

NEITHER ABSENCE NOR EXCESS OF FGF23 DISTURBS FETAL PHOSPHATE  
METABOLISM IN MICE UNTIL AFTER BIRTH

by

© YUE MA

A thesis submitted to the  
School of Graduate Studies  
in partial fulfillment of the requirements for the degree of  
Doctor of Philosophy

Division of Biomedical Sciences  
Faculty of Medicine  
Memorial University of Newfoundland

October 2020

St. John's

Newfoundland and Labrador

## ABSTRACT

Fibroblast growth factor 23 (FGF23) plays an important role in maintaining phosphate homeostasis in adults largely through actions on the kidneys to excrete phosphate and reduce calcitriol. However, whether FGF23 is essential in maintaining phosphate homeostasis in fetuses had been largely unknown prior to my Ph.D. project, which hypothesized that FGF23 was important in regulating not only fetal serum phosphate and skeletal development, but also placental phosphate transport. However, studies in *Phex* null fetuses showed that excess FGF23 did not disturb any phosphate parameter or placental phosphate transport. Although the expression of *Cyp24a1* was increased in the null placenta and kidneys and the expression of *Klotho* was decreased in the null kidneys, these changes did not disturb any physiological parameter related to phosphate, which suggests that FGF23 is not important in fetal phosphate regulation. Previous studies in *Fgf23* null fetuses showed FGF23 absence did not alter fetal phosphate parameters, placental phosphate transport or skeletal development. These results led to my hypothesis that other FGF members might compensate for FGF23 loss by acting on the FGFR/Klotho receptor complex. However, studies in *Klotho* null fetuses showed that serum FGF23 was normal and that they had a similar phenotype as *Fgf23* nulls – which rejected my hypothesis. Previous studies showed that *Pth* null fetuses developed hyperphosphatemia. I then studied *Pth/Fgf23* double knockout (DKO) fetuses to determine if absence of FGF23 would potentiate hyperphosphatemia in *Pth* nulls. The results showed that DKO had the same elevation in serum phosphate as *Pth* nulls and there were no skeletal mineral content changes between the two genotypes either. I finally examined the postnatal time course of phosphate metabolism in neonatal *Fgf23* nulls, *Klotho* nulls, and *Phex* nulls, respectively. The results showed *Fgf23* nulls and *Klotho* nulls were normal at birth, but developed hyperphosphatemia, increased renal gene

expression of *NaPi2a* and *NaPi2c*, and increased renal phosphate reabsorption between 5 and 7 days later. In contrast, excess FGF23 exerted effects in *Phex* nulls within 12 hours after birth, with the development of hypophosphatemia, reduced renal expression of *NaPi2a* and *NaPi2c*, and decreased renal phosphate reabsorption. In conclusion, my Ph.D. project suggests FGF23 is not an important regulator of fetal phosphate metabolism.

## ACKNOWLEDGEMENTS

I would like to thank my supervisor, Dr. Christopher Kovacs, for his supervision and support. I would also like to thank him for bringing me to medical conferences where I had the opportunities to present my work to peer researchers.

Thanks to Dr. Gary Paterno and Dr. Ann Dorward, my supervisory committee, for helping keep my Ph.D. project on track and providing valuable suggestions. I would like to acknowledge Dr. Beate Lanske for providing us with the *Fgf23* knockout mice. Thanks to Research Assistant Beth Kirby in Dr. Kovacs' Laboratory for her many years of technical support.

Last but not least, I would like to thank my dear mom and dad and my lovely wife Xiaoxi Liu for their support and encouragement.

## TABLE OF CONTENTS

NEITHER ABSENCE NOR EXCESS OF FGF23 DISTURBS FETAL PHOSPHATE METABOLISM IN MICE UNTIL AFTER BIRTH.....	I
ABSTRACT.....	I
ACKNOWLEDGEMENTS.....	III
TABLE OF CONTENTS.....	IV
LIST OF TABLES.....	VIII
LIST OF FIGURES.....	IX
LIST OF ABBREVIATIONS.....	XI
1 Introduction.....	1
1.1 Preamble.....	1
1.2 Phosphorus Homeostasis in Adults.....	1
1.2.1 Function and Distribution of Phosphorus.....	1
1.2.2 Phosphate Regulation in Adults: Intestine-Bone-Kidney Axis.....	2
1.2.2.1 Intestinal Phosphate Absorption.....	2
1.2.2.1.1 Phosphate Transport across the Intestines.....	2
1.2.2.1.2 Regulation of Intestinal Phosphate Transport.....	6
1.2.2.1.2.1 Dietary Phosphate.....	6
1.2.2.1.2.2 Calcitriol.....	7
1.2.2.1.2.3 PTH.....	9
1.2.2.1.2.4 FGF23.....	11
1.2.2.1.2.5 Other Hormones and Factors.....	13
1.2.2.2 Phosphate in the Bones.....	14
1.2.2.2.1 Phosphate-related Bone Metabolism.....	14
1.2.2.2.2 Regulation of Phosphate Storage and Release from the Bones.....	15
1.2.2.2.2.1 FGF23.....	15
1.2.2.2.2.2 PTH.....	16
1.2.2.2.2.3 Calcitriol.....	16
1.2.2.3 Phosphate Handling by the Kidneys.....	17
1.2.2.3.1 Phosphate Physiology at the Kidneys.....	17
1.2.2.3.2 Kidney Structure.....	18
1.2.2.3.3 Renal Phosphate Reabsorption.....	18
1.2.2.3.4 Regulation of Renal Phosphate Excretion and Reabsorption.....	21
1.2.2.3.4.1 PTH and PTHrP.....	21
1.2.2.3.4.2 FGF23.....	22
1.2.2.3.4.3 Calcitriol.....	24
1.2.3 Phosphate Disorders in Human Adults.....	24
1.2.3.1 FGF23-Dependent Hypophosphatemic Disorders.....	25
1.2.3.1.1 XLH.....	25
1.2.3.1.2 TIO.....	28
1.2.3.1.3 ADHR.....	28
1.2.3.1.4 ARHR.....	28
1.2.3.2 FGF23-Dependent Hyperphosphatemic Disorders.....	29
1.2.3.3 FGF23-Independent Phosphate Disorders.....	29
1.3 Phosphorus Homeostasis in Fetal Life.....	31
1.3.1 Phosphate Handling by the Placenta.....	31
1.3.1.1 Phosphate Transport across the Placenta.....	31
1.3.1.2 Regulation of Placental Phosphate Transport.....	32
1.3.1.2.1 PTHrP.....	32
1.3.1.2.2 PTH.....	33

1.3.1.2.3	Calcitriol.....	34
1.3.1.2.4	FGF23 .....	35
1.3.1.3	Summary of Key Points .....	35
1.3.2	Phosphate in Fetal Bone Development .....	35
1.3.2.1	Overview of Fetal Bone Development.....	35
1.3.2.2	Regulation of Phosphate in Fetal Bone Development .....	38
1.3.2.2.1	PTH.....	38
1.3.2.2.2	PTHrP .....	40
1.3.2.2.3	Combined Actions of PTH and PTHrP.....	40
1.3.2.2.4	Calcitriol.....	41
1.3.2.2.5	FGF23 .....	42
1.3.2.2.6	Other Factors.....	43
1.3.2.3	Summary of Key Points .....	43
1.3.3	Phosphate Handling by the Fetal Kidneys .....	44
1.3.3.1	Regulation of Phosphate in the Fetal Kidneys .....	45
1.3.3.1.1	PTH and PTHrP .....	45
1.3.3.1.2	Calcitriol.....	45
1.3.3.1.3	FGF23 .....	46
1.3.3.2	Summary of Key Points .....	47
1.4	Phosphorus Homeostasis during the Neonatal Stage .....	47
1.4.1	Serum Phosphate Changes during a Transition from Fetuses to Neonates.....	47
1.4.2	Intestinal Phosphate Absorption in Neonates .....	48
1.4.2.1	Regulators of Intestinal Phosphate Absorption in Neonates.....	50
1.4.2.1.1	Calcitriol.....	50
1.4.2.1.2	FGF23 .....	51
1.4.2.1.3	PTH and PTHrP .....	51
1.4.2.1.4	Phosphate Content in Food .....	52
1.4.2.2	Summary of Key Points .....	52
1.4.3	Skeletal Phosphate Metabolism in Neonates .....	52
1.4.4	Renal Phosphate Excretion in Neonates .....	53
1.4.4.1	Regulators of Renal Phosphate Excretion in Neonates.....	53
1.4.4.1.1	PTH.....	53
1.4.4.1.2	Calcitriol.....	54
1.4.4.1.3	FGF23 .....	54
1.4.4.2	Summary of Key Points .....	55
1.5	Summary of Animal Models.....	56
1.6	Overview of Ph.D. Project.....	56
2	Materials and Methods .....	60
2.1.1	Mouse Models Used in My Ph.D. Project.....	60
2.1.1.1	Phex Null Model.....	60
2.1.1.2	Fgf23 KO Model.....	62
2.1.1.3	Klotho KO Model .....	64
2.1.1.4	Fgf23/Pth Double KO Model.....	66
2.2	Description of Experiments in Aim 1 .....	69
2.2.1	Experiments on ED17.5 .....	69
2.2.2	Experiments on ED18.5 .....	69
2.3	Description of the Experiments in Aim 2 .....	70
2.4	Description of the Experiments in Aim 3 .....	70
2.5	Description of the Experiments in Aim 4 .....	70
2.6	Genotyping.....	71
2.6.1	Tagging and Tailing .....	71

2.6.2	DNA Extraction .....	71
2.6.3	PCR.....	71
2.6.3.1	PCR Programs for the <i>Phex</i> Mutant Model .....	71
2.6.3.2	PCR Programs for the <i>Klotho</i> KO model .....	75
2.6.3.3	PCR Programs for the <i>Fgf23</i> KO Model.....	75
2.6.3.4	PCR Programs for the <i>Fgf23/Pth</i> Double KO Model .....	76
2.6.4	Gel Electrophoresis.....	77
2.7	Fetal Serum Mineral and Hormone Analysis.....	78
2.7.1	Fetal Serum Collection.....	78
2.7.2	Serum Mineral Analysis.....	78
2.7.3	Serum Hormone Analysis .....	79
2.8	Amniotic Fluid Collection and Mineral Analysis .....	81
2.8.1	Amniotic Fluid Collection .....	81
2.8.2	Amniotic Fluid Mineral Analysis .....	81
2.9	Fetal Skeletal Mineral Analysis .....	81
2.9.1	Fetal Ash Collection.....	81
2.9.2	Skeletal Mineral Analysis .....	82
2.10	Placental Phosphorus Transfer.....	82
2.11	Fetal Tibial Morphology .....	83
2.12	Microarray.....	84
2.13	Neonatal Urine Collection .....	85
2.14	FGF23-Targeted Gene Expression Analysis on the Placenta and on the Fetal and Neonatal Kidneys .....	85
2.14.1	Placenta and Fetal and Neonatal Kidneys Collection .....	85
2.14.2	Real-time Quantitative RT-PCR (qPCR).....	85
2.14.2.1	RNA Extraction.....	86
2.14.2.2	cDNA Synthesis.....	86
2.14.2.3	Quantitative Real Time RT-PCR (qPCR).....	87
2.15	Statistical Analysis.....	87
3	Results .....	89
3.1	Results from <i>Phex</i> Null Fetuses.....	89
3.1.1	Serum Hormones in <i>Phex</i> Fetuses on ED18.5 .....	89
3.1.2	Serum Chemistries in <i>Phex</i> Fetuses on ED18.5.....	94
3.1.3	Amniotic Fluid Chemistries in <i>Phex</i> Fetuses on ED17.5.....	98
3.1.4	Placental Phosphate Transport in <i>Phex</i> Fetuses on ED17.5.....	101
3.1.5	Skeletal Mineral Content in <i>Phex</i> Fetuses on ED18.5 .....	104
3.1.6	Bone Morphology and Mineralization in <i>Phex</i> Fetuses on ED18.5.....	109
3.1.7	Gene Expression Analysis on the <i>Phex</i> Placenta and Kidneys on ED18.5.....	111
3.1.8	Control Studies in <i>Phex</i> WT Dams on ED18.5.....	113
3.1.9	Microarray Analysis on the <i>Phex</i> and <i>Fgf23</i> Null Placentas .....	116
3.2	Results from <i>Klotho</i> Null Fetuses .....	117
3.2.1	Serum Hormones in <i>Klotho</i> Fetuses on ED18.5 .....	117
3.2.2	Serum Chemistries in <i>Klotho</i> Fetuses on ED18.5.....	121
3.2.3	Amniotic Fluid Chemistries in <i>Klotho</i> Null Fetuses on ED17.5.....	124
3.2.4	Placental Phosphate Transport in <i>Klotho</i> Fetuses on ED17.5.....	127
3.2.5	Skeletal Mineral Content in <i>Klotho</i> Fetuses on ED18.5 .....	130
3.2.6	Bone Morphology and Mineralization in <i>Klotho</i> Fetuses on ED18.5.....	135
3.2.7	Gene Expression Analysis on the <i>Klotho</i> Placenta and Kidneys on ED18.5.....	137
3.3	Results from <i>Pth/Fgf23</i> DKO Fetuses .....	141
3.3.1	Serum Phosphorus in <i>Fgf23/Pth</i> DKO Fetuses on ED18.5 .....	141
3.3.2	Skeletal Mineral Content in <i>Fgf23/Pth</i> DKO Fetuses on ED18.5 .....	144

3.4	Results from Postnatal <i>Phex</i> Null, <i>Fgf23</i> Null, and <i>Klotho</i> Null Pups .....	146
4	Discussion.....	157
4.1	Excess FGF23 Does Not Disturb Fetal Phosphate Metabolism.....	157
4.2	Neither FGF23, Calcitriol nor PTH Is Required to Maintain Fetal Phosphate Homeostasis....	161
4.3	Maternal Phenotype Does Not Affect Fetal Phenotype .....	162
4.4	Why Were Fetal PTH Values High in My Study?.....	163
4.5	Potential Effects of Genetic Backgrounds on Fetal FGF23 .....	165
4.6	Calcitriol Does Not Respond to FGF23 during Pregnancy.....	166
4.7	Why Does an Abnormal FGF23 Signaling Pathway Fail to Alter Fetal Phosphate Parameters? 166	
4.8	FGF23 Is Important in Neonatal Phosphate Regulation .....	169
4.9	Clinical Implication .....	172
4.10	Study Limitations.....	172
4.11	Future Directions .....	175
4.12	Summary and Conclusion .....	179
5	References .....	181
6	Appendix .....	195
6.1	Mouse Tail DNA Extraction Protocol .....	195
6.2	Phosphorus Assay .....	196
6.3	Mouse PTH 1-84 ELISA Kit .....	199
6.4	1,25-Dihydroxy Vitamin D EIA kit .....	207
6.5	FGF23 ELISA Kit.....	218

## LIST OF TABLES

Table 1: List of FGF23-Targeted Genes in Placentas and Fetal Kidneys between <i>Phex</i> WT and Null Fetuses. ....	112
Table 2: List of FGF23-Targeted Genes in Placentas and Fetal Kidneys between <i>Klotho</i> WT and Null Fetuses. ....	139
Table 3: Renal Expression of <i>NaPi2a</i> , <i>NaPi2b</i> and <i>NaPi2c</i> in <i>Phex</i> Neonates.....	150
Table 4: Renal Expression of <i>NaPi2a</i> , <i>NaPi2b</i> and <i>NaPi2c</i> in <i>Fgf23</i> and <i>Klotho</i> Neonates...	155

## LIST OF FIGURES

Figure 1: A Tight Junction in The Small Intestines.....	4
Figure 2: Renal Phosphate Reabsorption by Proximal Tubular Cells.....	20
Figure 3: A Proposed Mechanism of How DMP1 Regulate the <i>Fgf23</i> Expression.....	27
Figure 4: Endochondral Bone Formation. ....	37
Figure 5: Naturally Occurring Mutations in <i>Phex</i> . ....	61
Figure 6: The Generation of <i>Fgf23</i> Null Mice. ....	63
Figure 7: The Generation of <i>Klotho</i> Null Mice.....	65
Figure 8: The Generation of <i>Fgf23/Pth</i> Double Mutant Mice.....	67
Figure 9: The Generation of <i>Pth</i> Null Mice.....	68
Figure 10: Serum FGF23 in <i>Phex</i> Fetuses on ED18.5.....	91
Figure 11: Serum Calcitriol in ED18.5 <i>Phex</i> Fetuses. ....	92
Figure 12: Serum PTH in ED 18.5 <i>Phex</i> Fetuses.....	93
Figure 13: Serum Phosphorus in <i>Phex</i> Fetuses on ED18.5 (Data of WT ♂ and WT ♀ Were Separated). ....	95
Figure 14: Serum Phosphorus in <i>Phex</i> Fetuses on ED18.5 (Data of WT ♂ and WT ♀ Were Pooled). ....	96
Figure 15: Serum Total Calcium in <i>Phex</i> Fetuses on ED18.5.....	97
Figure 16: Amniotic Fluid Phosphorus in <i>Phex</i> Fetuses on ED17.5. ....	99
Figure 17: Amniotic Fluid Total Calcium in ED 17.5 <i>Phex</i> Fetuses.....	100
Figure 18: Placental Phosphate Transport ( $^{32}\text{P}/^{51}\text{Cr}$ -EDTA) in ED 17.5 <i>Phex</i> Fetuses.....	102
Figure 19: Placental Phosphate Transport ( $^{32}\text{P}$ ) in ED17.5 <i>Phex</i> Fetuses. ....	103
Figure 20: Body Ash Weight in ED 18.5 <i>Phex</i> Fetuses.....	105
Figure 21: Skeletal Phosphate Content in ED 18.5 <i>Phex</i> Fetuses.....	106
Figure 22: Skeletal Calcium Content on in ED 18.5 <i>Phex</i> Fetuses. ....	107
Figure 23: Skeletal Magnesium Content in ED 18.5 <i>Phex</i> Fetuses. ....	108
Figure 24: Skeletal Morphology and Mineralization in ED 18.5 <i>Phex</i> Fetuses. ....	110
Figure 25: Serum FGF23 in <i>Phex</i> Fetuses from WT Dams Mated to <i>Phex</i> Null Males.....	114
Figure 26: Fetal Serum Phosphorus of Fetuses from <i>Phex</i> WT Dams Mated to <i>Phex</i> Null Males..	115
Figure 27: Serum FGF23 in ED18.5 <i>Klotho</i> Fetuses.....	118
Figure 28: Serum Calcitriol in ED18.5 <i>Klotho</i> Fetuses. ....	119
Figure 29: Serum PTH in ED 18.5 <i>Klotho</i> Fetuses.....	120
Figure 30: Serum Phosphorus in ED 18.5 <i>Klotho</i> Fetuses.....	122
Figure 31: Serum Total Calcium in ED 18.5 <i>Klotho</i> Fetuses. ....	123
Figure 32: Amniotic Fluid Phosphorus in ED 17.5 <i>Klotho</i> Fetuses. ....	125
Figure 33: Amniotic Fluid Total Calcium in ED 17.5 <i>Klotho</i> Fetuses. ....	126
Figure 34: Placental Phosphate Transport ( $^{32}\text{P}/^{51}\text{Cr}$ ) in ED 17.5 <i>Klotho</i> Fetuses.....	128
Figure 35: Placental Phosphate Transport ( $^{32}\text{P}$ ) in ED 17.5 <i>Klotho</i> Fetuses. ....	129
Figure 36: Body Ash Weight in ED 18.5 <i>Klotho</i> Fetuses.....	131
Figure 37: Skeletal Phosphate Content in ED 18.5 <i>Klotho</i> Fetuses.....	132
Figure 38: Skeletal Calcium Content on in ED 18.5 <i>Klotho</i> Fetuses.....	133
Figure 39: Skeletal Magnesium Content in ED 18.5 <i>Klotho</i> Fetuses. ....	134
Figure 40: Skeletal Morphology and Mineralization in ED 18.5 <i>Klotho</i> Fetuses. ....	136
Figure 41: Expression of <i>Cyp24a1</i> in the <i>Fgf23</i> , <i>Phex</i> , and <i>Klotho</i> Fetal Kidneys.....	140

Figure 42: Serum Phosphorus in <i>Fgf23/Pth</i> DKO Fetuses.....	143
Figure 43: Skeletal Mineral Content in ED17.5 <i>Fgf23/Pth</i> DKO Fetuses. ....	145
Figure 44: Serum Phosphorus in <i>Phex</i> Neonates.....	148
Figure 45: Urine Phosphorus in <i>Phex</i> Neonates. ....	149
Figure 46: Serum Phosphorus in <i>Fgf23</i> Neonates. ....	151
Figure 47: Serum Phosphorus in <i>Klotho</i> Neonates. ....	152
Figure 48: Urine Phosphorus in <i>Fgf23</i> Neonates.....	153
Figure 49: Urine Phosphorus in <i>Klotho</i> Neonates. ....	154
Figure 50: Serum PTH in <i>Fgf23</i> and <i>Klotho</i> Neonates.....	156

## LIST OF ABBREVIATIONS

1, 25(OH) <sub>2</sub> D <sub>3</sub> .....	1, 25-dihydroxyvitamin D
AC.....	Adenylate Cyclase
ADHR.....	Autosomal Dominant Hypophosphatemic Ricket
ASARM.....	Acidic Serine-Aspartate-Rich Motif
ATP.....	Adenosine Triphosphate
ARHR.....	Autosomal Recessive Hyperphosphatemic Ricket
BL.....	Baseline
cAMP.....	Cyclic Adenosine Monophosphate
CaSR.....	Calcium Sensing Receptor
DKO.....	Double Knockout
DMP1.....	Dentin Matrix Acidic Phosphoprotein 1
ED.....	Embryonic Day
EDTA.....	Ethylenediaminetetraacetic Acid
EGF.....	Epidermal Growth Factor
ERK.....	Extracellular Signal-Regulated Kinase
FGF23.....	Fibroblast Growth Factor 23
FGFR.....	FGF receptor
HET.....	Heterozygous
HRP.....	Horseradish Peroxidase
HSPG.....	Heparin Sulfate Proteoglycan
JAM-1.....	Junctional Adhesion Molecule 1
JNK.....	Jun N-Terminal Kinase
KO.....	Knockout
lincRNA.....	Long Intergenic Non-Coding RNA
LP.....	Late Pregnancy

OPN.....	Osteopontin
PD.....	Postnatal Day
PKA.....	Protein Kinase A
PKB.....	Protein Kinase B
PTH.....	Parathyroid Hormone
PTH1R.....	Type 1 PTH Receptor
PTH2R.....	Type 2 PTH Receptor
PTHrP.....	Parathyroid Hormone Related Peptide
qPCR.....	Real-Time Quantitative Polymerase Chain Reaction
RANKL.....	Receptor Activator Of Nuclear Factor kB
RIN.....	RNA Integrity Number
RXR.....	Retinoid X Receptor
SIBLING.....	Small Integrin-Binding Ligand, N-Linked Glycoprotein
Slc34a1.....	Solute Carrier Family 34, Member 1
Slc34a2.....	Solute Carrier Family 34, Member 2
Slc34a3.....	Solute Carrier Family 34, Member
3TAE.....	Tris-Acetate-EDTA
TC.....	Tumoral Calcinosis
TIO.....	Tumor-Induced Osteomalacia
TRPV6.....	Transient Receptor Potential Cation Channel Subfamily V Member 6
VDRE.....	Vitamin D Response Element
WT.....	Wildtype
XLH.....	X-Linked Hypophosphatemic Ricket
ZO-1.....	Zonula Occludens-1

# 1 Introduction

## 1.1 Preamble

Phosphorus plays an important role in normal physiological activities. Disturbance in phosphorus homeostasis can trigger severe disorders. In adults, it is well known that fibroblast growth factor 23 (FGF23), parathyroid hormone (PTH) and calcitriol regulate phosphorus homeostasis.

However, little had been known about the regulation of phosphorus homeostasis in fetuses and neonates by the time when I initiated my Ph.D. study. In my Ph.D. project, the main focus was on studying potential roles of FGF23 in fetal and neonatal phosphorus regulation. To achieve this goal, three mouse models were used: the *Phex* null model (also known as the *Hyp* model that develops spontaneous hypophosphatemia due to naturally occurring mutations in the *Phex* gene), the *Fgf23* knockout (KO) model, and the *Klotho* KO model. By studying the three models, I was hoping to answer the question as to whether FGF23 is physiologically important in maintaining fetal and neonatal phosphorus homeostasis.

## 1.2 Phosphorus Homeostasis in Adults

### 1.2.1 Function and Distribution of Phosphorus

Phosphorus is an essential element in all organisms [1, 2]. Compounds containing phosphorus have critical roles in maintaining cell structure integrity (cell membranes and nucleic acids have high content of phosphorus), cell metabolism (synthesis of adenosine triphosphate or ATP), cell signaling pathway (phosphorylation of enzymes), homeostasis of body fluids (urinary buffering), and bone health [3, 4]. Therefore, maintaining normal physiological phosphorus homeostasis is critical for well-being. A phosphorus imbalance can trigger severe disorders. Excess phosphorus

causes calcification of cardiovascular vessels and other soft tissues, while deficient phosphorus leads to undermineralized, weakened bone [i.e., osteomalacia (adults) or rickets (children)] and neuromuscular disturbances [5-9].

*In vivo*, phosphorus primarily is present in the form of phosphate. It is common to use the two terms interchangeably. The term phosphate is used in the following content. The majority of body phosphate (~85%) is deposited in the bones as hydroxyapatite [ $\text{Ca}_{10}(\text{PO}_4)_6(\text{OH})_2$ ] with calcium [10]. The remainder exists as inorganic and organic compounds that are distributed in other tissues (~14%) and extracellular fluids (~1%).

## 1.2.2 Phosphate Regulation in Adults: Intestine-Bone-Kidney Axis

Phosphate homeostasis in adults can be explained largely by an intestine-bone-kidney axis.

Phosphate intake is through intestinal absorption, the majority of phosphate is stored in the bones, and the kidneys are the primary route through which a phosphorus balance is fine-tuned.

### 1.2.2.1 Intestinal Phosphate Absorption

#### 1.2.2.1.1 Phosphate Transport across the Intestines

Phosphate is present in the majority of food sources. Milk and dairy products are the richest dietary sources, but others include bread, cereals, rice, meat, fish, and some non-alcoholic beverages. Phosphate is predominately absorbed in the duodenum and usually interacts with other minerals. For example, calcium and magnesium can bind to phosphate in the duodenum, reducing intestinal phosphate absorption. A proper amount of sodium under acidic pH promotes

the process [11].

The intestines absorb phosphate via two distinct mechanisms: paracellular diffusion and active transport. The former is a process of passive transport largely driven by an electrochemical gradient, whereas the latter involves energy-dependent sodium-phosphate co-transporters [12]. How phosphate passively diffuses across the intestines remains to be elucidated. In general, passive diffusion of a compound occurs at a tight junction complex where membranes of two cells join together to form barriers (**Figure 1**). Adhesive anchor proteins between neighbouring cells maintain the complex. Common adhesive proteins in a tight junction include occludin, claudin 1, E-cadherin, zonula occludens-1 (ZO-1), junctional adhesion molecule-1 (JAM-1), catenins, cingulin, and actin [13]. Recent studies suggested that cytoskeletal pathways regulate passive diffusion across a tight junction, and that occludins and claudins appear to play important roles. For example, mutations of claudin in the small intestine caused hypomagnesemia and hypercalciuria [14-17]. Although more and more studies are being carried out, the process of phosphate-specific diffusion through an intestinal tight junction is still unclear.

Unlike passive diffusion, the active transport of phosphate in the intestines has been intensively studied. In simple words, phosphate in the lumen is transferred into intestinal epithelial cells in a sodium-dependent manner. The process requires phosphate-specific transporters located on the surface of the epithelial cells. However, how phosphate is pumped out of intestinal epithelial cells at the basolateral side remains unknown. Those transporters required for the active process include two families of solute carriers, the SLC34 family (also known as type II sodium-phosphate co-transporters) and the SLC20 family (also known as type III) [18-20].

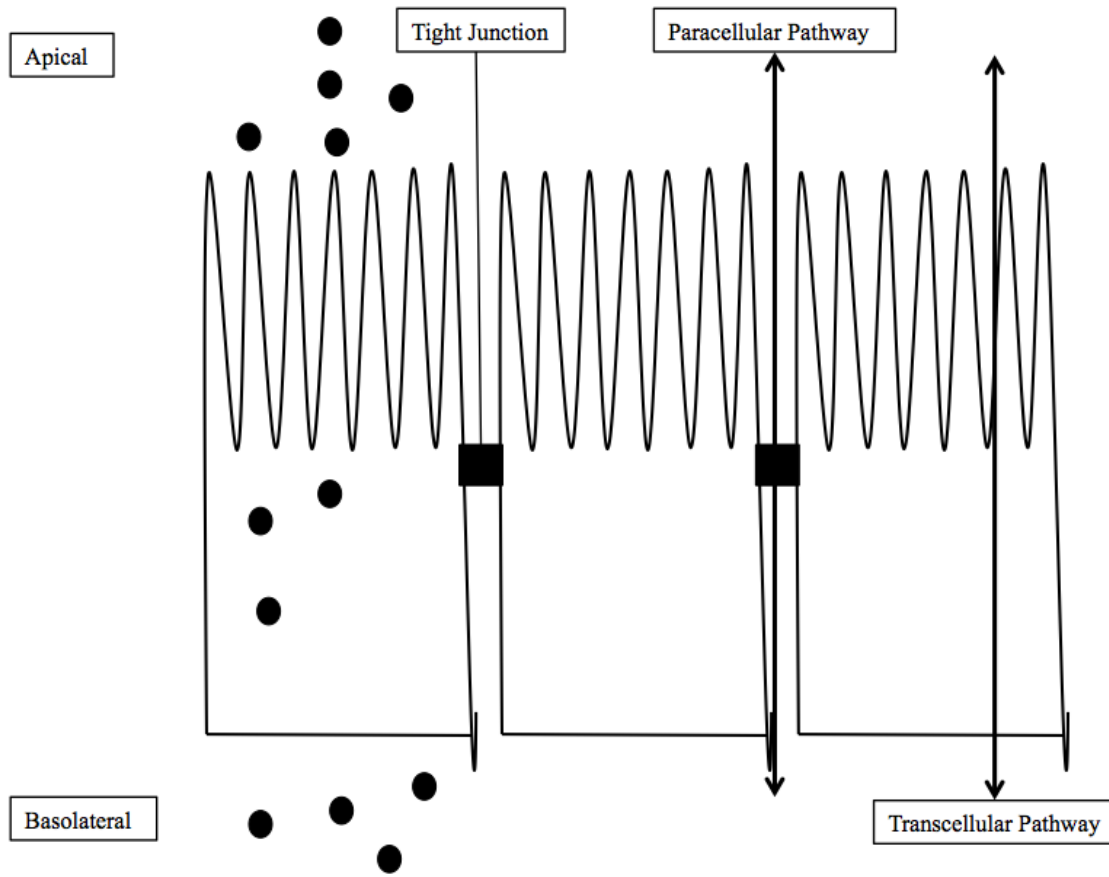


**Figure 1: A Tight Junction in the Small Intestines.** Intestinal absorption occurs via passive paracellular diffusion and/or active transcellular transport. A tight junction is formed where the membranes of two cells join together to form barriers.

The type II sodium-phosphate co-transporters are the major players in the phosphate transport across cell membranes. They are represented by the 2a subtype (NaPi2a), the 2b subtype (NaPi2b), and the 2c subtype (NaPi2c). It is well known that intestinal phosphate absorption is facilitated through NaPi2b whereas the renal reabsorption through NaPi2a and NaPi2c [12]. It is noteworthy that the genes encoding NaPi2a, NaPi2b, and NaPi2c are officially named *solute carrier family 34 member 1 (Slc34a1)*, *solute carrier family 34 member 2 (Slc34a2)*, and *solute carrier family 34 member 3 (Slc34a3)*, respectively. Several studies in KO mice implied that NaPi2b may play essential roles in sensing phosphate in the intestines and regulating the absorption. For example, 30 and 60 minutes after being gavaged with 0.5 M sodium phosphate bolus, adult mice with postnatal KO of *NaPi2b* had significantly lower concentrations of serum phosphate concentrations than normal wildtype (WT) mice receiving the same treatment [21]. Interestingly, despite decreased intestinal phosphate absorption, serum phosphate concentrations were normal in adult mice with intestine-specific *NaPi2b* KO. This might be achieved by a compensatory mechanism of increased renal phosphate reabsorption because quantitative immunoblot analysis showed that NaPi2a protein levels were significantly increased in the KO kidneys. In human patients with a *NaPi2b* mutation, the net changes of serum and urinary phosphate were found to be normal [22, 23].

The type III co-transporters, now often called Pit1 and Pit2, have been shown to be broadly expressed on membranes of polarized epithelial cells [24]. They play roles in mediating sodium and phosphate movements across cell membranes. Some prior studies showed the expression of both *Pit1* and *Pit2* in *Xenopus* oocytes could stimulate phosphate to move inward into the cells in the presence of sodium, i.e. the movement was sodium-dependent [25].

#### 1.2.2.1.2 Regulation of Intestinal Phosphate Transport

When diet can provide more than sufficient phosphate, it is predominately absorbed via passive diffusion in the intestines. Active phosphate absorption occurs when there is a dietary phosphate deficiency or renal phosphate wasting. The three key players of the active process are dietary phosphate, 1,25-dihydroxyvitamin D ( $1,25(\text{OH})_2\text{D}_3$ , also known as calcitriol), and parathyroid hormone (PTH). Calcitriol is the biologically active form of vitamin D. Other factors, such as calcium, glucocorticoids, estrogens, FGF23, epidermal growth factor (EGF), metabolic acidosis, and parathyroid hormone related peptide (PTHrP) are also indicated to regulate active intestinal phosphate absorption [2, 26-30].

##### 1.2.2.1.2.1 Dietary Phosphate

Low dietary phosphate stimulates intestinal phosphate absorption [31-33]. The original thought was that dietary phosphate exerted effects on intestinal phosphate absorption through changing the calcitriol signalling pathway – calcitriol increases intestinal phosphate absorption (This is discussed in Section 1.2.2.1.2.2 titled “Calcitriol”). Indeed, this hypothesis was straightforward because low dietary phosphate decreases serum phosphate, which in turn stimulates  $1\alpha$  hydroxylase (the enzyme required to produce calcitriol *in vivo*) [34-36]. However, it was not until recently that the phosphate content in diet was found to change active phosphate absorption independent of calcitriol. Katai’s group showed that a low phosphate diet stimulated NaPi2b in the rats’ intestines without changing the mRNA levels of the vitamin D receptor gene (*Vdr*) [32]. A previous study conducted by Segawa’s team illustrated that low dietary phosphate increased NaPi2b protein synthesis in both WT and *Vdr* KO mice [33]. These results suggest that dietary phosphate could change the process of intestinal phosphate absorption independent of

calcitriol. Studies by Hattenhauer's group showed that although dietary phosphate restriction increased NaPi2b protein levels in normal mice, *NaPi2b* mRNA expression was not changed, suggesting that dietary phosphate could adjust intestinal absorption through post-transcriptional modifications [31].

#### 1.2.2.1.2.2 Calcitriol

Calcitriol is produced by the key enzyme, 1 $\alpha$ -hydroxylase (encoded by the gene called *Cyp27b1*), at the proximal tubules in the kidneys. 1 $\alpha$ -hydroxylase uses 25-hydroxyvitamin D as a substrate and adds a hydroxyl group on the 1' site of the substrate molecule. Calcitriol is metabolised by the enzyme 1,25-dihydroxyvitamin D3 24-hydroxylase (encoded by the gene called *Cyp24a1*) – 1,25-dihydroxyvitamin D3 24-hydroxylase adds one hydroxyl on the 24' site of the calcitriol molecule to suppress its functions. Calcitriol's only known receptor, VDR, belongs to a nuclear receptor subfamily and is located in cytoplasm. Before being activated by calcitriol, VDR exists in a form of heterodimers with retinoid X receptor (RXR) [37]. After calcitriol binds to the heterodimer, the complex is translocated into the nucleus where it binds to the so-called vitamin D response element (VDRE) sequence on DNA, triggering expression of downstream genes.

Many animal studies have shown that calcitriol can increase intestinal phosphate absorption [38, 39]. However, the mechanism still needs further studies for several reasons. First, expression of *NaPi2b* as a response to calcitriol varies among different species. This prevents a generalizable statement about the mechanism of calcitriol-dependent intestinal phosphate absorption [40, 41]. Second, as explained above, low dietary phosphate has been shown to be able to stimulate the

NaPi2b protein independent of calcitriol. Third, the effect of calcitriol on *NaPi2b* mRNA expression seems to be age-dependent. This interesting phenomenon was shown in a rat study conducted by Xu [39]. In this study, calcitriol treatment increased intestinal phosphate absorption in 14-day-old suckling young rats and adult rats by 2.5-fold and 2.1-fold, respectively; however, *NaPi2b* mRNA expression in adult rats (90 – 100 days old) was not changed by calcitriol. *NaPi2b* mRNA levels were increased by 2-fold in the suckling rats under the same treatment.

How many effects on intestinal phosphate absorption are from calcitriol directly remains an unresolved question because calcitriol can interact with other phosphate-regulating hormones. [40]. For example, calcitriol can inhibit PTH secretion and stimulate FGF23 production. Both PTH and FGF23 decrease serum phosphate in adults mainly via suppressing renal phosphate reabsorption. Calcitriol's inhibitory effect on PTH has been suggested by studies showing that calcitriol suppressed *Pth* gene transcription and by the fact that calcitriol is clinically used to treat parathyroid hyperplasia [42-45]. In terms of calcitriol's stimulatory role in FGF23 production, Shimada showed that when *Vdr* was knocked out in mice, serum FGF23 levels were undetectable, even after dietary phosphate loading[46]. Ohnishi's group reported that serum FGF23 in *Cyp27b1* mutant mice was significantly lower than that in WT [47]. Similar results were also observed in Dr. Kovacs' laboratory, which showed that adult *Cyp27b1* null mice had very low FGF23 levels that slightly increased during pregnancy but were much lower than those achieved in pregnant normal mice [48]. It should be noted that loss of calcitriol is a more specific model than loss of VDR in that there could be a possibility that calcitriol might act on some unknown receptors. The functions of PTH and FGF23 in regulating intestinal phosphate absorption are discussed below.

### 1.2.2.1.2.3 PTH

PTH is synthesized in the parathyroid glands. PTH tightly maintains serum calcium concentrations. Hypocalcemia induces the production and secretion of PTH, which in turn increases serum calcium through several mechanisms. Calcium reversely acts as a suppressor of PTH by binding to calcium sensing receptors (CaSR), which inhibit a PTH synthesis and release. This negative feedback loop ensures that serum calcium concentrations stay within a tight range.

The mineral and skeletal functions of PTH are through its actions on type 1 PTH receptors (PTH1R) that are highly expressed in the skeleton and kidneys. On one hand, activated PTH1R can modify the Gs protein, which in turn activates adenylate cyclase (AC). The activated AC synthesizes cAMP, which further activates protein kinase A (PKA), which regulates downstream transcriptional factors and gene expression. On the other hand, PTH1R modifies the Gq protein, which activates downstream PLC-IP<sub>3</sub> and PLC-DAG-PKC pathways. The two pathways can further regulate downstream transcriptional factors and gene expression. Unlike PTH1R, type 2 PTH receptors (PTH2R) are primarily located in the central nervous system, placenta, pancreas, and testis. PTH2R is involved in a variety of physiological functions, depending on where the receptor is [49].

In terms of PTH-induced regulation of intestinal phosphate absorption, the current view is that PTH regulates *NaPi2b* gene expression in an indirect way – which is different from calcitriol that can place a direct effect on this process. That is, PTH indirectly stimulates *NaPi2b* by increasing calcitriol production and/or any other related regulators [50, 51]. As discussed above, biosynthesis of calcitriol *in vivo* is largely regulated by 1 $\alpha$ -hydroxylase (encoded by *Cyp27b1*),

while the metabolism by 1,25-dihydroxyvitamin D3 24-hydroxylase (encoded by *Cyp24a1*). Many studies have shown that PTH is a strong activator of *Cyp27b1* and a strong inhibitor of *Cyp24a1*[44, 52]. Calcitriol has an inhibitory effect on PTH production. This negative feedback loop ensures appropriate intestinal phosphate absorption.

FGF23, which is discussed in details below, is known to reduce intestinal phosphate absorption. Studies have suggested that PTH can increase FGF23 production in both *vivo* and *vitro*. Lavi-Moshayoff's group reported that PTH infusion for 3 days increased circulating FGF23 in normal adult healthy mice and the treatment elevated calvarial *Fgf23* mRNA expression. An *in vitro* experiment showed that PTH treatment increased *Fgf23* expression in osteoblast-like UMR106 cells [53]. DMP1-caPTH1 is a transgenic mouse model that expresses a constitutively active human PTHR1 gene in osteocytes, causing increased bone mass and bone remodeling. Rhee showed that in DMP1-caPTH1 transgenic mice *Fgf23* expression in osteocytes was significantly elevated compared to normal WT mice [54]. PTH's stimulatory effect on FGF23 can be both direct as well as indirect through calcitriol. Lopez used parathyroidectomized rats to show that PTH replacement therapy was able to create a dose-dependent increase in both serum FGF23 and calcitriol in rats without the parathyroid glands. In this experiment, calcitriol plus PTH replacement highly increased serum FGF23 in parathyroidectomized rats. Although calcitriol alone also elevated serum FGF23, the level was below that achieved by calcitriol plus PTH replacement. [55]. Although many studies indicate PTH stimulates FGF23, further work is still needed to confirm this because some studies found that PTH did not change FGF23. For example, Saji showed in an *in vitro* study that calvarial cells receiving PTH treatment increased neither *Fgf23* mRNA levels nor FGF23 concentrations in the medium [56].

#### 1.2.2.1.2.4 FGF23

FGF23 is a phosphate-regulating hormone synthesized largely by osteoblasts and osteocytes [57]. Precursor proteins of FGF23 have 251 amino acids, which are modified by a cleavage of a 24-amino acid signal peptide (AA1 – AA24) sequence before being secreted – thus secreted FGF23 has 227 amino acids. An intact structure of biologically active FGF23 consists of an N-terminal fragment that is an FGF homology region (AA25 – AA179) and a C-terminal fragment (AA180 – AA251) [58]. Some FGF23 proteins are cleaved at AA179 by Furin (a type I precursor convertase), yielding separate N-terminal and C-terminal fragments [59]. It should be noted that it is intact FGF23 that is biologically active, whereas the N- and C-terminal fragments are not.

The classic FGF23 signaling pathway involves three key elements: FGF23, FGF receptors (FGFRs), and a co-receptor called Klotho. There are four types of FGFRs: FGFR1, FGFR2, FGFR3, and FGFR4. These receptors belong to a tyrosine kinase superfamily. Like typical tyrosine kinase receptors, FGFRs have an extracellular domain to bind a ligand, a single transmembrane helix domain, and an intracellular domain associated with tyrosine kinase activity. A fifth type of FGFRs, FGFR5 (also known as fibroblast growth factor receptor-like 1), was recently identified. In contrast to FGFRs1-4, FGFR5 does not have a tyrosine kinase domain – it only has an extracellular ligand domain [60].

Based on how FGFs conduct cell signals, the FGF superfamily is divided into two categories: paracrine FGFs and endocrine FGFs. The former includes the FGF1 family, the FGF4 family, the FGF7 family, the FGF8 family, the FGF9 family, and the FGF11 family. The latter (also known

as the FGF19 family) includes FGF19, FGF21, and FGF23. The key factor to differentiate the paracrine family and FGF19 family is the affinity to heparin sulfate proteoglycans (HSPGs, also known as heparin). Paracrine FGFs have a much stronger affinity to HSPGs than endocrine FGFs [61]. HSPG is thus claimed to serve as the “co-receptor” of paracrine FGFs [62]. Due to their loose affinities to HSPG, FGF19 family members can “escape” from local HSPGs and circulate to other locations to function.

Klotho serves as a co-receptor of endocrine FGFs. Klotho is a single-pass transmembrane protein. It was initially discovered during a study in mice with a syndrome resembling rapid ageing [63]. The *Klotho* gene is expressed in various tissues, such as distal convoluted tubules in the kidneys, the parathyroid glands, and epithelial cells of the choroid plexus in the brain [64]. The essential role of Klotho in the classic FGF23 signaling pathway has been confirmed in several studies showing that adult mice with an inactivating mutation in *Klotho* had a identical phenotype as those with an inactivating mutation in *Fgf23* except the former had extremely high FGF23 levels due to end organ resistance while the latter had none[65-68].

Among the four types of FGFRs, the FGFR1c isoform (FGFR1c) is the principal receptor for FGF23 for phosphorus homeostasis [69, 70], while FGFR3 and FGFR4 are relatively unimportant [71]. When FGF23, FGFRs, and Klotho bind together to form a complex, downstream factors such as extracellular signal-regulated kinases (ERK), P38, c-Jun N-terminal kinases (JNK), and protein kinase B (PKB), are activated to trigger further signaling cascades [65, 68, 72].

FGF23's main functions are to reduce serum phosphate and control phosphate supply at a mineralizing surface of the bones. Although the primary functional site of FGF23 is at the kidneys, this hormone can also indirectly inhibit intestinal phosphate absorption. Miyamoto showed that FGF23 injection reduced the amount of NaPi2b in the brush border membrane vesicles; however, the reduction disappeared in *Vdr* null mice – suggesting that FGF23 depends on VDR to inhibit NaPi2b [73]. FGF23 has been shown to suppress the production of PTH as well [74, 75]. The regulation of renal phosphate metabolism by FGF23 is discussed in Section 1.2.2.3.4 titled “Regulation of Renal Phosphate Excretion and Reabsorption.”

#### 1.2.2.1.2.5 Other Hormones and Factors

Besides the key players discussed above, other hormones and factors could also play roles in intestinal phosphate absorption to some extent. Secreted by various types of normal or malignant cells, parathyroid hormone related peptide (PTHrP) is a 139- or 173-amino acid peptide with N-terminal homology to PTH. PTHrP is normally extremely low in adults; however, it can circulate at high levels in fetuses, lactating females, and patients with certain malignancies. When elevated in the circulation, PTHrP has a phosphaturic effect as a result of its N-terminal structural similarity as PTH. Dua's group showed in a sheep study that after being injected by PTHrP, normal sheep had a significant increase in the absorption rate of calcium and phosphate from the reticulorumen [76]. In normal adults PTHrP does not regulate phosphate homeostasis. However, in patients with humoral hypercalcemia of malignancy, PTHrP is usually high, which can stimulate FGF23. Excess calcium forms un-absorbable compounds with phosphate in the intestines, leading to a reduction in phosphate intake [77]. Calcium can also suppress PTH, leading to a reduction in the renal synthesis of calcitriol. Xu showed that estradiol increased

active intestinal phosphate absorption by 45% in rats via increasing NaPi2b expression and its synthesis in the intestines [29]. Glucocorticoids have been suggested to inhibit intestinal phosphate absorption. In 4-week-old suckling rabbits, methylprednisolone injection significantly reduced an uptake of phosphate compared to rabbits treated with placebo [78]. Epidermal growth factor (EGF) has been illustrated to decrease *NaPi2b* mRNA levels via suppressing the activity of the gene's promoter [27].

#### 1.2.2.2 Phosphate in the Bones

As briefly mentioned above, the adult skeleton contains ~85% of the body's phosphate content. One of the skeleton's key functions is to serve as a reservoir of minerals, including phosphate. Therefore, in order to understand phosphate homeostasis, it is necessary to know how phosphate is handled within the bones.

##### 1.2.2.2.1 Phosphate-related Bone Metabolism

Bone mineralization is an important step during skeletal development. Hydroxyapatite, a complex of calcium and phosphate, constitutes the majority of mineral content of the bones. Other contents normally include carbonate, magnesium, and acid phosphate. The chemical formation of hydroxyapatite initially occurs within matrix vesicles that originate from osteogenic cell membranes. These vesicles then migrate to extracellular skeletal matrix, where they attract phosphate to move into the vesicles, followed by a calcium influx [79]. Since ~85% of phosphate *in vivo* is stored in the bones in a form of hydroxyapatite, this acts as a reservoir of phosphate. When hypophosphatemia occurs, the bones can be resorbed to release phosphate.

#### 1.2.2.2.2 Regulation of Phosphate Storage and Release from the Bones

After phosphate is absorbed in the intestines, most of it is stored in the bones. However, it should be noted that the bones are a less responsive organ to serum phosphate changes than the intestines and the kidneys (which is discussed in Section 1.2.2.3 titled “Phosphate Handling by the Kidneys”). Factors that regulate the storage and release of phosphate from the bones are discussed below.

##### 1.2.2.2.2.1 FGF23

FGF23 affects skeletal phosphate handling through changing the process of bone mineralization and bone resorption – bone mineralization consumes serum phosphate while bone resorption releases phosphate into the circulation. FGF23 can inhibit bone mineralization through both direct and indirect mechanisms. The indirect mechanism refers to FGF23’s effect to reduce circulating phosphate levels – thereby, making fewer minerals available for bone formation/mineralization. The direct mechanism is discussed below.

FGF23 itself is an inhibitor of bone mineralization independent of circulating phosphate. The inhibitory effects have been shown in many studies. For example, when *Fgf23* was overexpressed during osteoblast development in fetal rat calvaria cells, nodule formation and mineralization was inhibited. The inhibition could be ablated by an FGFR1 inhibitor, SU5402 [80]. Similar results were demonstrated in Sitara’s and Shalhoub’s studies using primary calvarial osteoblast cell cultures and osteoblastic MC3T3 E1 cells, respectively [81, 82]. Yuan’s group showed that *Fgf23/Pth* double KO mice had improved trabecular bone volume and mineralized bone volume than *Fgf23* mutant mice, indicating that a possible effect of FGF23 on

bone development is dependent of PTH but not phosphate[83].

Interestingly, some studies also suggest that FGF23 may have some positive effects on bone mineralization. For example, mice with FGF23 deficiency had osteomalacia or osteodosis even though these mice exhibited hyperphosphatemia, hypercalcemia, decreased serum PTH, and high serum calcitriol. One potential explanation is that FGF23 could suppress osteopontin (OPN), which is a well-known inhibitor of bone mineralization [84, 85].

#### 1.2.2.2.2 PTH

PTH indirectly stimulates osteoclasts by increasing secretion of receptor activator of nuclear factor kB (RANKL) by osteoblasts. RANKL acts on its receptor RANK on the surface of osteoclasts to activate the cells. During a process of bone resorption, phosphate and calcium are released into the circulation. Besides stimulating bone resorption, PTH can directly stimulate osteoblasts, which use phosphate to generate osteoid and thereby form bone.

#### 1.2.2.2.3 Calcitriol

The effects of calcitriol on bone tissues are complex – calcitriol seems to be able to stimulate both bone resorption and mineralization independent of circulating phosphate [86].

As to the effects on osteoclasts, Takahashi's group showed that an addition of calcitriol to the co-culture medium of osteoblasts and bone marrow cells enhanced the differentiation of osteoclasts [87]. An *in vivo* study demonstrated that calcitriol induced *Rankl* expression by osteoblasts, a critical step to stimulate the differentiation and activation of osteoclasts for bone resorption [88].

Calcitriol's stimulatory effects on osteoclastogenesis are thought to be through VDR in osteoblasts, because VDR is mainly expressed in osteoblasts, and because studies showed conditional deletion of *Vdr* from osteoblasts ablated calcitriol's stimulatory effects [89].

As to calcitriol's stimulatory effects on bone mineralization, most evidence suggests they are indirect. That is, calcitriol enhances bone mineralization by stimulating the intestinal absorption of calcium and phosphate. For example, Xue's group demonstrated that global *Vdr* KO phenotypes were nearly prevented with a genetic reintroduction of *Vdr* into intestinal cells [90]. Another study showed a conditional KO of *Vdr* in the intestines had similar phenotypes as a global KO [91]. Interestingly, several recent studies illustrated that calcitriol could directly increase mineralization in the human pre-osteoblastic SV-HFO cell line by enhancing production of ALP-positive mature matrix vesicles [92].

### 1.2.2.3 Phosphate Handling by the Kidneys

#### 1.2.2.3.1 Phosphate Physiology at the Kidneys

Renal phosphate excretion is of particular importance for the maintenance of a phosphate balance, perhaps even more so than intestinal phosphorus absorption or bone formation and resorption [93]. In humans, approximately 20 g of phosphate is filtered by the kidneys per day, with 85% (~ 17 g) eventually reabsorbed [93]. In equilibrium, the amount of excreted phosphate should be equal to that of intestinal absorption; however, this is not always the case as renal handling of phosphate is subject to numerous factors. Main hormonal players in this process are discussed in the related sections below.

#### 1.2.2.3.2 Kidney Structure

The kidneys are surrounded by a thin capsule, made of the connective tissues, which holds their shape and protects them. Inside the capsule is cortex, and deep inside that is medulla. The renal medulla is made of several pyramid-like structures, which consist of straight tubules and blood vessels. The apices of the renal pyramids are each connected to a minor calyx which merges with other calyces to form major calyces. The major calyces eventually merge into renal pelvis from where urine flows into the ureters.

The functional unit of the kidneys is called nephron, which is located in the renal cortex. There are two types of nephrons: cortical nephrons which constitute ~85% of nephrons and are found in the renal cortex, and juxtamedullary nephrons which make up the remaining 15%, and are located near the renal medulla. Each nephron has three elements: a renal corpuscle, a tubule, and a capillary network. The renal corpuscle consists of a glomerulus and a Bowman's capsule surrounding it. The glomerulus is linked to a long renal tubule that can be divided into three sections: the loop of Henle (also known as nephritic loop), a proximal tubule, and a distal tubule. The distal tubule is further connected to collecting ducts, which merge with other collecting ducts and enter into the papillae of the medullary section. Urine flows through the glomerulus to be filtered and reabsorbed and then passes into the renal calyces and further into the bladder through the ureters.

#### 1.2.2.3.3 Renal Phosphate Reabsorption

Renal phosphate reabsorption occurs at brush border membranes of proximal tubular cells. The process is thought to be sodium ion ( $\text{Na}^+$ ) dependent with no paracellular diffusion [94].

Chief co-transporters responsible for renal phosphate reabsorption are NaPi2a and NaPi2c. This has been confirmed in studies showing that adult mice with NaPi2a deficiency developed renal phosphate wasting and hypophosphatemia [95]. Similar results were observed when *NaPi2c* was knocked out [18]. Some studies suggest NaPi2a plays a larger role than NaPi2c. For example, the brush border membrane isolated from *NaPi2a* KO mice had a 70% reduction in the Na<sup>+</sup> dependent phosphate reabsorption [96]. Interestingly, NaPi2c was found to decrease with age in one study [97]. NaPi2a and NaPi2c have different transport stoichiometries as the former is electrogenic while the latter is electroneutral. NaPi2a displays a Na<sup>+</sup>:Phosphate stoichiometry of 3:1, whereas NaPi2c shows 2:1 [93]. Some recent studies indicate that PiT2 should also be considered as a potential phosphate co-transporter since the protein was detected exclusively at the brush border membrane of proximal tubular cells [24, 93]. The process of phosphate reabsorption by proximal tubular cells is illustrated in **Figure 2**. How phosphate exits the tubular cells at the basolateral membrane remains to be elucidated.

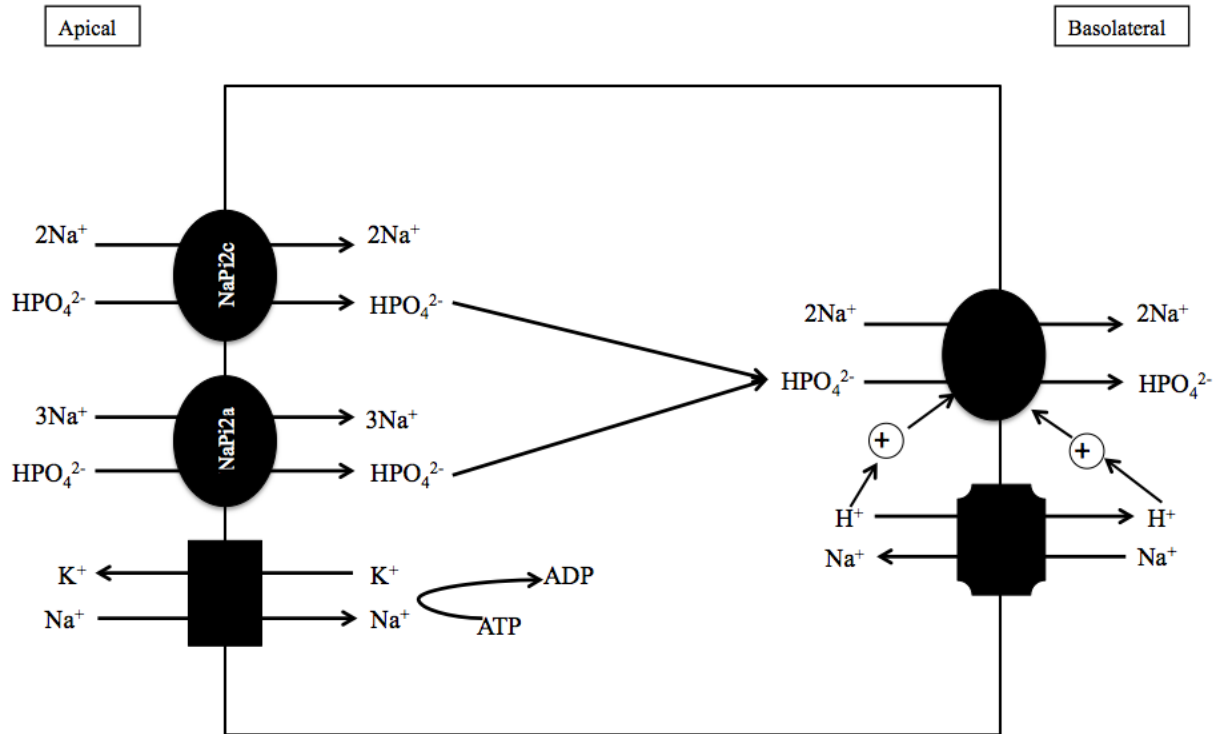


**Figure 2: Renal Phosphate Reabsorption by Proximal Tubular Cells.** Phosphate is transported across the brush border by NaPi2a and NaPi2c co-transporters. Phosphate enters the tubular cells and is transported across the basolateral membrane by a poorly understood mechanism. The Na/K -ATPase on the basolateral membrane (not shown in figure) pumps Na out of the cells thereby providing the driving force for the cell entry of Na<sup>+</sup>.

#### 1.2.2.3.4 Regulation of Renal Phosphate Excretion and Reabsorption

The regulation of renal phosphate reabsorption is through changes of the amount of NaPi2a and NaPi2c located on the brush border membrane of proximal tubular cells. The regulation process is complex and involves three major hormonal factors, including PTH, calcitriol, and FGF23. Interactions among the three hormones make the process even more complicated. Among the three players, PTH and FGF23 are thought to play more important roles.

##### 1.2.2.3.4.1 PTH and PTHrP

PTH reduces renal phosphate reabsorption, causing an increase in the excretion of the mineral [2]. When PTH is missing, renal excretion of phosphate is highly reduced. A study conducted in the 1970s showed that parathyroidectomized starlings developed significant hyperphosphatemia and decreased clearances of phosphate [98]. More recent studies also illustrated that *Pth* null animals suffered from renal phosphate retention [75]. It has been well established for decades that hypoparathyroidism – whether congenital (due to inactivating *Pth* mutations) or acquired (e.g. from thyroid/parathyroid surgery) – leads to hyperphosphatemia with elevated renal phosphate reabsorption [99]. When PTH is at excess levels, the body tends to excrete too much phosphate. Secondary hyperparathyroidism in vitamin D deficiency human patients was thought to be the cause of hyperphosphaturia [100].

Primary hyperparathyroidism, which is due to a tumor of one parathyroid gland or hyperplasia of all four parathyroid glands, could increase renal phosphate excretion [101]. In addition, PTH analog injections (a treatment for osteoporosis) and PTH infusion (a diagnostic test for pseudohypoparathyroidism) can also lead to hyperphosphaturia. Several studies showed that a

low phosphate diet could reduce renal phosphate excretion because PTH was suppressed due to the body not being able to get a sufficient amount of phosphate [102].

PTHrP and PTH have N-terminal homology that enables the two hormones to act on PTH1R to reduce renal phosphate reabsorption. It should be noted that PTHrP is normally undetectable in the circulation, suggesting it is unlikely to play a role in normal renal phosphate excretion.

However, during lactation PTHrP levels in the blood are increased – a possible response in order to excrete excess phosphate through the kidneys because serum phosphate is highly elevated during lactation (as a result of elevated bone resorption) [103]. It should also be mentioned that during lactation PTH is normally at low levels, indicating the stimulatory effect on renal phosphate excretion is from PTHrP alone and not a combination of PTH and PTHrP. During fetal development, PTHrP is increased while PTH circulates at low levels.

Some rodent studies showed that when PTH receptors were stimulated, within minutes the NaPi2a protein abundance in the brush border of proximal tubular cells decreased; however, the mRNA levels remained unchanged [104, 105]. Decreases in the protein level of NaPi2c were shown to take several hours [106, 107]. These results once again suggest that NaPi2a plays a more important role in renal phosphate reabsorption than NaPi2c.

#### 1.2.2.3.4.2 FGF23

FGF23 reduces renal phosphate reabsorption through down regulation of NaPi2a and NaPi2c in the proximal tubules. Supporting evidence comes from prior studies in human patients who had tumor-induced osteomalacia (TIO), autosomal-dominant hypophosphatemic rickets (ADHR),

recessive hyperphosphatemic rickets (ARHR) and X-linked hypophosphatemic rickets (XLH). These patients had increased circulating levels of FGF23, phosphaturia and bone disorders [93]. Conversely, studies in tumor calcinosis (a disorder in which FGF23 is absent) patients showed that these patients usually developed hyperphosphatemia and had low phosphate excretion. Details of these human disorders are discussed in Section 1.2.3 titled “Phosphate Disorders in Human Adults”.

Many *in vitro* studies suggest that FGF23’s phosphaturic effect is through a decrease in NaPi2a and NaPi2c in the kidneys [18, 108]. For example, isolated proximal tubular cells from rodents with a stable *R176Q* mutation had significantly reduced NaPi2a on the brush border. An *R176Q* mutation makes the FGF23 protein resistant to cleavage [109]. Shimada’s group previously showed that *Fgf23* null mice developed hyperphosphatemia and increased renal phosphate reabsorption [110].

Interestingly, some studies suggest that FGF23’s co-receptor, Klotho, could directly exert negative effects on NaPi2a. For example, Hu’s group illustrated that addition of Klotho in cultured proximal tubular cells first reduced the NaPi2a activity and then decreased its protein levels [111]. Even more interestingly, the *Klotho* gene was shown to be expressed in the renal distal convoluted tubules whereas phosphate reabsorption occurs in the proximal tubules [112]. How Klotho migrates from the distal tubules and acts in the proximal tubules remains unknown. Some researchers claim Klotho to be a humoral phosphaturic factor.

#### 1.2.2.3.4.3 Calcitriol

First, whether calcitriol increases or decreases renal phosphate reabsorption remains controversial [113]. For example, thyroparathyroidectomized rats on chronic calcitriol treatment reportedly had reduced renal phosphate reabsorption [114]. In that study, the effect of PTH was excluded since the parathyroid glands were surgically removed. However, some other studies showed that mice with *Vdr* or *Cyp27b1* knocked out had the same levels of NaPi2a in proximal tubular cells as WT mice, suggesting calcitriol may not have any effect on renal phosphate reabsorption [33, 115].

Second, it is difficult to determine whether calcitriol regulates renal phosphate reabsorption in a direct or indirect manner, or both. As described above, calcitriol interacts with FGF23 and PTH, both of which are important regulators of renal phosphate reabsorption. Repeated injection of calcitriol was shown to increase serum FGF23 levels in a rat study [116]. FGF23 was shown to reduce renal production of calcitriol by suppressing *Cyp27b1* expression and by increasing *Cyp24a1* expression [110, 117].

### 1.2.3 Phosphate Disorders in Human Adults

Serum minerals are tightly maintained within a proper range. Likewise, circulating phosphate needs to be regulated. Derangement in serum phosphate, either excess or deficiency, can cause severe human disorders. Here the phosphate related disorders, including both FGF23 dependent and independent, are briefly discussed.

### 1.2.3.1 FGF23-Dependent Hypophosphatemic Disorders

Defective bone mineralization results in rickets in childhood and osteomalacia in adulthood.

There are many different causes of rickets and osteomalacia, but almost all share hypophosphatemia as a common pathophysiological denominator [58]. Phosphate deposition is the first step required for skeletal mineralization; thus, low serum phosphate leads to an undermineralized skeleton.

There are several kinds of hypophosphatemic rickets and osteomalacia associated with an excess FGF23 action, including XLH, TIO, and ADHR/ARHR. These disorders share not only relatively increased intact FGF23, but renal phosphate wasting, reduced renal calcitriol production, and low-to-normal serum calcitriol.

#### 1.2.3.1.1 XLH

XLH is caused by an inactivating mutation in a phosphate-regulating gene with homologies to endopeptidases on the X chromosome – called the *Phex* gene [118]. *Phex* is expressed in osteocytes, osteoblasts, and odontoblasts [119]. Mutations in *Phex* indirectly lead to an increase in FGF23 serum levels, which results in renal phosphate wasting, hypophosphatemia, reduced renal synthesis of calcitriol and low-to-normal serum levels of calcitriol.

The mechanisms whereby *Phex* regulates the *Fgf23* expression remain to be elucidated. Initial studies suggested that the Phex protein cleaved FGF23 [120]. However, subsequent studies failed to prove the hypothesis as they showed that FGF23 was not a direct substrate of Phex [121].

Liu's group showed that an inactivating mutation in *Phex* led to an increase in *Fgf23*

transcription, which suggests *Phex* is somehow involved in controlling the FGF23 biosynthesis [122].

Some recent studies indicate that *Phex* and dentin matrix acidic phosphoprotein 1 (DMP1) share a common pathway to regulate *Fgf23* expression. DMP1 belongs to a class of small integrin-binding ligand, N-linked glycoprotein (SIBLING) proteins – SIBLING is a family of non-collagenous proteins that are components of extracellular matrix of bone and dentin. *Dmp1* is expressed by osteoblasts and osteocytes, and an inactivating mutation in *Dmp1* can increase *Fgf23* expression in the bones. The main function of DMP1 is to regulate mineralization of the extracellular matrix. A proposed mechanism of how DMP1 and *Phex* regulate *Fgf23* expression is illustrated in **Figure 3**. In brief, the acidic serine-aspartate-rich motif (ASARM) at the C-terminal of DMP1 binds to *Phex* located on the membrane of osteocytes, which subsequently inhibits expression of *Fgf23*. When there is a mutation on *Phex*, a biosynthesis of FGF23 is uninhibited and becomes uncontrolled. Detailed intermediate mechanisms remain unclear.

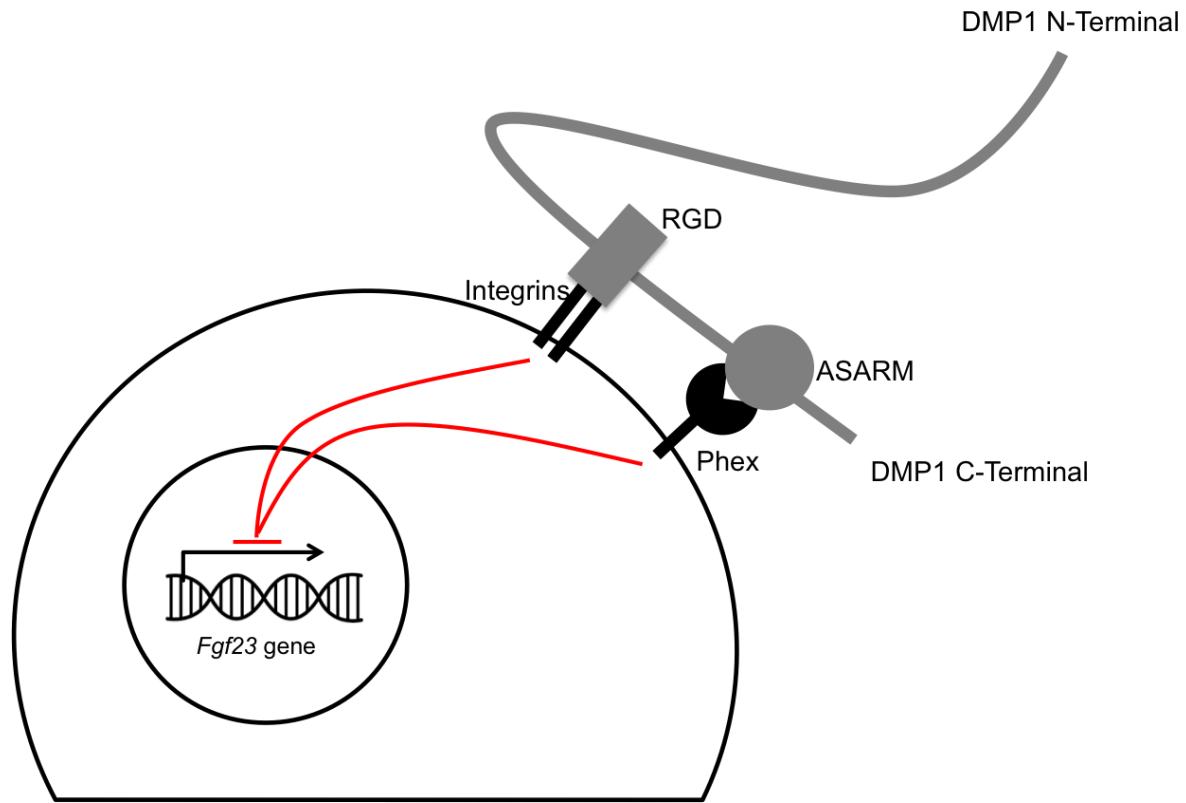


**Figure 3: A Proposed Mechanism of How DMP1 Regulate the *Fgf23* Expression.** The ASARM motif at the C-terminal of DMP1 binds to the PHEX protein located on the membrane of osteocytes to inhibit the expression of *Fgf23*. Detailed intermediate mechanisms remain unclear.

#### 1.2.3.1.2 TIO

The development of TIO is usually associated with slow-growing, benign, mucinous tumors that are often pathologically classified as phosphaturic mesenchymal tumors. These tumors secrete FGF23 which is considered a causative factor for TIO [123]. Many clinical cases showed that once the tumors were surgically removed, serum FGF23, serum phosphate and renal phosphate handling were then normalized – TIO was cured [58]. Recent human studies also showed that treatment with an antibody against FGF23 led to resolution of TIO [124].

#### 1.2.3.1.3 ADHR

ADHR is a rare genetic disorder caused by mutations on *Fgf23* [125]. Three missense mutations have been discovered to date, with each making the FGF23 protein resistant to cleavage – resulting in relative excess circulating FGF23, impaired mineralization of bone, rickets and/or osteomalacia, suppressed levels of calcitriol, renal phosphate wasting, and low serum phosphate. In clinical practice, calcitriol treatment – which is a common treatment for low serum phosphate – does not rescue hypophosphatemia in ADHR patients. Some studies showed that serum FGF23 levels in some ADHR patients with hypophosphatemia were not always high and might fluctuate [126].

#### 1.2.3.1.4 ARHR

ARHR is a rare genetic disorder that is often associated with increased serum FGF23, hypophosphatemia, low levels of serum calcitriol and hypophosphatemic rickets. Serum calcium, PTH and urinary calcium excretion in ARHR patients are normal [127, 128]. There are three types of ARHR, which are due to genetic mutations in *Dmp1* (Type 1), *Enpp1* (Type 2) and

*Fam20c* (Type 3), respectively [127, 128].

### 1.2.3.2 FGF23-Dependent Hyperphosphatemic Disorders

A common human disorder characterized by hyperphosphatemia is tumoral calcinosis (TC).

Familial TC is a rare autosomal recessive disease in which patients have ectopic calcifications, especially on blood vessels and joints [129, 130]. Familial TC patients also develop

hyperphosphatemia due to increased renal phosphate reabsorption and elevated serum calcitriol

levels [130]. The development of familial TC is mainly caused by a disruption in the FGF23

signaling pathway due to gene mutations – several responsible genes have been identified to

date, including *Galnt3*, *Fgf23*, and *Klotho* [131-133]. *Galnt3* encodes an enzyme involved in the

glycosylation of FGF23 – mutations on *Galnt3* result in higher sensitivity of FGF23 to cleavage

before it can exit the cell of origin. Therefore, *Galnt3* mutations can cause low serum intact

FGF23 levels – which should have a similar phenotype as inactivating *Fgf23* mutations [58].

A KO mouse model – *Fgf23* null – has been created to mimic inactivating *Fgf23* mutations in

humans. Those *Fgf23* null mice exhibit growth retardation, hyperphosphatemia, increased

calcium and calcitriol, and impaired bone mineralization and long bone growth in adulthood.

*Klotho* gene mutations result in functional loss of the FGF23 signaling pathway. However,

different from *Galnt3* and *Fgf23* mutations, *Klotho* mutations have high levels of serum FGF23,

which is regarded as a compensatory response to hyperphosphatemia.

### 1.2.3.3 FGF23-Independent Phosphate Disorders

Hereditary hypophosphatemic rickets with hypercalciuria (HHRH) is a rare autosomal recessive

disorder caused by mutations in *NaPi2c* [134]. HHRH patients normally develop urinary

phosphate wasting, hypophosphatemic rickets and appropriately elevated calcitriol. The elevated calcitriol further results in hypercalciuria due to enhanced intestinal calcium absorption and reduced PTH-dependent renal calcium reabsorption that can cause kidney stones and/or nephrocalcinosis.

Dent disease is an X-linked recessive chronic kidney disease that primarily affects males. It is mainly caused by mutations in either *Clcn5* (Type I, 60% of cases) or *Ocrl* (Type II, 15% of cases). The remaining 25% of Dent disease cases are due to unknown genetic mutations. The *Clcn5* and *Ocrl* genes are involved in the production of proteins needed for normal kidney function, particularly in the proximal tubules where nutrients, water, and other substances are reabsorbed. Mutations in the two genes impair the ability of the kidneys to reabsorb those substances. Dent disease patients usually develop proteinuria, hypercalciuria, nephrocalcinosis and kidney stones. Some patients with Dent disease may also develop bone diseases such as osteomalacia and hypophosphatemic rickets (a condition caused by impaired phosphate reabsorption and altered calcitriol metabolism in the kidneys).

Idiopathic infantile hypercalcemia (IIH) is a condition characterized by high levels of calcium in the blood. There are two types of IIH, which are caused by mutations in *Cyp24a1* (Type I) and *NaPi2a* (Type II), respectively. Mutations in either of the two genes result in too much calcitriol in the blood, causing hypercalcemia that further leads to hypercalciuria, kidney stones, vomiting, polyuria, dehydration, constipation, poor feeding, weight loss, and an inability to grow. Patients with Type II IIH can also develop hypophosphatemia, while phosphate levels are typically normal in Type I patients.

### 1.3 Phosphorus Homeostasis in Fetal Life

The preceding sections described regulation of phosphate homeostasis in young and adult stages. Phosphate metabolism during fetal development differs in several respects [135]. Normal human fetuses are hyperphosphatemic, with cord blood phosphate 0.5 mmol/L higher than maternal values; so are all mammals studied [135]. The fetal demand for phosphate is met by active transport across the placenta, which contributes to fetal hyperphosphatemia. Phosphate plays a significant role in fetal bone development. Renal and intestinal phosphate regulation during fetal life appears to be much less important than that in adulthood as a result of autophagia. That is, amniotic fluid (fetal urine) excreted by the fetal kidneys can be swallowed and absorbed by the intestines – it should be noted that intestinal absorption is a minor circuit and of little importance to fetal mineral homeostasis while this process is the primary and the only route of mineral delivery in the postnatal stage.

#### 1.3.1 Phosphate Handling by the Placenta

By the time of this dissertation, few studies had been conducted to investigate placental phosphate transport. In this section, the current findings were summarized.

##### 1.3.1.1 Phosphate Transport across the Placenta

Normally, two thirds of the phosphate stored in the human skeletons during fetal development is accreted within the third trimester [136]. Much evidence suggests that NaPi2b plays an important role in placental phosphate transport. For example, back in 1980s, Stule's group demonstrated that phosphate transport across the placenta was sodium ( $\text{Na}^+$ ) dependent in guinea pigs [137, 138]. The rodent placenta was demonstrated to express *Napi2a*, *NaPi2b*, and *NaPi2c*, with the

levels of *NaPi2a* and *NaPi2c* lower than those of *NaPi2b* [139, 140]. In addition, global *NaPi2b* KO is lethal during mid-gestation [21].

### 1.3.1.2 Regulation of Placental Phosphate Transport

Many studies have been conducted to investigate factors that regulate how calcium crosses the placenta. However, there were few studies about phosphate. Prior to my Ph.D. project (one of experiments was to measure the effect of FGF23 excess or absence on placental phosphate transport), researchers had examined effects of several other hormones, including PTHrP, PTH, and calcitriol.

#### 1.3.1.2.1 PTHrP

Multiple studies suggest that PTHrP is an important factor regulating placental calcium and magnesium transport. For example, Care's group demonstrated that injections of a mid-region portion of PTHrP increased the rate at which the calcium concentrations increased (as measured by  $^{45}\text{Ca}/^{51}\text{Cr}\text{-EDTA}$ ) in the umbilical veins – suggesting PTHrP stimulates placental calcium transport [141]. Conversely, the N-terminal section of PTHrP was shown to have no effect on the process [135]. Dr. Kovacs' group also independently showed that injections of mid-region but not N-terminal PTHrP could rescue a reduction in placental calcium transport in *Pthrp* null fetal mice [142]. Based on these observations, it should be logical to investigate whether mid-region PTHrP regulates placental phosphate transport; however, several studies in rats and ewes found that the mid-section of PTHrP could not stimulate phosphate to cross the placenta [143, 144].

#### 1.3.1.2.2 PTH

That the PTH receptor gene, *Pthr1*, is highly expressed by intraplacental yolk sacs and trophoblasts in rodents strongly suggests that PTH plays certain roles in placental mineral transport [145]. However, most studies in fetal lambs suggest that PTH has no effect on placental phosphate transport [146]. Abbas, Care, and Rodda's group independently showed that exogenous PTH did not change placental phosphate transport in thyroparathyroidectomized fetal sheep [141, 147, 148].

For placental calcium transport, results are mixed. The studies by Abbas, Care, and Rodda's groups in thyroparathyroidectomized fetal sheep showed PTH has no effect on this process, while Robinson's group illustrated that exogenous N-terminal (1-34) PTH modestly increased calcium transport in the placenta from decapitated rat fetuses that mimicked parathyroidectomy [149]. Dr. Kovacs' laboratory previously used *Pth* null and *Gcm2* null fetuses to study potential effects of PTH on placental calcium transport. *Gcm2* is a gene involved in the development of the parathyroid glands – knocking it out leads to the defective to absent parathyroid glands. *Gcm2* null fetuses have a similar phenotype as *Pth* nulls, except the former have low but detectable serum levels of PTH. The results showed that placental calcium transport in *Pth* null fetuses appeared normal [150]. In subsequent studies, *Pth* null fetuses treated *in utero* with PTH1–84 increased the accumulation rate of <sup>45</sup>Ca by 30%, indicating that exogenous PTH could stimulate placental calcium transport when endogenous PTH is absent. Different from *Pth* null fetuses, *Gcm2* nulls had a significant increase in the rate of placental calcium transport, which was attributed to increased expression of *Pth* mRNA within the *Gcm2* null placenta [150]. It is noteworthy that *Pthrp* null fetuses have decreased placental calcium transport despite a 3-fold

increase in PTH – therefore, PTH cannot make up for loss of PTHrP.

To sum up, current available data suggest that PTH has no effect on placental phosphate transfer but that PTH may have a modest effect to stimulate placental calcium transport.

#### 1.3.1.2.3 Calcitriol

Few studies directly examined whether calcitriol can regulate phosphate transport across the placenta. One group used an indirect method to measure the impact of calcitriol on this process in pregnant ewes. In this study, a single infusion of phosphorus isotope ( $^{32}\text{P}$ ) was injected into pregnant ewes that were later treated with either pharmacological doses of calcitriol or diluent (control) for one week. One week later, the amount of  $^{32}\text{P}$  in fetal ewes from the mothers treated with calcitriol was higher than that in fetal ewes from control mothers [151]. Placental calcium transport was also measured, showing similar results as phosphate. The same group conducted similar experiments in pregnant guinea pigs and obtained similar results – fetuses of the calcitriol-treated mothers had increased  $^{32}\text{P}$  and  $^{45}\text{Ca}$  compared to those of the control mothers [152].

The results above appear to suggest that maternal calcitriol can increase the rate of placental phosphate transport. However, it should be noted that their experimental approaches were too indirect because external phosphate injection on pregnant mothers could increase phosphate availability to fetuses independent of calcitriol. In addition, just because pharmacological doses of calcitriol could increase the rate of placental phosphate transfer does not mean physiological doses would do the same. One study in Dr. Kovacs' group demonstrated that *Vdr* null mouse

fetuses had no deficit in placental phosphate transport (unpublished data). These confounding results make the theory that calcitriol could regulate placental phosphate transport inconclusive.

#### 1.3.1.2.4 FGF23

Prior to my Ph.D. program few studies were carried out to investigate the role of FGF23 in placental phosphate transport. One study in Dr. Kovacs' laboratory demonstrated that *Fgf23* null fetuses had a similar rate of placental phosphate transport as WT fetuses, suggesting FGF23 plays no role in this process [139]. In my present study, I investigated if excess FGF23 in *Phex* null fetuses would change the rate of placental phosphate transport. Please refer to the results section of this dissertation.

#### 1.3.1.3 Summary of Key Points

Active transport of phosphate across the placenta is required to meet fetal requirements for minerals; however, the mechanisms are not well established. The mid-section of PTHrP seems to be able to increase placental transport for calcium but not for phosphate. PTH and calcitriol were tested in rats and lambs – no solid conclusions have been reached as to whether the two hormones can regulate placental phosphate transport. FGF23 seems to have no effect in this process.

### 1.3.2 Phosphate in Fetal Bone Development

#### 1.3.2.1 Overview of Fetal Bone Development

There are two essential mechanisms involved in fetal bone development: intramembranous and

endochondral. Intramembranous bone formation involves deposits of mesenchymal cells in places where the axial and appendicular skeletons will form. Those mesenchymal cells will differentiate directly into osteoblasts that then form the intramembranous bones.

Most of the fetal skeleton forms through endochondral bone formation, in which mesenchymal progenitor cells initially differentiate into proliferating chondroblasts and chondrocytes, forming a proliferating zone (**Figure 4**). Cells located on the end of the proliferating zone secrete PTHrP and other signals to delay chondrocyte differentiation. As the distance increases from the zone of proliferating chondrocytes, older chondrocytes no longer receive the signals, so they start differentiating, forming a differentiation zone. After differentiation is complete, those differentiated chondrocytes become hypertrophic and a hypertrophic zone is then formed. Eventually hypertrophic chondrocytes undergo apoptosis and the dead cells and matrix are removed by chondroclasts, after which new blood vessels form and osteoblasts begin to lay down primary spongiosa. Interestingly, some studies suggest that hypertrophic chondrocytes could become osteoblasts and osteocytes in fetal and postnatal endochondral bone formation [153]. Endochondral bone formation occurs at the primary ossification centers during fetal bone development. It is not until the primary ossification centers have formed that the skeletons begin to accrete substantial minerals. Most secondary ossification centers develop after birth.

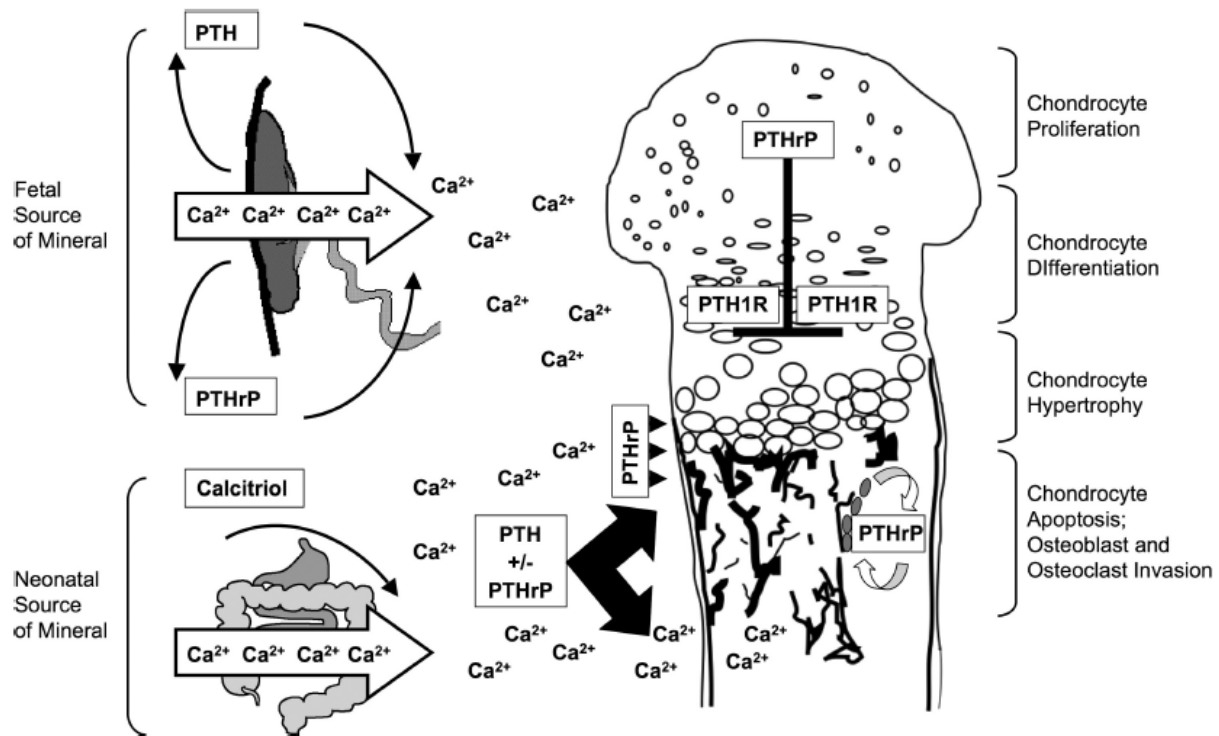


**Figure 4: Endochondral Bone Formation.** Mesenchymal progenitor cells initially differentiate into proliferating chondroblasts and chondrocytes (the proliferating zone). The cells located on the end of the proliferating zone secrete PTHrP and other signals to prevent chondrocytes from differentiation. As the distance increases from the zone of proliferating chondrocytes, older chondrocytes no longer receive the signals, so they start differentiating (the differentiation zone). After the process of differentiation is complete, these chondrocytes become hypertrophic (the hypertrophic zone). Eventually hypertrophic chondrocytes undergo apoptosis and the dead cells and matrix are removed by chondroclasts, after which new blood vessels form and osteoblasts begin to lay down. (from [135] with permission from Elsevier)

### 1.3.2.2 Regulation of Phosphate in Fetal Bone Development

Phosphate is important in endochondral bone formation in fetuses – phosphate stimulates apoptosis of hypertrophic chondrocytes [154, 155] and it is deposited into osteoid before forming hydroxyapatite with calcium [156, 157]. Therefore, serum phosphate is an important factor in regulating fetal bone formation and mineralization. Studies in rodents, lambs, pigs, calves and foals suggest that serum phosphate is typically higher in fetuses than in pregnant mothers, which is critical to maintain the healthy bone formation in fetuses [135]. In fetuses with hypophosphatemia, apoptosis of differentiated hypertrophic chondrocytes is impaired, leading to an expanded hypertrophic chondrocyte layer of the growth plate, as well as reduced mineral deposits in the bones [154, 155].

#### 1.3.2.2.1 PTH

Studies in fetal sheep suggest that PTH is necessary for normal fetal bone development because previous studies in fetal lambs showed that surgical removal of the parathyroids resulted in undermineralized skeletons with increased bone volume, trabecular thickness and osteoid [158]. Compared to studies in fetal lambs, studies in fetal rats indicate that PTH is not required since fetal decapitation that mimics thyroparathyroidectomy had little impact on endochondral bone formation [159].

Studies utilizing various genetic KO mouse models have also been carried out to assess potential roles of PTH in fetal skeletal development. Knocking out *Hoxa3* (a gene involved in the development of the parathyroid glands) causes absence of the parathyroid glands. Previous studies in Dr. Kovacs' laboratory showed that *Hoxa3* null fetuses had the normal long bones and

growth plate development, but their skeletons were significantly undermineralized [160]. Specifically, the total body ash weight, the calcium content and the magnesium content in *Hoxa3* nulls were reduced by approximately 10%, 20% and 10%, respectively. As to chondrocyte and osteoblast-specific genes, they were normally expressed. In *Pth* null fetuses, the skeletons were also undermineralized. However, unlike *Hoxa3* nulls, *Pth* nulls showed slightly shortened long bones, abnormally formed skulls, smaller vertebral bodies, and shorter metacarpal and metatarsal bones [161]. In addition, the long bones of *Pth* nulls had an enlarged hypertrophic zone, increased cortical thickness, and decreased osteoblast number. As to osteoblast-specific genes, their expression was reduced in *Pth* nulls.

A comparison between the phenotypes of *Pth* nulls and *Hoxa3* nulls leads to a question – why a loss of PTH cause a bone phenotype which a loss of the parathyroid glands does not possess? Different genetic backgrounds could be an answer because *Hoxa3* nulls in the study were generated in a Black Swiss background, while *Pth* nulls in C57BL/6 that is known to have lower levels of blood calcium compared to Black Swiss [162]. To resolve the puzzle, *Pth* nulls were re-examined in a Black Swiss background in Dr. Kovacs' laboratory. The results showed that *Pth* null fetuses had normal skeletal development, with a modestly reduced mineral content that was not as severe as in *Hoxa3* nulls [142, 160]. The results indicate that a loss of PTH would cause a defective bone phenotype only in a C57BL/6 background, which is likely due to lower serum calcium in C57BL/6 mice than Black Swiss ones [163-166]. As to the osteoblast-specific genes that were reduced in *Pth* nulls with a C57BL/6 background, their expression was not altered in *Pth* nulls with a Black Swiss background.

#### 1.3.2.2.2 PTHrP

During fetal bone development, PTHrP is synthesized by chondrocytes in the proliferating zone. PTHrP's N-terminal receptor, PTH1R, is located on the surface of chondrocytes within the pre-hypertrophic zone. Acting on the pre-hypertrophic chondrocytes, PTHrP delays their differentiation from proliferating to hypertrophic chondrocytes. That is, without PTHrP chondrocyte hypertrophy and the primary bone formation would occur prematurely, causing chondrodysplasia with shortened limbs [146, 167, 168]. Conversely, excess PTHrP during fetal bone development can result in the under-mineralized skeletons at birth (almost entirely cartilaginous) because endochondral bone development is so delayed [169, 170].

Previous animal studies showed that rodent *Pthrp* null fetuses developed hypocalcemia, hyperphosphatemia, and reduced placental calcium transport. Those null fetuses were originally expected to have reduced skeletal mineral content; however, they displayed normal skeletal ash weight and normal content of calcium and phosphate due to abnormally accelerated mineralization [160, 162]. In addition, not only the bones *in utero* were prematurely mineralized in *Pthrp* null fetuses, but some parts of their skeletons that normally remain cartilaginous – such as the sternal portions of the ribs – became the bones before birth. The expression of osteoblast-specific genes (collagen I, collagenase-3, osteocalcin and osteopontin) was normal to increased in *Pthrp* nulls. These results above confirm that PTHrP plays an important role in controlling bone mineralization (including phosphate) and growth plate development in fetuses.

#### 1.3.2.2.3 Combined Actions of PTH and PTHrP

PTH and PTHrP share the same receptor, PTHR1. Knocking out *Pthr1* causes characteristics

similar as combined phenotypes of PTH and PTHrP deficiencies. *Pthr1* null fetuses have chondrodysplasia plus under-mineralization[171]. *Hoxa3/Pthrp* double KO fetuses have neither PTH nor PTHrP. They have a small body size, severe chondrodysplasia, and under-mineralized skeletons [160]. This model is essentially a sum of the phenotypes of *Hoxa3* nulls and *Pthrp* nulls. *Pthrp/Pth* double KO fetuses show chondrodysplasia (observed in *Pthrp* nulls) combined with the under-mineralized bones (demonstrated in *Pth* nulls) [161].

In summary, prior mouse studies demonstrated that *Pth* nulls and *Hoxa3* nulls developed the under-mineralized bones; *Pthrp* nulls had normal skeletal mineral content but chondrodysplasia with shortened limbs; and *Pthr1* nulls had a combined phenotypes of *Pth* nulls and *Pthrp* nulls. These results suggest that during fetal development PTHrP functions locally in the process of endochondral bone development to maintain the cartilaginous proliferating zone and delay their terminal differentiation, whereas PTH stimulates normal skeletal mineralization via maintaining serum mineral levels and acting on osteoblasts.

#### 1.3.2.2.4 Calcitriol

Various animal studies have suggested calcitriol is not required for mineralization of endochondral ossification during fetal development. For example, fetal rats with vitamin D deficiency and fetal mice without *Vdr* had normal ash weight and skeletal mineral content [172-175]. Specifically, the skeletons in *Vdr* null fetuses displayed no abnormalities – the length and morphology of the long bones in the appendicular skeleton were normal. *Vdr* null fetuses and their WT siblings had similar growth plates (length and morphology). As to expression of skeletal development-related genes [types I, II, and X collagens, H4 histone, cartilage matrix

protein, osteoblast markers (osteopontin, osteocalcin, interstitial collagenase, and alkaline phosphatase), osteoclast marker (92-kDa gelatinase or type IV collagenase or matrix metalloproteinase-9)], no differences were detected in *Vdr* nulls.

It should be noted that *Vdr* null fetuses normally have high levels of calcitriol, which could potentially act on other receptors (not VDR) to regulate skeletal development and mineralization in fetuses. Recent studies using *Cyp27b1* KO mouse model in Dr. Kovacs' laboratory eliminated such possibility [176]. The results showed that *Cyp27b1* null fetuses derived from *Cyp27b1* null dams had normal skeletal mineral content and morphology relative to WT fetuses, which confirms that calcitriol is unimportant in regulating bone development and mineralization in fetuses.

#### 1.3.2.2.5 FGF23

The role of FGF23 in regulating phosphate during fetal bone development had not been studied before my Ph.D. project was carried out. Concurrent with my Ph.D. project, one student in Dr. Kovacs' laboratory carried out a study in *Fgf23* null fetuses, which demonstrated that those nulls had normal mineral content (phosphate, calcium and magnesium) in their body ash prior to birth. In addition, other skeletal parameters were also normal in *Fgf23* null fetuses. Specifically, *Fgf23* null tibias showed normal endochondral development with no alteration in the lengths or cellular morphology of the cartilaginous or bony compartments, as well as a normal distribution of minerals [139]. In my present study, I investigated if excess FGF23 in *Phex* null fetuses would alter phosphate deposit during bone development, as well as other skeletal parameters. Please refer to the results section of this dissertation.

#### 1.3.2.2.6 Other Factors

Animal and human studies indirectly suggest that sex hormones, including testosterone and estrogen, are not critical for fetal skeletal mineralization. Rodents and humans that have mutations in estrogen receptors or aromatase enzyme have normal bone morphology at birth and do not develop mineralization defects until older ages [177]. Calcitonin, which is encoded by the *Ctcgrp* gene, acts to lower serum calcium by preventing bone reabsorption. But calcitonin seems to be unimportant for fetal bone development and mineralization, as *Ctcgrp* null fetuses have normal endochondral skeletons (morphology, gene expression, and calcium and phosphate content) before birth [178].

#### 1.3.2.3 Summary of Key Points

Phosphate plays an important role in fetal skeletal development and mineralization. Phosphate stimulates the apoptosis in hypertrophic chondrocytes during endochondral bone formation. When hypophosphatemia develops in fetuses, the apoptosis of differentiated hypertrophic chondrocytes is inhibited, leading to an expanded hypertrophic chondrocyte layer of growth plates and reduced mineral deposits in the bones. PTH and PTHrP are arguably the two most important hormones regulating fetal bone development and mineralization. PTHrP functions locally in the process of endochondral bone development to maintain the cartilaginous proliferating zone, whereas PTH stimulates normal skeletal mineralization via maintaining serum mineral levels and acting on osteoblasts. FGF23 does not seem to regulate phosphate during fetal bone development.

### 1.3.3 Phosphate Handling by the Fetal Kidneys

Although the kidneys play an essential role in maintaining mineral homeostasis in adults, their roles may be less important in fetuses for three reasons: first, the placenta is the main organ that supplies minerals to fetuses [179]; second, minerals (phosphate and calcium) that are excreted by the kidneys into amniotic fluid can be swallowed and absorbed (autophagia), such that renal mineral excretion does not cause a permanent loss of mineral content [180]; and third, renal blood flow and glomerular filtration rates are low in fetuses until after birth, which contributes to relative inactivity of the kidneys during fetal development [181, 182].

Whether the fetal kidneys play a role in mineral regulation remains inconclusive. Moore's group and Ross' group respectively conducted related experiments in fetal lambs – they surgically removed the bilateral kidneys, leading to hyperphosphatemia, hypocalcemia, an increase in PTH, and a 60% calcitriol decrease [183, 184]. A control procedure was conducted on additional fetal lambs by bilateral ureteral sectioning to permit fetal urine to drain into peritoneal cavity while presumably preserving normal renal function – the control procedure had no effect on fetal minerals and related hormones [183]. These observations led the researchers to believe it was the decrease in renal calcitriol production that resulted in the fetal mineral changes, but not the loss of the fetal kidneys. Moritz's group nephrectomized five fetal lambs at 100 days of gestation (gestation in sheep normally varies from 142 to 152 days) and compared them to normal fetuses (control). The nephrectomized lambs displayed increased serum phosphate (two times as high as that in control), no changes in serum calcium, and a non-significant decrease in calcium excretion into amniotic fluid [185]. Unfortunately, calcitriol and PTH were not measured. Similar experiments have also been performed on fetal rats, with the results showing the same trend for

serum and amniotic fluid calcium but no phosphate changes[186].

In summary, the kidneys play relatively minor roles in regulating fetal phosphate homeostasis because the placenta is the main organ of mineral delivery, fetuses can swallow amniotic fluid, and renal blood flow and glomerular filtration rate are low in fetuses. Several studies in fetal lambs suggest that the fetal kidneys may adjust serum phosphate through the renal production of calcitriol. However, more studies are needed.

### 1.3.3.1 Regulation of Phosphate in the Fetal Kidneys

#### 1.3.3.1.1 PTH and PTHrP

In fetuses, PTH appears to have some role in phosphate excretion. For example, thyroparathyroidectomized fetal lambs had hyperphosphatemia and reduced renal phosphate excretion. Hypocalcemia and increased calcium excretion were also noticed in them [187]. However, one previous study showed that a pharmacological dose of N-terminal fragments of PTH or PTHrP did not change serum or urine phosphate concentrations in normal fetal lambs [187, 188]. Fetal mice with mutations in *Hoxa3*, *Gcm2*, *Pth1r*, or *Pth* have hyperphosphatemia, which is likely contributed to reduced phosphate excretion [135, 150, 189].

#### 1.3.3.1.2 Calcitriol

Functions of calcitriol in fetal phosphate regulation through the kidneys are inconclusive. One study in fetal lambs, which is discussed above in Section 1.3.3 titled “Phosphate Handling by the Fetal Kidneys,” concluded that a loss of renal production of calcitriol caused hypocalcemia and

hyperphosphatemia – indicating renal phosphate excretion might be reduced without calcitriol [183]. Unlike nephrectomized fetal lambs, nephrectomized fetal rats had no changes in serum phosphate – indicating calcitriol might not be important in renal phosphate excretion [186]. In *Vdr* null fetuses (mice), serum ionized and amniotic fluid phosphate concentrations were not changed compared to WT, which also indicates kidney-produced calcitriol is relatively unimportant in renal phosphate regulation in mouse fetuses [175]. *Cyp27b1* null fetuses had a similar phenotype – they had normal serum and amniotic fluid calcium and phosphate concentrations [190]. Why do rodent fetuses and fetal lambs show an opposite response to calcitriol deficiency? It is possibly because circulating calcitriol levels are relatively low in fetal rodents but high in fetal lambs [135].

#### 1.3.3.1.3 FGF23

Given that FGF23 regulates phosphate homeostasis in adults by suppressing renal phosphate reabsorption, FGF23 was initially expected to have an important role in fetuses. By the time when I started my Ph.D. project, there had been no relevant published data. One experiment (concurrent with my Ph.D. project) conducted in Dr. Kovacs' Laboratory showed that phosphate and calcium in fetal amniotic fluid, which represents fetal urine, were not different between *Fgf23* null and WT fetuses two days prior to birth. Renal expression of *NaPi2a* and *NaPi2c* was not altered in those nulls either. These results suggest that FGF23 plays no role in regulating renal phosphate during the fetal stage. In my Ph.D. project, I studied amniotic fluid phosphate and calcium, as well as renal expression of *NaPi2a* and *NaPi2c*, in *Phex* null mouse fetuses which have excess FGF23. Please refer to the results section of this dissertation.

### 1.3.3.2 Summary of Key Points

The kidneys appear to be less important during fetal development because amniotic fluid (largely consisting of fetal urine) can be recycled through a process called autophagia. The fetal kidneys are a likely source of low levels of calcitriol in the fetal circulation, and are capable of excreting and reabsorbing phosphate. Whether the fetal kidneys contribute importantly to fetal phosphate homeostasis is still uncertain. Studies have been conducted to examine whether PTH, PTHrP and calcitriol can regulate renal phosphate regulation in fetuses, with no solid conclusions having been reached. FGF23's role was examined in this Ph.D. project, and the results were to be presented below in the results section.

## 1.4 Phosphorus Homeostasis during the Neonatal Stage

### 1.4.1 Serum Phosphate Changes during a Transition from Fetuses to Neonates

After birth, a loss of the placenta forces a rapid change in mineral homeostasis because the source of minerals is lost and must be switched to intestinal absorption and renal reabsorption as quickly as possible.

In rodents, serum phosphate decreases significantly in the first 2 – 4 hours after birth, then sharply increases by 6 hours, and again drops over the following days to normal neonatal levels [191]. The initial decline is largely due to a loss of the placental phosphate supply while uptake into bone continues; the subsequent rise corresponds to a transient hypoparathyroidism which is physiologically normal in newborns [135]. Why is there a transient hypoparathyroidism? In rodent fetuses, PTH circulates at lower levels because it is suppressed by hypercalcemia. After fetuses are delivered, fetal calcium falls immediately, which stimulates PTH release – but the

whole process to produce a sufficient amount of PTH takes time. Interestingly, some scant data from WT mice showed that FGF23 spiked to 10-fold higher than adult values within 12 hours after birth, concurrent with the transient increase in serum phosphate [192]. Contrary to rodents, neonatal lambs have elevated serum phosphate for more than one week [193]. Human babies undergo a similar transient hypoparathyroidism, with serum phosphate increasing over the first 24 – 48 hours after delivery [194-196]. Subsequently, serum PTH rises and serum phosphate declines to adult levels [135].

#### 1.4.2 Intestinal Phosphate Absorption in Neonates

Very few studies have been conducted to investigate intestinal phosphate absorption in neonates. However, how calcium is intestinally absorbed may give some insights as to how phosphate is absorbed because both minerals are related.

In rodent neonates, intestinal calcium absorption occurs mainly in a passive manner and independent of calcitriol [197-199]. High levels of lactose contained in breast milk increase passive transport [135]. As days pass, intestinal epithelial cells start expressing necessary elements that drive active calcium absorption. These elements include VDR, calbindin-D<sub>9k</sub>, and transient receptor potential cation channel subfamily V member 6 (TRPV6).

Studies have been conducted to investigate whether a disruption in the calcitriol pathway would cause a disturbance in intestinal calcium absorption in neonates. Experiments conducted by Halloran's group showed that plasma calcium at 3 days postpartum was fairly normal in vitamin D-deficiency rat pups; however, plasma calcium decreased during the suckling period [199].

Several mouse models with a disrupted vitamin D pathway were studied, which included four different types of *Vdr* null neonates [200-203] and two different types of *Cyp27b1* null neonates [204, 205]. During the lactation period (first 2-3 weeks after birth), serum calcium and phosphate in *Vdr* nulls and *Cyp27b1* nulls were normal. When it approached weaning, the null pups started to develop hypocalcemia, hypophosphatemia, secondary hyperparathyroidism and signs of rickets. When *Vdr* null and *Cyp27b1* null pups were treated with a rescue diet made of increased content of calcium, phosphate and lactose, those pups could maintain normal serum calcium and phosphate and normal skeletal morphology and mineral content. The results described above suggest that passive calcium absorption (which may be stimulated by calcitriol to a small extent) progressively declines during the first 3 weeks after birth in rodent neonates, after which calcitriol-dependent active transport becomes the dominant way for calcium to be absorbed[135].

In terms of phosphate, there is no specific data. It is expected that intestinal phosphate absorption in neonates follow a similar pattern as to what happens with calcium absorption, since calcitriol regulates both calcium and phosphate.

In human neonates, calcium absorption is enhanced by lactose in breast milk, which is similar to rodent neonates [206, 207]. Intestinal absorption and retention of calcium increase with both postnatal age [135, 208, 209]. These findings suggest that intestinal absorption in human neonates develops toward an active, calcitriol-dependent process – which is what is seen in older children and adults. Much evidence suggested that the intestines in premature babies are unresponsive to calcitriol. A small study in preterm babies compared human milk, human milk plus vitamin D, and human milk plus vitamin D and phosphorus, and found that only the group

receiving phosphorus supplementation had a significant increase in calcium retention, suggesting there is a lack of effect of vitamin D/calcitriol to increase calcium absorption and retention in the preterm intestines [210]. An interventional study found that preterm infants showed no calcemic response to short courses of supraphysiological doses of calcitriol, also suggesting the preterm intestines are refractory to calcitriol [211]. It should be noted that these data could infer that the intestines in human neonates go through progressive up-regulation of *Vdr* expression. However, data of longitudinal changes in *Vdr* expression has not been available. Similarly, it is unclear when the intestines in neonates change from passive to active absorption. One study demonstrated the responsiveness to calcitriol at four weeks of age, which may indicate that active absorption should have occurred by that age [212]. Some human data from premature neonates highlights potential impacts of intestinal absorption on skeletal development. Studies demonstrated that prematurely born babies required more minerals to support bone development than what the intestines can possibly absorb. Thus, parenteral administration of minerals is needed to prevent premature rickets [213-215].

#### 1.4.2.1 Regulators of Intestinal Phosphate Absorption in Neonates

##### 1.4.2.1.1 Calcitriol

In adults, calcitriol is required to facilitate active phosphate transport across the intestines. Due to a lack of specific data in neonates, it is expected that calcitriol may not be important until after weaning when the active phase of intestinal phosphate absorption is more evident. This is partially supported by the fact that serum calcitriol does not elevate until the 3<sup>rd</sup> week after birth when lactation is almost over – calcitriol is barely synthesized before weaning [191, 216]. In newborn lambs, calcitriol is not produced until up to 11 days after birth, even in response to PTH

administration [191, 217].

#### 1.4.2.1.2 FGF23

Scant data is available regarding the role of FGF23 in intestinal mineral absorption in neonates. Studies have shown *Fgf23* null neonates (mice) developed hyperphosphatemia and increased calcitriol at 10 days after birth, as well as hypercalcemia by 2 weeks – these data suggests that FGF23 could suppress phosphate and calcium absorption in the intestines; however, whether the effects are mediated through calcitriol is still unknown as there have been no studies investigating if FGF23 could directly regulate *NaPi2b* in the neonatal intestines [110].

#### 1.4.2.1.3 PTH and PTHrP

PTH and PTHrP could affect intestinal phosphate absorption in neonates via changing renal calcitriol synthesis. Studies of the PTH1R signaling pathway, comparison of crystal structures of PTH and PTHrP, and clinical studies suggest that PTH is a more potent simulator of the calcitriol synthesis than PTHrP in humans and rodents [218-221]. However, the kidneys of neonatal lambs have a resistance to PTH during the first 11 days after birth [217]. Whether PTHrP is directly involved in the renal calcitriol synthesis in neonates is unknown. PTHrP disappears from the circulation at some time point postnatally, which suggests that PTHrP is unlikely to be involved in renal production of calcitriol. The parathyroids are important for mineral homeostasis in neonates since removal of the organ increases serum phosphate and decreases calcium. However, whether these effects are through intestinal phosphate absorption is unknown.

#### 1.4.2.1.4 Phosphate Content in Food

Mineral content of food sources affect mineral intestinal absorption. Over 90% of the phosphate content in breast milk is absorbed through the intestines. More importantly, studies showed that neonates consuming formula with a higher phosphate content had serum phosphate doubled compared to ones consuming breast milk [135]. This is reasonable because phosphate absorption is proportional to intake when it is initially absorbed via a passive transport mechanism.

#### 1.4.2.2 Summary of Key Points

Calcium studies suggest that intestinal mineral absorption (including phosphate) is through passive transport during the stage of breast feeding, after which minerals are actively transported across the intestines in a calcitriol-dependent manner. PTH is also an important hormone in this process as PTH is a potent stimulator of renal calcitriol production. Based on these conclusions from calcium studies in neonates, it is speculated that intestinal phosphate absorption follows a similar mechanism as calcium, and calcitriol and PTH are two critical hormones regulating the process after breast feeding.

#### 1.4.3 Skeletal Phosphate Metabolism in Neonates

It is known that skeletal development in neonates highly depends on the efficiency of intestinal mineral absorption. Neonatal rodents normally do not develop any skeletal abnormality before weaning because minerals are passively absorbed during this stage. After weaning, intestinal mineral absorption becomes a calcitriol-dependent, active process, in which the neonatal skeleton will develop deficits in mineral content if there are conditions of hypoparathyroidism, vitamin D deficiency, and/or a loss of VDR. As to the skeletal phosphate content, it is highly

dependent on the intestinal supply after weaning, as well as, the ability to reabsorb phosphate in the kidneys. Thus, any phosphate deficiency in the diet, inability to absorb sufficient phosphate from the diet, or renal phosphate wasting will cause neonatal rickets. It also should be noted that infants and neonates normally tend to have higher serum phosphate concentrations than adults, which is believed to be important to maintain healthy bone development. Factors that regulate intestinal phosphate absorption should have a significant impact on skeletal phosphate deposits in neonates.

#### 1.4.4 Renal Phosphate Excretion in Neonates

Renal regulation of phosphate in neonates needs further studies. Available data from rat studies showed that the neonatal kidneys started actively excreting or reabsorbing minerals within a few days after birth [222]. In addition, elements responsible for renal calcium reabsorption, such as TRPV6 and calbindin-D<sub>9k</sub>, showed a progressive expression increase, reaching maximum at the third week after birth [223]. Human data showed that renal phosphate excretion was low at birth and gradually increased with age [182, 224]. Longitudinal changes of NaPi2a and NaPi2c in the human neonatal kidneys have not been studied.

##### 1.4.4.1 Regulators of Renal Phosphate Excretion in Neonates

###### 1.4.4.1.1 PTH

PTH reduces renal phosphate reabsorption in adults. But whether PTH affects the process in neonates remains inconclusive. *In vitro* studies demonstrated that PTH treatment in renal cells from rodent neonates generated less cAMP (an important element in the PTH signaling pathway)

than in fetal renal cells, indicating PTH is of less importance in the neonatal kidneys [225].

Human data showed that there was an increasing trend in serum PTH after birth, which coincided with the elevation of renal phosphate excretion [182, 224]. Term and preterm infants also showed a developmental increase in the cAMP synthesis after PTH treatment, likely suggesting that PTH begins to suppress renal phosphate reabsorption during the neonatal stage in humans [226].

Some interesting data from studies in neonates with congenital hypoparathyroidism suggests that PTH may have a different effect on renal phosphate excretion between animals and humans. For example, animal pups with hypoparathyroidism had hypocalcemia, hyperphosphatemia, and impaired skeletal mineralization at birth; while human babies with hypoparathyroidism at birth did not develop hyperphosphatemia until later in childhood [135] [227-229].

#### 1.4.4.1.2 Calcitriol

Potential roles of calcitriol in renal phosphate excretion in neonates have not been studied specifically. Rat kidneys do not begin expressing *Vdr* or responding to calcitriol until the third week after birth, suggesting that calcitriol does not function at the kidneys until after weaning [222]. Other studies have suggested that a gradual increase in renal calcitriol production in neonates is likely to be due to an increasing responsiveness to PTH [225].

#### 1.4.4.1.3 FGF23

Until recently, very limited data have been available pertaining to the role of FGF23 in renal phosphate regulation in neonates. One mouse study demonstrated that reduced renal phosphate

excretion was present at 3 weeks after birth in *Fgf23* KO neonates – this timing was the earliest time point that had been studied until this project [81]. Those nulls also displayed hyperphosphatemia, increased calcitriol, and hypercalcemia. In *Phex* mutant neonates, serum phosphate surprisingly increased modestly from 2 hours to 10 hours after birth, and then dropped – causing hypophosphatemia at 24 hours after birth [192]. At the same time that hypophosphatemia developed, serum FGF23 and PTH in those *Phex* mutant neonates were elevated, and calcitriol was reduced. These results suggest that FGF23 starts playing a role in the neonatal kidneys within the first day after birth.

In humans, TC commonly presents during the first twenty years of life. In some cases, it has presented as early as 18 days after birth and as late as 65 years old [230-232]. XLH patients have been recognized to have hypophosphatemia during the first year after birth if there is family history that led to increased surveillance [233]. Without a family history, XLH with hypophosphatemia is often diagnosed at 2 or 3 years of age [234-236]. In one study involving four patients who were diagnosed early because of family history, all had hypophosphatemia between 2 and 6 weeks of age, one had reduced renal phosphate reabsorption at 9 days of age, and the rest did not have it until 6 months old [233].

#### 1.4.4.2 Summary of Key Points

The neonatal kidneys start actively excreting and reabsorbing phosphate within a few days after birth through their progressively increased responsiveness to PTH, calcitriol, and FGF23.

## 1.5 Summary of Animal Models

In this Ph.D. project, three main mouse models were applied, including *Phex* null model, *Fgf23* KO model, and *Klotho* KO model. Main phenotypes of each model were summarized below.

*Phex* null mice have naturally occurring mutations in the *Phex* gene located on Chromosome X, which leads to abnormally high serum levels of FGF23. Adult *Phex* nulls had impaired mineralization (rickets or osteomalacia), which occur as a consequence of excess renal phosphate excretion, reduced calcitriol and reduced intestinal phosphate absorption.

*Fgf23* null mice have mutations in the *Fgf23* gene located on chromosome 6, leading to loss of FGF23 in the blood. Adult *Fgf23* nulls develop hyperphosphatemia and extraskeletal calcifications, which occur as a result of impaired urine phosphorus excretion, increased calcitriol, and increased intestinal phosphorus absorption. Although PTH also lowers serum phosphate, it is unable to correct the hyperphosphatemia caused by absence of FGF23 in the null mice.

*Klotho* null mice have mutations in the *Klotho* gene located on chromosome 5. Adult *Klotho* nulls have a similar phenotype as *Fgf23* nulls except that the former has high levels of serum FGF23.

## 1.6 Overview of Ph.D. Project

In adults, FGF23 is a phosphate-regulating hormone produced largely by osteocytes and osteoblasts. It controls a supply of phosphate at a mineralizing surface of the bones through

actions on distal tissues. Within proximal renal tubules FGF23 down-regulates expression of *NaPi2a* and *NaPi2c*. FGF23 also inhibits renal expression of *Cyp27b1*, increases expression of *Cyp24a1*, and inhibits intestinal expression of *NaPi2b*. The combined effects of these actions lead to increased renal phosphate excretion and reduced active intestinal absorption of calcium and phosphate.

A loss of FGF23 causes hyperphosphatemia, extraskeletal calcifications, and early mortality, which occur as a result of impaired urine phosphate excretion, increased calcitriol, and increased intestinal phosphate absorption. Although PTH can also lower serum phosphate, PTH is unable to correct hyperphosphatemia caused by an absence of FGF23. Excess FGF23 leads to opposite phenotypes – hypophosphatemia with impaired mineralization (rickets or osteomalacia) and myopathy, which occur as a consequence of excess renal phosphate excretion, reduced calcitriol, normal-to-low PTH, and reduced intestinal phosphate absorption.

My Ph.D. project was to study potential effects of FGF23 on fetal phosphate regulation and skeletal development. In this project, I hypothesized that FGF23 could regulate fetal phosphate metabolism through actions on the placenta, kidneys, and skeletons. The whole project was divided into four aims. Each aim is briefly described below:

- Aim 1: To study effects of excess FGF23 on fetal phosphate metabolism and skeletal development by using the *Phex* null model;
- Aim 2: To study effects of a loss of *Klotho* on fetal phosphate metabolism and skeletal development by using the *Klotho* KO model;
- Aim 3: To study combined effects of PTH and FGF23 losses on fetal phosphate metabolism

and skeletal development by using the *Pth/Fgf23* double KO (DKO) model; and

- Aim 4: To determine effects of excess FGF23 and a loss FGF23 on neonatal phosphate metabolism by using the *Phex* null model and the *Fgf23* KO model, respectively. The *Klotho* KO model was also applied in this aim.

It should be noted that little had been known about the role of FGF23 in fetal and neonatal development by the time when this project was carried out. Concurrent with my studies, Dr. Samaraweera in Dr. Kovacs' laboratory measured effects of a loss of FGF23 on fetal phosphate regulation and skeletal development by utilizing *Fgf23* KO mouse model. Some of her results were cited in earlier subsections. Here I briefly summarized all of her results. In Dr. Samaraweera's project [139], *Fgf23* null fetuses were confirmed to have undetectable serum FGF23 on embryonic day (ED)18.5 compared to WT fetuses. *Fgf23* heterozygous (HET) dams had significantly higher serum FGF23 than fetuses of all genotypes. In adults, FGF23 inhibits the synthesis of calcitriol, so it was originally expected that a loss of FGF23 would lead to an increase in calcitriol in fetuses. However, serum calcitriol on ED 18.5 in *Fgf23* nulls was not changed. In terms of serum and plasma PTH, *Fgf23* null fetuses had numerically lower levels than WT. As to phosphorus and total calcium in serum and amniotic fluid, placental phosphate transport, and skeletal mineral content (phosphate, calcium and magnesium) and bone morphology, there were no significant differences in *Fgf23* nulls. Placental and renal expression of *Fgf23* and *Fgf23*-targeted genes (*Klotho*, *NaPi2a*, *NaPi2b*, *NaPi2c*, *Cyp27b1*, *Cyp24a1*, and *Fgfr1 – 4*) in *Fgf23* null fetuses on ED 18.5 was also studied by Dr. Samaraweera. The WT placenta showed a low level of *Fgf23* expression that was absent (no signal) in the null placenta. Those *Fgf23*-targeted genes were each expressed within the placenta, with *Klotho* and *NaPi2b* displaying the most

abundant expression. However, there were no significant differences between the WT and *Fgf23* null placenta in their expression. *Fgf23* was not expressed within the WT and null fetal kidneys whereas each of the *Fgf23*-targeted genes was well expressed. *Cyp24a1* expression was reduced 0.6-fold in the *Fgf23* null kidneys but there were no significant differences in the remaining target genes.

## 2 Materials and Methods

### 2.1.1 Mouse Models Used in My Ph.D. Project

All experiments were approved by Institutional Animal Care Committee of Memorial University of Newfoundland.

#### 2.1.1.1 *Phex* Null Model

*Phex* null mice (AKA *Hyp* mice) bear spontaneous mutations on the *Phex* gene that is located on the X chromosome. To date, five deletional mutations have been reported: *Phex*<sup>*Hyp*</sup>, *Gy*, *Phex*<sup>*Ska1*</sup>, *Phex*<sup>*Hyp-2J*</sup>, and *Phex*<sup>*Hyp-Duk*</sup> (**Figure 5**). The *Phex* model I used is based on the *Phex*<sup>*Hyp-2J*</sup> mutation. Adult *Phex* mutant mice develop excess FGF23, which causes hypophosphatemia, reduced renal phosphate reabsorption, low serum levels of calcitriol, reduced intestinal phosphate absorption and rickets or osteomalacia.



#### 2.1.1.2 *Fgf23* KO Model

The generation of *Fgf23* null mice was previously described [237]. In brief, the Exon 1-3 coding region of the *Fgf23* gene is replaced with the *lacZ* gene and the *neomycin (neo)* gene (**Figure 6**). Adult *Fgf23* null mice develop FGF23 deficiency, which leads to hyperphosphatemia, increased renal phosphorus reabsorption, increased serum levels of calcitriol, increased intestinal phosphorus absorption, skeletal abnormalities, extraskelatal calcifications and early mortality.

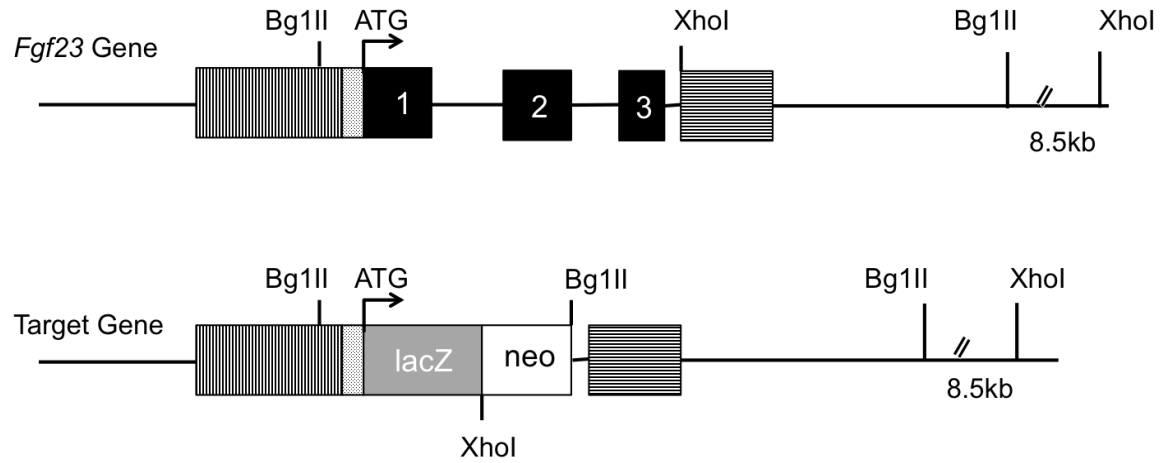


**Figure 6: The Generation of *Fgf23* Null Mice.** The Exon 1-3 coding region of the *Fgf23* gene is replaced with the *lacZ* gene and the *neomycin (neo)* gene.

### 2.1.1.3 *Klotho* KO Model

*Klotho* null mice were generated by an insertion of two unique plasmids, E50 and E70, which can trigger an 8-kb deletion of the *Klotho* gene, resulting in a functional loss of the gene [63]

(**Figure 7**). Adult *Klotho* null mice have a similar phenotype as *Fgf23* nulls –

hyperphosphatemia, increased renal phosphate reabsorption/excretion, high calcitriol, increased intestinal phosphorus absorption and skeletal abnormalities. Different from *Fgf23* nulls, *Klotho* nulls develop high serum levels of FGF23.

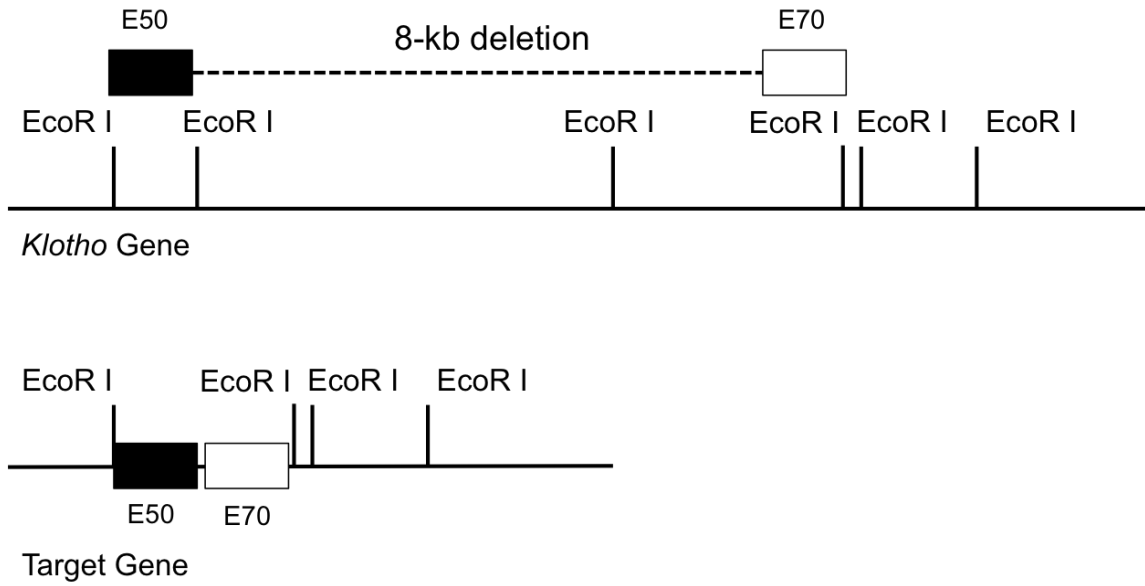


**Figure 7: The Generation of *Klotho* Null Mice.** An insertion of two unique plasmids, E50 and E70, triggers an 8-kb deletion of the *Klotho* gene, resulting in a functional loss of the gene.

#### 2.1.1.4 *Fgf23/Pth* Double KO Model

The *Fgf23/Pth* double KO mice were generated in Dr. Kovacs' Laboratory (**Figure 8**). In brief, *Fgf23* HET mice were mated with *Pth* HETs to obtain *Fgf23/Pth* double HETs ( $Fgf23^{+/-}/Pth^{+/-}$ ). The double HET mice were then mated with each other to generate WT ( $Fgf23^{+/+}/Pth^{+/+}$ ), double nulls ( $Fgf23^{-/-}/Pth^{-/-}$ ), *Pth* nulls ( $Fgf23^{+/+}/Pth^{-/-}$ ), *Fgf23* nulls ( $Fgf23^{-/-}/Pth^{+/+}$ ), as well as 5 other genotypes that weren't relevant to current project. The generation of the *Pth* KO model was previously described [161]. In brief, part of Exon 3 of the *Pth* gene is replaced by a *neo* gene via a homologous recombination with the pPNT vector (**Figure 9**).

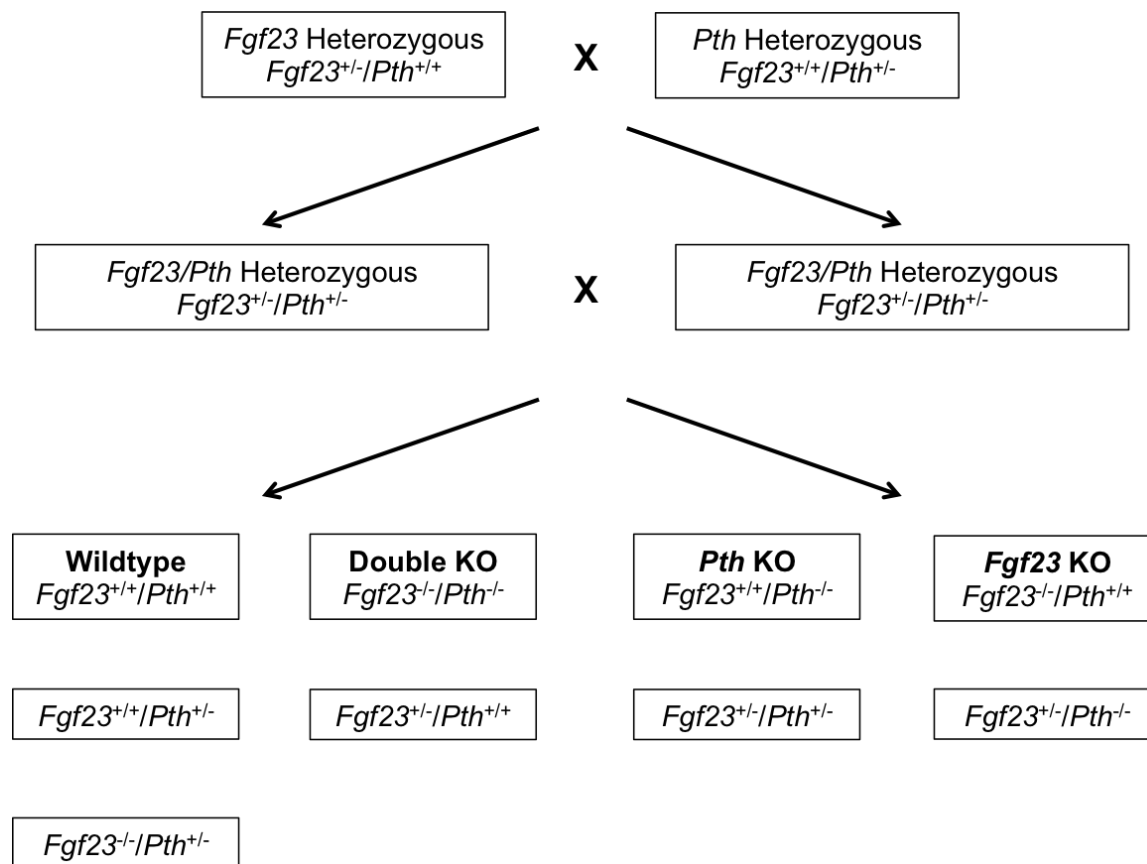


**Figure 8: The Generation of  $Fgf23/Pth$  Double Mutant Mice.**  $Fgf23$  HET mice were mated with  $Pth$  HETs to obtain  $Fgf23/Pth$  double HET ( $Fgf23^{+/-}/Pth^{+/-}$ ). The double HET mice were then mated with each other to generate WT ( $Fgf23^{+/+}/Pth^{+/+}$ ), double mutants ( $Fgf23^{-/-}/Pth^{-/-}$ ),  $Pth$  nulls ( $Fgf23^{+/+}/Pth^{-/-}$ ),  $Fgf23$  nulls ( $Fgf23^{-/-}/Pth^{+/+}$ ), and other 5 mixed genotypes.

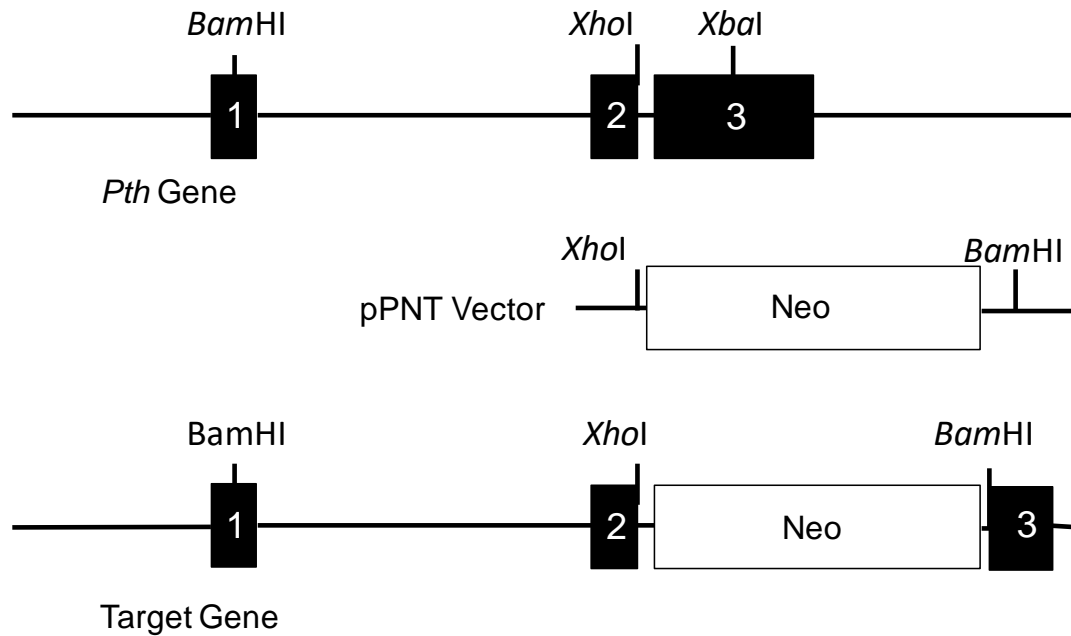


**Figure 9: The Generation of *Pth* Null Mice.** To generate *Pth* null mice, part of the coding sequence of the *Pth* gene on Exon 3 is replaced with a neomycin-resistant gene via a homologous recombination with the pPNT vector. Each box with a number represents an exon of the *Pth* gene.

## 2.2 Description of Experiments in Aim 1

All mice used in Aim 1 were raised on standard laboratory mouse diet (1% calcium, 0.75% phosphorus) and maintained in the Animal Care Facility at Memorial University of Newfoundland. Males and females were weaned at 3 weeks old. To generate experimental fetuses, 7-week-old female HET ( $\text{♀ } Phex^{+/-}$ ) and male WT ( $\text{♂ } Phex^{+/+}$ ) mice were mated overnight and then separated the next morning. The female mice were checked for a mucus plug, which is a sign that mating has occurred. Those females with a mucus plug were put into separate cages and the day was marked as Day 0.5 of pregnancy (ED 0.5).

### 2.2.1 Experiments on ED17.5

On ED 17.5, the pregnant mothers were sacrificed to collect amniotic fluid from each fetus. The amniotic fluid was frozen at  $-20^{\circ}\text{C}$  for future phosphorous and calcium measurements.

### 2.2.2 Experiments on ED18.5

On ED18.5, the pregnant mothers were sacrificed to harvest fetuses. Serum from each fetus was collected and frozen immediately for subsequent phosphorous, calcium and hormone (FGF23, PTH and calcitriol) measurements. After blood collection, carcasses were frozen at  $-20^{\circ}\text{C}$  for subsequent skeletal mineral and morphological analysis. The placenta and kidneys of each fetus were harvested and snap frozen for future expression analysis of FGF23-targeted genes by qPCR and microarray. On ED18.5, the amount of phosphorous transferred across the placenta from a pregnant dam to each of her fetus within a period of 5 minutes was also measured.

### 2.3 Description of the Experiments in Aim 2

To generate experimental fetuses, 7-week-old female HET ( $\text{♀ } Klotho^{+/-}$ ) and male HET ( $\text{♂ } Klotho^{+/-}$ ) mice were mated. Sample collection details are the same as those in Aim 1.

### 2.4 Description of the Experiments in Aim 3

To generate experimental fetuses, 7-week old female double HET ( $\text{♀ } Pth^{+/-}/Fgf23^{+/-}$ ) and male double HET ( $\text{♂ } Pth^{+/-}/Fgf23^{+/-}$ ) were mated. On ED17.5, the pregnant mothers were sacrificed to harvest fetuses, following which serum of each fetus was collected and frozen immediately for future phosphate measures. The bodies of the used fetuses were frozen for later mineral content measures.

### 2.5 Description of the Experiments in Aim 4

For the *Phex* mutant model, 7-week-old female HET ( $\text{♀ } Phex^{+/-}$ ) and male WT ( $\text{♂ } Phex^{+/+}$ ) mice were mated to generate experimental neonates; for the *Fgf23* KO and *Klotho* KO models, female HET ( $\text{♀ } Fgf23^{+/-}, Klotho^{+/-}$ ) and male HET ( $\text{♂ } Fgf23^{+/-}, Klotho^{+/-}$ ) mice were mated. Neonatal serum and urine were collected and frozen on postnatal day 1 (PD 1, within 24 hours after birth), PD 3, PD 5, PD 7, and PD 10. Serum and urine phosphorous concentrations were later measured. The neonatal kidneys were harvested at the postnatal day when urine phosphorous of null pups showed a significant difference. qPCR was used to measure *NaPi2a* and *NaPi2c* mRNA expression on those harvested kidneys.

## 2.6 Genotyping

Polymerase chain reaction (PCR) was carried out to determine mice genotypes. The genotyping process included tagging and tailing, DNA extraction, PCR, and gel electrophoresis.

### 2.6.1 Tagging and Tailing

Mice were briefly anaesthetized with isoflurane (Baxter, Toronto). Their right ear was pierced with an ear tag containing a unique number and a 0.5 cm tail clipping was collected and put into a sterile Eppendorf tube.

### 2.6.2 DNA Extraction

The Puregene Mouse Tail Kit (Qiagen, Toronto) was used to extract genomic DNA from tail clippings. Details can be found in the kit insert (see Appendix).

### 2.6.3 PCR

PCR was carried out on genomic DNA extracted from mouse tails. PCR conditions and primer sequences for each study are described below.

#### 2.6.3.1 PCR Programs for the *Phex* Mutant Model

To identify male fetuses in the litter, PCR for the *Sry* gene was used to distinguish between male and females, with  *$\beta$ -actin* used as a positive control.

The *Sry* primers were:

- Forward 5'-GAG AGC ATG GAG GGC CAT-3',
- Reverse 5'-CCA CTC CTC TGT GAC ACT-3' (product size 200bp).

The *β-actin* primers were:

- Forward 5'-TGT GAT GGT GGG AAT GGG TCA G-3',
- Reverse 5'-TTT GAT GTC ACG CAC GAT TTC C-3' (product size 514bp).

The PCR program was as follows:

- Initial denaturation at 95°C for 5 minutes
- Denaturation at 94°C for 5 seconds
- Annealing at 60°C for 30 seconds
- Extension at 72°C for 30 seconds
- Repeat for 30 cycles
- Final extension at 72°C for 5 minutes

To distinguish between null and WT, male fetuses were then genotyped by PCR to detect Exon 15 (absent in *Phex* male nulls) and Exon 11 (present in both WTs and nulls and used as a positive control).

The Exon 15 primers were [238]:

- Forward 5'-AGT CTT GCC AAA CTG TGC TC-3',
- Reverse 5'-GTC ACT TAC ATT GAA AAC ACT C-3' (product size 387bp).

The Exon 11 primers were:

- Forward 5'-GAC TGG TGT GGG ATG GAA TC-3',
- Reverse 5'-TCT TGT CTG TCA GAT CTG CC-3' (product size 280bp).

The PCR program was as follows:

- Initial denaturation at 95°C for 5 minutes
- Denaturation at 95°C for 30 seconds
- Annealing at 60°C for 30 seconds
- Extension at 72°C for 30 seconds
- Repeat for 35 cycles
- Final extension at 72°C for 5 minutes

Because the mutation is X-linked, males are either null or WT and these 2 genotypes can be easily distinguished using primers to detect Exon 15 (above). But HET females mated to WT males can bear WT or HET fetuses and we were unable to distinguish between these 2 genotypes with the Exon 15 primers, which only allow us to detect the presence or absence of Exon 15 but not to distinguish between one copy of Exon 15 (as in HET) vs 2 copies (in WT). The *Phex* gene has not been sequenced adjacent to Exon 15 to enable efficient primer design to be used in conventional PCR genotyping. Instead, RNA extracted from female tails was first reverse-transcribed to create cDNA and then amplified by PCR using primers designed to detect the *Phex* sequence. Female WTs (*Phex*<sup>+/+</sup>) should have a single band while female HETs (*Phex*<sup>+/-</sup>) should have two bands that include a normal band and a shorter mutant band. RNA extraction and cDNA synthesis steps are explained in the qPCR section below.

The specific PCR primers for on cDNA Exon 15 primers were:

- Forward 5'-GGC AAC GTA CTG CAA ACC CGC-3',
- Reverse 5'-CCA CAG ACC ACC ACG GAT CAA GG-3'.

The Exon 11 primers (positive control) were:

- Forward 5'-GAC TGG TGT GGG ATG GAA TC-3',
- Reverse 5'-TCT TGT CTG TCA GAT CTG CC-3' (product size 280bp).

The PCR program was as follows:

- Initial denaturation at 95°C for 5 minutes
- Denaturation at 95°C for 15 seconds
- Annealing at 68°C for 30 seconds
- Extension at 68°C for 1 minute
- 6 cycles, -1°C/cycle
- Denaturation at 95°C for 15 seconds
- Annealing at 62°C for 30 seconds
- Extension at 68°C for 1 minute
- Repeat for 35 cycles
- Final extension at 72°C for 10 minutes

### 2.6.3.2 PCR Programs for the *Klotho* KO model

A 3-primer system was applied to separate WT (*Klotho*<sup>+/+</sup>), HET (*Klotho*<sup>+/-</sup>), and null (*Klotho*<sup>-/-</sup>). The *GKL-01* and *GKU01* primers detected the mutant allele while *GKL-02* and *GKU01* detected the WT allele.

- *GKU01* sense primer: 5'-TTG TGG AGA TTG GAA GTG GAC GAA AGA G-3'
- *GKL-01* null antisense primer: 5'-CGC CCC GAC CGG AGC TGA GAG TA-3' (product size 491bp)
- *GKL-02* wildtype antisense primer: 5'-CTG GAC CCC CTG AAG CTG GAG TTA C-3' (product size 815bp)

The PCR Procedure was as follows:

- Initial denaturation at 94°C for 5 minutes
- Denaturation at 94°C for 30 seconds
- Annealing at 60°C for 1 minute
- Extension at 72°C for 45 seconds
- Repeat for 30 cycles
- Final extension at 72°C for 10 minutes

### 2.6.3.3 PCR Programs for the *Fgf23* KO Model

A 3-primer system was used to separate WT (*Fgf23*<sup>+/+</sup>), HET (*Fgf23*<sup>+/-</sup>), and null (*Fgf23*<sup>-/-</sup>). The *Fgf23* primers (forward and reverse) detected *Fgf23* WT allele while the *Fgf23* forward primer and the *LacZ* primer detected the mutant allele.

- *Fgf23* forward primer: 5'-AGT CTT GCC AAA CTG TGC TC-3'
- *Fgf23* reverse primer: 5'-GTC ACT TAC ATT GAA AAC ACT C-3' (product size 252 bp)
- *LacZ* primer: 5'-TCT TGT CTG TCA GAT CTG CC-3' (product size 366 bp)

The PCR program was as follows:

- Initial denaturation at 94°C for 5 minutes
- Denaturation at 94°C for 1 minute
- Annealing at 62°C for 1 minute
- Extension at 72°C for 1 minute
- 5 cycles, -1°C/cycle
- Denaturation at 94°C for 1 minute
- Annealing at 56°C for 1 minute
- Extension at 72°C for 1 minute
- Repeat for 35 cycles
- Final extension at 72°C for 5 minutes

#### 2.6.3.4 PCR Programs for the *Fgf23/Pth* Double KO Model

*Fgf23* and *Pth* genotyping was carried out to select *Fgf23/Pth* double HET males ( $\sigma^7$  *Fgf23*<sup>+/-</sup>/*Pth*<sup>+/-</sup>) and females ( $\text{♀}$  *Fgf23*<sup>+/-</sup>/*Pth*<sup>+/-</sup>) as parents. The same technique was also used to determine genotypes of the offspring. *Fgf23* genotyping was done using the same primer set and procedure described above. *Pth* genotyping was performed using the following 3-primer system:

- *Pth* common primer: 5'-AAG ATG ATG TCT GCA AAC ACC GTG G-3'
- *Pth* wildtype primer: 5'-GGT GTT TGC CCA GGT TGT GCA TAA-3' (product size 250bp)

- *Pth* mutant primer: 5'-TCC AGA CTG CCT TGG GAA AAG CGC-3' (product size 200bp)

The *Pth* PCR program was as follows:

- Initial denaturation at 94°C for 5 minutes
- Denaturation at 94°C for 1 minute
- Annealing at 63°C for 1 minute
- Extension at 72°C for 1 minute
- Repeat for 34 cycles
- Final extension at 72°C for 10 minutes

#### 2.6.4 Gel Electrophoresis

Horizontal gel electrophoresis was used to separate and visualize PCR products. The 1.2% agarose gel in TAE buffer was made as follows: 1.2 g agarose (Invitrogen, Toronto) was dissolved by heating in 100 ml 1X TAE buffer (10ml 10x Tris-acetate-EDTA (TAE) buffer [0.12M EDTA, 0.40M Tris, 11.5% Glacial Acetic Acid, pH 8.0], 90 ml deionized water). 10µL SYBR Safe DNA Gel Stain (Invitrogen, Toronto) was added. Once slightly cooled, the gel was poured into the gel casting tray with comb in place and allowed to solidify.

1X TAE was used as the gel running buffer (10X TAE diluted to 1X by adding 70ml to 630ml distilled water). 4µL of 6X gel loading dye (2% coomassie blue, 2% xylene cyanol, 30% glycerine) was added to the 20µL PCR product and mixed well. 15µL was pipetted into each well of the gel. The gel ran at 200V for 20 min.

The gel was imaged under UV excitation using Gel Doc<sup>TM</sup> XR+ with Image Lab<sup>TM</sup> Software (BIO-RAD, Toronto) to visualize the bands.

## 2.7 Fetal Serum Mineral and Hormone Analysis

### 2.7.1 Fetal Serum Collection

Fetal serum was collected on ED 18.5. Pregnant dams were first anesthetized with isoflurane and then sacrificed by cervical dislocation. A Caesarean section (C-section) was performed to remove fetuses. Fetal whole blood was collected by severing the carotid artery and collecting blood using microhematocrit capillary tubes (Fisher Scientific, Toronto).

To separate serum, the capillary tubes containing whole blood were centrifuged at 14,000 rpm for 20 minutes in the Micro-MB microcentrifuge (Thermo Scientific, Toronto). A glass cutter was used to cut the capillary tubes at the interface between serum and clotted blood. The serum in each capillary tube was decanted into 0.6 ml tubes and stored at -20 °C.

### 2.7.2 Serum Mineral Analysis

Serum phosphorous and calcium were measured using commercial assays (Sekisui Diagnostics, Charlottetown). In terms of the mechanism of the phosphorus kit, inorganic phosphorus reacts with ammonium molybdate in the presence of sulfuric acid to produce an unreduced phosphomolybdate complex. The increase in absorbance at 340 nm is directly proportional to the concentration of phosphomolybdate complex, which also reflects the concentration of inorganic

phosphorus in the sample. In terms of the mechanism of the calcium kit, calcium reacts with Arsenazo III [2,2'-(1,8-dihydroxy-3,6-disulfonaphthylene-2,7-bisazo) bisbenzenearsonic acid] in an acid solution to form a blue-purple complex. The color developed has a maximum absorbance at 650 nm and is proportional to the calcium concentration in the sample. The experimental procedure followed the product inserts (see Appendix). Samples were analyzed using the Ultrospec 2000 UV spectrophotometer (Pharmacia Biotech, Toronto).

### 2.7.3 Serum Hormone Analysis

PTH, FGF23, and calcitriol concentrations in fetal serum were measured using commercial ELISA kits for mouse use (Immutopics Inc., CA; Kainos Laboratories Inc., Japan; and Immunodiagnostic Systems, UK; respectively).

In the two-site rat intact PTH ELISA kit two different goat polyclonal antibodies to rat intact PTH have been purified by affinity chromatography. The antibody which recognizes epitopes within the mid-region/C-terminal portion (39-84) of the peptide is biotinylated for capture. The other antibody which recognizes epitopes within the N-terminal region (1-34) is conjugated with the enzyme horseradish peroxidase (HRP) for detection. A sample containing PTH is incubated simultaneously with the biotinylated capture antibody and the HRP conjugated antibody in a streptavidin coated microtiter well. Intact PTH (1-84) contained in the sample is immunologically bound by the capture antibody and the detection antibody to form a “sandwich” complex: Well/Avidin-Biotin Anti-Rat PTH — Rat Intact PTH — HRP Anti-Rat PTH. At the end of this incubation period, the well is washed to remove any unbound antibody and other components. The enzyme bound to the well is then incubated with a substrate solution in a timed

reaction and then measured in a spectrophotometric microtiter plate reader. The enzymatic activity of the antibody complex bound to the well is directly proportional to the amount of PTH in the sample.

The FGF23 kit follows a similar mechanism as the PTH kit. Two specific murine monoclonal antibodies bind to full-length FGF23. One antibody is immobilized onto the microtiter plate well for capture. The other antibody is conjugated to HRP for detection. In enzyme reaction, a “sandwich” complex immobilized on the well is incubated with a substrate solution and then measured by a spectrophotometric microtiter plate reader. The enzymatic activity of the complex bound to the well is directly proportional to the amount of FGF23 in the sample.

The calcitriol kit is a complete assay system for the purification of calcitriol in samples by immunoextraction followed by quantitation by EIA. Samples are delipidated and calcitriol extracted from potential cross-reactants by incubation for 90 minutes with a highly specific solid phase monoclonal anti-calcitriol. The immunoextraction gel is then washed and purified calcitriol eluted directly into glass assay tubes. Reconstituted eluates and calibrators are incubated overnight with a highly specific sheep anti-calcitriol. A portion of this is incubated for 90 minutes with shaking in microplate wells which are coated with a specific anti-sheep antibody. Calcitriol linked to biotin is then added and the plate shaken for a further 60 minutes before aspiration and washing. HRP labelled avidin is added and binds selectively to complexed biotin and, following a further wash step, colour is developed using a chromogenic substrate. The absorbance of the stopped reaction mixtures are read in a microtitre plate reader, colour intensity developed being inversely proportional to the concentration of calcitriol in the sample.

The procedure of each experiment followed the product manual (see Appendix).

## 2.8 Amniotic Fluid Collection and Mineral Analysis

### 2.8.1 Amniotic Fluid Collection

Amniotic fluid was collected because it essentially represents fetal urine. On ED17.5, when amniotic fluid is more plentiful and less viscous, pregnant dams were anesthetized with isoflurane and then sacrificed by cervical dislocation. C-section was performed to reveal fetuses in their amniotic sacs. Amniotic sacs were lanced with a sterile blade, and the fluid was collected into microhematocrit capillary tubes which was then transferred to 0.6 ml tubes and stored at -20 °C.

### 2.8.2 Amniotic Fluid Mineral Analysis

Amniotic fluid phosphorous and calcium were measured using the same commercial assays used for serum measurements. Samples were analyzed using the Ultrospec 2000 UV spectrophotometer (Pharmacia Biotech, Toronto).

## 2.9 Fetal Skeletal Mineral Analysis

### 2.9.1 Fetal Ash Collection

Previously genotyped fetuses were weighed in crucibles (wet weight) and were reduced to ash in a furnace (make and manufacturer) at 500°C for 24 hours. The ash was then weighed (dry weight) and this represented the total amount of mineral in the fetuses. Samples were transferred to 20 ml scintillation vials and stored at room temperature.

### 2.9.2 Skeletal Mineral Analysis

Fetal ash was dissolved in 253  $\mu$ l of nitric acid. The samples were left at room temperature for one week until all ash was dissolved after which 10 ml of deionized water was added to each vial. Ash calcium and magnesium was measured by flame atomic absorption spectrophotometry on the 2380 Atomic Absorption Spectrophotometer (Perkin-Elmer, MA) while phosphorous content was measured using the same commercial phosphorous assay that was used to measure serum phosphorous. Samples were diluted 1:10 in distilled water prior to measurement. The measuring procedure followed the manual of the atomic absorption spectrophotometer. Five measurements per sample were done and averaged. Samples were further diluted 1:5 for phosphorous measurement.

### 2.10 Placental Phosphorus Transfer

Placental phosphorus transfer methodology was adapted from our previously reported placental calcium transfer procedure [162]. On ED 17.5 pregnant dams were anesthetized with isoflurane and given an intra-cardiac injection of 50  $\mu$ Ci  $^{32}$ P and 50  $\mu$ Ci  $^{51}$ Cr-EDTA in 0.9% saline. EDTA is passively transferred and serves as a blood diffusional marker. The mothers were then placed in a lead-coated box. After 5 minutes the mothers were sacrificed by cervical dislocation, and a C-section was performed to remove the fetuses from amniotic sacs. Fetal tails were collected for genotyping and the fetuses were placed in 12 mm x 75 mm disposable round bottom polystyrene culture test tubes (Fisher Scientific), and their brains were pithed using forceps. The tubes were then capped and the  $^{51}$ Cr-EDTA activity in each fetus was measured using a 1480 Wizard automatic  $\gamma$  counter (Perkin Elmer, MA). To dissolve the fetuses, 1 ml of Scintigest (Fisher Scientific, Toronto) was added to each tube and the tube was vortexed until to loosen the fetus so

that it could be transferred to a 20 ml scintillation vial (Fisher Scientific). A further 9 ml of Scintigest was added. All vials were incubated at 55°C in an isotherm oven (Fisher Scientific) for 24-48 hours, with periodic vortexing to aid in solubilization. When the fetuses were fully solubilized, the tubes were removed from the oven, and 10 ml of ScintiVerse (Fisher Scientific) and 5 drops of glacial acetic acid (Fisher Scientific) were added to each vial. The vials were wrapped in aluminum foil and placed in the dark for 24 hours to reduce bioluminescence. The activity of  $^{32}\text{P}$  was then measured using an LS 6500 Multi-Purpose Scintillation Counter (Beckman Coulter, CA). The ratio of  $^{32}\text{P}$  activity to  $^{51}\text{Cr}$ -EDTA activity for each fetus was calculated to determine the rate of phosphorous transfer from mother to fetus. The ratio of each fetus was normalized to the mean HET value within its litter for the *Klotho* fetuses or to the mean male null value within its litter for the *Phex* fetuses. Normalization allowed aggregate results from different litters to be analyzed. In addition,  $^{32}\text{P}$  activity alone (not as a ratio to  $^{51}\text{Cr}$ -EDTA) was analyzed after normalization.

### 2.11 Fetal Tibial Morphology

On ED 18.5, at the time of fetal serum collection, tibias were also removed, stored in 10% buffered formalin and subsequently embedded in paraffin for sectioning. 5  $\mu\text{m}$  sections were cut and collected. The slides were placed on a slide warmer (Fisher Scientific, Toronto) for 30 minutes and were deparafinized and rehydrated using the following series: xylene for 2 minutes (2x), 100% Ethanol for 2 minutes (2x), 95% ethanol for 2 minutes, 70% Ethanol for 2 minutes, 50% ethanol for 2 minutes, and distilled water for 1 minute. Von Kossa staining for mineral was then conducted. The steps were explained here. The sections were placed in a 1% aqueous silver nitrate solution and exposed to direct light for one hour. The sections were then washed 3 times

with distilled water, 2 minutes per wash. Sections were transferred to a 2.5% sodium thiosulphate solution for 5 minutes, and then washed three times (2 minutes per wash) in distilled water. The sections were counterstained with methyl green (Sigma, Toronto) for 2 minutes. Excess dye was blotted from the slides, which were then washed in 1- butanol (Fisher Scientific, Toronto) for 10 seconds, (2X), and then in xylene for 10 seconds (2X). Permount (Fisher Scientific, Toronto) was then added to the slides to mount the coverslips.

## 2.12 Microarray

Placental RNA samples were shipped on dry ice to The Centre for Applied Genomics, Microarray Facility, at the Hospital for Sick Children (Toronto, ON). The Affymetrix GeneChip Mouse Gene ST 2.0 Array (Affymetrix, CA), which is a whole-transcript array that includes probes to measure both mRNA and long intergenic non-coding RNA transcripts (lincRNA) (lincRNA transcripts can impact the mRNA expression profile), was then utilized to assess gene expression in the placenta of *Fgf23* WT, *Fgf23* null, *Phex* WT and *Phex* null fetuses. In total, 16 arrays were conducted, which included 4 samples in each of the 4 groups. Raw data obtained from the Mouse Gene ST 2.0 Arrays, which summarizes all probes into a single gene expression value, were analyzed by a third-party person hired by Dr. Kovacs' Laboratory. Raw data were normalized in R Version 3.2.1 (R Foundation for Statistical Computing) using the robust multi-array average algorithm. Differentially expressed genes were identified using the Local-Pooled-Error Test. False discovery rate, which is commonly used to evaluate statistical significance, was set at 0.01 such that genes with adjusted p-values < 0.01 were considered statistically significant. In this method, errors within genes and between replicate arrays for genes in which expression

values are similar are pooled, and it has been shown to have an advantage in identifying subtle changes in gene expression.

### 2.13 Neonatal Urine Collection

Neonatal urine was collected at the time of neonatal serum collection. The abdomen of each neonate was resected to reveal the bladder, which was removed intact and transferred to a clean 0.6 mL tube. Within the tube, the bladder was pierced to release the urine. Bladder tissue was then removed. Phosphorous in the neonatal urine was measured.

### 2.14 FGF23-Targeted Gene Expression Analysis on the Placenta and on the Fetal and Neonatal Kidneys

#### 2.14.1 Placenta and Fetal and Neonatal Kidneys Collection

The placenta and fetal kidneys were collected on ED18.5, at the time of fetal blood collection. Placentas were removed, immediately snap-frozen in liquid nitrogen and stored at -70 °C. Immediately after fetal blood was collected, the abdomen of the fetuses was resected to reveal the kidneys. The kidneys were removed, immediately snap-frozen in liquid nitrogen and stored at -70°C. A similar procedure was carried out to collect the kidneys in neonates at the time point when neonatal urine phosphorous was analyzed.

#### 2.14.2 Real-time Quantitative RT-PCR (qPCR)

qPCR was used to measure differential expression of select FGF23-targeted genes in the placenta and kidneys of *Phex* and *Klotho* null fetuses compared to their respective WT fetuses. qPCR was

also used to determine differential expression in the kidneys of *Phex*, *Klotho*, and *Fgf23* null neonates compared to their respective WT littermates. FGF23-targeted genes measured in the fetal kidneys included *Fgf23*, *Cyp27b1*, *Cyp24a1*, *NaPi2a*, *NaPi2b*, *NaPi2c*, *Fgfr1*, *Fgfr2*, *Fgfr3*, *Fgfr4*, and *Klotho*. In the neonatal kidneys, expression of *Napi2a* and *Napi2c* was measured.

Differential gene expression analysis consisted of three separate steps: RNA extraction from tissue samples, cDNA synthesis and finally, qPCR.

#### 2.14.2.1 RNA Extraction

To extract RNA from the placenta and fetal kidneys, the snap frozen organs were first transferred to clean tubes containing Qiazol (Qiagen, Toronto), which was followed by tissue disruption and homogenization using the Precellys system (Bertin Instruments, MD). Then, the RNeasy Midi Lipid Kit (Qiagen, Toronto) and RNeasy Mini Lipid Kit (Qiagen, Toronto) were applied to extract total RNA from placentas and fetal kidneys, respectively. The experimental steps followed the manual in each kit. RNA was quantified and the the RNA Integrity Number (RIN) was determined for each sample using the Agilent 2100 Bioanalyzer platform (Agilent Technologies, CA).

#### 2.14.2.2 cDNA Synthesis

cDNA was synthesized from 2 µg of RNA using the Superscript III First-strand Synthesis Kit (Invitrogen, Toronto). The synthesis program was as follows:

- Step 1: 25°C for 10 minutes
- Step 2: 37°C for 2 hours

- Step 3: 85°C for 5 minutes
- Step 4: 4°C indefinitely

#### 2.14.2.3 Quantitative Real Time RT-PCR (qPCR)

Differential gene expression analysis was done by qPCR using Taqman® Gene Expression Assays (commercially available manufacturer's pre-designed primers and probes for optimal amplification) (Life Technologies, Toronto) and Taqman Fast Advanced Master Mix (Life Technologies, Toronto). Briefly, a minor groove binder (MGB) probe with a 6-carboxyfluorescein (FAM) reporter dye at the 5' end and a non-fluorescent quencher at the 3' end is used in the assay. When targeted cDNA is amplified, the MGB probe is digested by DNA polymerase and the FAM reporter dye is released. Florescence from the free FAM reporter dye is detected by a real-time PCR system. The intensity of florescence is directed to the concentration of the targeted cDNA within proper range.

Samples were prepared using the Fast Advanced Master Mix kit (Life Technologies, Toronto). All samples were run in triplicate and the threshold cycle value ( $C_T$ ) was used as an indicator of gene expression. *Gapdh* was used as an endogenous control. All samples were run on the ViiA™ 7 Real-Time PCR System (Life Technologies, Toronto). qPCR results were analyzed using the comparative  $C_T$  method ( $2^{\Delta C_T}$ ).

#### 2.15 Statistical Analysis

All experimental results (except the qPCR results) were expressed as mean  $\pm$  standard error (SE). The results were analyzed using StatPlus:Mac Professional 2009, Build 6.0.3 (AnalystSoft Inc).

ANOVA was used for analysis of the following experiments, with a post-hoc Tukey test conducted to determine which pairs of means differed significantly: fetal serum and amniotic fluid chemistries, fetal serum hormones, fetal ash and mineral content, and placental phosphate transport. qPCR data was analyzed using the comparative  $C_T$  method ( $2^{\Delta C_T}$ ) with two-tailed probabilities reported as mean  $\pm$  SD. In the graphs of all results, significant differences were denoted and the number of the samples studied was indicated in parentheses.

Based on experience from previous studies in Dr. Kovacs' laboratory, the minimum sample size per group to find significant differences in the studies of serum chemistries, urine chemistries, serum hormones and bone mineral content is six. For qPCR experiments, the minimum sample size per group is five.

### 3 Results

#### 3.1 Results from *Phex* Null Fetuses

In this aim, I mainly examined whether excess FGF23 would impact fetal phosphate homeostasis and skeletal development, as well as placental phosphate transport by studying *Phex* null male fetuses. In contrast to the *Phex* null model, *Fgf23* null fetuses were studied in a simultaneous project carried out by Dr. Samaraweera in Dr. Kovacs' laboratory. To complement the studies in *Fgf23* nulls, I would also investigate phosphate-related phenotypes in *Klotho* null fetuses in which the FGF23 pathway is blocked (see results in Aim 2 below). If *Phex* null fetuses demonstrate an opposite phenotype against *Fgf23* nulls and *Klotho* nulls, it would imply FGF23 plays some critical roles in regulating fetal phosphate homeostasis. If *Phex* null fetuses have a similar phenotype as *Fgf23* nulls and *Klotho* nulls, it would imply FGF23 is relatively unimportant in this process.

##### 3.1.1 Serum Hormones in *Phex* Fetuses on ED18.5

Serum FGF23 in *Phex*<sup>+/-</sup> female fetuses (*Phex* ♀) and male null fetuses was up to 8-fold higher than that in WT fetuses (♂ and ♀) – which confirmed the effect of the *Phex* mutation was active *in utero*, but more importantly, proved that this model was valid in studying the effect of excess FGF23 in fetal phosphate regulation because FGF23 was increased up to 8-fold in *Phex* nulls (**Figure 10**). It should be noted that FGF23 was also increased over 7-fold in *Phex*<sup>+/-</sup> dams compared to WT fetuses. Despite the high maternal value, the FGF23 levels in WT fetuses were largely in-line with those in fetuses from WT dams – implying that FGF23 is unlikely going to cross the placenta from dams to fetuses.

Fetal serum calcitriol, as well as serum PTH, was measured to determine if there was any compensatory mechanism when serum FGF23 was ultra-high. FGF23 is known to inhibit calcitriol in adult mice – therefore, I expected serum calcitriol levels to be low in male *Phex* nulls. The results were in-line with my expectation, which showed that calcitriol was significantly reduced more than 30% in male *Phex* nulls compared to male WT fetuses (**Figure 11**). Calcitriol in *Phex*<sup>+/-</sup> dams was at least 5 times as high as in fetuses regardless their genotypes.

In terms of serum PTH, it showed no response to higher FGF23 in male *Phex* null fetuses as both WT and null fetuses had identical levels (**Figure 12**). Fetal serum PTH appeared to be about 8 fold as high as in *Phex*<sup>+/-</sup> dams, although the differences were non-significant. The high concentrations of serum PTH in fetuses was opposite of what was originally expected as PTH is normally maintained at a relatively low level in fetuses.

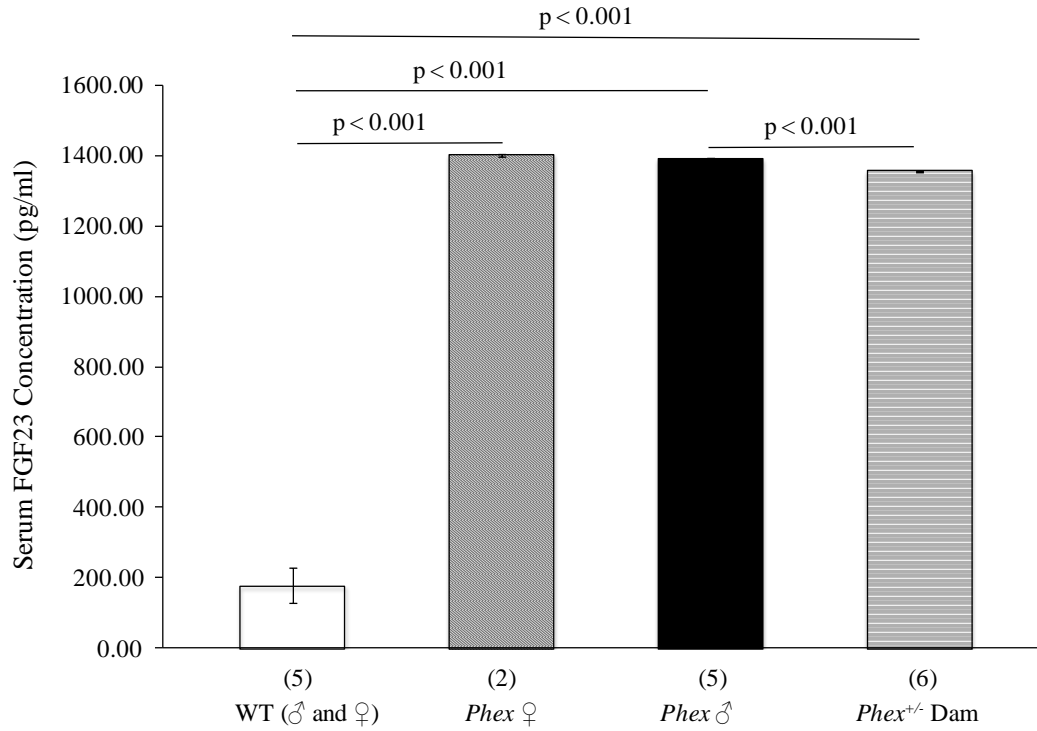


**Figure 10: Serum FGF23 in *Phex* Fetuses on ED18.5.** Fetal serum FGF23 on ED 18.5 was significantly increased in *Phex*<sup>+/-</sup> (*Phex* ♀) and male null (*Phex* ♂) fetuses compared to WT (♂ and ♀) fetuses. *Phex*<sup>+/-</sup> dams on ED 18.5 had significantly higher FGF23 than WT fetuses. The numbers in parentheses indicate the number of fetuses studied.

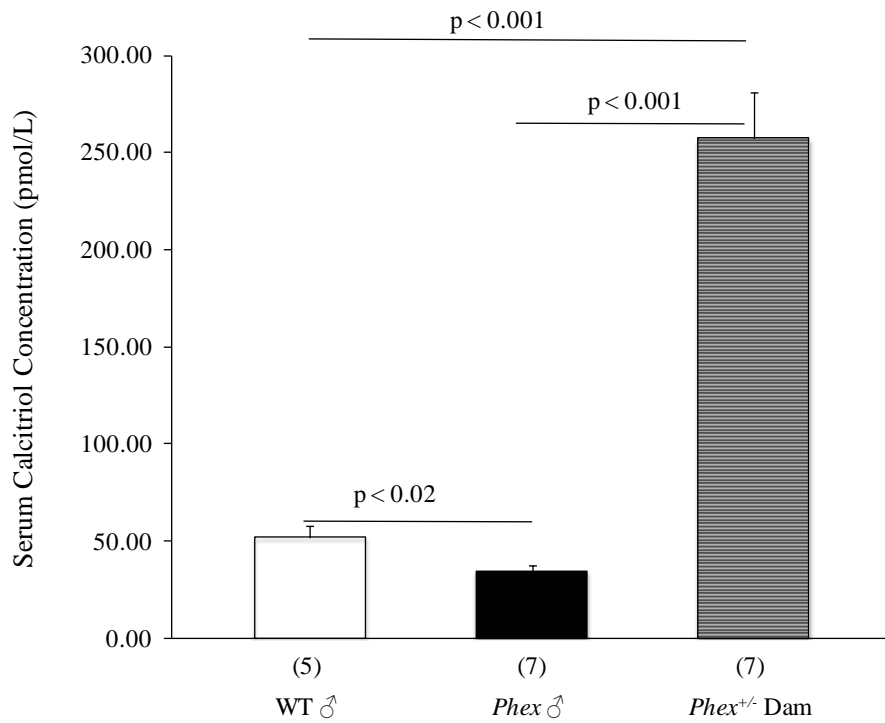


**Figure 11: Serum Calcitriol in ED18.5 *Phex* Fetuses.** Serum calcitriol in male *Phex* null fetuses (*Phex* ♂) on ED 18.5 was significantly lower than that in male WT (WT ♂). *Phex*<sup>+/-</sup> dams had higher serum calcitriol than all fetuses. The numbers in parentheses indicate the number of fetuses studied.

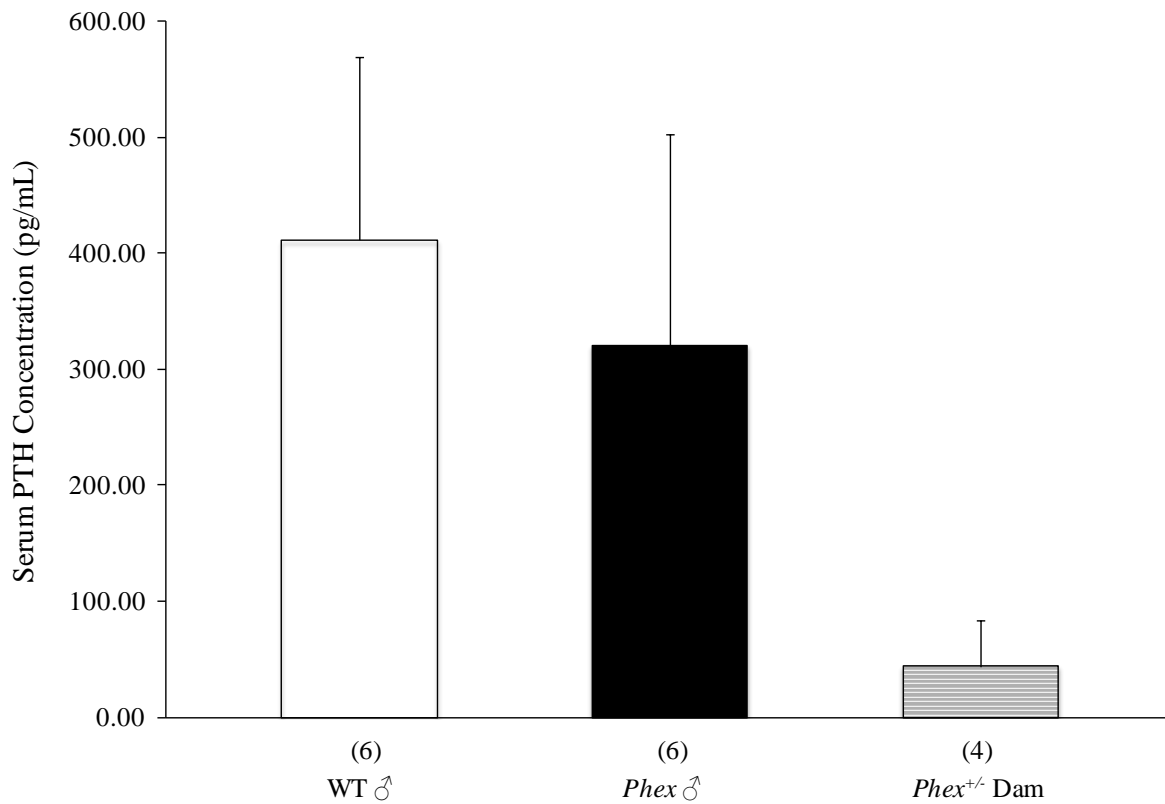


**Figure 12: Serum PTH in ED 18.5 *Phex* Fetuses.** On ED 18.5, male *Phex* null fetuses (*Phex* ♂) had similar levels of serum PTH as male WT fetuses (WT ♂). Fetal serum PTH appeared to be higher than maternal levels. The numbers in parentheses indicate the number of fetuses studied.

### 3.1.2 Serum Chemistries in *Phex* Fetuses on ED18.5

FGF23 lowers serum phosphate in adults. If FGF23 acts in fetuses in the same way, I expected serum phosphate to decrease in *Phex* null fetuses. Opposite to my original expectation, the results demonstrated that fetal serum phosphorus among *Phex* WT ♂, WT ♀, *Phex* ♀, and *Phex* ♂ was not significantly different on ED 18.5 (**Figure 13**). Serum phosphorus in fetuses was significantly 2.5-fold higher than that in *Phex*<sup>+/-</sup> dams on ED 18.5 – which was expected as higher levels of phosphate are normally seen in fetuses. Since there were no differences in serum phosphorus between WT ♂ and WT ♀, data from these two groups were pooled together for an analysis – serum phosphorus of *Phex* WT fetuses was still not significantly different from that in *Phex* ♀ or *Phex* ♂ (**Figure 14**). On ED 18.5, *Phex* WT (♂ and ♀), *Phex* ♀, and *Phex* ♂ fetuses had similar levels of serum total calcium. *Phex*<sup>+/-</sup> dams had non-significantly higher levels of serum total calcium (**Figure 15**). Normally, fetuses have hypercalcemia compared to dams when the ionized form of calcium is measured. The results shown in Figure 15 represent the total calcium that includes ionized, albumin-bound, and complexed forms of calcium.

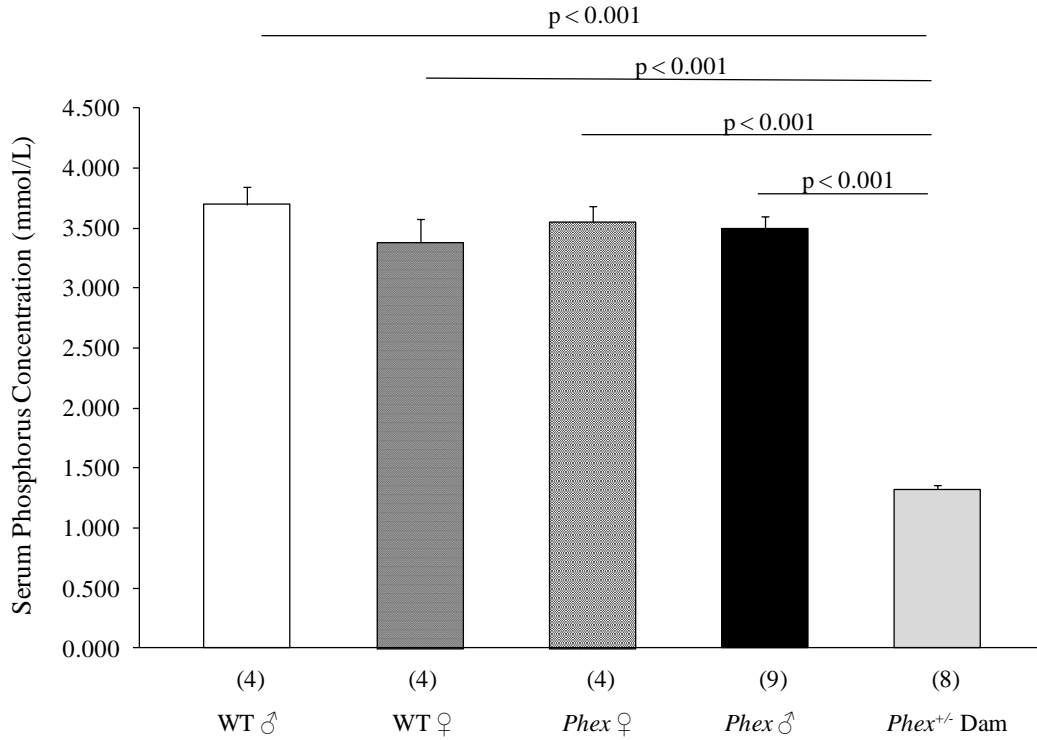


**Figure 13: Serum Phosphorus in *Phex* Fetuses on ED18.5 (Data of WT ♂ and WT ♀ Were Separated).** Fetal serum phosphorus was not significantly changed in *Phex* ♀ and *Phex* ♂ fetuses when compared to WT ♂ and WT ♀ fetuses. The numbers in parentheses indicate the number of fetuses studied.

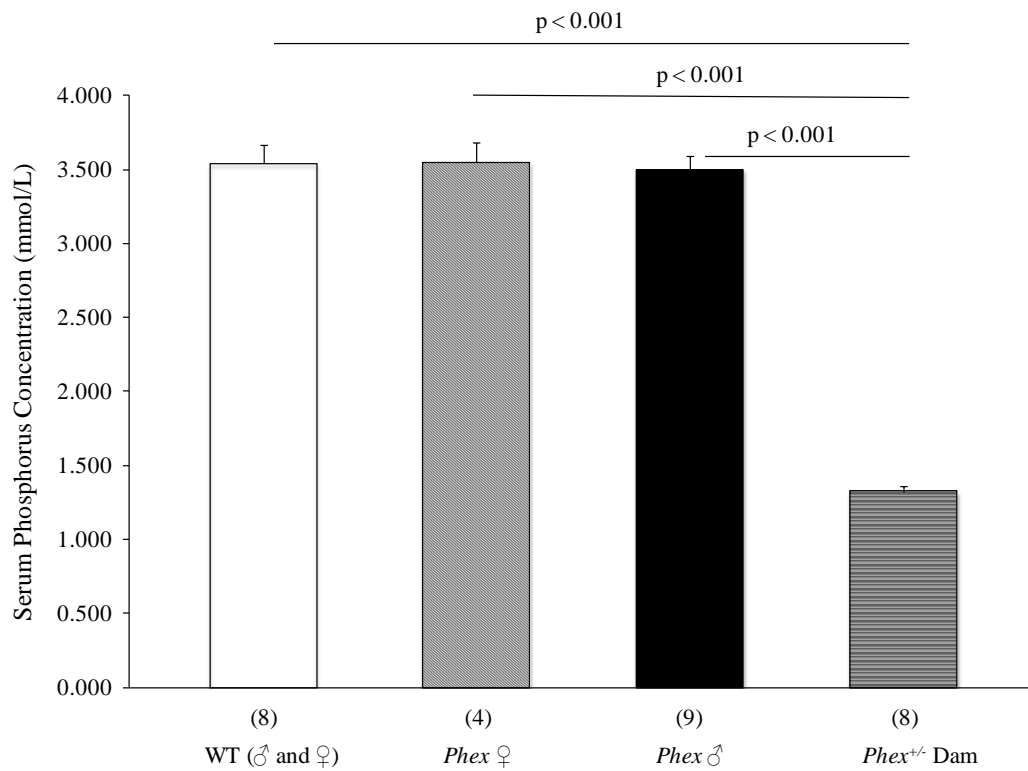


**Figure 14: Serum Phosphorus in *Phex* Fetuses on ED18.5 (Data of WT ♂ and WT ♀ Were Pooled).** There were no significant differences in serum phosphorus on ED 18.5 among *Phex* WT, *Phex* ♀, and *Phex* ♂ fetuses. Fetal serum phosphorus was higher than *Phex*<sup>+/-</sup> dams'. The numbers in parentheses indicate the number of fetuses studied.

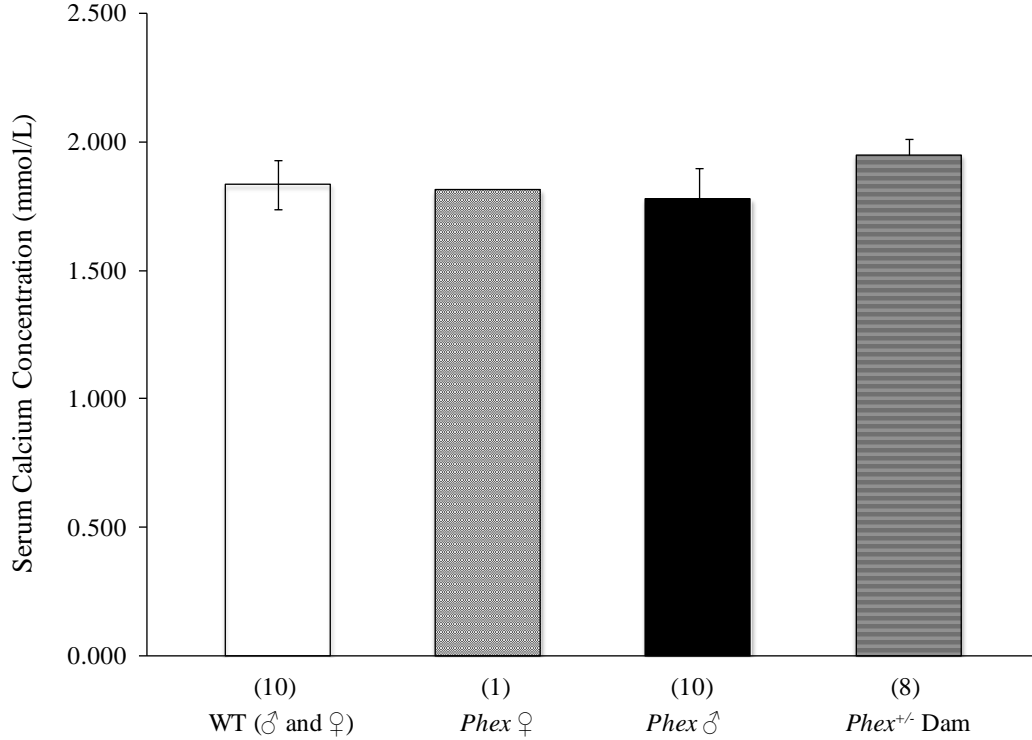


**Figure 15: Serum Total Calcium in *Phex* Fetuses on ED18.5.** There were no significant differences in serum total calcium on ED 18.5 among *Phex* WT, *Phex* ♀, and *Phex* ♂ fetuses. Regardless of genotypes, fetuses normally have hypercalcemia compared to dams when the ionized form of calcium is measured. The results presented here represent serum total calcium that include both free ionized calcium and albumin-binding calcium. The numbers in parentheses indicate the number of fetuses studied.

### 3.1.3 Amniotic Fluid Chemistries in *Phex* Fetuses on ED17.5

Amniotic fluid is mainly made of fetal urine. It is commonly used to measure minerals that the fetal kidneys excrete. Based on previous studies in Dr. Kovacs' laboratory, the amount of amniotic fluid on ED 18.5 is too thick and scant. Thus, I used amniotic fluid on ED 17.5 to measure concentrations of phosphorus and calcium. It is known that FGF23 decreases renal phosphate reabsorption in adults. If FGF23 has the same effect in fetuses, phosphorus in amniotic fluid from *Phex* null fetuses should increase. However, the results showed that WT (♂ and ♀), *Phex* ♀, and *Phex* ♂ fetuses had no significant differences in amniotic fluid phosphorus on ED 17.5 (**Figure 16**). The levels of total calcium in amniotic fluid on ED 17.5 were also similar among WT (♂ and ♀), *Phex* ♀, and *Phex* ♂ fetuses (**Figure 17**).

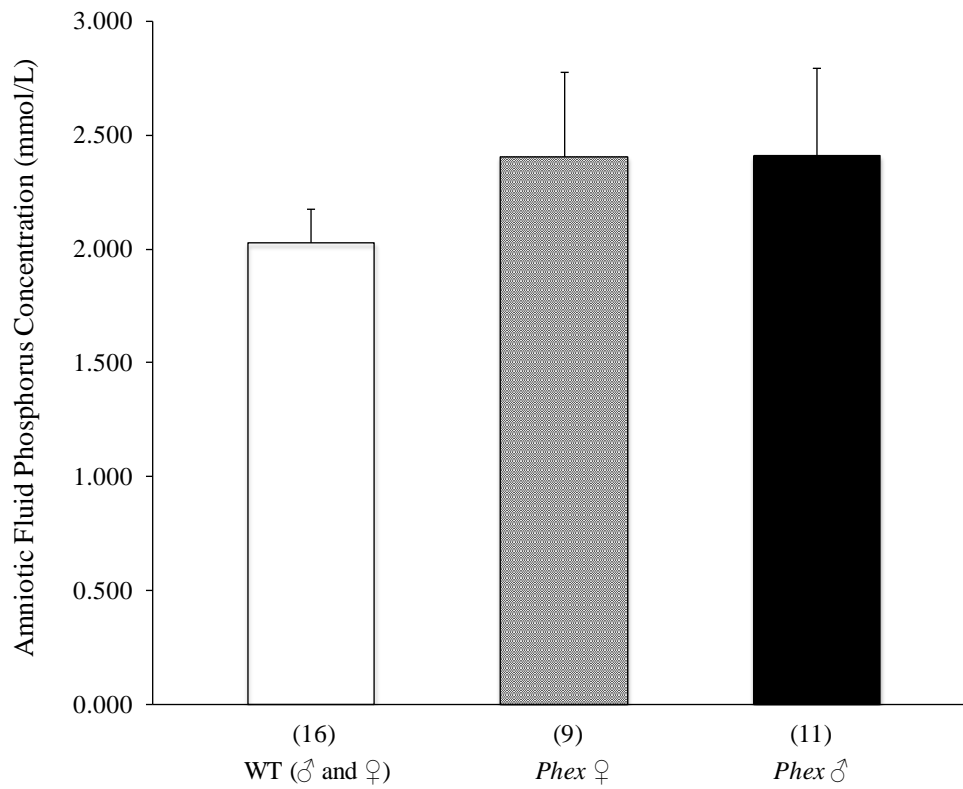


**Figure 16: Amniotic Fluid Phosphorus in *Phex* Fetuses on ED17.5.** There were no significant differences in amniotic fluid phosphorus on ED 17.5 among WT (♂ and ♀), *Phex* ♀, and *Phex* ♂ fetuses. The numbers in parentheses indicate the number of fetuses studied.

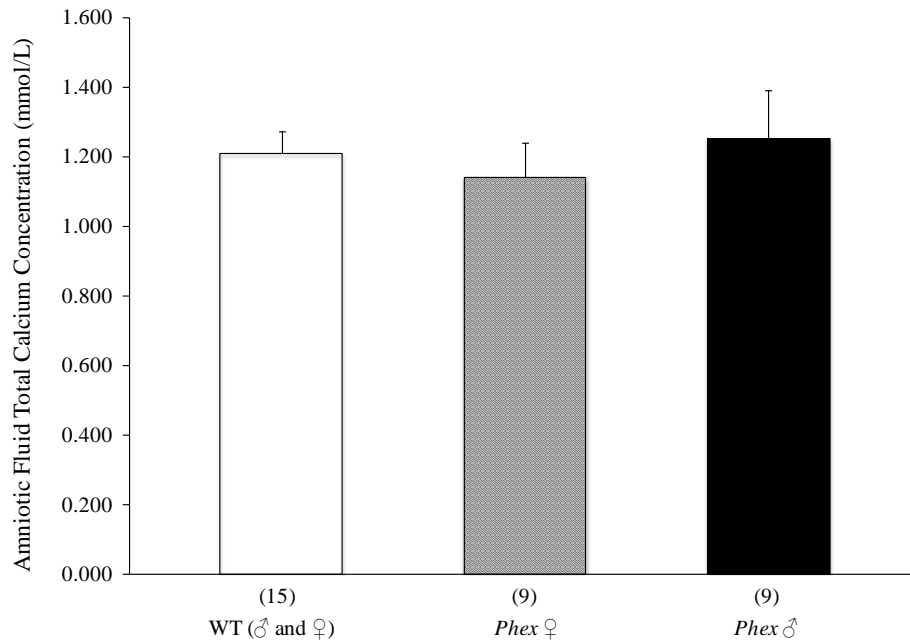


**Figure 17: Amniotic Fluid Total Calcium in ED 17.5 *Phex* Fetuses.** Compared to WT fetuses, *Phex* ♂ had similar levels of amniotic fluid total calcium on ED 17.5. The numbers in parentheses indicate the number of fetuses studied.

### 3.1.4 Placental Phosphate Transport in *Phex* Fetuses on ED17.5

The placenta is arguably the most important organ in fetal development as it represents the only source of input from mothers. Prior to this project, little had been known about potential roles of FGF23 in placental phosphate transport. FGF23 could conceivably stimulate or even inhibit this process. In this study, I measured the amount of  $^{32}\text{P}$  relative to  $^{51}\text{Cr}$ -EDTA transferred from dams to each of their fetuses in a 5-minute period following a maternal intracardiac injection. Because  $^{51}\text{Cr}$ -EDTA only diffuses across the placenta passively, it serves as a control for differences in the flow rate among individual placentas in one litter.  $^{32}\text{P}$ , however, is actively transported across the placenta from dams to fetuses. Thus, by normalizing for the rate of diffusion (using  $^{51}\text{Cr}$ -EDTA) the relative rate of placental phosphate transfer in each fetus in the same litter can be determined. The results seemed to suggest there was no effect of FGF23 on placental phosphate transport as this process was not changed in *Phex* ♂ fetuses relative to WT ♂ fetuses (**Figure 18**). The placental transfer of  $^{32}\text{P}$  without normalization to  $^{51}\text{Cr}$ -EDTA was also measured, showing no differences in *Phex* ♂ fetuses (**Figure 19**).

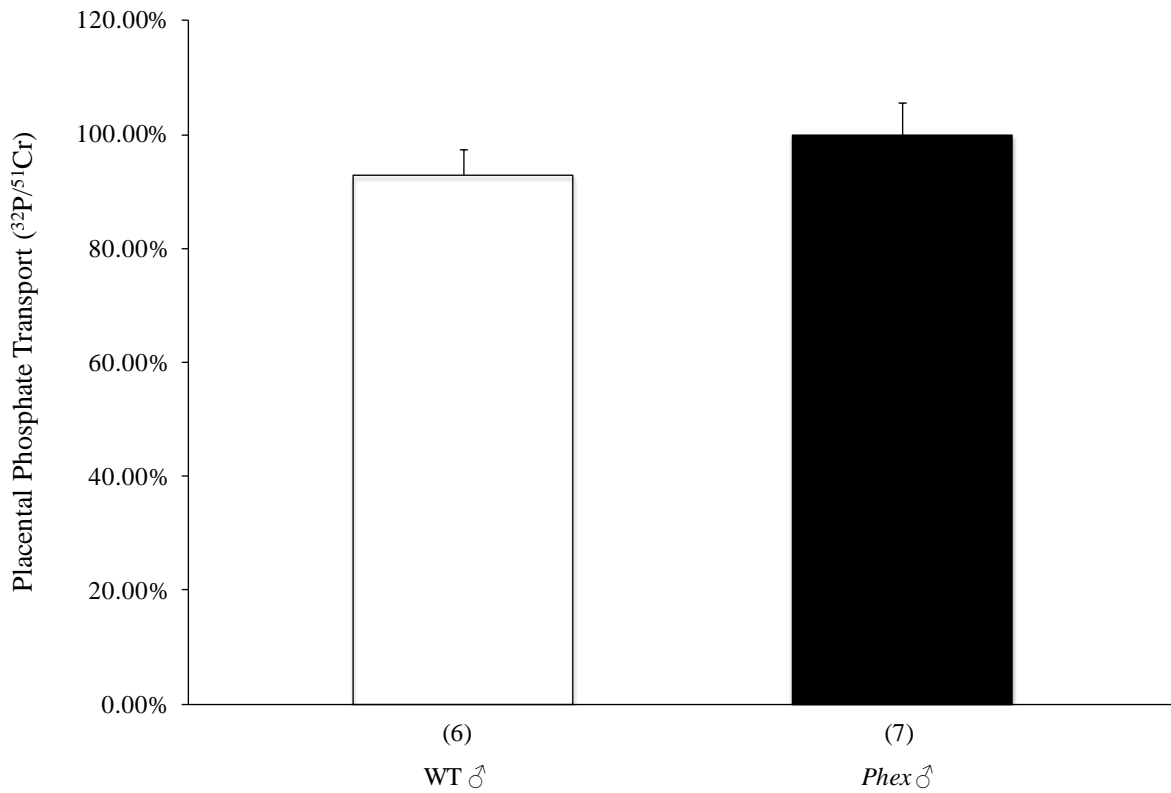


**Figure 18: Placental Phosphate Transport (<sup>32</sup>P/<sup>51</sup>Cr-EDTA) in ED 17.5 *Phex* Fetuses.** When normalized to <sup>51</sup>Cr, placental phosphate transfer on ED 17.5 was not different in *Phex* ♂ fetuses compared to WT ♂. The numbers in parentheses indicate the number of fetuses studied.

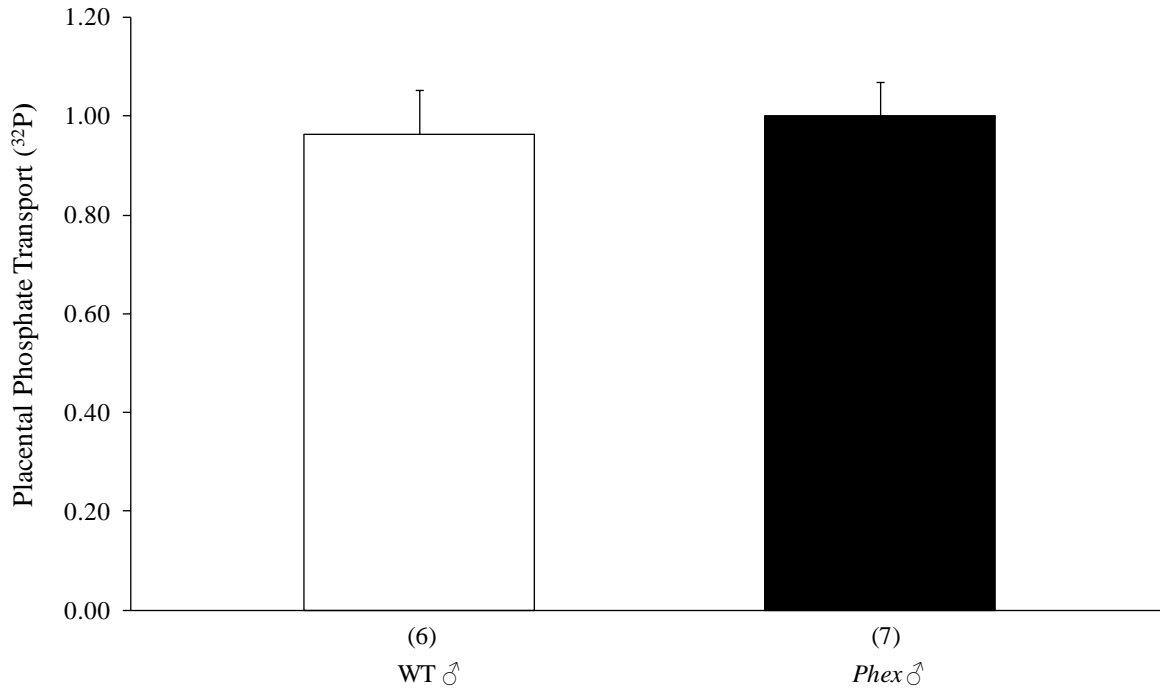


**Figure 19: Placental Phosphate Transport (<sup>32</sup>P) in ED17.5 *Phex* Fetuses.** Without normalization to <sup>51</sup>Cr, placental phosphate transfer on ED 17.5 was not changed in *Phex* ♂ fetuses either. The numbers in parentheses indicate the number of fetuses studied.

### 3.1.5 Skeletal Mineral Content in *Phex* Fetuses on ED18.5

The results above demonstrated that serum and amniotic fluid phosphate was not significantly changed in *Phex* ♂ fetuses, as well as placental phosphate transport. It could be possible that the methods of measuring serum/amniotic phosphate levels and placental phosphate transport were not sensitive enough to detect small differences that were present between *Phex* nulls and WT. If there were true differences between the two genotypes, the skeletal mineral content would be more likely to show a difference since it represents the net effect of phosphate metabolism over gestation, especially the last five days of it. Additionally, high levels of FGF23 are known to cause hypophosphatemic rickets and osteomalacia in adults. If excess FGF23 in fetuses has similar skeletal effects as in adults, skeletal mineral content and morphology in fetuses should be significantly altered. In this section, fetal bodies on ED 18.5 were reduced to ash in order to assess their mineral content. The results were presented by mineral content normalized to dry weights in order to eliminate the impact of different body weights. The results showed that *Phex* WT (♂ and ♀), *Phex* ♀ and *Phex* ♂ had identical body ash weight; more importantly, there were no significant changes in skeletal mineral content (phosphate, calcium and magnesium) in *Phex* ♂ fetuses compared to WT fetuses (**Figures 20 – 23**). Body ash weight and skeletal phosphate content of the fetuses of the *Phex* null model were also largely in-line with those of the fetuses of the *Fgf23* KO model [139].

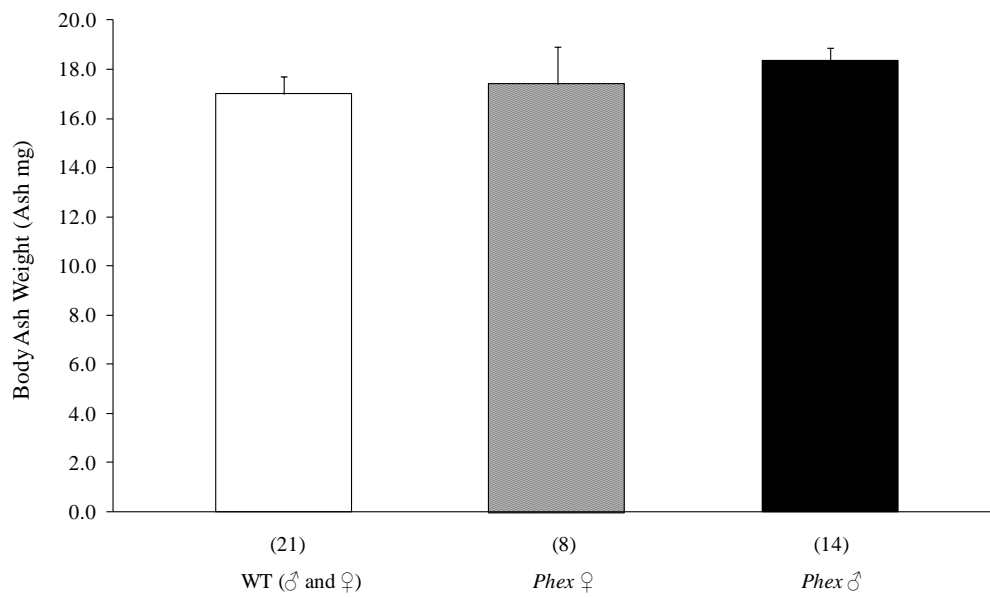


**Figure 20: Body Ash Weight in ED 18.5 *Phex* Fetuses.** There were no significant differences in body ash weight among *Phex* WT (♂ and ♀), *Phex* ♀ and *Phex* ♂ fetuses on ED 18.5. The numbers in parentheses indicate the number of fetuses studied.

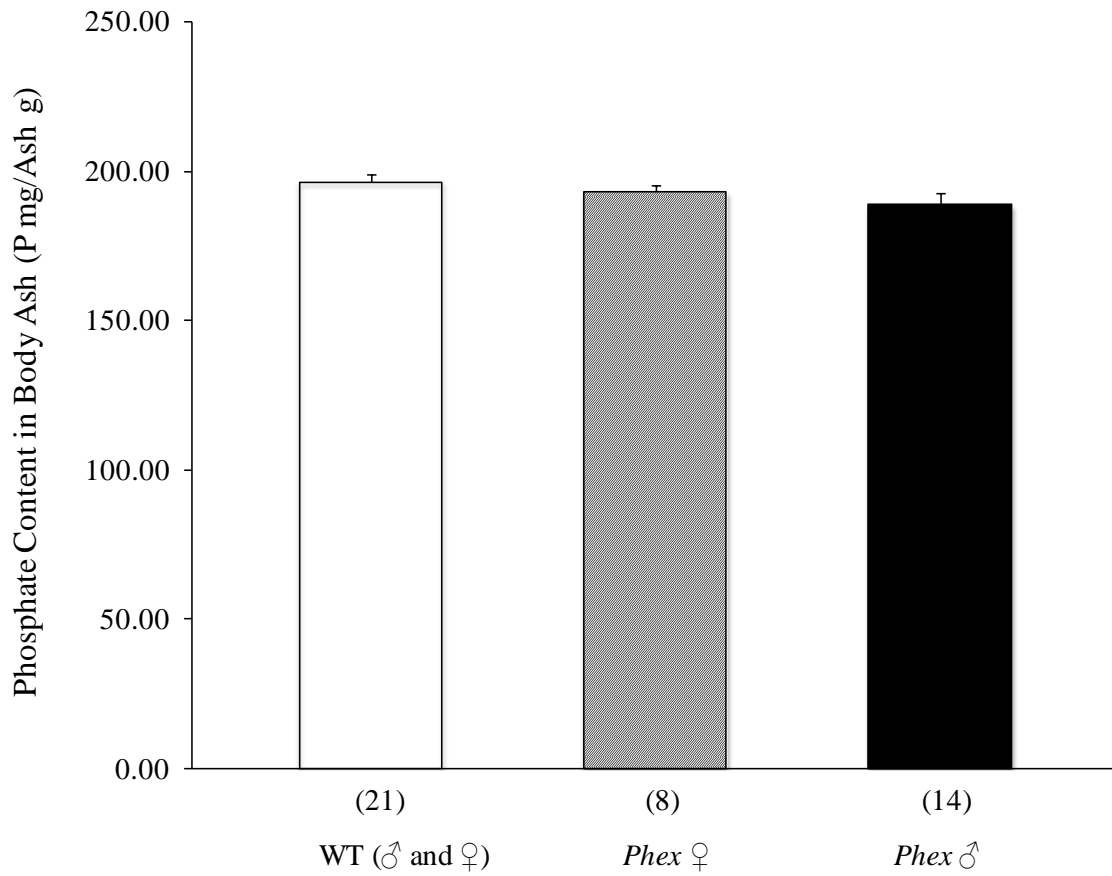


**Figure 21: Skeletal Phosphate Content in ED 18.5 *Phex* Fetuses.** Compared to WT fetuses, *Phex* ♂ fetuses demonstrated no significant changes in the skeletal content of phosphate on ED 18.5. The numbers in parentheses indicate the number of fetuses studied.

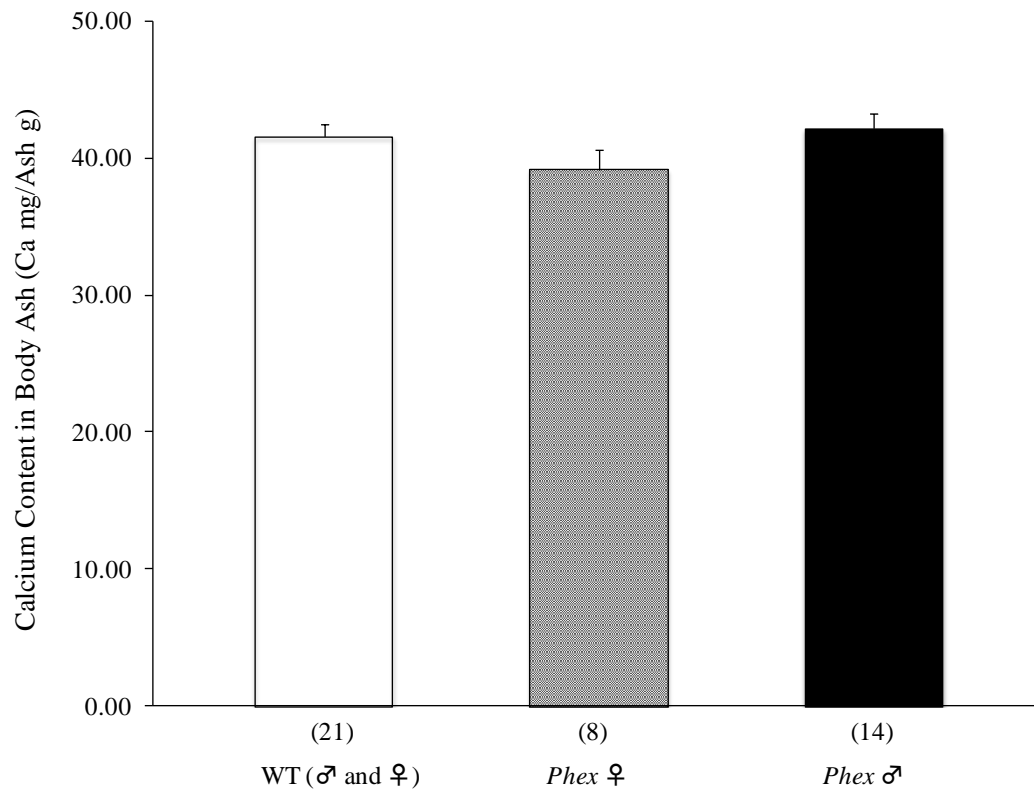


**Figure 22: Skeletal Calcium Content on in ED 18.5 *Phex* Fetuses.** Compared to WT fetuses, *Phex* ♂ fetuses had similar skeletal content of calcium on ED 18.5. The numbers in parentheses indicate the number of fetuses studied.

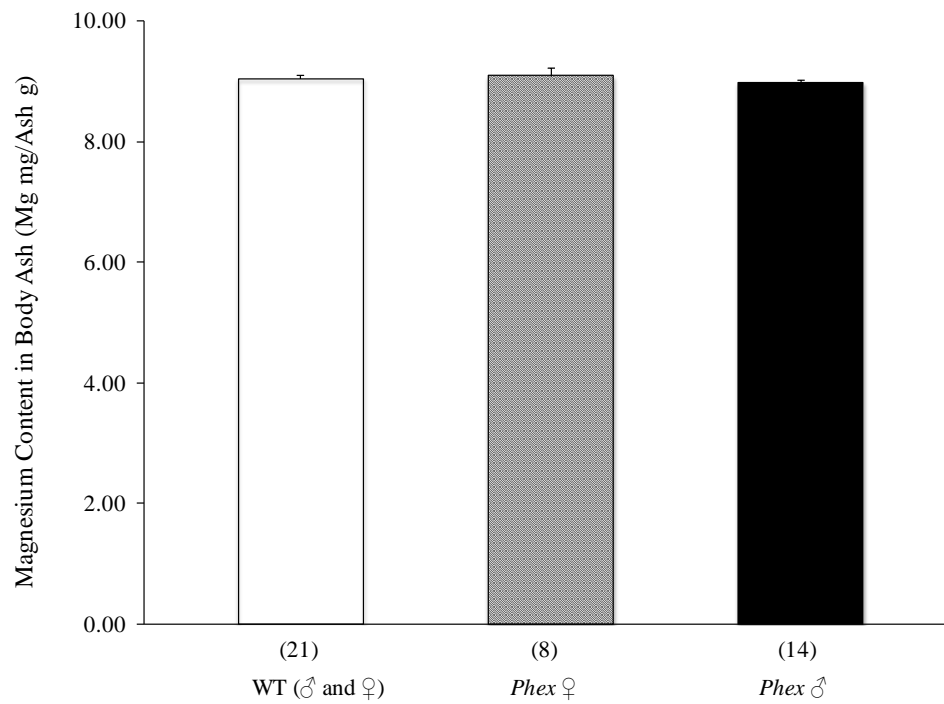
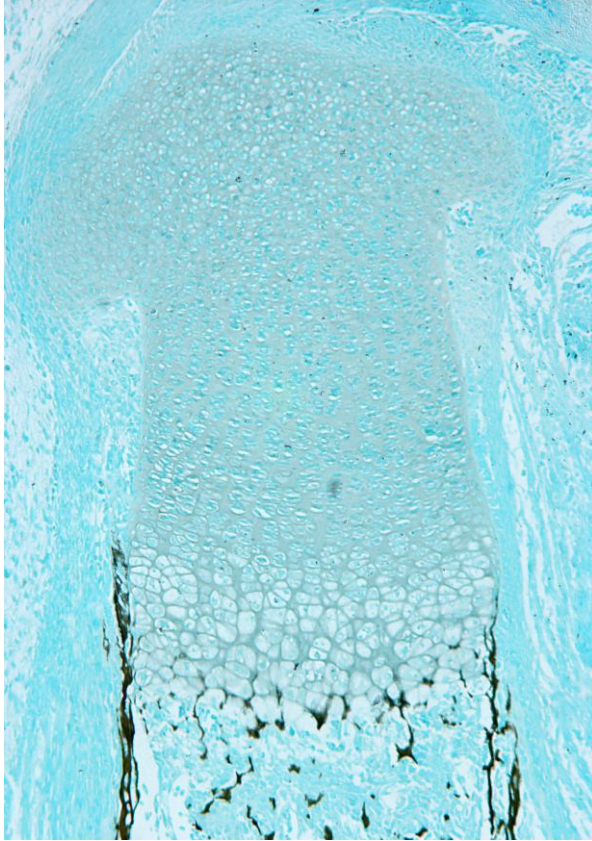


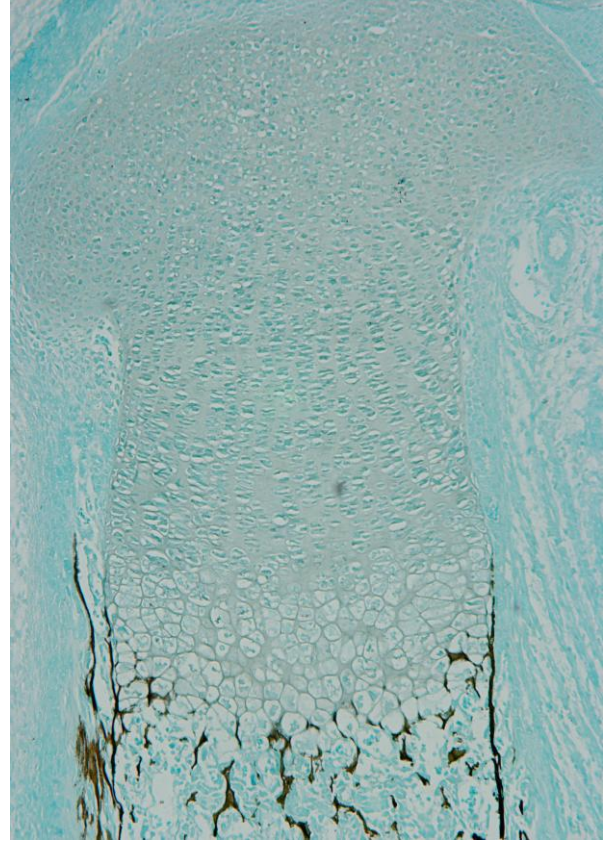
**Figure 23: Skeletal Magnesium Content in ED 18.5 *Phex* Fetuses.** There were no significant differences in skeletal magnesium content among *Phex* WT, *Phex* ♀ and *Phex* ♂ fetuses. The numbers in parentheses indicate the number of fetuses studied.

### 3.1.6 Bone Morphology and Mineralization in *Phex* Fetuses on ED18.5

It is known that phosphate stimulates apoptosis of hypertrophic chondrocytes during endochondral bone formation in fetuses – which is a critical step to ensure the bone develops robustly. In fetuses with hypophosphatemia, apoptosis of differentiated hypertrophic chondrocytes is impaired, leading to an expanded hypertrophic chondrocyte layer of the growth plate, as well as reduced mineral deposits in the bone. I originally expected the growth plate would be abnormal and mineral deposits would be highly decreased in *Phex* null fetuses; however, the results showed that the skeletal morphology and the mineralization pattern of *Phex* ♂ fetuses on ED 18.5 appeared similar to those of WT fetuses (**Figure 24**), suggesting that the skeletal scaffold of *Phex* ♂ fetuses develops robustly before birth, with normal tibial length and diaphysis and appropriate mineralization. The cellular morphology and growth plates were largely identical in *Phex* WT and *Phex* ♂ fetuses. In addition, both genotypes had no obvious differences in mineral deposition (the black areas in Figure 24 represent von Kossa's stain). It should be noted that the skeletal morphology and mineralization results were confirmed by the skeletal mineral (phosphate, calcium, and magnesium) content data discussed above, which demonstrated that *Phex* ♂ fetuses had similar content of phosphate, calcium, and magnesium as WT fetuses in the skeletons.



WT ♂



*Phex* ♂

**Figure 24: Skeletal Morphology and Mineralization in ED 18.5 *Phex* Fetuses.** Compared to WT fetuses, *Phex* ♂ fetuses appeared normal in terms of the amount of mineral deposition (the black areas) within the tibia and the morphology of growth plates.

### 3.1.7 Gene Expression Analysis on the *Phex* Placenta and Kidneys on ED18.5

FGF23 was significantly elevated in *Phex* ♂ fetuses, which might alter expression of its targeted genes. I examined expression of FGF23-targeted genes in the placenta and kidneys because the placenta represents the only source of phosphate to fetuses and the kidneys the only exit for phosphate – if excess FGF23 could impact serum phosphate in fetuses, the placenta and kidneys should be the most likely organs to act on. Although FGFR1 is the main receptor for FGF23, I also studied gene expression of the other three types of FGFR (FGFR2 – 4) as FGF23 might act on them when its serum concentrations were ultra-high in *Phex* ♂ fetuses. Normally, *Fgf23* expression in the placenta is low, which has been confirmed by the study conducted in the *Fgf23* KO model [139]. In the present experiment, the *Phex* ♂ placenta showed an increase in *Fgf23* expression, which approached statistical significance ( $p = 0.054$ ). *Fgf23* expression was absent in the kidneys of WT and male null fetuses. In terms of FGF23-targeted genes, *Cyp24a1* expression was significantly increased in the *Phex* ♂ kidneys and placenta – which might explain why serum calcitriol was significantly reduced in *Phex* ♂ fetuses (Figure 11) The majority of the remaining target genes showed no significant expression changes in the *Phex* ♂ kidneys and placenta, except for *Klotho* and *Fgfr2* in the kidneys (**Table 1**). However, the changes in these two genes were of small magnitude and questionable physiological significance – these changes might be chance findings.

**Table 1: List of FGF23-Targeted Genes in Placentas and Fetal Kidneys between *Phex* WT and Null Fetuses.**

Gene	Placenta			Fetal Kidneys		
	<i>Phex</i> WT (♂)	<i>Phex</i> ♂	p value	<i>Phex</i> WT (♂)	<i>Phex</i> ♂	p value
<i>Fgf23</i>	1.00±0.87	3.15±1.94	0.054	Undetectable	Undetectable	N/A
<i>Klotho</i>	1.00±0.16	1.17±0.12	0.103	<b>1.00±0.18</b>	<b>0.59±0.19</b>	<b>0.014</b>
<i>NaPi2a</i>	1.00±0.35	1.16±0.12	0.348	1.00±0.09	0.98±0.25	0.867
<i>NaPi2b</i>	1.00±0.31	1.01±0.29	0.953	1.00±0.20	0.81±0.05	0.071
<i>NaPi2c</i>	1.00±0.48	0.98±0.27	0.953	1.00±0.10	0.86±0.38	0.446
<i>Cyp24a1</i>	<b>1.00±0.36</b>	<b>7.00±3.54</b>	<b>0.030</b>	<b>1.00±0.46</b>	<b>5.58±1.77</b>	<b>0.001</b>
<i>Cyp27b1</i>	1.00±0.17	1.10±0.35	0.495	1.00±0.34	1.05±0.48	0.637
<i>Fgfr1</i>	1.00±0.19	0.85±0.08	0.276	1.00±0.09	0.87±0.11	0.068
<i>Fgfr2</i>	1.00±0.12	0.97±0.10	0.776	<b>1.00±0.08</b>	<b>0.83±0.08</b>	<b>0.011</b>
<i>Fgfr3</i>	1.00±0.40	0.76±0.07	0.357	1.00±0.11	0.89±0.19	0.283
<i>Fgfr4</i>	1.00±0.22	0.83±0.12	0.289	1.00±0.09	0.84±0.13	0.056

Gene	Gene Name
<i>Fgf23</i>	Fibroblast growth factor 23
<i>Klotho</i>	Klotho
<i>NaPi2a</i> or <i>Slc34a1</i>	Sodium-dependent phosphate transporter 2A or Solute carrier family 34 member 1
<i>NaPi2b</i> or <i>Slc34a2</i>	Sodium-dependent phosphate transporter 2B or Solute carrier family 34 member 2
<i>NaPi2c</i> or <i>Slc34a3</i>	Sodium-dependent phosphate transporter 2C or Solute carrier family 34 member 3
<i>Cyp24a1</i>	1,25-dihydroxyvitamin D(3) 24-hydroxylase
<i>Cyp27b1</i>	25-hydroxyvitamin D-1 alpha hydroxylase
<i>Fgfr1</i>	Fibroblast growth factor receptor 1
<i>Fgfr2</i>	Fibroblast growth factor receptor 2
<i>Fgfr3</i>	Fibroblast growth factor receptor 3
<i>Fgfr4</i>	Fibroblast growth factor receptor 4

### 3.1.8 Control Studies in *Phex* WT Dams on ED18.5

In the studies above, the *Phex*<sup>+/-</sup> dams were abnormal because serum FGF23 was highly increased and serum phosphorus was reduced. In order to determine if maternal phenotypes would have an impact on fetuses via serum phosphorus and FGF23 or somehow via the genotypes, I measured serum phosphorus and FGF23 in fetuses derived from WT females mated to *Phex* null males – the genotypes of offspring included *Phex* WT ♂ and *Phex* ♀ fetuses.

As to serum FGF23 in *Phex* WT ♂ and *Phex* ♀ fetuses, the results showed that serum FGF23 in the latter was 10 fold as high as that in the former. In addition, serum FGF23 in *Phex* ♀ fetuses was highly increased compared to values of WT dams. Serum FGF23 in WT dams at late pregnancy (LP) on ED 18.5 was 2.5 fold as high as that in WT dams at baseline (BL) – which was consistent with what Dr. Kovacs's Laboratory has previously reported that maternal intact FGF23 doubled during pregnancy compared with pre-pregnant values [165] (**Figure 25**).

As to serum phosphorus, there were no significant differences between WT ♂ and *Phex* ♀ fetuses (**Figure 26**). Serum phosphorus in fetuses was significantly higher than that in WT dams. These results confirm that neither fetal genotype nor maternal genotype would affect fetal serum phosphorus.

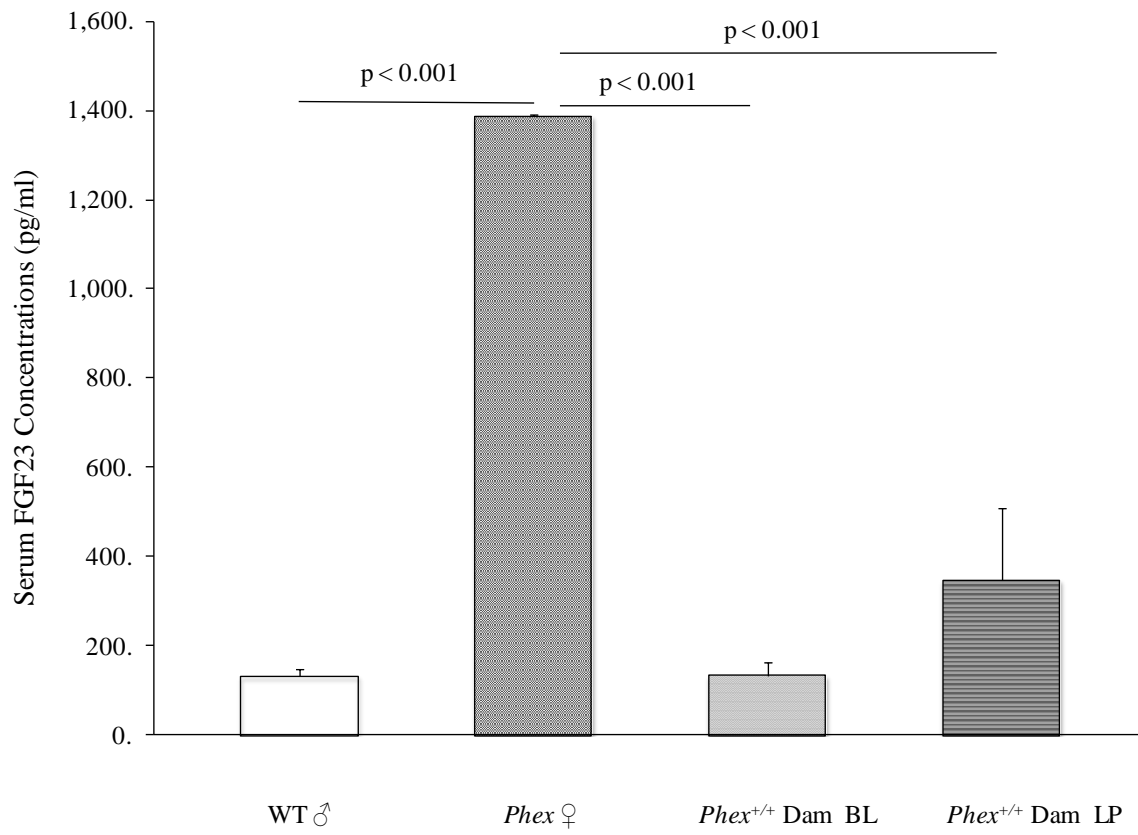


**Figure 25: Serum FGF23 in *Phex* Fetuses from WT Dams Mated to *Phex* Null Males.** *Phex* ♀ fetuses from WT dams mated to *Phex* null males had significant higher serum FGF23 than WT ♂ siblings, *Phex*<sup>+/+</sup> (WT) dams at baseline (BL), and at late pregnancy on ED 18.5 (LP). The numbers in parentheses indicate the number of fetuses studied.

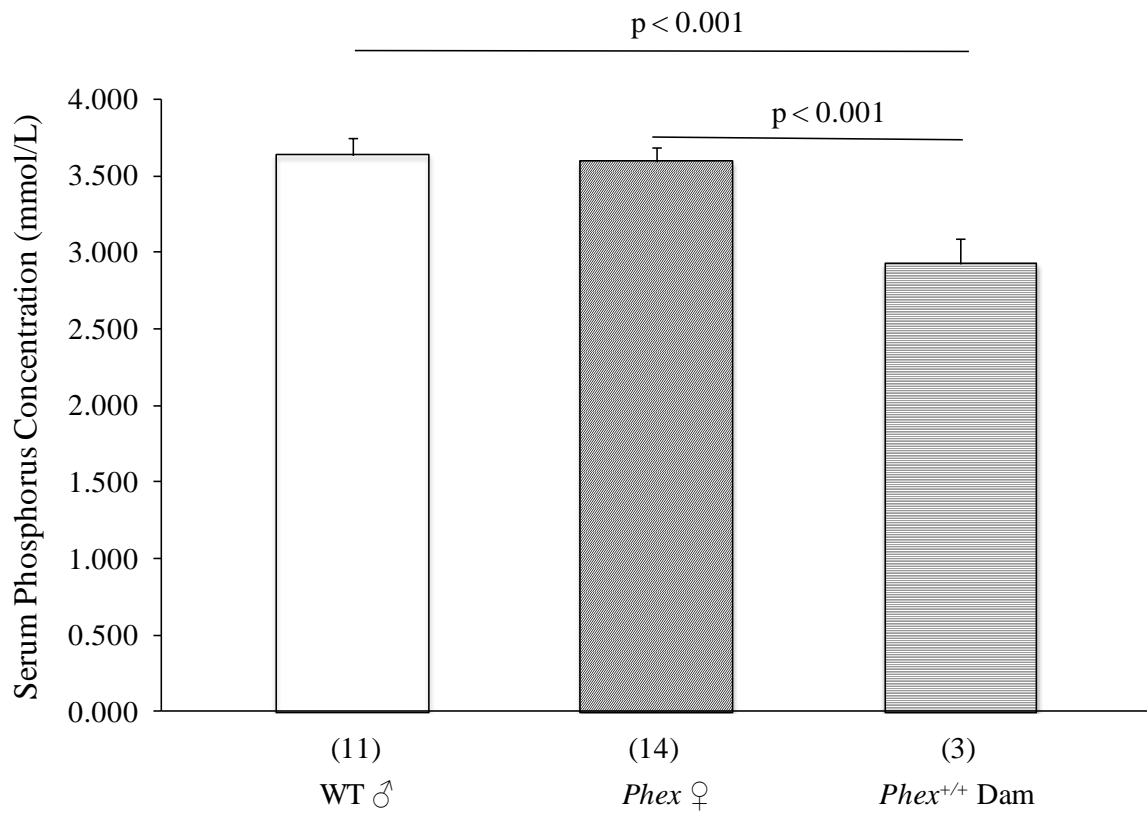


**Figure 26: Fetal Serum Phosphorus of Fetuses from *Phex* WT Dams Mated to *Phex* Null Males.** WT ♂ and *Phex* ♀ fetuses from WT dams mated to *Phex* null males had similar levels of serum phosphorus. Fetal serum phosphorus was significantly higher than WT dams'. The numbers in parentheses indicate the number of fetuses studied.

### 3.1.9 Microarray Analysis on the *Phex* and *Fgf23* Null Placentas

To confirm that excess or deficient FGF23 does not importantly alter placental expression of *Fgf23*-targeted genes (apart from the change in *Cyp24a1* expression), genome-wide microarray analyses were carried out on the *Fgf23* null, *Phex* null and matching WT littermate placentas. No significant changes in gene expression were noted between the *Phex* null and WT placentas, or between the *Fgf23* null and corresponding WT placentas (data not shown). It should be noted that  $p < 0.01$  was used in the microarray analysis to determine whether a gene expression change was significant. Although qPCR analysis showed the expression of *Cyp24a1* in the *Phex* null placenta was significantly increased (**Table 1**), the p value in that experiment was only 0.03. It could be the reason why microarray analysis did not show a significant change in placental *Cyp24a1* expression.

### 3.2 Results from *Klotho* Null Fetuses

In the experiments above, it was shown that excess FGF23 in *Phex* null fetuses did not change any parameter of fetal mineral homeostasis, including serum and amniotic fluid phosphate, skeletal morphology, skeletal mineral content, and placental phosphate transport. Although *Cyp24a1* was significantly increased in the *Phex* null placenta and fetal kidneys, the increase in gene expression did not disturb any parameter related to phosphate. It is also discussed in the introduction section that loss of FGF23 in *Fgf23* null fetuses did nothing to phosphate metabolism and fetal bone development either, although expression of *Cyp24a1* in the *Fgf23* null kidneys was significantly reduced. The purpose of studying phosphate related phenotypes in *Klotho* null fetuses was to confirm that loss of *Klotho* should be equivalent to loss of FGF23, as well as, to ensure that another FGF would not be compensating for absence of FGF23 by acting on *Klotho*.

#### 3.2.1 Serum Hormones in *Klotho* Fetuses on ED18.5

Serum FGF23 is significantly increased in adult *Klotho* nulls to compensate a disruption in the FGF23 pathway. Therefore, I originally expected serum FGF23 to behave in the same way in *Klotho* null fetuses. Contrarily, there were no significant differences in serum FGF23 on ED 18.5 among WT, HET, and null fetuses (**Figure 27**). *Klotho* HET dams on ED 18.5 had significantly higher FGF23 compared to fetuses of all genotypes. Similar to calcitriol in *Fgf23* null fetuses, calcitriol in *Klotho* null fetuses was not altered on ED18.5 either (**Figure 28**). As to serum PTH, it was numerically decreased in *Klotho* null fetuses compared to WT on ED18.5 (**Figure 29**). In adults PTH is normally suppressed in *Klotho* nulls due to hypercalcemia as a result of high serum calcitriol.

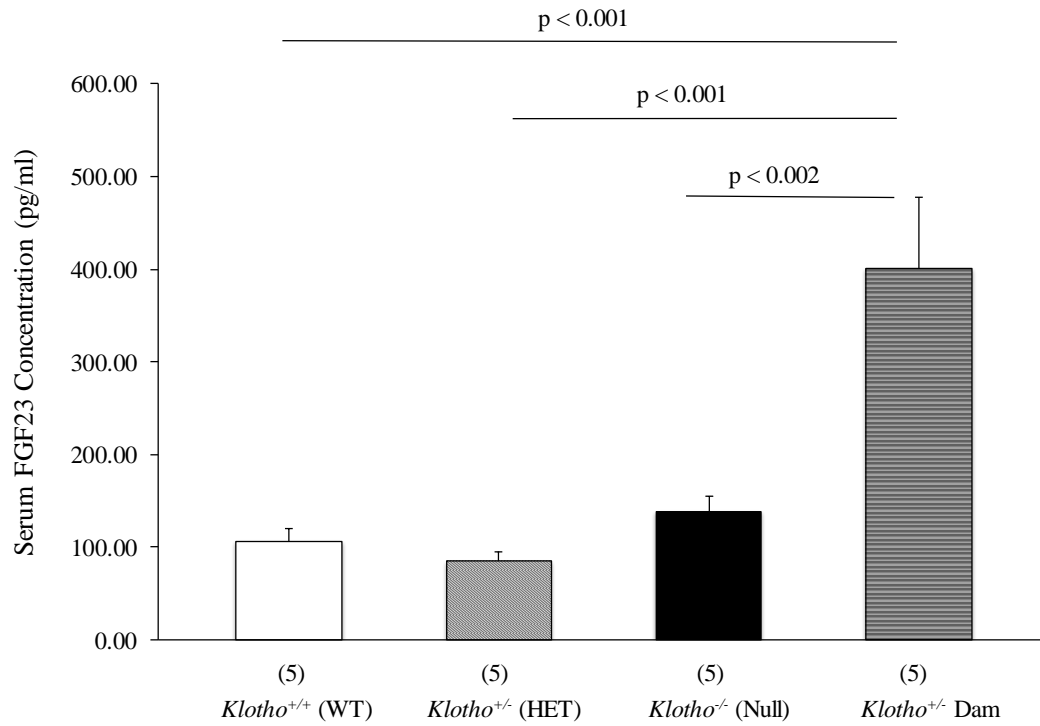


**Figure 27: Serum FGF23 in ED18.5 *Klotho* Fetuses.** There were no significant differences in serum FGF23 on ED 18.5 among *Klotho* WT, HET, and null fetuses. *Klotho* HET dams on ED 18.5 had significantly higher FGF23 than all fetuses. The numbers in parentheses indicate the number of fetuses studied.

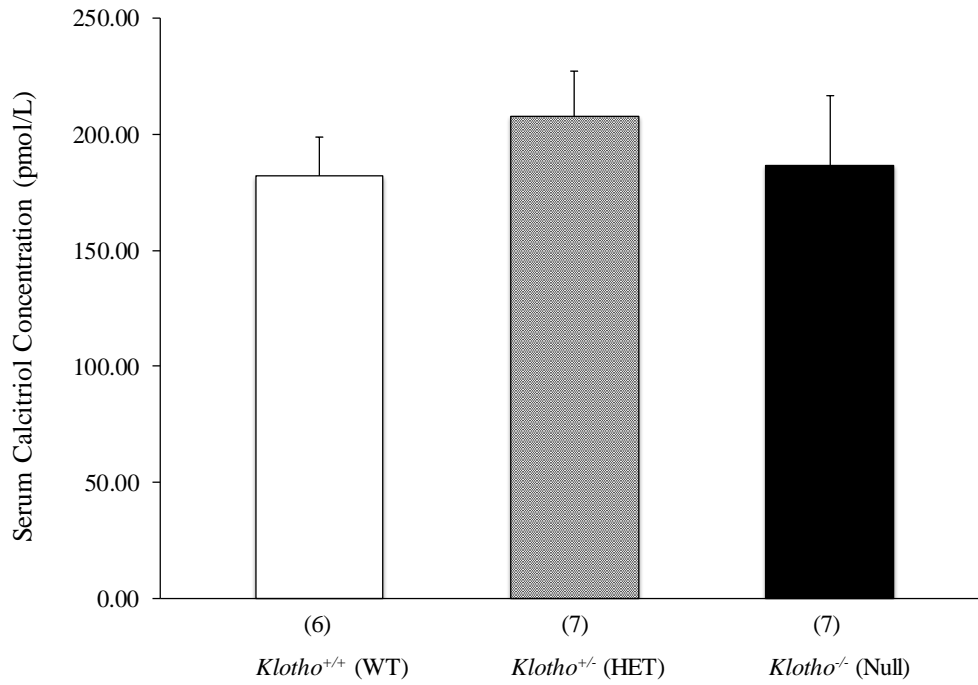


**Figure 28: Serum Calcitriol in ED18.5 *Klotho* Fetuses.** Serum calcitriol in *Klotho* null fetuses was not different as compared to that in WT. The numbers in parentheses indicate the number of fetuses studied.

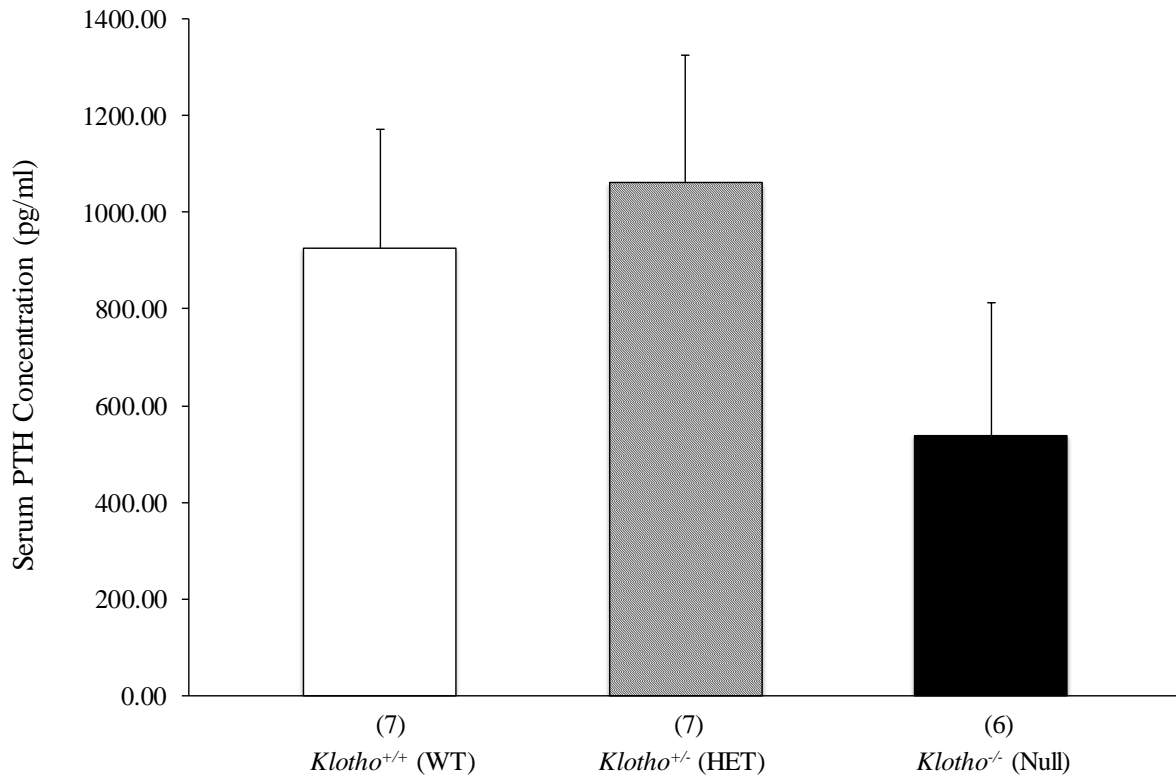


**Figure 29: Serum PTH in ED 18.5 *Klotho* Fetuses.** On ED 18.5, *Klotho* null fetuses had numerically lower serum PTH than WT fetuses (non-significant). The numbers in parentheses indicate the number of fetuses studied.

### 3.2.2 Serum Chemistries in *Klotho* Fetuses on ED18.5

*Klotho* nulls develop hyperphosphatemia postnatally as the FGF23 pathway does not function. I originally expected serum phosphorus to increase in *Klotho* null fetuses. However, results demonstrated that *Klotho* null fetuses on ED 18.5 had similar levels of serum phosphorus as WT and HET fetuses – a similar case as in *Fgf23* null fetuses (**Figure 30**). Fetuses of all genotypes had hyperphosphatemia compared to HET dams ( $1.94 \pm 0.04$  mmol/L), which was physiologically normal. *Klotho* WT, HET, and null fetuses on ED 18.5 had the same levels of serum total calcium (**Figure 31**). HET dams had non-significantly higher serum total calcium than all fetuses.

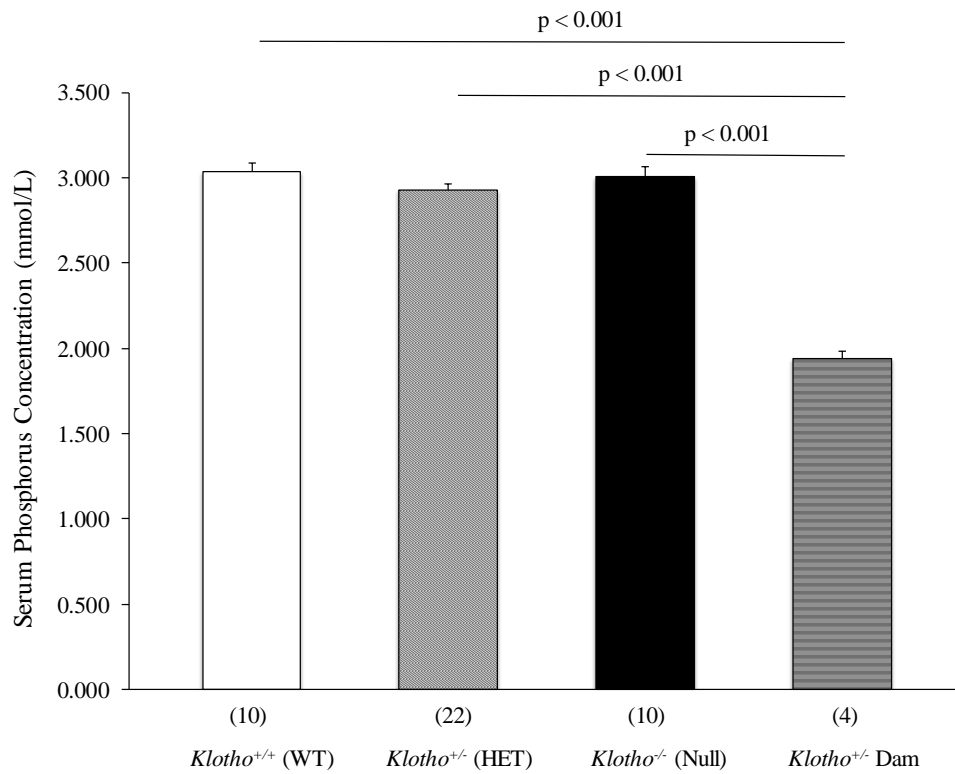


**Figure 30: Serum Phosphorus in ED 18.5 *Klotho* Fetuses.** There were no significant differences in serum phosphorus on ED 18.5 among *Klotho* WT, HET, and null fetuses. All *Klotho* fetuses had hyperphosphatemia compared to HET dams. The numbers in parentheses indicate the number of fetuses studied.

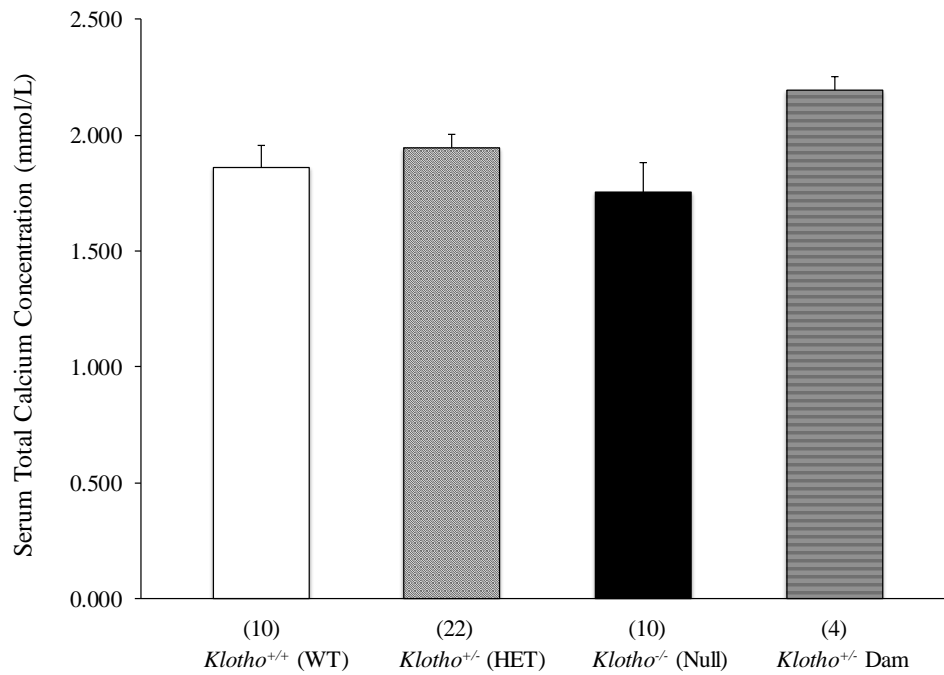


**Figure 31: Serum Total Calcium in ED 18.5 *Klotho* Fetuses.** There were no significant differences in serum total calcium on ED 18.5 among *Klotho* WT, HET, and null fetuses. HET dams had non-significantly higher serum total calcium than all fetuses. The numbers in parentheses indicate the number of fetuses studied.

### 3.2.3 Amniotic Fluid Chemistries in *Klotho* Null Fetuses on ED17.5

Because amniotic fluid is largely fetal urine and because renal phosphate excretion is largely reduced in *Klotho* nulls postnatally, I originally expected loss of *Klotho* to lead to a reduction in amniotic fluid phosphorus in *Klotho* null fetuses. However, the results demonstrated that there were no significant differences in amniotic fluid phosphorus among *Klotho* WT, HET, and null fetuses (**Figures 32**).

As to calcium, it is not impacted during postnatal period by lack of *Klotho*. Therefore, I did not expect amniotic fluid calcium to be changed in *Klotho* null fetuses – the results were in-line with my expectations. It should be pointed out that if the non-significant reduction in PTH observed in *Klotho* nulls is real (**Figure 29**), amniotic fluid calcium should increase – however, this was not seen in **Figure 33**, suggesting the observed reduction in PTH in *Klotho* nulls is just a numerical change and not a physiologically significant one.

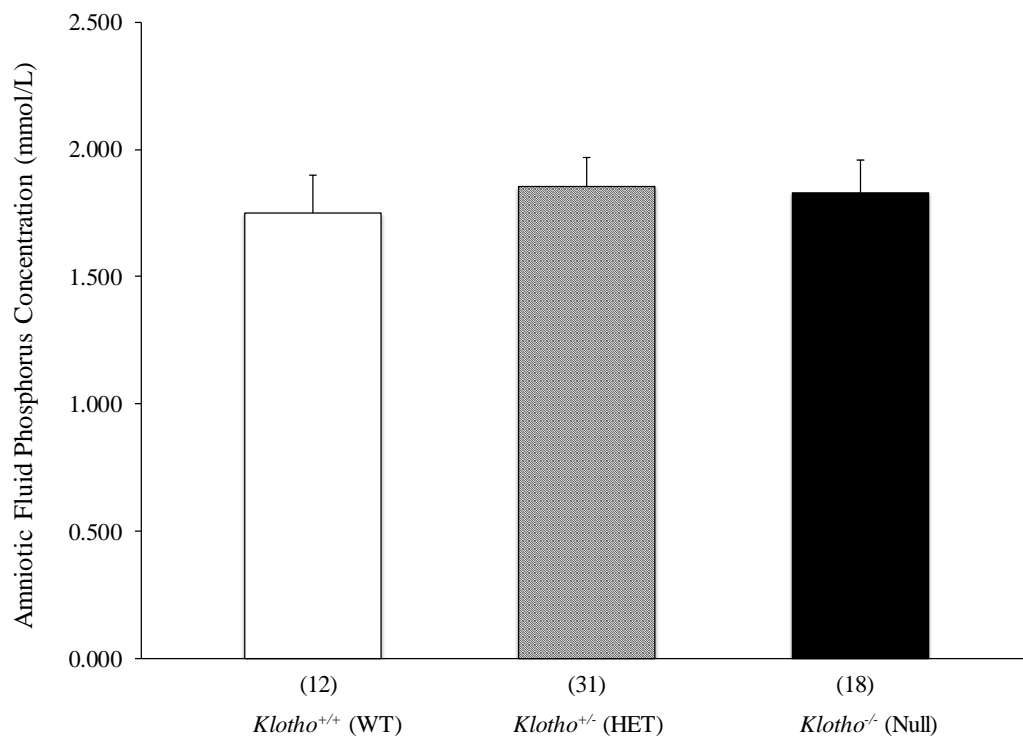


**Figure 32: Amniotic Fluid Phosphorus in ED 17.5 *Klotho* Fetuses.** *Klotho* WT, HET, and null fetuses had similar levels of amniotic fluid phosphorus on ED 17.5. The numbers in parentheses indicate the number of fetuses studied.

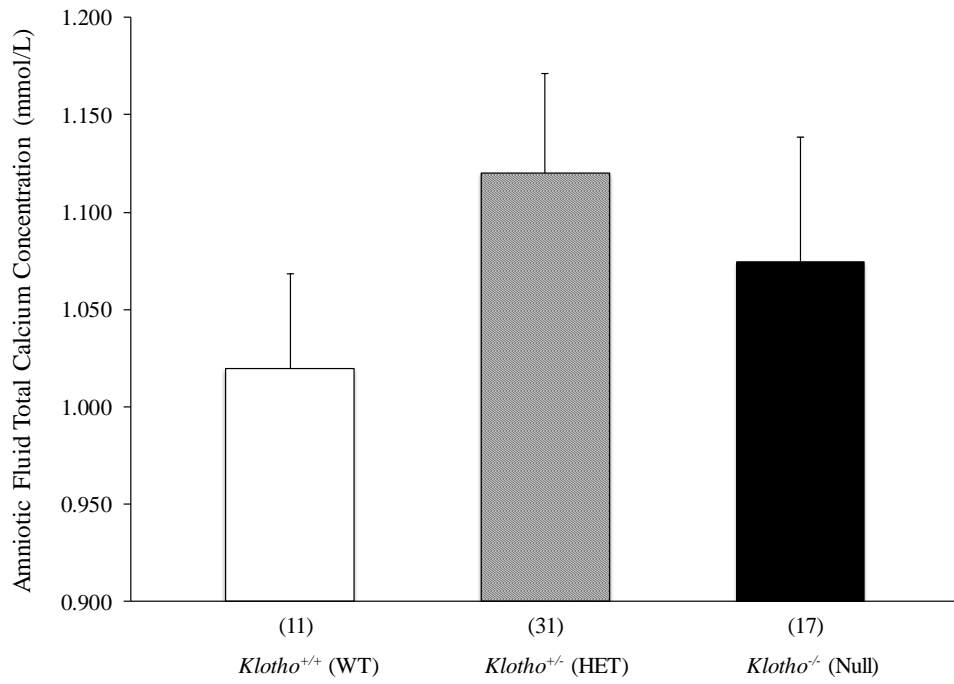


**Figure 33: Amniotic Fluid Total Calcium in ED 17.5 *Klotho* Fetuses.** There were no significant differences in amniotic fluid calcium on ED 17.5 among *Klotho* WT, HET, and null fetuses. The numbers in parentheses indicate the number of fetuses studied.

### 3.2.4 Placental Phosphate Transport in *Klotho* Fetuses on ED17.5

The rate of placental phosphate transport was measured in two ways: with a  $^{51}\text{Cr}$ -EDTA correction and without the correction. Because  $^{51}\text{Cr}$ -EDTA only diffuses across the placenta passively, it serves as a control for differences in flow rate among individual placentas in one litter.  $^{32}\text{P}$ , however, is actively transported across the placenta from dams to fetuses. Thus, by normalizing for the rate of diffusion (using the  $^{51}\text{Cr}$ -EDTA) the relative rate of placental phosphate transfer in each fetus in the same litter can be determined. The results demonstrated that placental phosphate transport as measured by  $^{32}\text{P}$  normalized to  $^{51}\text{Cr}$  in *Klotho* null fetuses was not changed compared to WTs and HETs. Without  $^{51}\text{Cr}$  normalization, the results were the same (**Figures 34 & 35**).

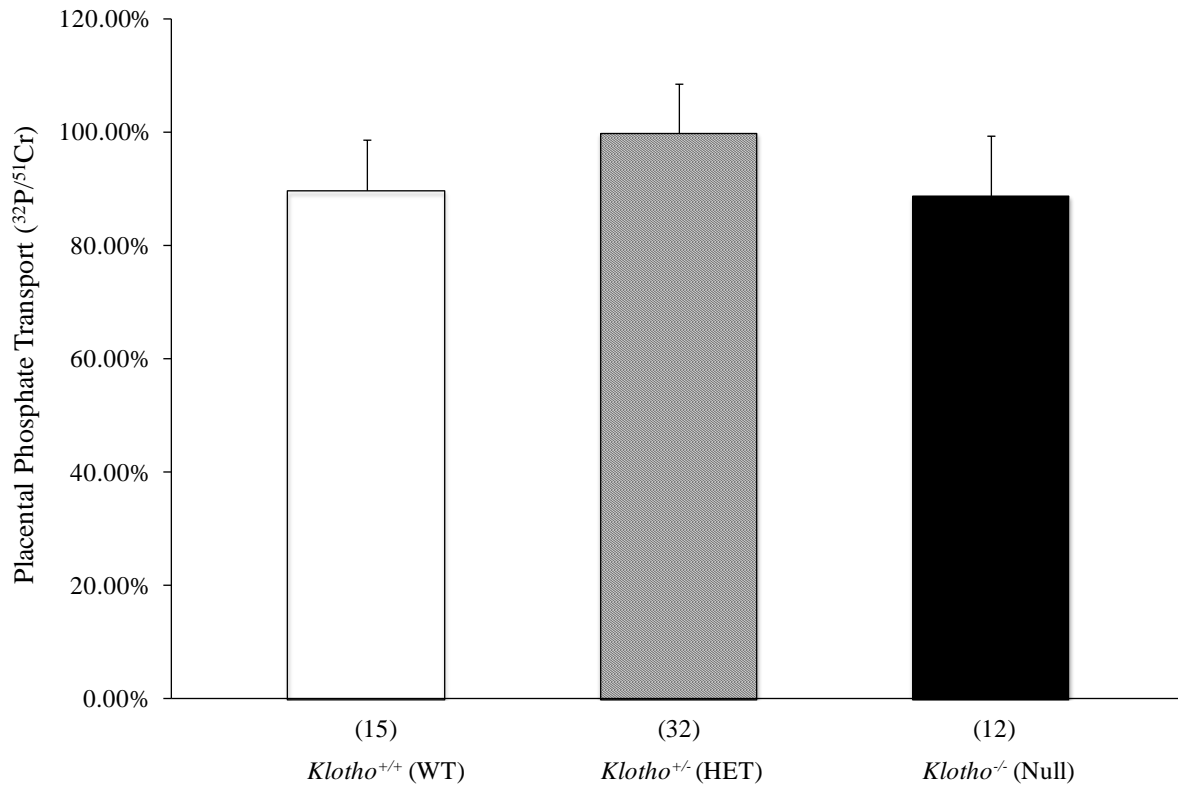


**Figure 34: Placental Phosphate Transport ( $^{32}\text{P}/^{51}\text{Cr}$ ) in ED 17.5 *Klotho* Fetuses.** *Klotho* WT, HET, and null fetuses had a similar process of placental phosphate transport (as measured by  $^{32}\text{P}$  normalized to  $^{51}\text{Cr}$ ) on ED 17.5. The numbers in parentheses indicate the number of fetuses studied.

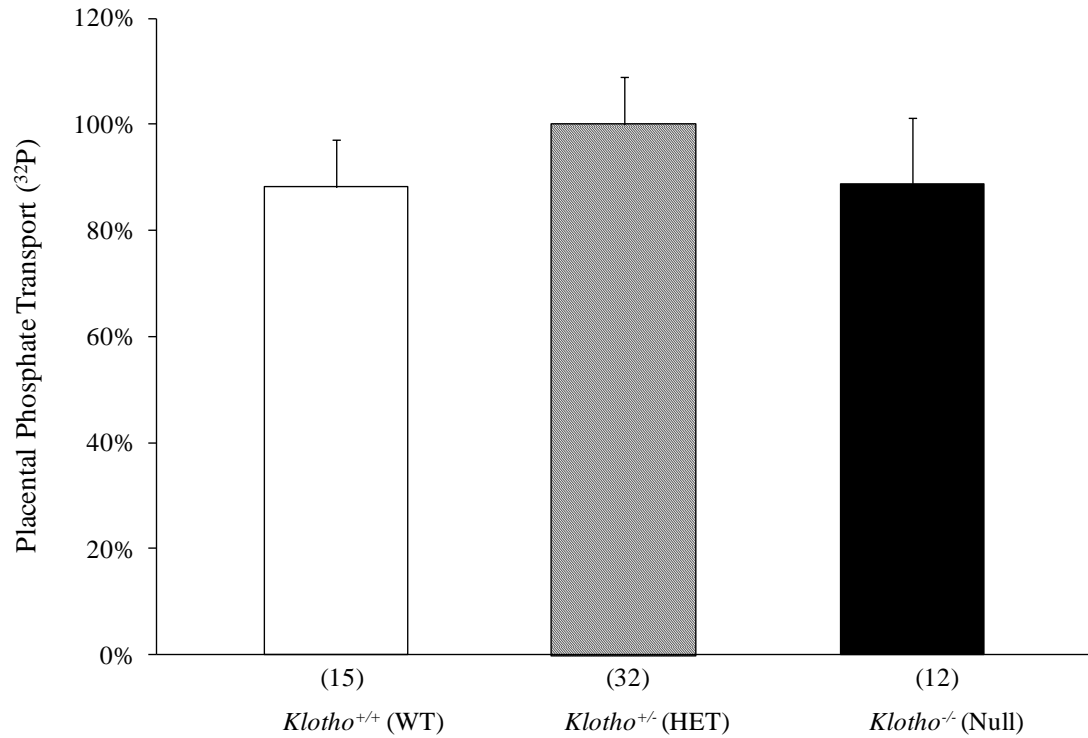


**Figure 35: Placental Phosphate Transport (<sup>32</sup>P) in ED 17.5 *Klotho* Fetuses.** *Klotho* WT, HET, and null fetuses had a similar process of placental phosphate transport (as measured by <sup>32</sup>P without <sup>51</sup>Cr normalization) on ED 17.5. The numbers in parentheses indicate the number of fetuses studied.

### 3.2.5 Skeletal Mineral Content in *Klotho* Fetuses on ED18.5

Since the skeleton contains the largest amount of phosphate in the body, any difference in serum/amniotic fluid phosphate or placental phosphate transport should lead to a change in ash weight and, more specifically, skeletal phosphate content. In adult *Klotho* null mice, skeletal phosphate content is increased due to hyperphosphatemia. Based on the adult phenotype, I originally expected body ash weight and skeletal phosphate content to increase in *Klotho* null fetuses – however, the results showed that there was no difference between WT and null, which was consistent with no changes in serum/amniotic fluid phosphate or placental phosphate transport. Skeletal content of calcium and magnesium was not altered in *Klotho* null fetuses either. It is noteworthy that if there were any extraskeletal calcium/phosphate deposits, they would be registered in body ash weight measurement because the minerals all remained behind regardless of whether they were in the skeleton or not. The results showed *Klotho* WT and null fetuses had equal weight of body ash – confirming the total amount of phosphate in the null was not changed (**Figures 36 – 39**). Body ash weight and skeletal phosphate content of the fetuses of the *Klotho* model were also largely in-line with those of the fetuses of the *Fgf23* KO model [139].

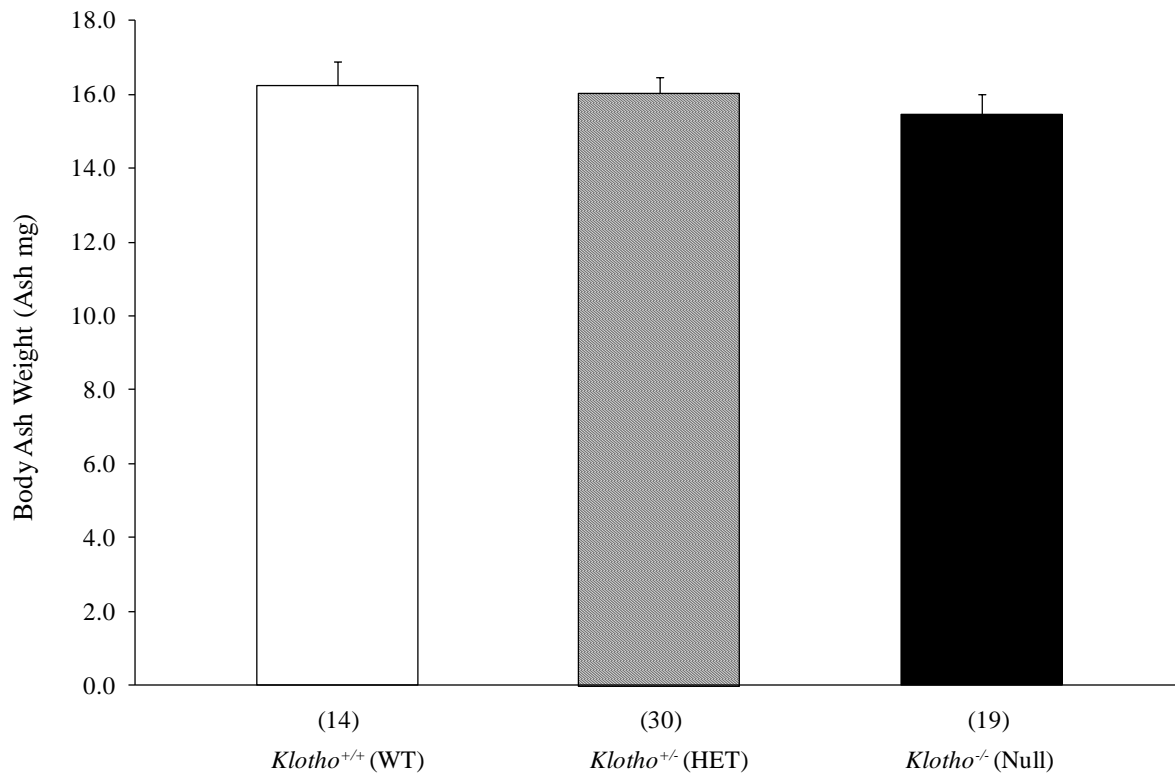


**Figure 36: Body Ash Weight in ED 18.5 *Klotho* Fetuses.** There were no changes in body ash weight in *Klotho* null fetuses on ED 18.5. The numbers in parentheses indicate the number of fetuses studied.

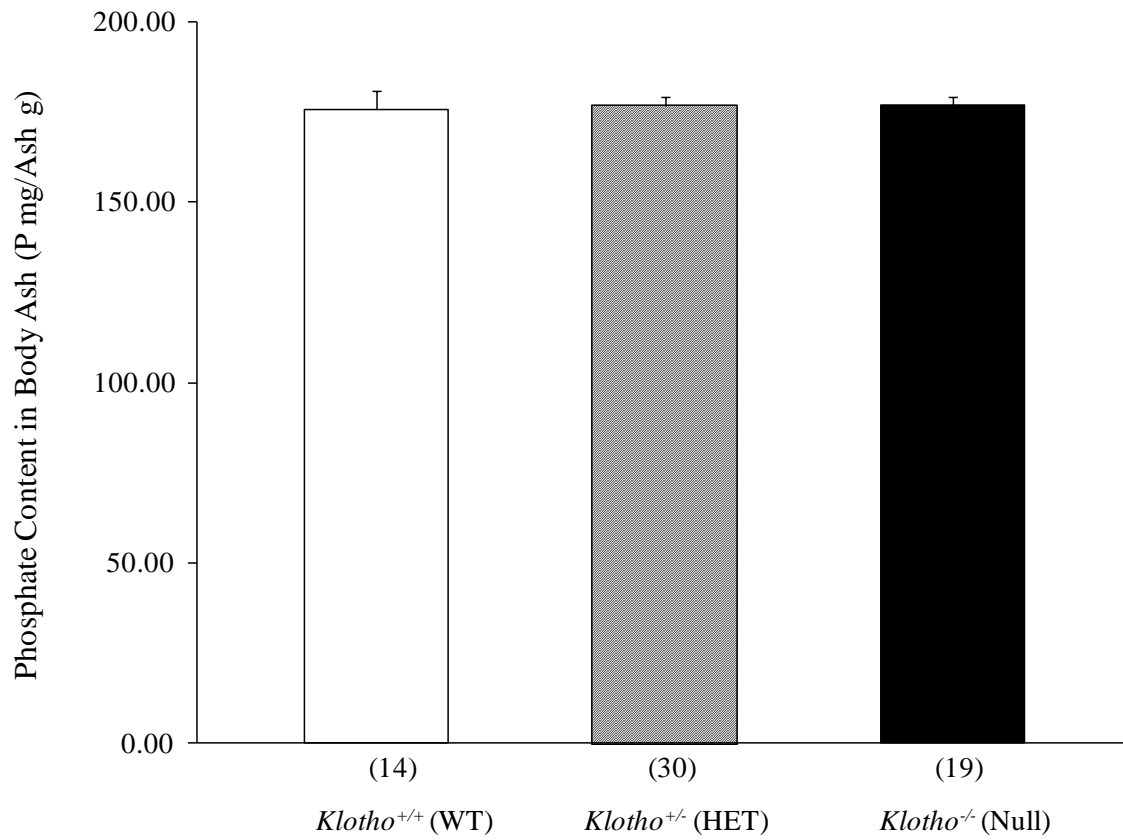


**Figure 37: Skeletal Phosphate Content in ED 18.5 *Klotho* Fetuses.** *Klotho* null fetuses demonstrated no significant changes in the skeletal content of phosphate on ED 18.5. The numbers in parentheses indicate the number of fetuses studied.

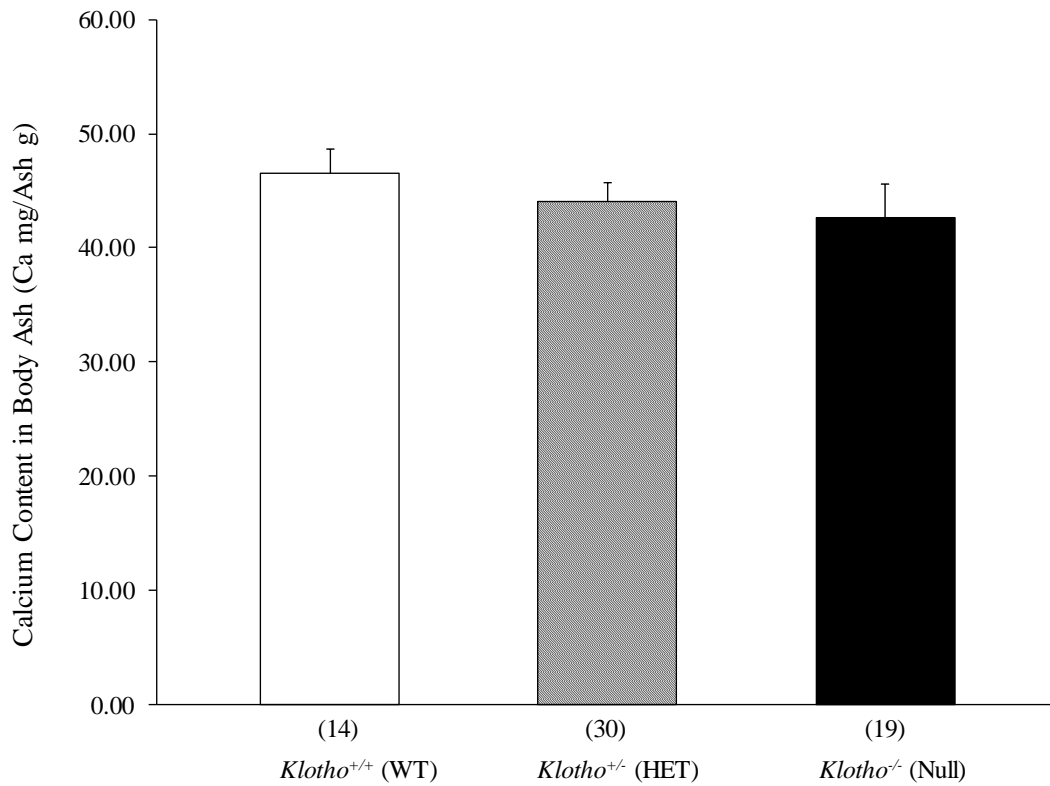


**Figure 38: Skeletal Calcium Content on in ED 18.5 *Klotho* Fetuses.** *Klotho* null fetuses had a similar skeletal content of calcium on ED 18.5. The numbers in parentheses indicate the number of fetuses studied.

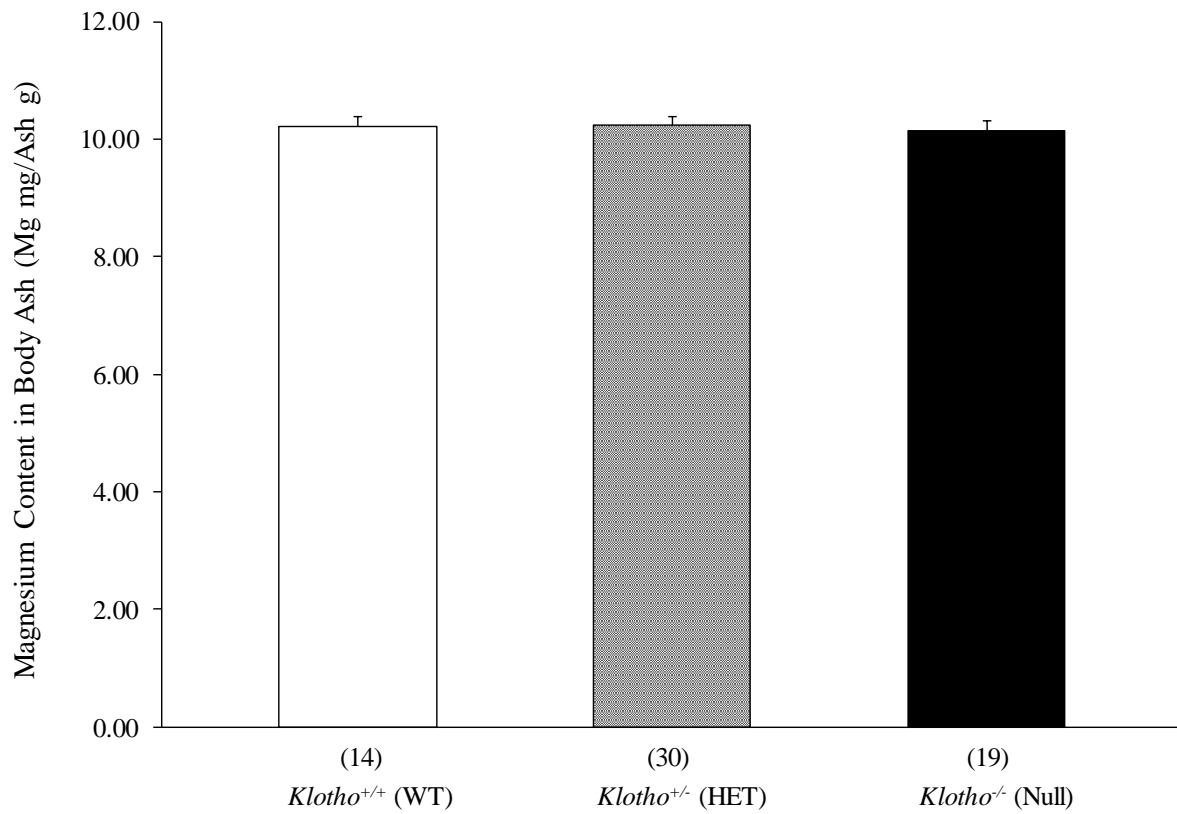
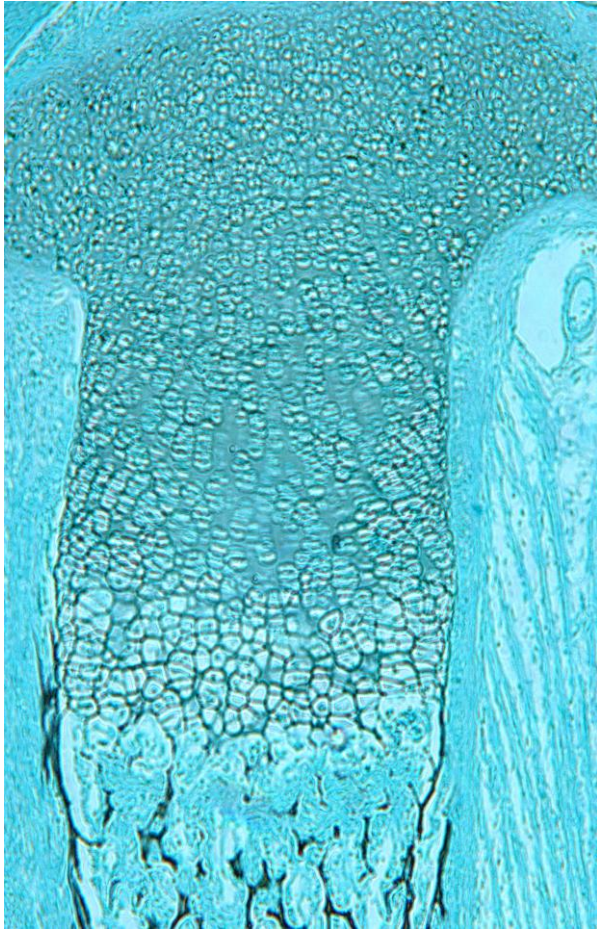


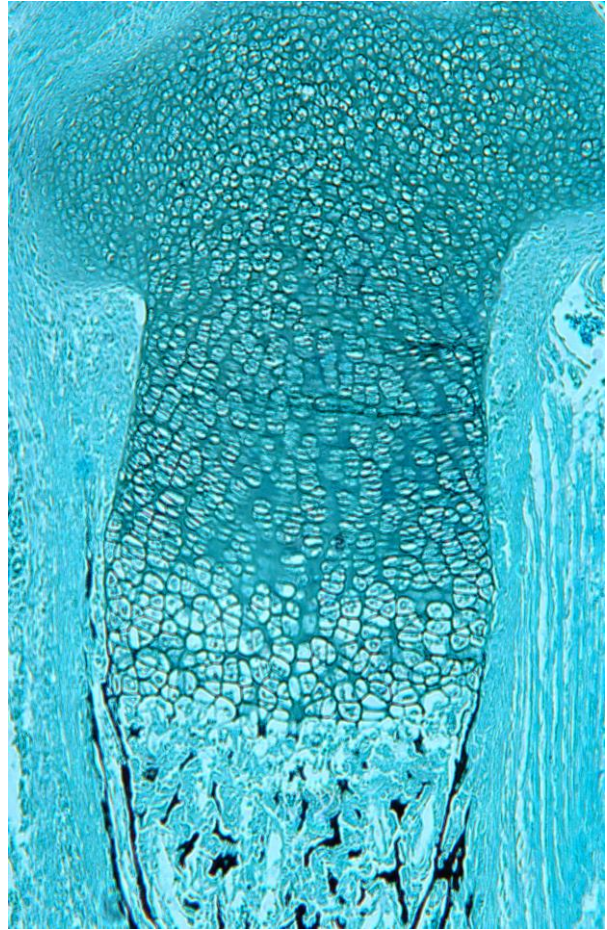
**Figure 39: Skeletal Magnesium Content in ED 18.5 *Klotho* Fetuses.** There were no significant differences in the skeletal magnesium content among *Klotho* WT, HET, and null fetuses. The numbers in parentheses indicate the number of fetuses studied.

### 3.2.6 Bone Morphology and Mineralization in *Klotho* Fetuses on ED18.5

Phosphate stimulates apoptosis of hypertrophic chondrocytes during endochondral bone formation in fetuses, a critical step to ensure robust bone development. Fetuses with hyperphosphatemia develop premature apoptosis of hypertrophic chondrocytes – leading to a shortened growth plate, as well as impaired mineral deposits. Based on this, I originally expected the growth plate would be impaired and mineral deposits would be increased in *Klotho* null fetuses; however, the results showed *Klotho* WT and nulls on ED18.5 had a largely identical pattern of tibia morphology (including growth plate) and mineralization (**Figure 40**).



*Klotho*<sup>+/+</sup> (WT)



*Klotho*<sup>-/-</sup> (Null)

**Figure 40: Skeletal Morphology and Mineralization in ED 18.5 *Klotho* Fetuses.** *Klotho* WT and null fetuses appeared to have a similar pattern of the growth plate morphology and mineralization. The black areas represent mineralization.

### 3.2.7 Gene Expression Analysis on the *Klotho* Placenta and Kidneys on ED18.5

It is known that in *Klotho* null adults serum FGF23 is significantly increased due to a compensatory mechanism. In contrast, Figure 27 demonstrated that serum FGF23 was only numerically elevated in *Klotho* null fetuses. While the increase in the fetuses was not as profound as that in the adults, it might still be able to alter expression of FGF23-targeted genes in the placenta and kidneys. The placenta represents the only source of phosphate to fetuses and the kidneys the only exit for phosphate – if loss of *Klotho* could alter serum phosphate in fetuses, FGF23-targeted gene expression should be changed on the two organs. The results first showed that *Klotho* WT fetuses had robust *Klotho* expression in the placenta and kidneys, which was absent in the null organs – confirming the *Klotho* KO model was valid. FGF23-targeted genes (*NaPi2a*, *NaPi2b*, *NaPi2c*, *Cyp27b1*, *Cyp24a*, and *Fgfr1–4*) were each expressed within the WT and null placentas, with *NaPi2b* displaying the most abundant expression among the sodium-phosphate co-transporters. Originally, I expect the expression of *Cyp27b1* to increase and the expression of *Cyp24a1* to decrease as calcitriol in adult *Klotho* nulls is elevated. I also expected the expression of *NaPi2a* and *NaPi2c* to increase as renal phosphate excretion in adult *Klotho* nulls is reduced. However, the results in *Klotho* null fetuses demonstrated the expression of none of those genes was altered (**Table 2**). A very low level of *Fgf23* expression (near the limit of detection) was detected in the WT and null placentas, which was also confirmed in the *Fgf23* KO model.

Since the *Fgf23* null kidneys showed a modest reduction in *Cyp24a1* expression that reached the threshold of statistical significance, and since the *Phex* null kidneys (and the placenta) showed opposite, and since the *Klotho* null kidneys showed no changes, I repeated the qPCR analysis

using a larger sample size of the fresh kidneys from *Fgf23* null, *Klotho* null, and *Phex* null fetuses. The results confirmed that the *Cyp24a1* expression was significantly increased in the *Phex* null kidneys. However, the expression was not changed in the *Fgf23* null or *Klotho* null kidneys (**Figure 41**).

**Table 2: List of FGF23-Targeted Genes in Placentas and Fetal Kidneys between *Klotho* WT and Null Fetuses.**

Gene	Placenta			Fetal Kidneys		
	<i>Klotho</i> <sup>+/+</sup> (WT)	<i>Klotho</i> <sup>-/-</sup> (Null)	p value	<i>Klotho</i> <sup>+/+</sup> (WT)	<i>Klotho</i> <sup>-/-</sup> (Null)	p value
<i>Fgf23</i>	1.00±0.25	1.00±0.22	0.917	Undetectable	Undetectable	N/A
<i>Klotho</i>	<b>1.00±0.22</b>	<b>Undetectable</b>	<b>0.000</b>	<b>1.00±0.11</b>	<b>Undetectable</b>	<b>0.000</b>
<i>NaPi2a</i>	1.00±0.23	1.00±0.38	0.825	1.00±0.10	1.20±0.20	0.109
<i>NaPi2b</i>	1.00±0.08	0.90±0.24	0.559	1.00±0.10	1.00±0.00	0.673
<i>NaPi2c</i>	1.00±0.16	1.10±0.15	0.431	1.00±0.30	1.20±0.30	0.258
<i>Cyp24a1</i>	1.00±0.20	0.80±0.36	0.364	1.00±0.10	1.10±0.30	0.537
<i>Cyp27b1</i>	1.00±0.00	0.90±0.00	0.379	1.00±0.30	1.20±0.70	0.614
<i>Fgfr1</i>	1.00±0.08	1.20±0.33	0.341	1.00±0.20	1.20±0.10	0.225
<i>Fgfr2</i>	1.00±0.14	1.10±0.19	0.284	1.00±0.20	1.20±0.10	0.080
<i>Fgfr3</i>	1.00±0.21	1.00±0.27	0.881	1.00±0.30	1.20±0.10	0.323
<i>Fgfr4</i>	1.00±0.18	1.20±0.27	0.217	1.00±0.20	1.10±0.10	0.610

Gene	Gene Name
<i>Fgf23</i>	Fibroblast growth factor 23
<i>Klotho</i>	Klotho
<i>NaPi2a or Slc34a1</i>	Sodium-dependent phosphate transporter 2A or Solute carrier family 34 member 1
<i>NaPi2b or Slc34a2</i>	Sodium-dependent phosphate transporter 2B or Solute carrier family 34 member 2
<i>NaPi2c or Slc34a3</i>	Sodium-dependent phosphate transporter 2C or Solute carrier family 34 member 3
<i>Cyp24a1</i>	1,25-dihydroxyvitamin D(3) 24-hydroxylase
<i>Cyp27b1</i>	25-hydroxyvitamin D-1 alpha hydroxylase
<i>Fgfr1</i>	Fibroblast growth factor receptor 1
<i>Fgfr2</i>	Fibroblast growth factor receptor 2
<i>Fgfr3</i>	Fibroblast growth factor receptor 3
<i>Fgfr4</i>	Fibroblast growth factor receptor 4

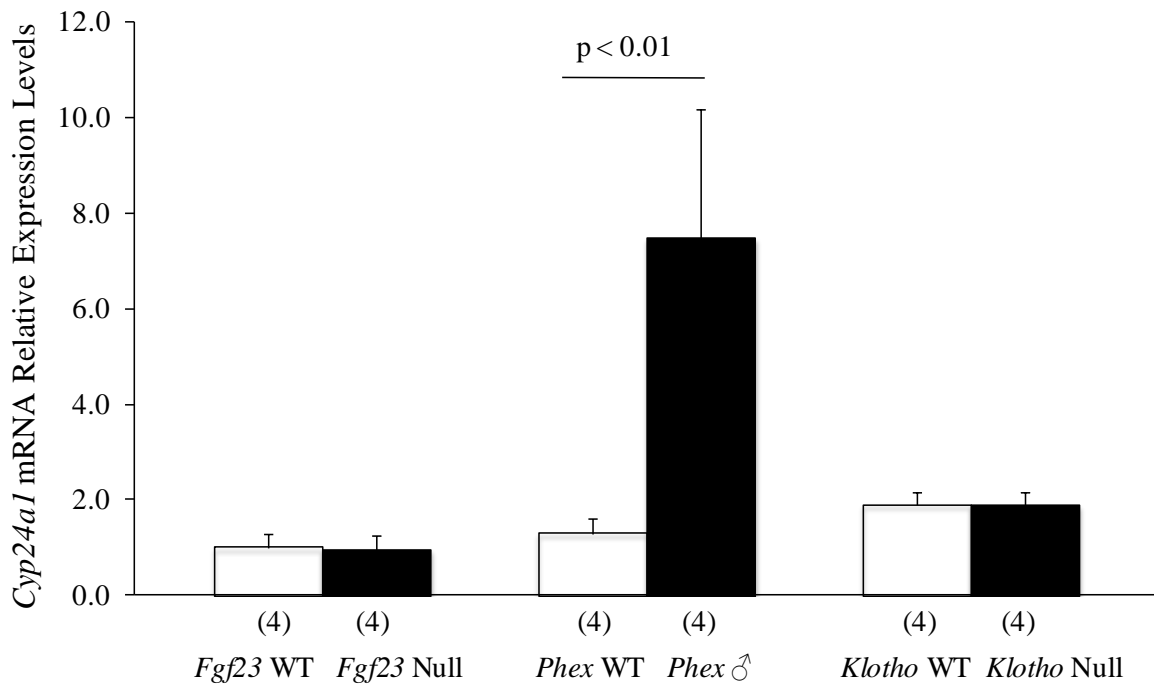


**Figure 41: Expression of *Cyp24a1* in the *Fgf23*, *Phex*, and *Klotho* Fetal Kidneys.** *Phex* ♂ kidneys had significantly higher expression of *Cyp24a1* while no changes were detected in *Fgf23* or *Klotho* null kidneys. The numbers in parentheses indicate the number of fetuses studied.

### 3.3 Results from *Pth/Fgf23* DKO Fetuses

PTH and FGF23 both regulate serum phosphate and both hormones affect the same renal genes postnatally. It was previously found in Dr. Kovacs' Laboratory that unlike *Fgf23* nulls, *Pth* null fetuses on ED18.5 had increased serum phosphorus compared to WT siblings; meanwhile, those nulls had significantly reduced serum FGF23 [139, 150]. Therefore, two questions were raised: (i) in *Fgf23* nulls and *Klotho* nulls, could PTH somehow compensate to keep phosphorus normal even though there was no increase in PTH in either model? (ii) conversely, could FGF23 compensate *in utero* for loss of PTH? To answer the two questions, the approach was to take the hyperphosphatemic *Pth* null fetus and to see if hyperphosphatemia would worsen with absence of FGF23. If PTH could compensate loss of FGF23, *Fgf23/Pth* DKO fetuses should have a phenotype different from *Fgf23* nulls; if PTH could not, the DKO should have an identical phenotype as *Fgf23* nulls. If FGF23 could compensate loss of PTH, *Fgf23/Pth* DKO and *Pth* null fetuses should have a different phenotype; if FGF23 could not, the DKO should have an identical phenotype as *Pth* nulls.

#### 3.3.1 Serum Phosphorus in *Fgf23/Pth* DKO Fetuses on ED18.5

My results in **Figure 42** showed that *Pth* nulls had significantly increased serum phosphorus relative to the normal fetal hyperphosphatemia – which was consistent with what was observed previously in Dr. Kovacs' Laboratory. If FGF23 could compensate for loss of PTH, *Fgf23/Pth* DKO should have an even higher serum phosphorus than *Pth* nulls – however, there was no significant difference between the values. In fact, serum phosphorus was non-significantly lower in the DKO rather than increased, confirming that FGF23 does not compensate for loss of PTH.

As discussed above, serum phosphorus was not altered in *Fgf23* nulls relative to WT [139]. In this experiment, serum phosphorus in *Fgf23* nulls was only numerically decreased when compared to DKO, suggesting there is lack of any synergistic effect of PTH and FGF23 being both absent, which further indicates that PTH is likely not compensating for loss of FGF23 in *Fgf23* null fetuses. This note also fits with PTH levels not changing in *Fgf23* nulls.

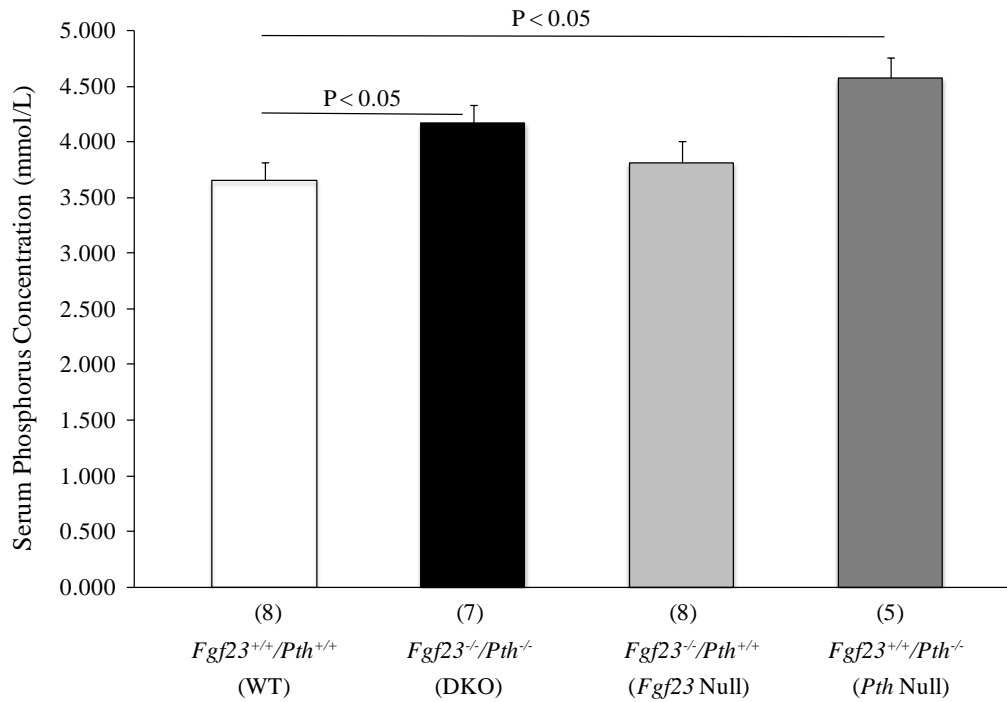


**Figure 42: Serum Phosphorus in *Fgf23/Pth* DKO Fetuses.** DKO and *Pth* null fetuses had increased serum phosphorus compared to WT siblings. However, no differences were detected between DKO and *Pth* null. The numbers in parentheses indicate the number of fetuses studied.

### 3.3.2 Skeletal Mineral Content in *Fgf23/Pth* DKO Fetuses on ED18.5

The skeleton contains the largest amount of phosphate in the body, so any difference in serum/amniotic fluid phosphate or placental phosphate transport should cause a change in ash weight and, more specifically, skeletal phosphate content. As discussed in the introduction section, skeletal mineral content was not altered in *Fgf23* nulls – thus, in this study I explored if this was due to a compensatory mechanism by PTH. The calcium content is known to be reduced in *Pth* null fetuses. My results showed that the calcium content was significantly reduced in both DKO and *Pth* nulls, with no differences between the two genotypes – suggesting no added change in calcium content due to loss of FGF23 (**Figure 43B**). The phosphate content was significantly increased in *Fgf23* nulls compared to WTs (**Figure 43A**) – which was different from the results of a prior study with a much bigger sample size showing the phosphate content was unchanged in *Fgf23* nulls. In the present study, with a small sample size and with a double-heterozygous dams (*Fgf23<sup>+/-</sup>/Pth<sup>+/-</sup>*), the skeletal phosphate content in *Fgf23* nulls was modestly increased, just reaching statistical significance. No changes in the magnesium content were observed among genotypes (**Figure 43C**). Other analyses as in the *Phex* null and *Klotho* KO models were not done in the DKO model because: (i) serum phosphate and skeletal mineral content in *Fgf23/Pth* double null fetuses were not changed compared to *Pth* nulls – suggesting that no further insights are likely to be gained and that it would be low yield to further pursue those experiments, and (ii) those studies are quite time consuming and expensive because of the many genotypes involved.

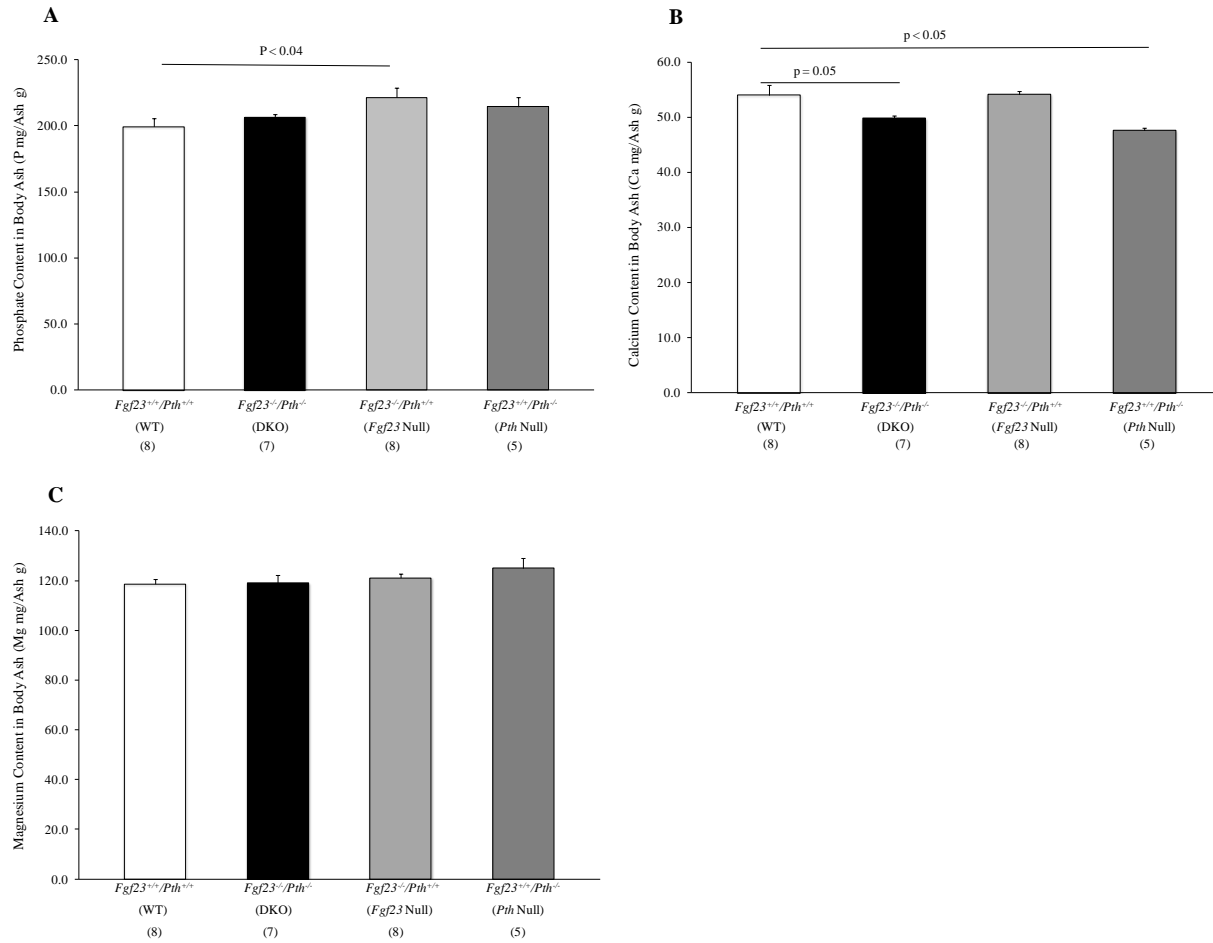


**Figure 43: Skeletal Mineral Content in ED17.5 *Fgf23/Pth* DKO Fetuses.** (A) *Fgf23* null fetuses had increased skeletal phosphate content as compared to their WT siblings. (B) DKOs and *Pth* nulls had a higher skeletal calcium content than WT fetuses; however, there were no differences between DKOs and *Pth* nulls. (C) No different skeletal magnesium content was observed among the genotypes. The numbers in parentheses indicate the number of fetuses studied.

### 3.4 Results from Postnatal *Phex* Null, *Fgf23* Null, and *Klotho* Null Pups

The results in *Phex* null and *Klotho* null fetuses, as well as previous data in *Fgf23* null fetuses, suggest that FGF23 has no role in fetal phosphate regulation. However, it is well known that excess or deficient FGF23 will cause marked abnormalities postnatally – so, when does FGF23 become important postnatally? In this aim, I investigated when serum and urine phosphorus, as well as renal expression of *NaPi2a-c*, would be changed in postnatal *Phex*, *Fgf23* and *Klotho* null pups. I considered the first time point to be within 12 hours of birth because dams usually delivered pups at midnight and the experiments were conducted between 10 a.m. and 12 p.m. Serum phosphorus was significantly decreased 30% within approximate 12 hours of delivery [i.e. postnatal day (PD) 1] in *Phex* ♂ pups (**Figure 44**). At the same time point, urine phosphorus was analyzed. Due to a limit of urine volume available, creatinine was not measured to normalize urine phosphorus. Within PD 1, *Phex* ♂ pups had significantly increased renal phosphate excretion by 2.5 fold (**Figure 45**) relative to WT pups. To confirm the observed changes of renal phosphate excretion, I analyzed renal expression of *NaPi2a*, *NaPi2b*, and *NaPi2c*, concurrently with the urine phosphate measures. The results demonstrated that in *Phex* ♂ pups within PD 1, renal expression of both *NaPi2a* and *NaPi2c* was significantly reduced while expression of *NaPi2b* was not altered (**Table 3**).

Conversely, absence of FGF23 or *Klotho* had a slower onset to effects in neonatal pups. The results showed that serum phosphorus was not increased until PD7 and PD5 in *Fgf23* nulls and *Klotho* nulls, respectively (**Figures 46 – 47**). On PD 7, *Fgf23* null pups started to have a modest but significant 10% reduction in renal phosphate excretion (**Figure 48**). On PD 5, *Klotho* null pups had a non-significant downward trend in renal phosphate excretion (**Figure 49**). I also

measured urine phosphorus levels after PD 5 in *Klotho* null pups, with no significant differences from the levels in WTs (data not shown). The failure to detect the urine phosphorus changes in *Klotho* nulls might be due the technical aspect of not being able to normalize for urine concentration by correcting for urine creatinine. To complement the urine phosphorus results, renal expression of *NaPi2a*, *NaPi2b*, and *NaPi2c* was analysed in *Fgf23* nulls on PD 7 and *Klotho* nulls on PD 5. The results showed that the expression of *NaPi2a* and *NaPi2c* was significantly elevated while there was no change in *NaPi2b* (**Table 4**).

*Fgf23* and *Klotho* null neonates did not have increased serum phosphorus immediately after birth – therefore, I wondered if PTH would transiently compensate loss of the FGF23 pathway, given the fact that PTH decreases serum phosphate in adults. The results showed that serum PTH in *Fgf23* nulls did not differ as compared to that in WTs at any postnatal time points, nor did serum PTH in *Klotho* nulls (**Figure 50**). The only significant trend observed was that serum PTH decreased during the postnatal time course.

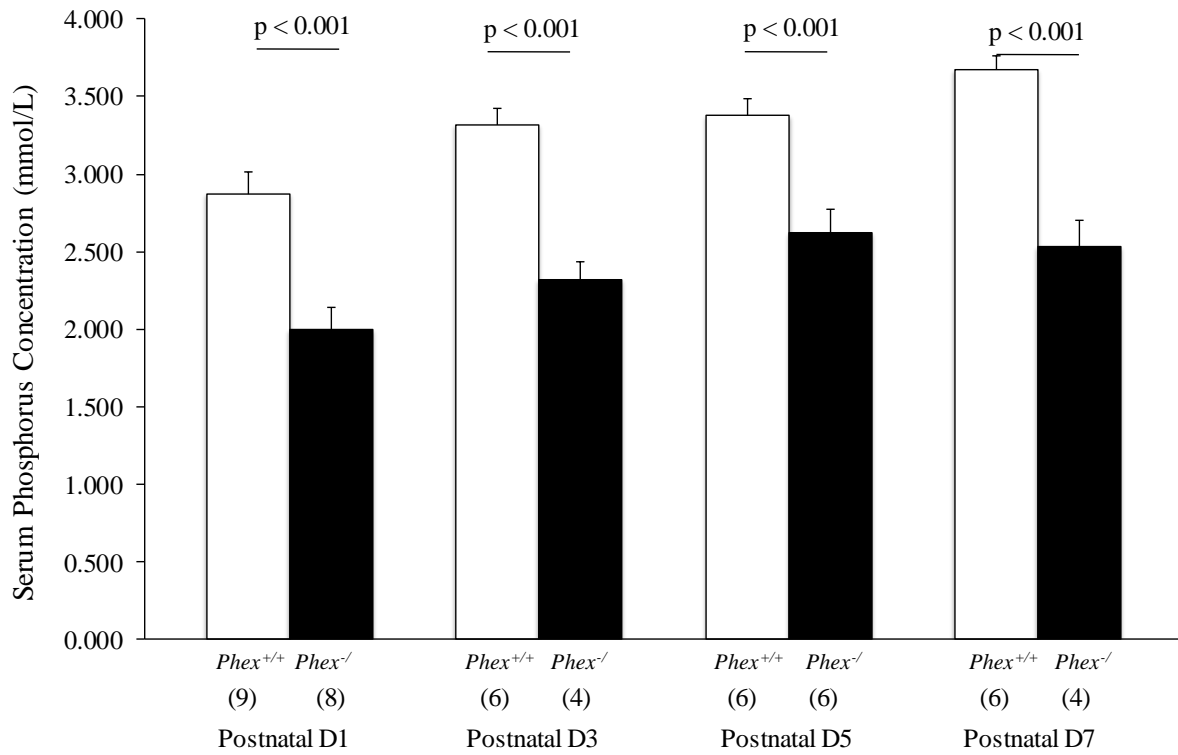


**Figure 44: Serum Phosphorus in *Phex* Neonates.** *Phex* null pups demonstrated decreased serum phosphorus immediately after birth (PD 1). The numbers in parentheses indicate the number of fetuses studied.

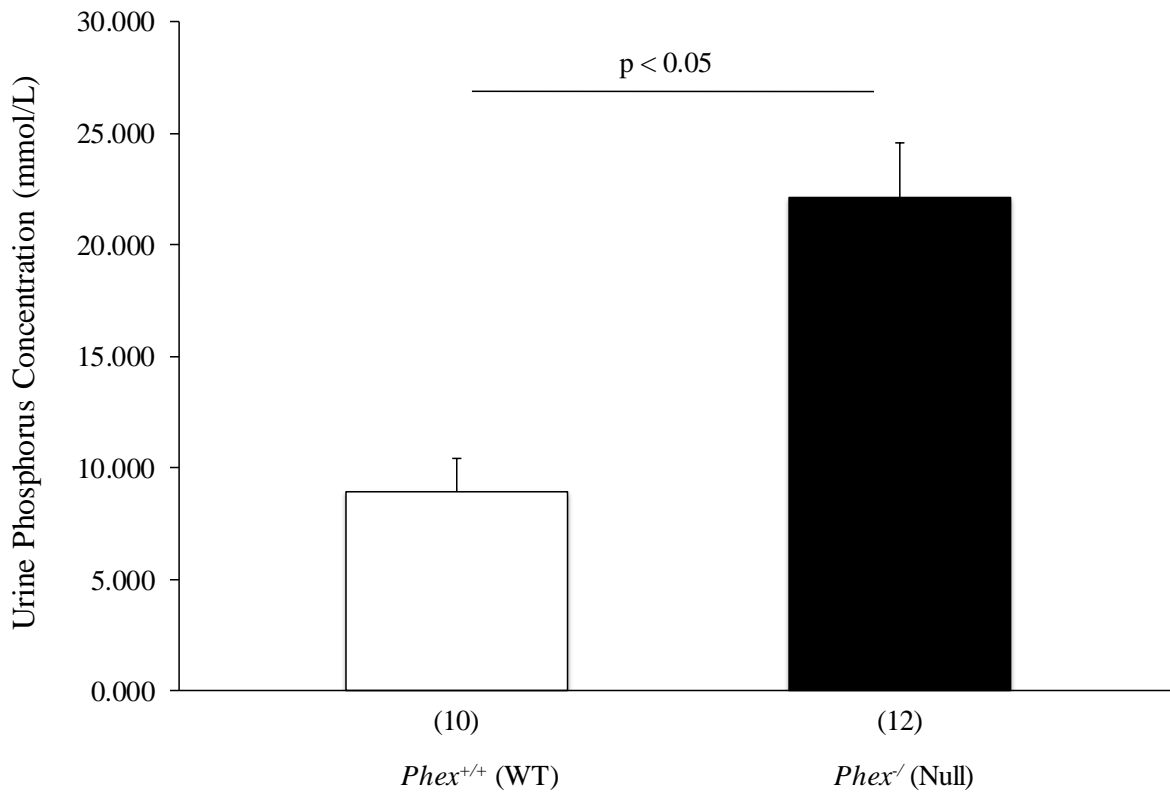


**Figure 45: Urine Phosphorus in *Phex* Neonates.** *Phex* null pups had a significant increase in renal phosphorus excretion at PD 1. The numbers in parentheses indicate the number of fetuses studied.

**Table 3: Renal Expression of *NaPi2a*, *NaPi2b* and *NaPi2c* in *Phex* Neonates.**

Gene	<i>Phex</i>		P value
	<i>Phex</i> <sup>+/+</sup> (WT)	<i>Phex</i> <sup>-/-</sup> (Null)	
<i>NaPi2a</i>	<b>1.00±0.08</b>	<b>0.78±0.17</b>	<b>&lt; 0.03</b>
<i>NaPi2b</i>	1.00±0.08	1.04±0.04	NS
<i>NaPi2c</i>	<b>1.00±0.24</b>	<b>0.60±0.32</b>	<b>&lt; 0.05</b>

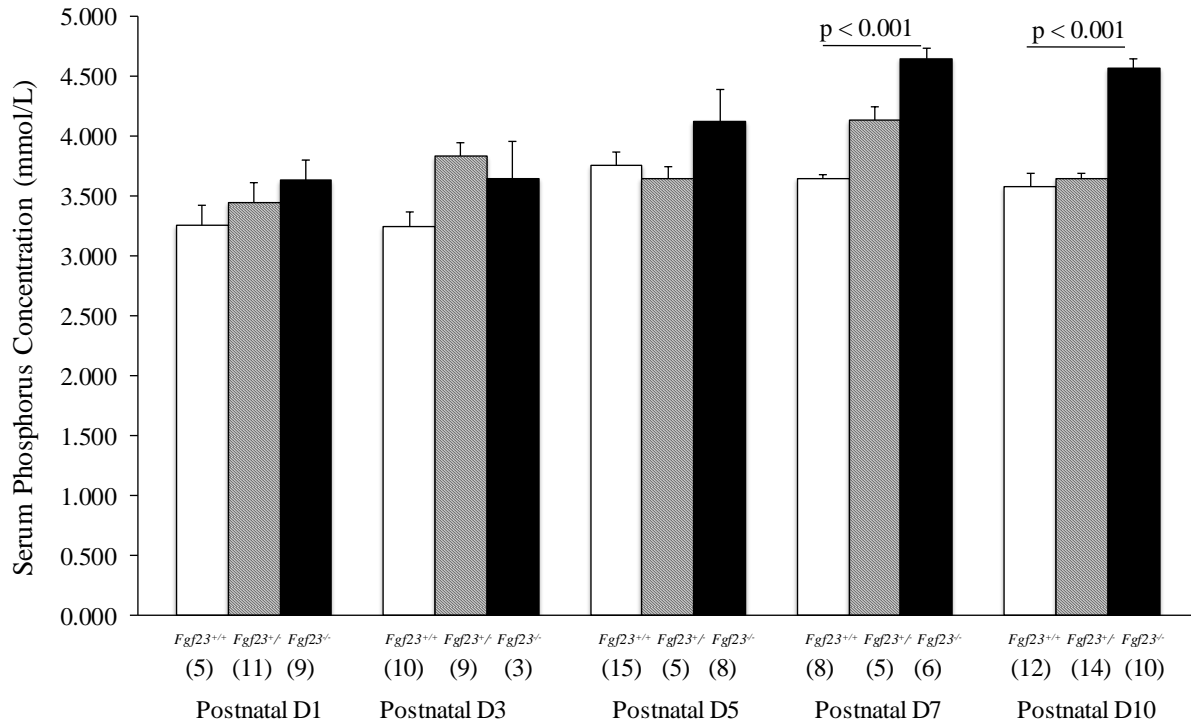


**Figure 46: Serum Phosphorus in *Fgf23* Neonates.** *Fgf23* nulls did not have increased serum phosphorus until PD 7. The numbers in parentheses indicate the number of fetuses studied.

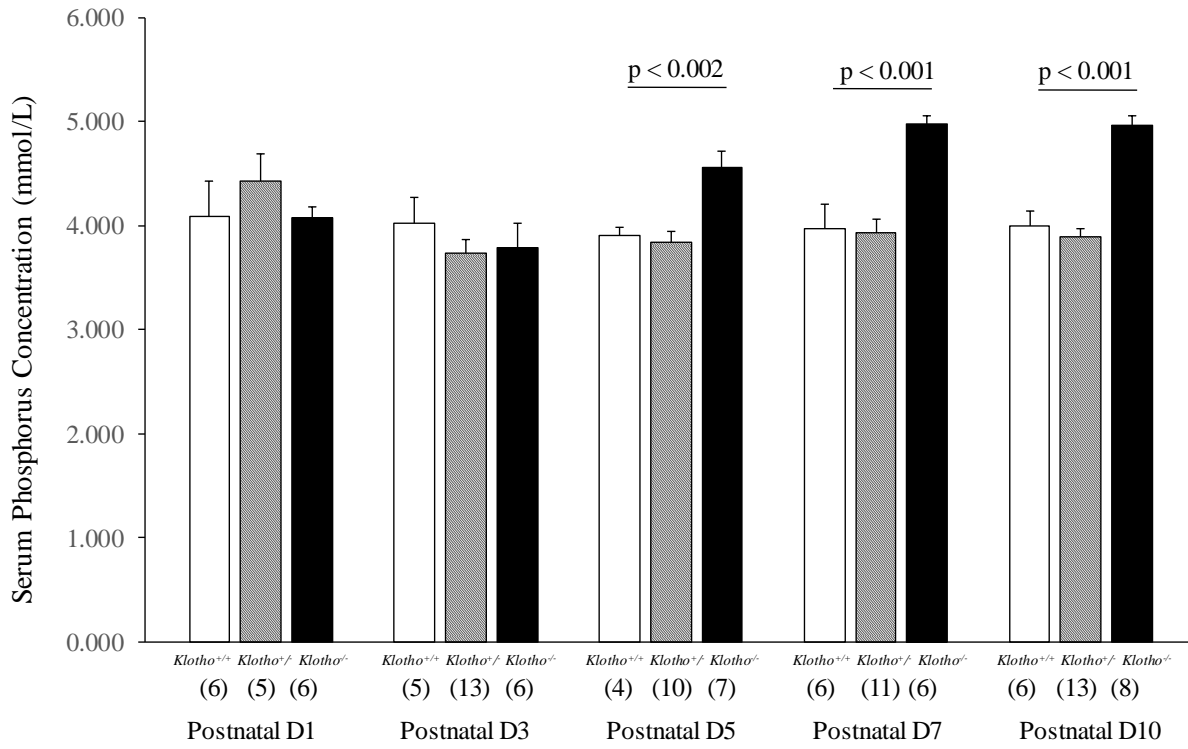


**Figure 47: Serum Phosphorus in *Klotho* Neonates.** *Klotho* nulls did not have increased serum phosphorus until PD 5. The numbers in parentheses indicate the number of fetuses studied.

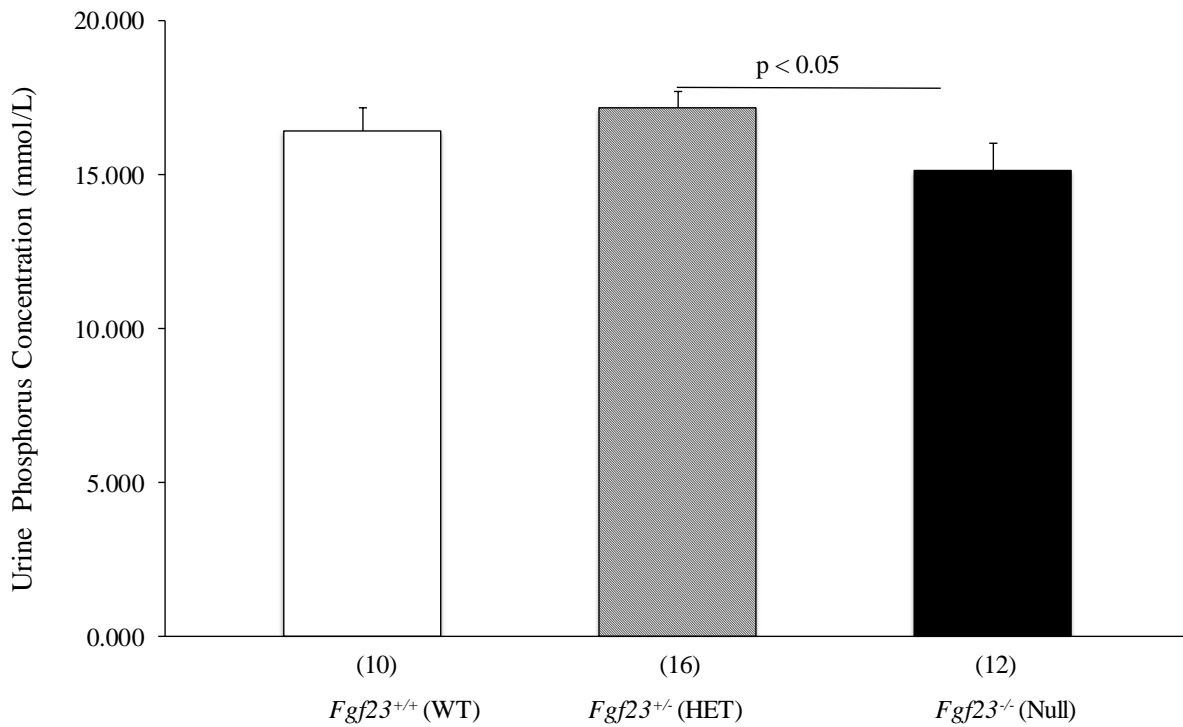


**Figure 48: Urine Phosphorus in *Fgf23* Neonates.** *Fgf23* nulls had a modest but significant reduction in renal phosphorus excretion at PD 7. The numbers in parentheses indicate the number of fetuses studied.

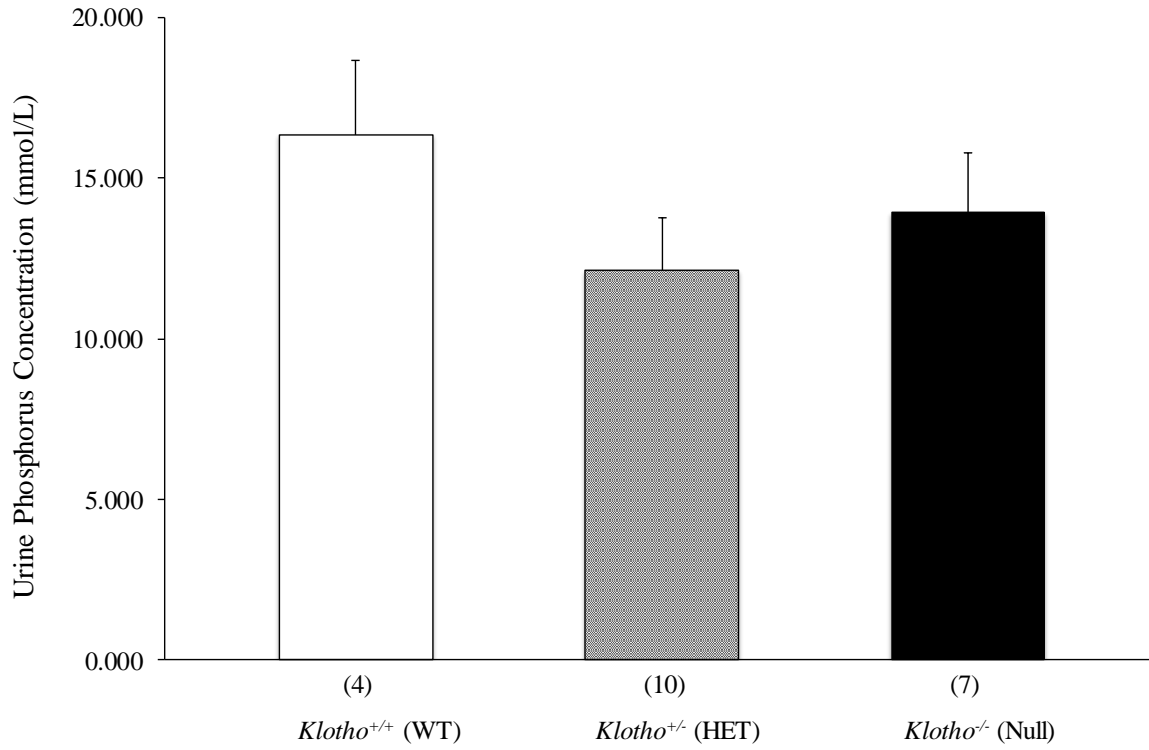


**Figure 49: Urine Phosphorus in *Klotho* Neonates.** *Klotho* nulls had a non-significant trend for reduced renal phosphorus excretion. The numbers in parentheses indicate the number of fetuses studied.

**Table 4: Renal Expression of *NaPi2a*, *NaPi2b* and *NaPi2c* in *Fgf23* and *Klotho* Neonates.**

Gene	<i>Fgf23</i>			<i>Klotho</i>		
	<i>Fgf23</i> <sup>+/+</sup> (WT)	<i>Fgf23</i> <sup>-/-</sup> (Null)	P value	<i>Klotho</i> <sup>+/+</sup> (WT)	<i>Klotho</i> <sup>-/-</sup> (Null)	P value
<i>NaPi2a</i>	<b>1.00±0.08</b>	<b>1.39±0.12</b>	<b>&lt; 0.05</b>	<b>1.00±0.29</b>	<b>1.67±0.36</b>	<b>&lt; 0.02</b>
<i>NaPi2b</i>	1.00±0.23	1.30±0.29	NS	1.00±0.29	1.05±0.26	NS
<i>NaPi2c</i>	<b>1.00±0.10</b>	<b>1.57±0.39</b>	<b>&lt; 0.05</b>	<b>1.00±0.28</b>	<b>1.83±0.39</b>	<b>&lt; 0.005</b>

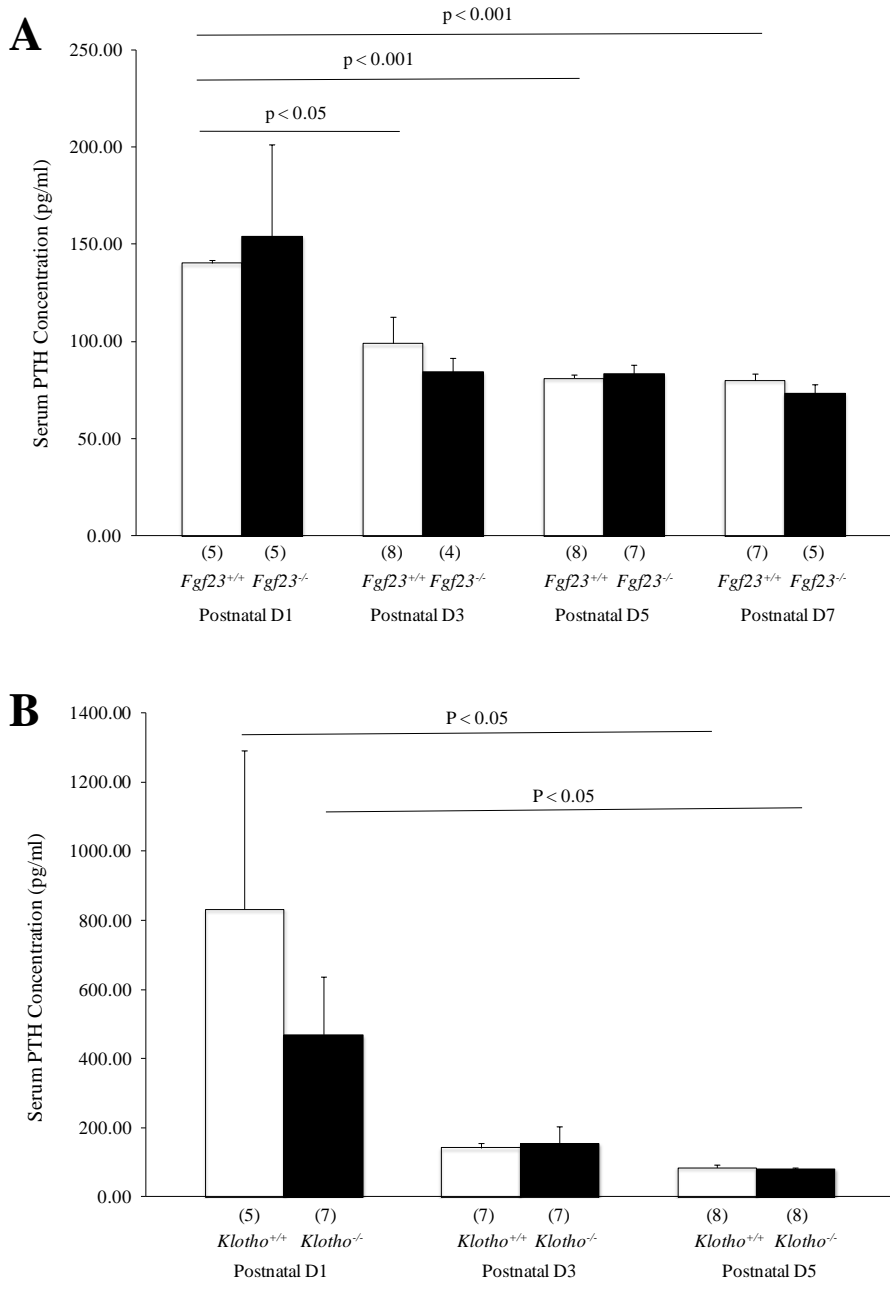


**Figure 50: Serum PTH in *Fgf23* and *Klotho* Neonates.** (A – B) PTH did not differ between genotypes at any postnatal time points in *Fgf23* and *Klotho* neonates. Serum PTH decreased during the postnatal time course. The numbers in parentheses indicate the number of fetuses studied.

## 4 Discussion

It has been established that FGF23 plays important roles in regulating phosphate homeostasis in adults – it decreases serum phosphate mainly by reducing renal phosphate reabsorption and reducing renal production of calcitriol, which in turn decreases intestinal phosphate absorption. This Ph.D. project examined potential roles of FGF23 in fetal-placental phosphate and bone metabolism as little had been known about expression of *Fgf23* and its target genes in the placenta or fetal kidneys, or whether FGF23 plays a significant role in regulating fetal phosphate. It was initially hypothesized that FGF23 plays an important role in regulating not only fetal blood phosphate and skeletal development, but also placental phosphate transfer. However, results of this project demonstrated that: (i) neither excess FGF23 nor loss of *Klotho* disturbed fetal-placental phosphate parameters, (ii) loss of FGF23 did not further alter phosphate homeostasis in *Pth* null fetuses, but (iii) excess FGF23 altered serum and urine phosphate within 12 hours of birth while loss of FGF23 or *Klotho* took 5-7 days to change serum and urine phosphate. The following sections discuss those results in detail.

### 4.1 Excess FGF23 Does Not Disturb Fetal Phosphate Metabolism

In adults excess FGF23 causes a severe disruption in phosphate metabolism, mainly including hypophosphatemia, renal phosphate wasting and osteomalacia or rickets. Extrapolating those findings in adults to fetuses, I initially hypothesized that FGF23 would also be a critical phosphate regulator through reducing serum phosphate, decreasing renal phosphate reabsorption and lowering placental phosphate transport during fetal development. However, I found in *Phex* null fetuses that excess FGF23 resulted in no disturbance in serum and amniotic fluid (fetal urine) phosphate and calcium, placental phosphate transport, skeletal morphology, or skeletal ash

weight and mineral content. WT, *Phex* null male, and *Phex*<sup>+/-</sup> female fetuses were able to maintain normal phosphate parameters despite marked hypophosphatemia in their *Phex*<sup>+/-</sup> dams. These results were surprisingly the opposite of what was expected initially, suggesting that FGF23 did not regulate phosphate homeostasis or bone development in fetuses – this is in sharp contrast to its critical roles in regulating phosphorus and skeletal metabolism in adults and children.

It should be noted that a Japanese group also conducted mice studies in *Phex* male null fetuses independently [239]. Their key findings are summarized here. The protein expression of FGFR1 and Klotho was initially confirmed in the WT placenta by immunohistochemical analysis. This group next examined potential effects of excess FGF23 in male *Phex* null fetuses derived from the *Phex*<sup>+/-</sup> (HET) female and *Phex*<sup>+/-</sup> (WT) male mating. Specifically, plasma FGF23 in *Phex*<sup>+/-</sup> dams was significantly elevated by 10 fold than that in normal WT dams. FGF23 in male *Phex* null fetuses was about 20-fold higher than that in *Phex*<sup>+/-</sup> dams, as well as 100-fold higher than that in male WT fetuses. The Japanese group also found that *Cyp24a1* expression was significantly increased in the placenta of fetuses (including both null and WT) from *Phex*<sup>+/-</sup> dams when compared with WT fetuses from normal WT dams; however, there was no significant difference in *Cyp24a1* expression between null and WT placentas (both were from *Phex*<sup>+/-</sup> dams).

The Japanese group then did an experiment in which they directly injected FGF23 into the WT placentas from normal WT dams, which led to an increase in *Cyp24a1* expression. In the fetal kidneys, *Cyp24a1* expression was significantly increased in male *Phex* nulls than in male WT;

however, serum calcitriol in male *Phex* nulls was only decreased numerically (non-significantly) when compared to that in male WT fetuses. It should be noted that despite those changes in male *Phex* nulls, serum phosphate and calcium, as well as amniotic fluid phosphate, were not altered. The Japanese group then did an *in vitro* organ culture experiment with the WT placenta (from normal WT dams). In this experiment, treatment with plasma from *Phex*<sup>+/-</sup> dams significantly increased placental *Cyp24a1* expression, which was abolished by a simultaneous addition of an anti-FGF23 antibody.

In the end, the Japanese group concluded that excess FGF23 in pathological conditions (such as in male *Phex* null fetuses) exerted direct effects on the placenta and affected fetal vitamin D metabolism via the up-regulation of *Cyp24a1* expression. Comparing my results and the Japanese group's, I noticed that we both observed that excess FGF23 in male *Phex* null fetuses did not cause changes in phosphate metabolism. The Japanese group did some experiments in which exogenous FGF23 treatment was introduced to change *Cyp24a1* expression. My study should be more complete as I directly measured the rate of placental phosphate transport and phosphate deposits in the fetal skeleton. What is quite interesting is that this Japanese group claimed that FGF23 seemed important in fetal phosphate homeostasis – a conclusion that was based solely on some modest changes in placental gene expression. It would be the same as I were to claim FGF23 is important due to a few modest changes in gene expression that I found. However, I know that those important physiological parameters (serum phosphate, amniotic fluid phosphate, skeletal phosphate content, and placental phosphate transport) were unchanged.

PTH is known to reduce serum phosphate via suppressing its renal reabsorption in adults. It is also known from other *in vitro* studies that excess FGF23 inhibits PTH. However, in the present study serum PTH levels were not different between WT male and *Phex* null male fetuses, suggesting there is no interaction between FGF23 and PTH in fetuses.

Interestingly, I found that increased FGF23 in *Phex* null male fetuses resulted in an increase in *Cyp24a1* expression in the fetal kidneys and placenta, which may explain the small but statistically significant reduction in serum calcitriol in *Phex* null male fetuses. I also found that expression of *Klotho* and *Fgfr2* was significantly reduced in the *Phex* null kidneys. Overall, these results suggest that fetal kidneys are likely to respond to high FGF23 levels as they do in adults by increasing *Cyp24a1* expression and reducing renal calcitriol production. However, these changes did not cause any detectable disturbance in renal phosphate handling or serum phosphate, indicating that calcitriol is not an important phosphate regulator in fetuses either and that the kidneys only play a very minor role during fetal development. Studies in Dr. Kovacs' laboratory previously demonstrated that neither loss of VDR nor loss of calcitriol would disturb fetal phosphate regulation – thus, it is not surprising that modest lowering of calcitriol in *Phex* null male fetuses had no effect [175, 176]. *Fgfr2* expression was reduced only 17% in the *Phex* null kidneys, and so this may not be a physiologically significant difference. It would be interesting to study the phenotype of *Fgfr2* null fetuses; however, knocking out the gene is fetal lethal [240].

#### 4.2 Neither FGF23, Calcitriol nor PTH Is Required to Maintain Fetal Phosphate Homeostasis

As presented in the introduction section, it was recently discovered in Dr. Kovacs' Laboratory that loss of FGF23 did not cause any significant disturbance in phosphate metabolism in *Fgf23* null fetuses, except a modest reduction in renal *Cyp24a1* expression which did not alter serum calcitriol. These data suggest that FGF23 is not required to maintain phosphate homeostasis during fetal development. Based on these results, I then hypothesized that there could be other FGF members compensating FGF23 deficiency in fetuses by acting on the FGFR/Klotho receptor complex. In order to address this hypothesis, I studied phenotypes of *Klotho* null fetuses in Aim 2. The results demonstrated that *Klotho* null fetuses had a similar phosphate and bone development phenotype as *Fgf23* nulls – thus, my hypothesis should be rejected.

Gene expression analysis showed that *Klotho* expression was absent in the *Klotho* null placenta and kidneys and that *Klotho* nulls had normal renal expression of *Cyp24a1* – which was different from *Fgf23* nulls that had decreased expression. It should be noted that studies in *Phex* null fetuses suggest calcitriol is not important in fetal phosphate homeostasis – thus, the *Cyp24a1* expression difference between *Klotho* null and *Fgf23* null is physiologically unimportant.

Additionally, upon a repeat assessment with the new placentas from WT and *Fgf23* nulls in a larger sample size, I found *Cyp24a1* expression was not reduced in the *Fgf23* null placenta – confirming neither an absence of FGF23 or *Klotho* alters *Cyp24a1* expression, which is consistent with lack of changes in serum calcitriol in both genotypes. Collectively, these results indicate that calcitriol does not compensate to regulate phosphate in fetuses when the FGF23 signaling pathway is impaired.

PTH is well known to decrease renal phosphate reabsorption in adults, leading to increased renal excretion of the mineral. However, in my fetal experiment, serum PTH levels were not significantly altered in *Klotho* nulls. Similar results were also observed in *Fgf23* nulls. These results should reinforce the notion that fetal phosphate homeostasis is not altered by absence of *Klotho* or FGF23 since PTH did not need to increase to compensate. It was previously observed in Dr. Kovacs' laboratory that both *Pth* null and *Gcm2* null fetuses developed hyperphosphatemia, reduced body ash weight and reduced skeletal calcium and magnesium content. Although skeletal phosphorus content was not measured, the mineral would be highly likely reduced in the bone as the calcium content was lower. These results imply that PTH could potentially lower blood phosphate by stimulating bone mineralization in fetuses. In the present study (Aim 3), by comparing *Pth* nulls and *Fgf23/Pth* DKO fetuses in Aim 3, I found that whereas loss of PTH had its previously established effect to cause hyperphosphatemia and reduced the skeletal calcium content, simultaneous loss of FGF23 did not potentiate those effects. These results further support the notion that PTH does not compensate loss of FGF23 to regulate phosphate homeostasis in fetuses, otherwise there would be phenotype differences between *Pth* nulls and DKOs. Meanwhile, the lack of difference between *Pth* nulls and *Fgf23/Pth* DKO once again highlighted that FGF23 is not important in regulating fetal phosphate.

#### 4.3 Maternal Phenotype Does Not Affect Fetal Phenotype

My results confirmed that *Phex*<sup>+/-</sup> dams have lower serum phosphate than WT dams during pregnancy. To determine whether hypophosphatemia in *Phex*<sup>+/-</sup> dams would affect fetal serum phosphate, I studied serum FGF23 and phosphate in fetuses (WT male and *Phex*<sup>+/-</sup> female) from

*Phex* WT dams mated to *Phex* null males. The results showed that fetal serum phosphate was no different across genotypes (WT vs. *Phex*<sup>+/-</sup>). More importantly, the results demonstrated that WT fetuses from the WT dams and WT fetuses from the HET dams had similar levels of serum phosphate, and that HET fetuses from the WT dams and HET fetuses from the HET dams had similar levels of serum phosphate as well. In terms of FGF23, it was significantly increased in *Phex*<sup>+/-</sup> female fetuses when compared to WT males. What is more important is that when comparing serum FGF23 between fetuses from *Phex* WT dams vs. HET dams, I noticed that serum FGF23 was unaltered by maternal genotypes. Additionally, in Dr. Samaraweera's studies WT fetuses from *Fgf23*<sup>+/-</sup> dams (which had FGF23 deficiency) had largely identical serum phosphate and FGF23 as WT fetuses from *Fgf23*<sup>+/+</sup> dams [139]. Overall, these results suggest that fetal phenotypes of serum phosphate and FGF23 are independent of maternal phenotypes. This is similar to what was previously found about fetal serum calcium in Dr. Kovacs' laboratory, that fetal serum calcium was generally set and maintained independent of maternal levels. It is also noteworthy that a recent project carried out in Dr. Kovacs' laboratory using WT dams (mated with WT males) demonstrated that altering maternal serum phosphate through low, normal or high phosphate diets did not change fetal serum phosphate either (data not published). For details, please refer to the first point discussed in the "Future Directions" section below.

#### 4.4 Why Were Fetal PTH Values High in My Study?

PTH is normally suppressed at a relatively low level in fetuses. However, it was observed in Aim 1 and Aim 2 that fetuses had higher-than-expected serum PTH. It could be due to a problem with the mouse PTH enzyme immunoassay (EIA) I used – it might measure fragments of PTH at times rather than true intact PTH because such fragments may accumulate in the fetal circulation.

Human PTH assays have gone through an evolution of becoming more and more specific to measure intact PTH without binding to the N-terminal or C-terminal fragments of PTH that are not biologically active. Unfortunately, this has not been done with rodent assays which still measure N-terminal PTH but not full-length – that is, current rodent PTH kits still include measuring inactive PTH fragments which the human assays now exclude. It should be pointed out that recent experiments in Dr. Kovacs' laboratory using the mouse PTH EIA kits that were ordered recently saw appropriately low fetal PTH values – however, this did not occur in the past by using the PTH EIA kits that were ordered earlier. The variation from batch to batch could suggest there are between-kit problems. Additionally, a mouse PTH EIA kit is also not as specific or reliable as a rat/rodent PTH immunoradiometric assay (IRMA) kit. Earlier studies in Dr. Kovacs' laboratory and others used the rat/rodent IRMA kit for measurements in mice and later switched to the mouse EIA kit – that is when this kit-to-kit variability started. I've been tempted to look at this in more details by comparing the IRMA and EIA, mouse and rat, but it would be expensive.

Another explanation for high PTH in those fetuses is that maternal HET phenotype may be affecting serum levels of PTH in fetuses. Why? It is known that *Phex*<sup>+/-</sup> dams have hypophosphatemia, which may require fetuses to up-regulate the mechanisms responsible for placental phosphorus transport in order to obtain the needed amount of phosphorus. Conceivably, secondary hyperparathyroidism in fetuses may stimulate placental phosphate transport. However, other studies of the perfused placenta from fetal lambs demonstrated that exogenous PTH or PTHrP did not stimulate this process [241].

Regardless of PTH being higher than maternal levels or lower (as it is supposed to be), readers should know that PTH was not changed between the fetal genotypes in the *Fgf23*, *Phex* and *Klotho* KO models. Therefore, whether high levels of fetal PTH in my studies are an assay problem or due to some aspects of maternal genotypes/phenotypes, it is not an issue of any of the fetal genotypes. However, the possibility that variability of the mouse PTH EIA (as explained earlier) might mask some true differences in serum PTH between WT and null fetuses cannot be completely ruled out.

#### 4.5 Potential Effects of Genetic Backgrounds on Fetal FGF23

Serum FGF23 was previously measured in WT fetuses of *Pth*<sup>+/-</sup> dams in Dr. Kovacs' Laboratory [139]. Comparing serum FGF23 levels among WT fetuses of *Pth*<sup>+/-</sup> dams, *Phex*<sup>+/-</sup> dams, and *Fgf23*<sup>+/-</sup> dams, I observed that *Pth* WT fetuses had higher serum FGF23 than *Phex* WT and *Fgf23* WT fetuses [139]. At this time, I do not have a solid reason to explain why there was such a difference. The lower FGF23 in the latter two ones may be due to genetic background differences as the *Phex* null and *Fgf23* KO models are based on the C56BL/6 background while the *Pth* KO model on the Black Swiss. It has been known that Black Swiss fetuses have higher ionized calcium and bone mineral density than C57BL/6 fetuses [162]. The genetic differences between the Black Swiss and C57BL/6 may impact the overall physiology of fetuses and result in phenotypic differences. As a result, FGF23 in Black Swiss fetuses was higher than that in C57BL/6 fetuses. It should also be pointed out that there are even significant phenotypic differences between Black Swiss-based and C57BL/6-based *Pth* null fetuses. For example, C57BL/6-based ones are modestly abnormal in skeletal development (i.e. slightly shortened long bones, shorter metacarpals and tetatarsals) while Black Swiss-based ones are normal in those

parameters. Clearly, other factors, besides genetic differences, may also contribute to higher FGF23 observed in *Pth* WT fetuses. More studies are needed to identify them.

#### 4.6 Calcitriol Does Not Respond to FGF23 during Pregnancy

I did not comprehensively examine maternal physiology during pregnancy in the *Phex* null and *Klotho* KO models. However, I noted in Aim 1 that 7-fold increased FGF23 in *Phex*<sup>+/-</sup> dams did not suppress maternal serum calcitriol during pregnancy – suggesting that *Cyp27b1* and *Cyp24a1* do not respond to FGF23 in pregnant dams and that whatever stimulates *Cyp27b1* and inhibits *Cyp24a1* should be more powerful than the effects of high FGF23 that normally suppresses *Cyp27* and stimulates *Cyp24a1*. It should be pointed out that increased calcitriol during pregnancy is likely not due to contributions from the placenta and other fetal sources. Calcitriol normally increases 2- to 5-fold during pregnancy, primarily as a result of increased production within the maternal kidneys and without the need for stimulation by PTH [165, 242]. The placenta normally contributes little if any calcitriol to the maternal circulation, as shown by an anephric woman who had low calcitriol before and during a pregnancy and by 30-fold higher expression of *Cyp27b1* in the maternal kidneys vs. placenta in mice [48, 165, 176, 243].

#### 4.7 Why Does an Abnormal FGF23 Signaling Pathway Fail to Alter Fetal Phosphate Parameters?

There are two key points to answer this question – first, the placenta is the main organ for regulating phosphate in fetuses; and second, the placenta does not depend upon FGF23 to regulate phosphate transport. Active transport of phosphate across the placenta is the main route of phosphate delivery to fetuses. The fetal kidneys and intestines provide only a route for

recycling of minerals that come across the placenta, are excreted by the kidneys into amniotic fluid, and are then swallowed and reabsorbed. This is evidently a trivial route compared with the substantial forward flow of phosphate across the placenta. Other studies have demonstrated that the fetal kidneys have a reduced glomerular filtration rate and blood flow relative to the neonatal kidneys, and that maturational changes in glomerular filtration and renal blood flow after birth lead to an improved ability to reabsorb and excrete minerals[135]. A combination of all these pieces of evidence suggests that the placenta is the main organ to regulate phosphate (as well as other minerals) in fetuses while the kidneys and intestines play a much less important role. In terms of FGF23, it is evidently not a major regulator of active placental transport of phosphate as studies in Aims 1 & 2, as well as studies by Dr. Samaraweera, demonstrated neither excess FGF23 nor an impaired FGF23 pathway altered placental phosphate transport or placental gene expression of any of the sodium-phosphate co-transporters. As discussed in the introduction section, FGF23 acts primarily on the kidneys and to a lesser extent on the intestines to regulate phosphate metabolism in adults and children (postnatally). But during fetal development the kidneys and intestines provide only a trivial route for mineral exchange.

Besides the two points discussed above, the normally low concentrations of intact FGF23 in fetal mice of the C57BL/6 background may also be contributing to why the absence of FGF23 or *Klotho* has no effect; in other words, low concentrations of FGF23 in normal fetal mice may imply that FGF23 per se is relatively unimportant for fetal mineral homeostasis. However, it should be pointed out that fetal mice in the Black Swiss background were found to have intact FGF23 concentrations equal to the maternal values[139], and another study found fetal intact FGF23 concentrations to equal maternal values in the C57BL/6 background[239]. Moreover, low

levels of FGF23 in normal fetuses aren't the sole explanation for why FGF23 absence has no effect, because the absence of *Klotho* did not disturb fetal serum FGF23 concentrations, whereas it led to 1000- to 5000-fold higher levels in neonates and adults[74, 244, 245]. Taken together with the fact that high levels of FGF23 do not disturb fetal phosphate parameters but begin to do so within 12 hours after birth, it is clear that the fetal-placental unit is unresponsive to FGF23 or a loss of *Klotho*. The microarray studies in the placentas of WT, *Fgf23* null, and *Phex* null male placentas (in Aim 1) revealed no evidence of compensatory changes in phosphate-regulating or other genes. The lack of changes in the phosphotrophic hormone PTH (in Aims 1 & 2 and Dr. Samaraweera's studies) is further evidence that the compensatory changes do not occur during fetal development when FGF23 or *Klotho* is absent, or when FGF23 excess is present. In a real sense, fetuses do not care about a loss of FGF23 signaling, nor about excess FGF23 signaling, whereas neonates are adversely affected.

It is noteworthy that in my studies, as well as in Dr. Samaraweera's studies, the pregnant dams were on normal phosphate diet. Since their fetuses would also get a normal phosphate load, maybe that is why there was no FGF23 response. It is possible that hyperphosphatemia in pregnant dams as a result of phosphate-rich diet would trigger a FGF23 response in fetuses.

My experiments do not rule out the potential importance of the sodium-phosphate co-transporters (mainly *NaPi2b*) in regulating placental phosphate transport, because their expression was normal in *Klotho* null, *Fgf23* null, and *Phex* null male placentas. Instead, factors other than FGF23 must be regulating their expression during normal fetal development. Mouse fetuses with a global KO of *Napi2b* die at mid-gestation[246], but whether this is due in part to altered

placental phosphate transport is unknown. In addition, there are other possibilities that may explain why abnormal FGF23 fails to alter fetal phosphate metabolism. First, FGF23 might be different in fetal life from postnatal life in terms of its structure. That is, the structure of the FGF23 protein could be modified in fetuses to have no effect in phosphate regulation. Second, actions of FGF23 in fetal life may be blocked by some other undiscovered agents. Third, receptors of FGF23 (mainly FGFR1) may be altered or expressed at low protein levels even though my experiments showed that gene expression of *Fgfr1 – 4* was normal in the fetal kidneys and placenta. Fourth, the FGF23 assay is known to measure intact FGF23 which is biologically active. However, whether the assay can capture the first two N-terminal acids of FGF23 is unknown. If the assay does not, then there is a possibility that “intact” FGF23 that I measured in those *Phex* and *Klotho* fetuses was not intact at all or biologically active. That is, whether the two models are truly valid is unknown. A similar situation happens with PTH where loss of the first two amino acids of the protein causes inactivity but the protein is picked up as intact by most assays. Fifth, we know that the C-terminal fragment levels of FGF23 (biologically inactive) are higher in fetuses. If those fragments can block the action of intact FGF23, intact FGF23 cannot function properly in fetuses.

#### 4.8 FGF23 Is Important in Neonatal Phosphate Regulation

Since the results in Aims 1-3 suggest FGF23 is not an important regulator in phosphate homeostasis in fetuses, I further hypothesized that FGF23 would start being critical in this process during the neonatal stage. The results in Aim 4 demonstrated that by PD5 in *Klotho* nulls, and by PD7 in *Fgf23* nulls, serum phosphate became significantly increased, whereas the urine phosphate showed a slight decrease that was statistically significant in *Fgf23* nulls but not

significant in *Klotho* nulls. The non-significance of the urine phosphate results in *Klotho* nulls may be due to lack of the creatinine correction which likely increased the variability of the urine phosphate results (I did not measure the creatinine concentrations in urine because obtainable urine volumes from mouse neonates were too small). This apparent reduction in renal phosphate excretion in both *Fgf23* nulls and *Klotho* nulls was accompanied by an increase in renal expression of *NaPi2a* and *NaPi2c*, which was not present at ED 18.5. Collectively, these results suggest that my hypothesis should be accepted – that is, FGF23 is required during the neonatal stage to maintain normal phosphate homeostasis. The renal gene expression changes in *NaPi2a* and *NaPi2c* indicate that the kidneys start becoming an important organ to regulate phosphate excretion in neonates – which is strikingly opposite to what happens in fetuses where the kidneys only play some minor roles. My results in Aim 4 also showed that *Klotho* nulls appeared to have an earlier onset of hyperphosphatemia (day 5 vs. day 7) than *Fgf23* nulls but whether this is a real or chance difference from the *Fgf23* null phenotype is not certain; PD6 was not assessed.

In contrast to the slow emergence of hyperphosphatemia in *Fgf23* null and *Klotho* null neonates, excess FGF23 in *Phex* null males caused a reduction in serum phosphate and a significant increase in urine phosphate within 12 hours after birth. These results once again indicate that a normal level of FGF23 is important in maintaining phosphate homeostasis in neonates.

Accompanying with the urine phosphate results, renal expression of *NaPi2a* and *NaPi2c* was significantly reduced, as compared with no difference 24 hours earlier (ED 18.5) – suggesting the kidneys in neonates become important and responsive to FGF23 within 12 hours after birth whereas in fetuses the kidneys are much less critical.

The results also demonstrated that *Phex* null neonates had much earlier onset of phosphate abnormalities than *Fgf23* nulls and *Klotho* nulls, which could be due to a compensatory increase of PTH in the latter two ones. However, measurements of PTH in neonatal *Fgf23* nulls and *Klotho* nulls showed this hormone was not significantly altered – thus, such possibility should be ruled out. That is, the delayed onset of the *Fgf23* null and *Klotho* null phenotypes was not due to compensatory secondary hyperparathyroidism. FGF23 could be modified or blocked by other agents in fetuses, therefore ultra-high FGF23 in *Phex* null fetuses did not exert any effect on phosphate regulation. Once the fetus is delivered, the modification or blockade of FGF23 would disappear within several hours after birth. Therefore, *Phex* null pups demonstrated hypophosphatemia and increased renal phosphate excretion. There is also a possibility that intact FGF23 could be interfered by high levels of the C-terminal fragment of FGF23. A Japanese group previously reported that the C-terminal fragment was abundant in normal human cord blood despite low levels of intact FGF23 [247]. Once a fetus is delivered, the high levels of the C-terminal fragment of FGF23 should be cleared, which could allow FGF23 to begin acting on the kidneys of the pup right away. Another potential explanation for why *Fgf23* and *Klotho* null pups showed the abnormalities several days later than *Phex* null pups is that immediately after birth there is a very high need for phosphate in the developing skeleton, therefore, from a developmental perspective, an early neonate does not need to excrete phosphate but instead needs to hold on to it – so FGF23 normally do not begin to act until days later. The high demand of phosphate is especially seen in premature neonates where dietary calcium/phosphate intake is not sufficient, the neonates have to be treated parenterally to get enough calcium/phosphate to mineralize the early postnatal skeleton before the rate of mineralization slows.

#### 4.9 Clinical Implication

There have been no systematic studies of serum phosphate or urine phosphate excretion in human fetuses and/or neonates that are homozygous for mutations that lead to loss of biologically active FGF23 or Klotho; this is because their autosomal recessive inheritance leads to unexpected, sporadic appearance of affected offspring. Based on my Ph.D. project, it can be predicted that phosphate should be normal in cord blood of human fetuses that have null mutations in *Fgf23*, *Klotho*, and/or other genetic causes of hyperphosphatemic tumor calcinosis. Human conditions with a calcific mass and hyperphosphatemia (such as TC) can be presented as early as 18 days after birth – which is quite similar to the phenotypes observed in *Fgf23* null and *Klotho* null mouse neonates [230, 231].

In the opposite condition of excess FGF23, XLH (due to the *PheX* mutation) in humans can be diagnosed as early as the first year if there is a positive family history of the condition. Some abnormalities in this disorder, such as reduced but normal renal phosphate reabsorption, can be observed as early as 9 days of age – humans seem to have a slower occurrence of symptoms than what would be predicted from the *PheX* null model, likely due to a species difference between humans and rodents. Generally speaking, the human data, although limited, suggest a similar postnatal onset of FGF23 action as predicted in the mouse model.

#### 4.10 Study Limitations

As with all researches, the experiments in this Ph.D. project had some limitations which are discussed below.

First, the technique used to measure placental phosphate transport (studies in Aims 1 – 2) may not count the effect of  $^{32}\text{P}$  backflux (flow of phosphate from fetuses to dams) – which might mask true differences in placental phosphate transport between WT and null fetuses. Previous studies in Dr. Kovacs' Laboratory in *Pthrp* KO mice showed that extending the time between calcium isotope administration and surgical removal of fetuses could increase the relative differences in placental calcium transfer between the genotypes – which may indicate that the longer the interval, the more likely that placental mineral transport results would show significant differences. With only a 5-minute interval, there could be less time for  $^{32}\text{P}$  transferred from the maternal to the fetal side; in addition, a certain amount of  $^{32}\text{P}$  could cross the placenta to dams – the net result is a dilution in circulating phosphate in fetuses which could mask a small but true difference in placental phosphate transport between WT and null. It should be noted that in my studies, the *NaPi2b* gene expression was not significantly changed in *Phex* null or *Klotho* null placentas. Since there could be post-transcriptional modifications in NaPi2b, a protein analysis should be conducted to confirm there are no real changes in NaPi2b on protein levels.

Second, the measured urine phosphate concentrations in neonatal pups (studies in Aim 4) were not normalized by creatinine concentrations – this is likely the reason why no significant differences in urine phosphate between *Klotho* WT and null pups across all postnatal timepoints were detected. Normally, urine mineral concentration measures should be normalized by creatinine concentrations to eliminate the confounding effect of urine volume. However, urine volume available for collection in my postnatal experiments was too small to support creatinine measurements. It should be noted no creatinine correction may not be a big limitation, since

significant differences in urine phosphate without being corrected by creatinine were detected in *Phex* null and *Fgf23* null neonates.

Third, KO mouse models are great tools to investigate potential effects of certain gene(s) on physiological activities *in vivo*, especially given the fact that certain studies cannot be conducted in human bodies. However, there are various structural differences between rodents and humans, which may cause findings in mouse models to be inapplicable to humans. Take the placenta for example, rodents have a haemotrichorial placenta, while humans have a haemomonochorial placenta [248]. In addition, rodents have an intricate labyrinth where the maternal and fetal blood contact closely, whereas in humans villi from the fetal side extend into the intervillous maternal blood-filled space and float freely [249]. Due to these structural differences, it is possible that the human and rodent placenta function differently – however, it remains unknown. Therefore, our findings in mouse models may not necessarily be applicable to humans.

Fifth, in this project KO mouse models allowed me to investigate the potential roles of FGF23 in fetal phosphate regulation. However, there are limitations when using such models. One challenge is that when a gene of interest is knocked out, another hormone or mechanism may be triggered to compensate the loss of such gene. Moreover, a phenotype due to the knockout of a gene of interest might not be directly related to the gene loss. That is, knocking out a gene of interest may change expression of another gene, which in turn leads to a certain genotype.

Sixth, PTH normally circulates at low levels in fetuses; however, in studies in Aim 1 fetal PTH levels were unexpectedly high compared to the maternal values. It could be due to our mouse

PTH kit not being reliable, because one batch had given low PTH values in fetuses (which is what is expected) and then another had given high levels (based on our historical use experience). The PTH kit may vary in its sensitivity and specificity, and may pick up inactive PTH fragments in fetuses at times. The mouse PTH kits do not seem to be subjected to the same quality control that human kits are.

#### 4.11 Future Directions

My Ph.D. project suggests that FGF23 is not an important regulator in phosphate homeostasis and skeletal development in fetuses. Further efforts should still be taken to discover potential important regulators in this process.

First, dams' diet during pregnancy could be an important factor that would potentially change the process of fetal mineral metabolism. Few studies have been carried out to determine potential effects of low-phosphate diet on fetal phosphate regulation and bone development. In my Ph.D. project, all fetuses were delivered from dams on regular diet – thus, all fetuses got a normal phosphate load, which could be a potential reason that there were no FGF23 responses in *Phex* null, *Fgf23* null or *Klotho* null fetuses. Two studies were conducted in Dr. Kovacs's Laboratory to investigate if maternal hyperphosphatemia that was induced by phosphate-rich diet would provoke FGF23 responses in fetuses [250, 251]. The first study examined whether serum phosphate in WT fetuses from WT dams (mated to WT males) responds to different maternal phosphate diets (low vs. normal vs. high with corresponding effects on maternal serum phosphate). In this study, 30 WT C57BL/6 dams received low, normal or high phosphate diets prior to mating. The results showed that increasing phosphate intake led to progressively higher

maternal serum phosphate and FGF23 during pregnancy, while PTH stayed suppressed. As to fetal serum phosphate, there were no differences among fetuses from the dams on high, normal, low phosphate diets – that is, serum phosphate in fetuses was maintained independent of maternal serum phosphate. Fetal FGF23 and PTH remained low and unchanged. There were no differences in fetal ash weight, phosphate, or calcium content either; and no changes in placental expression of genes relevant to phosphate transport or FGF23 physiology. The second study examined whether serum phosphate in fetuses from *Fgf23*<sup>+/-</sup> dams (mated to *Fgf23*<sup>+/-</sup> males) responds to different maternal phosphate diets (normal vs. high). In this study, 20 *Fgf23*<sup>+/-</sup> dams received normal or high phosphate diets prior to mating. The results showed that high phosphate diet increased maternal FGF23 while PTH stayed suppressed. Similar to the results in the WT C57BL/6 fetuses, there were no differences in serum phosphate, FGF23 or PTH between WT fetuses from the dams on high and normal phosphate diets. What was interesting was that *Fgf23* null fetuses from mothers on the high phosphate diet had very high serum phosphate compared to *Fgf23* null fetuses from dams on the normal diet. Additionally, in the *Fgf23* null placenta from the high phosphate diet, *Cyp27b1* was down-regulated. There were no differences across genotypes or diets in fetal ash weight, phosphate, or calcium content. In general, combined results from both studies suggest that fetal phosphate is independent of maternal phosphate levels and that fetal FGF23 is only required to defend against hyperphosphatemia induced by maternal phosphate loading. I studied fetuses from *PheX*<sup>+/-</sup> dams and WT dams which were all fed with normal phosphate diets – that is, I examined the effect of low vs. normal maternal serum phosphate on WT fetuses. As discussed above, there was no difference in serum phosphate between WT fetuses from the *PheX*<sup>+/-</sup> dams and WT fetuses from the WT dams. Comparing my results and the results in the first study, we had a similar observation that abnormal levels of

maternal serum phosphate (either due to genetic mutations or phosphate diets) had no effect on fetal serum phosphate. Comparing my results and the results in the second study, we had a similar observation in WT fetuses, which was also similar to the first study. Although the results in the second study suggest potential effect in null fetuses due to high maternal phosphate diets, these results do not conflict with my data.

Second, the phenotype of *Klotho* null fetuses of the HET dam (*Klotho*<sup>+/-</sup>) on high-phosphate diet should also be explored in comparison to *Klotho* null fetuses of the HET dam on regular phosphate diet. If results replicate what was observed in the second study discussed in the last paragraph (i.e. hyperphosphatemia and reduced placental expression of *Cyp27b1* in the null fetuses of the dam on high phosphate diet), it should suggest that the potential role of fetal FGF23 in defending against hyperphosphatemia induced by maternal phosphate loading is through the classic FGF23/FGFR/*Klotho* pathway. If the null fetuses of the dam on high phosphate diet show a same phenotype as the null fetuses of the dam on regular phosphate diet, it should imply that the potential role of fetal FGF23 in defending against hyperphosphatemia could be through a *Klotho*-independent pathway.

Third, fetuses of the *Phex* HET dam (*Phex*<sup>+/-</sup>) were able to defend their serum phosphate levels against maternal hypophosphatemia, implying that when pregnant dams are hypophosphatemic, the rate of placental phosphate transport could potentially be increased to fulfill normal hyperphosphatemia in fetuses. A placental <sup>32</sup>P transport study could be conducted to compare the rate of phosphate transport between WT fetuses of the *Phex* HET dam and those of the *Fgf23* HET dam. If the fetuses of the *Phex* HET dam accumulate more <sup>32</sup>P than those of the *Fgf23*

HET dam within a period of time, it should suggest the placenta can self regulate the rate of phosphate transport to defend against maternal phosphate abnormalities. Additionally, an exploratory experiment could be conducted to mine potential changes on both gene expression (microarray and/or RNAseq) and protein (proteomics) levels between the placenta of WT pregnant dams on regular diet vs. on low-phosphate diet. Significant changes in a gene or protein imply this candidate may play roles in regulating placental phosphate transport, which may further impact fetal phosphate homeostasis and bone development.

Fourth, previous studies showed that *Pth* null fetuses had increased serum phosphate concentrations by ED18.5, which suggests that PTH could be a critical regulator of fetal phosphate homeostasis. However, placental phosphate transport was not measured in *Pth* null fetuses. It would be interesting to see if a loss of PTH could change this process.

Fifth, as discussed above, the sequence and structure of the FGF23 protein in fetal stage could be different from those in the adult stage – if so, FGF23 might have no effect in regulating phosphate metabolism in fetuses. In order to address this possibility, fetal FGF23 and adult FGF23 can be extracted and purified to analyze their amino acid sequences, respectively, followed by bioinformatics analysis that compare their structure. In addition, although our gene expression and microarray analysis showed that *Fgfr1* (FGF23's main receptor) was not changed in *Phex* null fetuses, it cannot be ruled out that the protein levels of FGFR1 could be low, leading to no effect of ultra-high levels of FGF23 in the nulls. Western blot can be applied to study the protein levels of FGFR1 in the placenta and kidneys of *Phex* null fetuses.

Sixth, FGF23 could be bound by other agents (proteins) that block its functions in *Phex* null fetuses. If so, the complex should have a higher molecular weight than FGF23. Proteomics techniques can be applied to study whether FGF23 interacts with other proteins in *Phex* null fetuses.

Seventh, as discussed above, the C-terminal fragment of FGF23 is known to be high in human cord blood. High serum levels of the C-terminal fragment could act on FGF23's receptors to block intact FGF23. Whether the C-terminal fragment is also high in rodents is unknown, which is worth being measured. Additional studies should also be conducted to study if there is an interaction between the C-terminal fragment and FGFR1 in the placenta. If so, it could explain why abnormally high FGF23 in the *Phex* null placenta had no effect in placental phosphate transport.

#### 4.12 Summary and Conclusion

In summary, Deletion of *Klotho*, as well as 7.8-fold higher serum FGF23 due to a mutation in *Phex*, does not disturb any measured parameters of fetal mineral homeostasis, including serum and amniotic fluid phosphate, skeletal morphology, skeletal mineral content, and placental phosphate transport. It is only after birth that disturbance in FGF23 signaling begins to significantly alter phosphate homeostasis. In neonates, excess FGF23 exerts its effects as early as 12 hours after birth; whereas a loss of *Klotho* or FGF23 has no effect until 5 to 7 days after birth. My results predict that human babies with abnormalities of FGF23 signaling will be normal at birth, with disturbance in phosphate metabolism beginning over the days to weeks or months after birth.

In conclusion, my original hypothesis (FGF23 was important in regulating not only fetal serum phosphate and skeletal development, but also placental phosphate transport) was rejected.

Although intact FGF23 is present in the fetal circulation at levels that range from low to equal to adult values, and although there is robust expression of FGF23-targeted genes in the placenta and kidneys, FGF23 itself is not an important regulator of fetal phosphate metabolism. Instead, factors other than FGF23 must dominate to regulate the transport of phosphate across the placenta, as well as expression of the sodium-phosphate co-transporters. The magnitude of phosphate delivery across the placenta may override any effect that an absence of FGF23 or Klotho, or excess FGF23, might otherwise have on the fetal kidneys. It is in hours to days after a loss of placental phosphate pump that FGF23 becomes an important regulator of renal phosphate reabsorption and intestinal phosphate absorption (to some less extent).

## 5 References

1. Debnam ES Marks J, Unwin RJ., *Phosphate Homeostasis and the Renal-Gastrointestinal Axis*. American Journal of Physiology. Renal Physiology, 2010. **299**(2): F285-296.
2. Berndt TJ , Schiavi S, Kumar R, "*Phosphatonins*" and the Regulation of Phosphorus Homeostasis. American Journal of Physiology. Renal Physiology, 2005. **289**: F1170-1182.
3. Amanzadeh J , Reilly RF., *Hypophosphatemia: An Evidence-Based Approach to Its Clinical Consequences and Management*. Nat Clin Pract Nephrol, 2006. **2**(3): 136-148.
4. Alizadeh Naderi AS , Reilly RF., *Hereditary Disorders of Renal Phosphate Wasting*. Nat Rev Nephrol, 2010. **6**: 657-665.
5. Moe SM , Chen NX, *Mechanisms of Vascular Calcification in Chronic Kidney Disease*. Journal of the American Society of Nephrology, 2008. **19**(2): 213-216.
6. Kendrick J , Chonchol M, *The Role of Phosphorus in the Development and Progression of Vascular Calcification*. Am J Kidney Dis, 2011. **58**(5): 826-834.
7. Goldsweig BK , Carpenter TO, *Hypophosphatemic Rickets: Lessons from Disrupted Fgf23 Control of Phosphorus Homeostasis*. Curr Osteoporos Rep, 2015. **13**(2): 88-97.
8. Tuchman S *Disorders of Mineral Metabolism in the Newborn*. Curr Pediatr Rev, 2014. **10**(2): 133-141.
9. Kocelak P , Olszanecka-Glinianowicz M, Chudek J., *Fibroblast Growth Factor 23--Structure, Function and Role in Kidney Diseases*. Adv Clin Exp Med, 2012. **21**(3): 391-401.
10. Junqueira LC , José C. Foltin J, Lebowitz H, Boyle PJ, eds. In *Basic Histology, Text & Atlas (10th Ed.)*, 144: McGraw-Hill Companies, 2003.
11. Penido M , Alon US, *Phosphate Homeostasis and Its Role in Bone Health*. Pediatric Nephrology, 2012. **27**(11): 2039-2048.
12. Sabbagh Y , Giral H, Caldas Y, Levi M, Schiavi SC, *Intestinal Phosphate Transport*. Adv Chronic Kidney Dis, 2011. **18**(2): 85-90.
13. Gonzalez-Mariscal L , Betanzos A, Nava P, Jaramillo BE, *Tight Junction Proteins*. Prog Biophys Mol Biol, 2003. **81**(1): 1-44.
14. Balda MS , Gonzalez-Mariscal L, Matter K, Cerejido M, Anderson JM, *Assembly of the Tight Junction: The Role of Diacylglycerol*. J Cell Biol, 1993. **123**(2): 293-302.
15. Benais-Pont G , Punn A, Flores-Maldonado C, Eckert J, Raposo G, Fleming TP, Cerejido M, Balda MS, Matter K, *Identification of a Tight Junction-Associated Guanine Nucleotide Exchange Factor That Activates Rho and Regulates Paracellular Permeability*. J Cell Biol, 2003. **160**(5): 729-740.
16. Will C , Fromm M, Muller D, *Claudin Tight Junction Proteins: Novel Aspects in Paracellular Transport*. Perit Dial Int, 2008. **28**(6): 577-584.
17. Krause G , Winkler L, Mueller SL, Haseloff RF, Piontek J, Blasig IE, *Structure and Function of Claudins*. Biochim Biophys Acta, 2008. **1778**(3): 631-645.
18. Miyamoto K , Ito M, Tatsumi S, Kuwahata M, Segawa H, *New Aspect of Renal Phosphate Reabsorption: The Type Iic Sodium-Dependent Phosphate Transporter*. Am J Nephrol, 2007. **27**(5): 503-515.
19. Murer H , Forster I, Biber J, *The Sodium Phosphate Cotransporter Family Slc34*. Pflugers Arch, 2004. **447**(5): 763-767.
20. Virkki LV , Biber J, Murer H, Forster IC, *Phosphate Transporters: A Tale of Two Solute Carrier Families*. Am J Physiol Renal Physiol, 2007. **293**(3): F643-654.
21. Sabbagh Y , O'Brien SP, Song W, Boulanger JH, Stockmann A, Arbeeny C, Schiavi SC, *Intestinal Npt2b Plays a Major Role in Phosphate Absorption and Homeostasis*. J Am Soc Nephrol, 2009. **20**(11): 2348-2358.
22. Corut A , Senyigit A, Ugur SA, Altin S, Ozcelik U, Calisir H, Yildirim Z, Gocmen A, Tolun A, *Mutations in Slc34a2 Cause Pulmonary Alveolar Microlithiasis and Are Possibly Associated with Testicular Microlithiasis*. Am J Hum Genet, 2006. **79**(4): 650-656.

23. Huqun , Izumi S, Miyazawa H, Ishii K, Uchiyama B, Ishida T, Tanaka S, Tazawa R, Fukuyama S, Tanaka T, Nagai Y, Yokote A, Takahashi H, Fukushima T, Kobayashi K, Chiba H, Nagata M, Sakamoto S, Nakata K, Takebayashi Y, Shimizu Y, Kaneko K, Shimizu M, Kanazawa M, Abe S, Inoue Y, Takenoshita S, Yoshimura K, Kudo K, Tachibana T, Nukiwa T, Hagiwara K., *Mutations in the Slc34a2 Gene Are Associated with Pulmonary Alveolar Microlithiasis*. Am J Respir Crit Care Med, 2007. **175**(3): 263-268.
24. Collins JF , Bai L, Ghishan FK., *The Slc20 Family of Proteins: Dual Functions as Sodium-Phosphate Cotransporters and Viral Receptors*. Pflugers Arch, 2004. **447**(5): 647-652.
25. Kavanaugh MP , Miller DG, Zhang W, Law W, Kozak SL, Kabat D, Miller AD, *Cell-Surface Receptors for Gibbon Ape Leukemia Virus and Amphotropic Murine Retrovirus Are Inducible Sodium-Dependent Phosphate Symporters*. Proc Natl Acad Sci U S A, 1994. **91**(15): 7071-7075.
26. Farrow EG , White KE, *Recent Advances in Renal Phosphate Handling*. Nat Rev Nephrol, 2010. **6**: 207-217.
27. Xu H , Collins JF, Bai L, Kiela PR, Ghishan FK, *Regulation of the Human Sodium-Phosphate Cotransporter Napi-Iib Gene Promoter by Epidermal Growth Factor*. Am J Physiol Cell Physiol, 2001. **280**: C628-C636.
28. Arima K , Hines ER, Kiela PR, Drees JB, Collins JF, Ghishan FK., *Glucocorticoid Regulation and Glycosylation of Mouse Intestinal Type Iib Na-Pi Cotransporter During Ontogeny*. Am J Physiol Gastrointest Liver Physiol, 2002. **283**: G426-G434.
29. Xu H , Uno JK, Inouye M, Xu L, Drees JB, Collins JF, Ghishan FK, *Regulation of Intestinal Napi-Iib Cotransporter Gene Expression by Estrogen*. Am J Physiol Gastrointest Liver Physiol, 2003. **285**: G1317-G1324.
30. Stauber A , Radanovic T, Stange G, Murer H, Wagner CA, Biber J, *Regulation of Intestinal Phosphate Transport. Ii. Metabolic Acidosis Stimulates Na+-Dependent Phosphate Absorption and Expression of the Na+-Pi Cotransporter Napi-Iib in Small Intestine*. Am J Physiol Gastrointest Liver Physiol, 2005. **288**: G501-G506.
31. Hattenhauer O , Traebert M, Murer H, Biber J., *Regulation of Small Intestinal Na-P(I) Type Iib Cotransporter by Dietary Phosphate Intake*. Am J Physiol, 1999. **227**: G756-762.
32. Katai K , Miyamoto K, Kishida S, Segawa H, Nii T, Tanaka H, Tani Y, Arai H, Tatsumi S, Morita K, Taketani Y, Takeda E, *Regulation of Intestinal Na+-Dependent Phosphate Co-Transporters by a Low-Phosphate Diet and 1,25-Dihydroxyvitamin D3*. Biochem J, 1999. **343**(Pt3): 705-712.
33. Segawa H , Kaneko I, Yamanaka S, Ito M, Kuwahata M, Inoue Y, Kato S, Miyamoto K, *Intestinal Na-P(I) Cotransporter Adaptation to Dietary P(I) Content in Vitamin D Receptor Null Mice*. Am J Physiol Renal Physiol, 2004. **287**(1): F39-47.
34. Levine BS , Ho K, Hodsman A, Kuorokawa K, Coburn JW, *Early Renal Brush Border Membranes Adaptation to Dietary Phosphorous*. Miner. Electrolyte Metab, 1984. **10**: 222-227.
35. Portale AA , Halloran BP, Curtis R, *Physiological Regulation of the Serum Concentration of 1,25-Dihydroxyvitamin D by Phosphorous in Normal Men*. J. Clin. Invest, 1989. **83**: 1494-1499.
36. Tenenhouse HS , Martel J, *Renal Adaptation to Phosphate Deprivation: Lessons from the X-Linked Hyp Mouse*. Pediatr. Nephrol, 1993. **7**: 312-318.
37. Hosoi T *Polymorphisms of Vitamin D Receptor Gene*. Nihon Rinsho, 2002. **60 Suppl 3**: 106-110.
38. Fukumoto S *Phosphate Metabolism and Vitamin D*. Bonekey Rep, 2014. **5**(3): 497.
39. Xu H , Bai L, Collins JF, Ghishan FK, *Age-Dependent Regulation of Rat Intestinal Type Iib Sodium-Phosphate Cotransporter by 1,25-(OH)(2) Vitamin D(3)*. Am J Physiol Cell Physiol, 2002. **282**(3): C487-493.
40. Lederer E *Regulation of Serum Phosphate*. J Physiol, 2014. **592**(18): 3985-3995.
41. Marks J , Debnam ES, Unwin RJ, *Phosphate Homeostasis and the Renal-Gastrointestinal Axis*. Am J Physiol Renal Physiol, 2010. **299**(2): F285-296.

42. Fukagawa M , Okazaki R, Takano K, Kaname S, Ogata E, Kitaoka M, Harada S, Sekine N, Matsumoto T, Kurokawa K, *Regression of Parathyroid Hyperplasia by Calcitriol-Pulse Therapy in Patients on Long-Term Dialysis*. N Engl J Med, 1990. **323**(6): 421-422.
43. Silver J , Russell J, Sherwood LM, *Regulation by Vitamin D Metabolites of Messenger Ribonucleic Acid for Preproparathyroid Hormone in Isolated Bovine Parathyroid Cells*. Proc Natl Acad Sci USA, 1985. **82**: 4270-4273.
44. Silver J , Naveh-Many T, Mayer H, Schmelzer HJ, Popovtzer MM, *Regulation by Vitamin D Metabolites of Parathyroid Hormone Gene Transcription in Vivo in the Rat*. J Clin Invest, 1986. **78**(5): 1296-1301.
45. Russell J , Lettieri D, Sherwood LM, *Suppression by 1,25(OH)2d3 of Transcription of the Pre-Parathyroid Hormone Gene*. Endocrinology, 1986. **119**: 1296-1301.
46. Shimada T , Yamazaki Y, Takahashi M, Hasegawa H, Urakawa I, Oshima T, Ono K, Kakitani M, Tomizuka K, Fujita T, Fukumoto S, Yamashita T, *Vitamin D Receptor-Independent Fgf23 Actions in Regulating Phosphate and Vitamin D Metabolism*. Am J Physiol Renal Physiol, 2005. **289**(5): F1088-1095.
47. Ohnishi M , Nakatani T, Lanske B, Razzaque MS, *Reversal of Mineral Ion Homeostasis and Soft-Tissue Calcification of Klotho Knockout Mice by Deletion of Vitamin D 1alpha-Hydroxylase*. Kidney Int, 2009. **75**(11): 1166-1172.
48. Gillies BR , Ryan BA, Tonkin BA, Poulton IJ, Ma Y, Kirby BJ, St-Arnaud R, Sims NA, Kovacs CS, *Absence of Calcitriol Causes Increased Lactational Bone Loss and Lower Milk Calcium but Does Not Impair Post-Lactation Bone Recovery in Cyp27b1 Null Mice*. J Bone Miner Res., 2018. **33**(1): 16-26.
49. Usdin TB , Bonner TI, Hoare SR., *The Parathyroid Hormone 2 (Pth2) Receptor*. Receptors Channels, 2002. **8**(3-4): 211-218.
50. Lee DB , Walling MW, Corry DB, *Phosphate Transport across Rat Jejunum: Influence of Sodium, Ph, and 1,25-Dihydroxyvitamin D3*. Am J Physiol Gastrointest Liver Physiol, 1986. **251**: G90 –G95.
51. Murer H , Hernando N, Forster L, Biber J, *Molecular Mechanisms in Proximal Tubular and Small Intestinal Phosphate Reabsorption*. Mol Membr Biol, 2001. **18**: 3-11.
52. Shinki T , Ueno Y, DeLuca HF, Suda T, *Calcitonin Is a Major Regulator for the Expression of Renal 25-Hydroxyvitamin D3-1alpha-Hydroxylase Gene in Normocalcemic Rats*. Proc Natl Acad Sci U S A., 1999. **96**(14): 8253-8258.
53. Lavi-Moshayoff V , Wasserman G, Meir T, Silver J, Naveh-Many T., *Pth Increases Fgf23 Gene Expression and Mediates the High-Fgf23 Levels of Experimental Kidney Failure: A Bone Parathyroid Feedback Loop*. Am J Physiol Renal Physiol, 2010. **299**(4): F882-889.
54. Rhee Y , Bivi N, Farrow E, Lezcano V, Plotkin LI, White KE, Bellido T., *Parathyroid Hormone Receptor Signaling in Osteocytes Increases the Expression of Fibroblast Growth Factor-23 in Vitro and in Vivo*. Bone, 2011. **49**(4): 636-643.
55. López I , Rodríguez-Ortiz ME, Almadén Y, Guerrero F, de Oca AM, Pineda C, Shalhoub V, Rodríguez M, Aguilera-Tejero E, *Direct and Indirect Effects of Parathyroid Hormone on Circulating Levels of Fibroblast Growth Factor 23 in Vivo*. Kidney Int, 2011. **80**(5): 475-482.
56. Saji F , Shigematsu T, Sakaguchi T, Ohya M, Orita H, Maeda Y, Ooura M, Mima T, Negi S, *Fibroblast Growth Factor 23 Production in Bone Is Directly Regulated by 1{Alpha},25-Dihydroxyvitamin D, but Not Pth*. Am J Physiol Renal Physiol, 2010. **299**(5): F1212-1217.
57. Silver J , Naveh-Many T, *Fgf23 and the Parathyroid Glands*. Pediatr Nephrol, 2010. **25**(11): 2241-2245.
58. Saito T , Fukumoto S, *Fibroblast Growth Factor 23 (Fgf23) and Disorders of Phosphate Metabolism*. Int J Pediatr Endocrinol, 2009. **2009**: 496-514.
59. Smith ER , Cai MM, McMahon LP, Holt SG, *Biological Variability of Plasma Intact and C-Terminal Fgf23 Measurements*. J Clin Endocrinol Metab, 2012. **97**(9): 3357-3365.

60. Sleeman M , Fraser J, McDonald M, Yuan S, White D, Grandison P, Kumble K, Watson JD, Murison JG, *Identification of a New Fibroblast Growth Factor Receptor, Fgfr5*. Gene, 2001. **271**(2): 171-182.
61. Beenken A , Mohammadi M, *The Fgf Family: Biology, Pathophysiology and Therapy*. Nat Rev Drug Discov, 2009. **8**(3): 235-253.
62. Sarrazin S , Lamanna WC, Esko JD., *Heparan Sulfate Proteoglycans*. Cold Spring Harb Perspect Biol, 2011. **3**(7).
63. Kuro-o M , Matsumura Y, Aizawa H, Kawaguchi H, Suga T, Utsugi T, Ohyama Y, Kurabayashi M, Kaname T, Kume E, Iwasaki H, Iida A, Shiraki-Iida T, Nishikawa S, Nagai R, Nabeshima YI., *Mutation of the Mouse Klotho Gene Leads to a Syndrome Resembling Ageing*. Nature, 1997. **390**(6655): 45-51.
64. Fukagawa M , Nii-Kono T, Kazama JJ, *Role of Fibroblast Growth Factor 23 in Health and in Chronic Kidney Disease*. Curr Opin Nephrol Hypertens, 2005. **14**(4): 325-329.
65. Kurosu H , Ogawa Y, Miyoshi M, Yamamoto M, Nandi A, Rosenblatt KP, Baum MG, Schiavi S, Hu MC, Moe OW, Kuro-o M, *Regulation of Fibroblast Growth Factor-23 Signaling by Klotho*. J Biol Chem, 2006. **281**(10): 6120-6123.
66. Nakatani T , Sarraj B, Ohnishi M, Densmore MJ, Taguchi T, Goetz R, Mohammadi M, Lanske B, Razzaque MS, *In Vivo Genetic Evidence for Klotho-Dependent, Fibroblast Growth Factor 23 (Fgf23) -Mediated Regulation of Systemic Phosphate Homeostasis*. FASEB J, 2009. **23**(2): 433-441.
67. Razzaque MS , Lanske B., *Hypervitaminosis D and Premature Aging: Lessons Learned from Fgf23 and Klotho Mutant Mice*. Trends Mol Med, 2006. **12**(7): 298-305.
68. Urakawa I , Yamazaki Y, Shimada T, Iijima K, Hasegawa H, Okawa K, Fujita T, Fukumoto S, Yamashita T, *Klotho Converts Canonical Fgf Receptor into a Specific Receptor for Fgf23*. Nature, 2006. **444**(7120): 770-774.
69. Razzaque MS *The Fgf23-Klotho Axis: Endocrine Regulation of Phosphate Homeostasis*. Nat Rev Endocrinol, 2009. **5**(11): 611-619.
70. Gattineni J , Bates C, Twombly K, Dwarakanath V, Robinson ML, Goetz R, Mohammadi M, Baum M, *Fgf23 Decreases Renal Napi-2a and Napi-2c Expression and Induces Hypophosphatemia in Vivo Predominantly Via Fgf Receptor 1*. Am J Physiol Renal Physiol, 2009. **297**(2): F282-291.
71. Liu S , Vierthaler L, Tang W, Zhou J, Quarles LD, *Fgfr3 and Fgfr4 Do Not Mediate Renal Effects of Fgf23*. J Am Soc Nephrol, 2008. **19**(12): 2342-2350.
72. Yamazaki Y , Tamada T, Kasai N, Urakawa I, Aono Y, Hasegawa H, Fujita T, Kuroki R, Yamashita T, Fukumoto S, Shimada T, *Anti-Fgf23 Neutralizing Antibodies Show the Physiological Role and Structural Features of Fgf23*. J Bone Miner Res, 2008. **23**(9): 1509-1518.
73. Miyamoto K , Ito M, Kuwahata M, Kato S, Segawa H, *Inhibition of Intestinal Sodium-Dependent Inorganic Phosphate Transport by Fibroblast Growth Factor 23*. Ther Apher Dial, 2005. **9**(4): 331-335.
74. Yuan Q , Sato T, Densmore M, Saito H, Schüler C, Erben RG, Lanske B, *Fgf-23/Klotho Signaling Is Not Essential for the Phosphaturic and Anabolic Functions of Pth*. J Bone Miner Res, 2011. **26**(9): 2026-2035.
75. Bergwitz C , Jüppner H., *Regulation of Phosphate Homeostasis by Pth, Vitamin D, and Fgf23*. Annu Rev Med, 2010. **61**: 91-104.
76. Dua K , Leonhard S, Martens H, Abbas SK, Care AD., *Effects of Parathyroid Hormone and Parathyroid Hormone-Related Protein on the Rates of Absorption of Magnesium, Calcium, Sodium, Potassium and Phosphate Ions from the Reticulo-Rumen of Sheep*. Exp Physiol, 1994. **79**(3): 401-408.
77. Clark I *Importance of Dietary Ca:Po4 Ratios on Skeletal, Ca, Mg, and Po4 Metabolism*. Am J Physiol, 1969. **217**(3): 865-870.

78. Borowitz SM , Granrud GS., *Glucocorticoids Inhibit Intestinal Phosphate Absorption in Developing Rabbits*. J Nutr, 1992. **122**(6): 1273-1279.
79. Bonjour JP *Calcium and Phosphate: A Duet of Ions Playing for Bone Health*. J Am Coll Nutr, 2011. **30**(5): 438S-448S.
80. Wang H , Yoshiko Y, Yamamoto R, Minamizaki T, Kozai K, Tanne K, Aubin JE, Maeda N, *Overexpression of Fibroblast Growth Factor 23 Suppresses Osteoblast Differentiation and Matrix Mineralization in Vitro*. J Bone Miner Res, 2008. **23**(6): 939-948.
81. Sitara D , Kim S, Razzaque MS, Bergwitz C, Taguchi T, Schüler C, Erben RG, Lanske B, *Genetic Evidence of Serum Phosphate-Independent Functions of Fgf-23 on Bone*. PLoS Genet., 2008. **4**(8): e1000154.
82. Shalhoub V , Ward SC, Sun B, Stevens J, Renshaw L, Hawkins N, Richards WG, *Fibroblast Growth Factor 23 (Fgf23) and Alpha-Klotho Stimulate Osteoblastic Mc3t3.E1 Cell Proliferation and Inhibit Mineralization*. Calcif Tissue Int., 2011. **89**(2): 140-150.
83. Yuan Q , Sitara D, Sato T, Densmore M, Saito H, Schüler C, Erben RG, Lanske B., *Pth Ablation Ameliorates the Anomalies of Fgf23-Deficient Mice by Suppressing the Elevated Vitamin D and Calcium Levels*. Endocrinology, 2011. **152**(11): 4053-4061.
84. Yuan Q , Jiang Y, Zhao X, Sato T, Densmore M, Schüler C, Erben RG, McKee MD, Lanske B., *Increased Osteopontin Contributes to Inhibition of Bone Mineralization in Fgf23-Deficient Mice*. J Bone Miner Res, 2014. **29**(3): 693-704.
85. Sodek J , Ganss B, McKee MD, *Osteopontin*. Crit Rev Oral Biol Med, 2000. **11**(3): 279-303.
86. Yoshida T , Stern PH, *How Vitamin D Works on Bone*. Endocrinol Metab Clin North Am, 2012. **41**(3): 557-569.
87. Takahashi N , Akatsu T, Sasaki T, Nicholson GC, Moseley JM, Martin TJ, Suda T, *Induction of Calcitonin Receptors by 1 Alpha, 25-Dihydroxyvitamin D3 in Osteoclast-Like Multinucleated Cells Formed from Mouse Bone Marrow Cells*. Endocrinology, 1988. **123**(3): 1504-1510.
88. Suda T , Takahashi N, Udagawa N, Jimi E, Gillespie MT, Martin TJ, *Modulation of Osteoclast Differentiation and Function by the New Members of the Tumor Necrosis Factor Receptor and Ligand Families*. Endocr Rev., 1999. **20**(3): 345-357.
89. Takeda S , Yoshizawa T, Nagai Y, Yamato H, Fukumoto S, Sekine K, Kato S, Matsumoto T, Fujita T, *Stimulation of Osteoclast Formation by 1,25-Dihydroxyvitamin D Requires Its Binding to Vitamin D Receptor (Vdr) in Osteoblastic Cells: Studies Using Vdr Knockout Mice*. Endocrinology, 1999. **140**(2): 1005-1008.
90. Xue Y , Fleet JC., *Intestinal Vitamin D Receptor Is Required for Normal Calcium and Bone Metabolism in Mice*. Gastroenterology, 2009. **136**(4): 1317-1327.
91. Suda T , Masuyama R, Bouillon R, Carmeliet G, *Physiological Functions of Vitamin D: What We Have Learned from Global and Conditional Vdr Knockout Mouse Studies*. Curr Opin Pharmacol. , 2015. **22**: 87-99.
92. Woeckel VJ , Alves RD, Swagemakers SM, Eijken M, Chiba H, van der Eerden BC, van Leeuwen JP, *1alpha,25-(Oh)2d3 Acts in the Early Phase of Osteoblast Differentiation to Enhance Mineralization Via Accelerated Production of Mature Matrix Vesicles*. J Cell Physiol., 2010. **225**(2): 593-600.
93. Biber J , Hernando N, Forster I, Murer H., *Regulation of Phosphate Transport in Proximal Tubules*. Eur J Physiol, 2009. **458**(1): 39-52.
94. Ullrich KJ , Murer H, *Sulphate and Phosphate Transport in the Renal Proximal Tubule*. Philos Trans R Soc Lond B Biol Sci, 1982. **299**(1097): 549-558.
95. Beck L , Karaplis AC, Amizuka N, Hewson AS, Ozawa H, Tenenhouse HS., *Targeted Inactivation of Npt2 in Mice Leads to Severe Renal Phosphate Wasting, Hypercalciuria, and Skeletal Abnormalities*. Proc Natl Acad Sci U S A, 1998. **95**(9): 5372-5377.
96. Tenenhouse HS , Martel J, Gauthier C, Segawa H, Miyamoto K, *Differential Effects of Npt2a Gene Ablation and X-Linked Hyp Mutation on Renal Expression of Npt2c*. Am J Physiol, 2003. **285**: F1271-F1278.

97. Segawa H , Kaneko I, Takahashi A, Kuwahata M, Ito M, Ohkido I, Tatsumi S, Miyamoto K, *Growth-Related Renal Type Ii Na/Pi Cotransporter*. J Biol Chem, 2002. **277**(22): 19665-19672.
98. Clark NB. , *Renal Excretion of Phosphate and Calcium in Parathyroidectomized Starlings*. Am J Physiol., 1977. **233**(2): 138-144.
99. In *Primer on the Metabolic Bone Diseases and Disorders of Mineral Metabolism*, edited by Rosen CJ 579-589: Wiley Online Library.
100. Fraser D , Kooh SW, Scriver CR., *Hyperparathyroidism as the Cause of Hyperaminoaciduria and Phosphaturia in Human Vitamin D Deficiency*. Pediatr Res., 1967. **1**(6): 425-435.
101. Murray RD , Lederer ED, Khundmiri SJ., *Role of Pth in the Renal Handling of Phosphate*. AIMS Medical Science, 2015. **2**(3): 162-181.
102. Prasad N , Bhadauria D, *Renal Phosphate Handling: Physiology*. Indian J Endocrinol Metab., 2013. **17**(4): 620-627.
103. Kovacs CS *The Role of Pthrp in Regulating Mineral Metabolism During Pregnancy, Lactation, and Fetal/Neonatal Development*. Clin Rev Bone Miner Metab, 2014. **12**: 142-164.
104. Bacic D , Lehir M, Biber J, Kaissling B, Murer H, Wagner CA., *The Renal Na<sup>+</sup>/Phosphate Cotransporter Napi-Iia Is Internalized Via the Receptor-Mediated Endocytic Route in Response to Parathyroid Hormone*. Kidney Int, 2006. **69**(3): 495-503.
105. Kempson SA , Löttscher M, Kaissling B, Biber J, Murer H, Levi M, *Parathyroid Hormone Action on Phosphate Transporter Mrna and Protein in Rat Renal Proximal Tubules*. Am J Physiol., 1995. **268**(4 Pt 2): F784-791.
106. Picard N , Capuano P, Bacic D, Biber J, Murer H, Le Hir M, Kaissling B, Wagner C, *Differential Regulation of Renal Na/Phosphate Cotransporters Napi-Lla and Napi-Llc in Response to Parathyroid Hormone (Pth)*. J Am Soc Nephrol, 2007. **18**: 109A.
107. Segawa H , Yamanaka S, Onitsuka A, Tomoe Y, Kuwahata M, Ito M, Taketani Y, Miyamoto K, *Parathyroid Hormone-Dependent Endocytosis of Renal Type Iic Na-Pi Cotransporter*. Am J Physiol Renal Physiol, 2007. **292**(1): F395-403.
108. Miyamoto K , Segawa H, Ito M, Kuwahata M, *Physiological Regulation of Renal Sodium-Dependent Phosphate Cotransporters*. Jpn J Physiol, 2004. **54**(2): 93-102.
109. Baum M , Schiavi S, Dwarakanath V, Quigley R, *Effect of Fibroblast Growth Factor-23 on Phosphate Transport in Proximal Tubules*. Kidney Int, 2005. **68**(3): 1148-1153.
110. Shimada T , Kakitani M, Yamazaki Y, Hasegawa H, Takeuchi Y, Fujita T, Fukumoto S, Tomizuka K, Yamashita T., *Targeted Ablation of Fgf23 Demonstrates an Essential Physiological Role of Fgf23 in Phosphate and Vitamin D Metabolism*. J Clin Invest, 2004. **113**(4): 561-568.
111. Hu MC , Shi M, Zhang J, Pastor J, Nakatani T, Lanske B, Razzaque MS, Rosenblatt KP, Baum MG, Kuro-o M, Moe OW., *Klotho: A Novel Phosphaturic Substance Acting as an Autocrine Enzyme in the Renal Proximal Tubule*. FASEB J., 2010. **24**(9): 3438-3450.
112. Kuro-o M *Klotho as a Regulator of Fibroblast Growth Factor Signaling and Phosphate/Calcium Metabolism*. Curr Opin Nephrol Hypertens., 2006. **15**(4): 437-441.
113. Kurnik BR , Hruska KA, *Mechanism of Stimulation of Renal Phosphate Transport by 1,25-Dihydroxycholecalciferol*. Biochim Biophys Acta., 1985. **817**(1): 42-50.
114. Mühlbauer RC , Bonjour JP, Fleisch H, *Tubular Handling of Pi: Localization of Effects of 1,25(Oh)2d3 and Dietary Pi in Tptx Rats*. Am J Physiol, 1981. **241**(2): F123-128.
115. Capuano P , Radanovic T, Wagner CA, Bacic D, Kato S, Uchiyama Y, St-Arnoud R, Murer H, Biber J., *Intestinal and Renal Adaptation to a Low-Pi Diet of Type Ii Napi Cotransporters in Vitamin D Receptor- and 1alphaohase-Deficient Mice*. Am J Physiol Cell Physiol, 2005. **288**(2): C429-434.
116. Shimada T , Hasegawa H, Yamazaki Y, Muto T, Hino R, Takeuchi Y, Fujita T, Nakahara K, Fukumoto S, Yamashita T., *Fgf-23 Is a Potent Regulator of Vitamin D Metabolism and Phosphate Homeostasis*. J Bone Miner Res, 2004. **19**(3): 429-435.

117. Perwad F , Zhang MY, Tenenhouse HS, Portale AA., *Fibroblast Growth Factor 23 Impairs Phosphorus and Vitamin D Metabolism in Vivo and Suppresses 25-Hydroxyvitamin D-1alpha-Hydroxylase Expression in Vitro*. Am J Physiol Renal Physiol. , 2007. **293**(5): F1577-1583.
118. Francis F , Hennig S, Korn B, Reinhardt R, de Jong P, Poustka A, Lehrach H, Rowe PSN, Goulding JN, Summerfield T, Mountford R, Read AP, Popowska E, Pronicka E, Davies KE, O'Riordan JLH, Econs MJ, Nesbitt T, Drezner MK, Oudet C, Pannetier S, Hanauer A, Strom TM, Meindl A, Lorenz B, Cagnoli B, Mohnike KL, Murken J, Meitinger T, *A Gene (Pex) with Homologies to Endopeptidases Is Mutated in Patients with X-Linked Hypophosphatemic Rickets. The Hyp Consortium*. Nat Genet., 1995. **11**(2): 130-136.
119. Beck L , Soumounou Y, Martel J, Krishnamurthy G, Gauthier C, Goodyer CG, Tenenhouse HS, *Pex/Pex Tissue Distribution and Evidence for a Deletion in the 3' Region of the Pex Gene in X-Linked Hypophosphatemic Mice*. J Clin Invest., 1997. **99**(6): 1200-1209.
120. Gordon JS *Fgf23, Hypophosphatemia, and Rickets: Has Phosphatonin Been Found?* Proc Natl Acad Sci U S A, 2001. **98**: 5945-5946.
121. Benet-Pagès A , Lorenz-Depiereux B, Zischka H, White KE, Econs MJ, Strom TM., *Fgf23 Is Processed by Proprotein Convertases but Not by Phex*. Bone, 2004. **35**(2): 455-462.
122. Liu S , Guo R, Simpson LG, Xiao ZS, Burnham CE, Quarles LD., *Regulation of Fibroblastic Growth Factor 23 Expression but Not Degradation by Phex*. J Biol Chem. , 2003. **278**(39): 37419-37426.
123. Shimada T , Mizutani S, Muto T, Yoneya T, Hino R, Takeda S, Takeuchi Y, Fujita T, Fukumoto S, Yamashita T., *Cloning and Characterization of Fgf23 as a Causative Factor of Tumor-Induced Osteomalacia*. Proc Natl Acad Sci U S A, 2001. **98**(11): 6500-6505.
124. Florenzano P , Gafni RI, Collins MT, *Tumor-Induced Osteomalacia*. Bone Rep., 2017. **20**(7): 90-97.
125. ADHR Consortium *Autosomal Dominant Hypophosphatemic Rickets Is Associated with Mutations in Fgf23*. Nat Genet., 2000. **26**(3): 345-348.
126. Imel EA , Hui SL, Econs MJ., *Fgf23 Concentrations Vary with Disease Status in Autosomal Dominant Hypophosphatemic Rickets*. J Bone Miner Res, 2007. **22**(4): 520-526.
127. Lorenz-Depiereux B , Bastepe M, Benet-Pagès A, Amyere M, Wagenstaller J, Müller-Barth U, Badenhop K, Kaiser SM, Rittmaster RS, Shlossberg AH, Olivares JL, Loris C, Ramos FJ, Glorieux F, Vikkula M, Jüppner H, Strom TM., *Dmp1 Mutations in Autosomal Recessive Hypophosphatemia Implicate a Bone Matrix Protein in the Regulation of Phosphate Homeostasis*. Nat Genet., 2006. **38**(11): 1248-1250.
128. Feng JQ , Ward LM, Liu S, Lu Y, Xie Y, Yuan B, Yu X, Rauch F, Davis SI, Zhang S, Rios H, Drezner MK, Quarles LD, Bonewald LF, White KE., *Loss of Dmp1 Causes Rickets and Osteomalacia and Identifies a Role for Osteocytes in Mineral Metabolism*. Nat Genet., 2006. **38**(11): 1310-1315.
129. Topaz O , Indelman M, Chefetz I, Geiger D, Metzker A, Altschuler Y, Choder M, Bercovich D, Uitto J, Bergman R, Richard G, Sprecher E., *A Deleterious Mutation in Samd9 Causes Normophosphatemic Familial Tumoral Calcinosis*. Am J Hum Genet, 2006. **79**(4): 759-764.
130. Lyles KW , Halsey DL, Friedman NE, Lobaugh B., *Correlations of Serum Concentrations of 1,25-Dihydroxyvitamin D, Phosphorus, and Parathyroid Hormone in Tumoral Calcinosis*. J Clin Endocrinol Metab., 1988. **67**(1): 88-92.
131. Ichikawa S , Imel EA, Kreiter ML, Yu X, Mackenzie DS, Sorenson AH, Goetz R, Mohammadi M, White KE, Econs MJ., *A Homozygous Missense Mutation in Human Klotho Causes Severe Tumoral Calcinosis*. J Clin Invest., 2007. **117**(9): 2684-2691.
132. Topaz O , Shurman DL, Bergman R, Indelman M, Ratajczak P, Mizrachi M, Khamaysi Z, Behar D, Petronius D, Friedman V, Zelikovic I, Raimer S, Metzker A, Richard G, Sprecher E., *Mutations in Galnt3, Encoding a Protein Involved in O-Linked Glycosylation, Cause Familial Tumoral Calcinosis*. Nat Genet., 2004. **36**(6): 579-581.

133. Araya K , Fukumoto S, Backenroth R, Takeuchi Y, Nakayama K, Ito N, Yoshii N, Yamazaki Y, Yamashita T, Silver J, Igarashi T, Fujita T., *A Novel Mutation in Fibroblast Growth Factor 23 Gene as a Cause of Tumoral Calcinosis*. J Clin Endocrinol Metab., 2005. **90**(10): 5523-5527.
134. Bergwitz C , Miyamoto KI., *Hereditary Hypophosphatemic Rickets with Hypercalciuria: Pathophysiology, Clinical Presentation, Diagnosis and Therapy*. Pflugers Arch., 2019. **471**(1): 149-163.
135. Kovacs CS *Bone Development and Mineral Homeostasis in the Fetus and Neonate: Roles of the Calcitropic and Phosphotropic Hormones*. Physiol Rev, 2014. **94**(4): 1143-1218.
136. Brunette MG , Allard S, *Phosphate Uptake by Syncytial Brush Border Membranes of Human Placenta*. Pediatr Res. , 1985. **19**(11): 1179-1182.
137. Stulc J , Stulcová B., *Transport of Inorganic Phosphate by the Fetal Border of the Guinea-Pig Placenta Perfused in Situ*. Placenta., 1984. **5**(1): 9-19.
138. Stulc J , Stulcová B, Svihovec J., *Uptake of Inorganic Phosphate by the Maternal Border of the Guinea Pig Placenta*. Pflugers Arch., 1982. **395**(4): 326-330.
139. Ma Y , Samaraweera M, Cooke-Hubley S, Kirby BJ, Karaplis AC, Lanske B, Kovacs CS, *Neither Absence nor Excess of Fgf23 Disturbs Murine Fetal-Placental Phosphorus Homeostasis or Prenatal Skeletal Development and Mineralization*. Endocrinology, 2014. **155**(5): 1596-605.
140. Lederer E , Miyamoto K., *Clinical Consequences of Mutations in Sodium Phosphate Cotransporters*. Clin J Am Soc Nephrol., 2012. **7**(7): 1179-1187.
141. Care AD , Abbas SK, Pickard DW, Barri M, Drinkhill M, Findlay JB, White IR, Caple IW., *Stimulation of Ovine Placental Transport of Calcium and Magnesium by Mid-Molecule Fragments of Human Parathyroid Hormone-Related Protein*. Exp Physiol., 1990. **75**(4): 605-608.
142. Simmonds CS , Kovacs CS., *Role of Parathyroid Hormone (Pth) and Pth-Related Protein (Pthrp) in Regulating Mineral Homeostasis During Fetal Development*. Crit Rev Eukaryot Gene Expr., 2010. **20**(3): 235-273.
143. Barlet JP , Davicco MJ, Rouffet J, Coxam V, Lefavre J., *Short Communication: Parathyroid Hormone-Related Peptide Does Not Stimulate Phosphate Placental Transport*. Placenta., 1994. **15**(4): 441-444.
144. Stulc J , Stulcová B., *Placental Transfer of Phosphate in Anaesthetized Rats*. Placenta., 1996. **17**(7): 487-493.
145. Kovacs CS , Chafe LL, Woodland ML, McDonald KR, Fudge NJ, Wookey PJ., *Calcitropic Gene Expression Suggests a Role for the Intraplacental Yolk Sac in Maternal-Fetal Calcium Exchange*. Am J Physiol Endocrinol Metab., 2002. **282**(3): E721-732.
146. Karsenty G , Kronenberg HM, Settembre C, *Genetic Control of Bone Formation*. Annu Rev Cell Dev Biol, 2009. **25**: 629-648.
147. Abbas SK , Pickard DW, Rodda CP, Heath JA, Hammonds RG, Wood WI, Caple IW, Martin TJ, Care AD., *Stimulation of Ovine Placental Calcium Transport by Purified Natural and Recombinant Parathyroid Hormone-Related Protein (Pthrp) Preparations*. Q J Exp Physiol, 1989. **74**: 549-552.
148. Rodda CP , Kubota M, Heath JA, Ebeling PR, Moseley JM, Care AD, Caple IW, Martin TJ, *Evidence for a Novel Parathyroid Hormone-Related Protein in Fetal Lamb Parathyroid-Glands and Sheep Placenta: Comparisons with a Similar Protein Implicated in Humoral Hypercalcaemia of Malignancy*. J Endocrinol, 1988. **117**: 261-271.
149. Robinson NR , Sibley CP, Mughal MZ, Boyd RD., *Fetal Control of Calcium Transport across the Rat Placenta*. Pediatr Res, 1989. **26**: 109-115.
150. Simmonds CS , Karsenty G, Karaplis AC, Kovacs CS, *Parathyroid Hormone Regulates Fetal-Placental Mineral Homeostasis*. J Bone Miner Res, 2010. **25**: 594-605.
151. Durand D , Braithwaite GD, Barlet JP., *The Effect of 1 Alpha-Hydroxycholecalciferol on the Placental Transfer of Calcium and Phosphate in Sheep*. Br J Nutr., 1983. **49**(3): 475-480.
152. Durand D , Barlet JP, Braithwaite GD., *The Influence of 1,25-Dihydroxycholecalciferol on the Mineral Content of Foetal Guinea Pigs*. Reprod Nutr Dev., 1983. **23**(2a): 235-244.

153. Yang L , Tsang KY, Tang HC, Chan D, Cheah KS., *Hypertrophic Chondrocytes Can Become Osteoblasts and Osteocytes in Endochondral Bone Formation*. Proc Natl Acad Sci U S A., 2014. **111**(33): 12097-12102.
154. Donohue MM , Demay MB, *Rickets in Vdr Null Mice Is Secondary to Decreased Apoptosis of Hypertrophic Chondrocytes*. Endocrinology, 2002. **143**: 3691-3694.
155. Sabbagh Y , Carpenter TO, Demay MB., *Hypophosphatemia Leads to Rickets by Impairing Caspase-Mediated Apoptosis of Hypertrophic Chondrocytes*. Proc Natl Acad Sci USA, 2005. **102**: 9637-9642.
156. Omelon S , Georgiou J, Henneman ZJ, Wise LM, Sukhu B, Hunt T, Wynnyckyj C, Holmyard D, Bielecki R, Grynblas MD, *Control of Vertebrate Skeletal Mineralization by Polyphosphates*. PLoS One, 2009. **4**: e5634.
157. Zhang R , Lu Y, Ye L, Yuan B, Yu S, Qin C, Xie Y, Gao T, Drezner MK, Bonewald LF, Feng JQ., *Unique Roles of Phosphorus in Endochondral Bone Formation and Osteocyte Maturation*. J Bone Miner Res, 2011. **26**: 1047-1056.
158. Aaron JE , Abbas SK, Colwell A, East11 R, Oakley BA, Russell RG, *Parathyroid Gland Hormones in the Skeletal Development of the Ovine Foetus: The Effect of Parathyroidectomy with Calcium and Phosphate Infusion*. Bone Miner., 1992. **16**(2): 121-129.
159. Rebut-Bonneton C , Garel JM, Delbarre F, *Parathyroid Hormone, Calcitonin, 1,25-Dihydroxycholecalciferol, and Basal Bone Resorption in the Rat Fetus*. Calc if Tissue Int., 1983. **35**(2): 183-189.
160. Kovacs CS , Chafe LL, Fudge NJ, Friel JK, Manley NR, *Pth Regulates Fetal Blood Calcium and Skeletal Mineralization Independently of Pthrp*. Endocrinology, 2001. **142**(11): 4983-4993.
161. Miao D , He B, Karaplis AC, Goltzman D, *Parathyroid Hormone Is Essential for Normal Fetal Bone Formation*. J Clin Invest., 2002. **109**(9): 1173-1182.
162. Kovacs CS , Lanske B, *Parathyroid Hormone-Related Peptide (Pthrp) Regulates Fetal-Placental Calcium Transport through a Receptor Distinct from the Pth/Pthrp Receptor*. Proc Natl Acad Sci U S A, 1996. **93**(26): 15233-15238.
163. Fudge NJ , Kovacs CS, *Pregnancy up-Regulates Intestinal Calcium Absorption and Skeletal Mineralization Independently of the Vitamin D Receptor*. Endocrinology, 2010. **151**: 886-895.
164. Kirby BJ , Ardeshirpour L, Woodrow JP, Wysolmerski JJ, Sims NA, Karaplis AC, Kovacs CS, *Skeletal Recovery after Weaning Does Not Require Pthrp*. J Bone Miner Res, 2011. **26**: 1242-1251.
165. Kirby BJ , Ma Y, Martin HM, Buckle Favaro KL, Karaplis AC, Kovacs CS., *Upregulation of Calcitriol During Pregnancy and Skeletal Recovery after Lactation Do Not Require Parathyroid Hormone*. Journal of Bone and Mineral Research, 2013. **28**(9): 1987-2000.
166. Woodrow JP , Sharpe CJ, Fudge NJ, Hoff AO, Gagel RF, Kovacs CS, *Calcitonin Plays a Critical Role in Regulating Skeletal Mineral Metabolism During Lactation*. Endocrinology, 2006. **147**: 4010-4021.
167. Vortkamp A , Lee K, Lanske B, Segre GV, Kronenberg HM, Tabin CJ, *Regulation of Rate of Cartilage Differentiation by Indian Hedgehog and Pth-Related Protein*. Science, 1996. **273**(5275): 613-622.
168. Karaplis AC , Luz A, Glowacki J, Bronson RT, Tybulewicz VL, Kronenberg HM, Mulligan RC, *Lethal Skeletal Dysplasia from Targeted Disruption of the Parathyroid Hormone-Related Peptide Gene*. Genes Dev., 1994. **8**(3): 277-289.
169. Weir EC , Philbrick WM, Amling M, Neff LA, Baron R, Broadus AE, *Targeted Overexpression of Parathyroid Hormone-Related Peptide in Chondrocytes Causes Chondrodysplasia and Delayed Endochondral Bone Formation*. Proc Natl Acad Sci U S A., 1996. **93**(19): 10240-10245.
170. Schipani E , Lanske B, Hunzelman J, Luz A, Kovacs CS, Lee K, Pirro A, Kronenberg HM, Jüppner H, *Targeted Expression of Constitutively Active Receptors for Parathyroid Hormone and Parathyroid Hormone-Related Peptide Delays Endochondral Bone Formation and Rescues Mice*

- That Lack Parathyroid Hormone-Related Peptide.* Proc Natl Acad Sci U S A, 1997. **94**(25): 13689-13694.
171. Lanske B , Karaplis AC, Lee K, Luz A, Vortkamp A, Pirro A, Karperien M, Defize LH, Ho C, Mulligan RC, Abou-Samra AB, Jüppner H, Segre GV, Kronenberg HM, *Pth/Pthrp Receptor in Early Development and Indian Hedgehog-Regulated Bone Growth.* Science, 1996. **273**(5275): 663-666.
  172. Halloran BP , De Luca HF, *Effect of Vitamin D Deficiency on Skeletal Development During Early Growth in the Rat.* Arch Biochem Biophys., 1981. **209**(1): 7-14.
  173. Miller SC , Halloran BP, DeLuca HF, Jee WS, *Studies on the Role of Vitamin D in Early Skeletal Development, Mineralization, and Growth in Rats.* Calcif Tissue Int., 1983. **35**(4-5): 455-460.
  174. Lachenmaier-Currie U , Harmeyer J., *Placental Transport of Calcium and Phosphorus in Pigs.* J Perinat Med., 1989. **17**(2): 127-136.
  175. Kovacs CS , Woodland ML, Fudge NJ, Friel JK., *The Vitamin D Receptor Is Not Required for Fetal Mineral Homeostasis or for the Regulation of Placental Calcium Transfer in Mice.* Am J Physiol Endocrinol Metab., 2005. **289**(1): E133-144.
  176. Ryan BA , Alhani K, Sellars KB, Kirby BJ, St-Arnaud R, Kaufmann M, Jones G, Kovacs CS., *Mineral Homeostasis in Murine Fetuses Is Sensitive to Maternal Calcitriol but Not to Absence of Fetal Calcitriol.* J Bone Miner Res, 2018: Epub ahead of print.
  177. Kovacs CS *Fetal Mineral Homeostasis.* Pediatric Bone: Biology and Diseases (2nd Ed.), Edited by Pettifor JM Glorieux FH, Jüppner H. San Diego: Elsevier/Academic, 2011.
  178. McDonald KR , Fudge NJ, Woodrow JP, Friel JK, Hoff AO, Gagel RF, Kovacs CS., *Ablation of Calcitonin/Calcitonin Gene-Related Peptide-Alpha Impairs Fetal Magnesium but Not Calcium Homeostasis.* Am J Physiol Endocrinol Metab., 2004. **287**(2): E218-226.
  179. Kovacs CS *Bone Metabolism in the Fetus and Neonate.* Pediatr Nephrol., 2014. **29**(5): 793-803.
  180. Ross MG , Beall MH. *Amniotic Fluid Dynamics.* Maternal-Fetal Medicine: Principles and Practice, Edited by Resnik R Creasy RK, Iams JD, Lockwood CJ, Moore TR, Greene MF. Philadelphia, PA: Elsevier, 2014.
  181. Guignard JP , Torrado A, Da Cunha O, Gautier E, *Glomerular Filtration Rate in the First Three Weeks of Life.* J Pediatr, 1975. **87**: 268-272.
  182. Linarelli LG *Newborn Urinary Cyclic Amp and Developmental Renal Responsiveness to Parathyroid Hormone.* Pediatrics, 1972. **50**: 14-23.
  183. Moore ES , Langman CB, Favus MJ, Coe FL, *Role of Fetal 1,25-Dihydroxyvitamin D Production in Intrauterine Phosphorus and Calcium Homeostasis.* Pediatr Res., 1985. **19**: 566-569.
  184. Ross R , Care AD, Robinson JS, Pickard DW, Weatherley AJ., *Perinatal 1,25-Dihydroxycholecalciferol in the Sheep and Its Role in the Maintenance of the Transplacental Calcium Gradient.* J Endocrinol, 1980. **87**: 179-189.
  185. Moritz KM , Macris M, Talbo G, Wintour EM, *Foetal Fluid Balance and Hormone Status Following Nephrectomy in the Foetal Sheep.* Clin Exp Pharmacol Physiol, 1999. **26**: 857-864.
  186. Chalon S , Garel JM, *Plasma Calcium Control in the Rat Fetus. Ii. Influence of Fetal Hormones.* Biol Neonate, 1985. **48**: 323-328.
  187. MacIsaac RJ , Horne RS, Caple IW, Martin TJ, Wintour EM., *Effects of Thyroparathyroidectomy, Parathyroid Hormone, and Pthrp on Kidneys of Ovine Fetuses.* Am J Physiol Endocrinol Metab, 1993. **264**: E37-E44.
  188. Davicco MJ , Coxam V, Lefavre J, Barlet JP., *Parathyroid Hormone-Related Peptide Increases Urinary Phosphate Excretion in Fetal Lambs.* Exp Physiol, 1992. **77**: 377-383.
  189. Kovacs CS , Manley NR, Moseley JM, Martin TJ, Kronenberg HM, *Fetal Parathyroids Are Not Required to Maintain Placental Calcium Transport.* J Clin Invest., 2001. **107**(8): 1007-1015.
  190. Ryan BA , Sellars KB, Alhani K, Kirby BJ, St-Arnaud R, Kovacs CS "Complete Absence of Calcitriol in Cyp27b1 Null Fetal Mice Does Not Disturb Mineral Metabolism or Skeletal Development." In *ASBMR.* Denver, Colorado, USA 2017.

191. Garel JM , Barlet JP, *Calcium Metabolism in Newborn Animals: The Interrelationship of Calcium, Magnesium, and Inorganic Phosphorus in Newborn Rats, Foals, Lambs, and Calves*. *Pediatr Res.*, 1976. **10**: 749-754.
192. Bai X , Miao D, Goltzman D, Karaplis AC., *Early Lethality in Hyp Mice with Targeted Deletion of Pth Gene*. *Endocrinology*, 2007. **148**(10): 4974-4983.
193. Malan AJ. , *Studies in Mineral Metabolism. Viii. Comparison of Phosphorus Partition in the Blood of Calf Foetus, Sheep Foetus, and Lambs, with Corresponding Maternal Blood*. *J Agric Sci*, 1928. **18**: 397-400.
194. Bagnoli F , Bruchi S, Sardelli S, Buonocore G, Vispi L, Franchi F, Bracci R., *Calcium Homeostasis in the First Days of Life in Relation to Feeding*. *Eur J Pediatr*, 1985. **144**: 41-44.
195. Salle BL , Glorieux FH, Delvin EE, David LS, Meunier G, *Vitamin D Metabolism in Preterm Infants. Serial Serum Calcitriol Values During the First Four Days of Life*. *Acta Paediatr Scand*, 1983. **72**: 203-206.
196. Schauburger CW , Pitkin RM, *Maternal-Perinatal Calcium Relationships*. *Obstet Gynecol*, 1979. **53**: 74-76.
197. Ghishan FK , Jenkins JT, Younoszai MK, *Maturation of Calcium Transport in the Rat Small and Large Intestine*. *J Nutr*, 1980. **110**: 1622-1628.
198. Ghishan FK , Parker P, Nichols S, Hoyumpa A, *Kinetics of Intestinal Calcium Transport During Maturation in Rats*. *Pediatr Res.*, 1984. **18**: 235-239.
199. Halloran BP , DeLuca HF, *Calcium Transport in Small Intestine During Early Development: Role of Vitamin D*. *Am J Physiol Gastrointest Liver Physiol*, 1980. **239**: G473-G479.
200. Erben RG , Soegiarto DW, Weber K, Zeitz U, Lieberherr M, Gniadecki R, Moller G, Adamski J, Balling R., *Deletion of Deoxyribonucleic Acid Binding Domain of the Vitamin D Receptor Abrogates Genomic and Nongenomic Functions of Vitamin D*. *Mol Endocrinol*, 2002. **16**: 1524-1537.
201. Li YC , Amling M, Pirro AE, Priemel M, Meuse J, Baron R, Delling G, Demay MB, *Normalization of Mineral Ion Homeostasis by Dietary Means Prevents Hyperparathyroidism, Rickets, and Osteomalacia, but Not Alopecia in Vitamin D Receptor-Ablated Mice*. *Endocrinology*, 1998. **139**: 4391-4396.
202. Van Cromphaut SJ , Dewerchin M, Hoenderop JG, Stockmans I, Van Herck E, Kato S, Bindels RJ, Collen D, Carmeliet P, Bouillon R, Carmeliet G., *Duodenal Calcium Absorption in Vitamin D Receptor-Knockout Mice: Functional and Molecular Aspects*. *Proc Natl Acad Sci USA*, 2001. **98**: 13324-13329.
203. Yoshizawa T , Handa Y, Uematsu Y, Takeda S, Sekine K, Yoshihara Y, Kawakami T, Arioka K, Sato H, Uchiyama Y, Masushige S, Fukamizu A, Matsumoto T, Kato S., *Mice Lacking the Vitamin D Receptor Exhibit Impaired Bone Formation, Uterine Hypoplasia and Growth Retardation after Weaning*. *Nat Genet.*, 1997. **16**: 391-396.
204. Dardenne O , Prud'homme J, Arabian A, Glorieux FH, St-Arnaud R., *Targeted Inactivation of the 25-Hydroxyvitamin D<sub>3</sub>-1(Alpha)-Hydroxylase Gene (Cyp27b1) Creates an Animal Model of Pseudovitamin D-Deficiency Rickets*. *Endocrinology*, 2001. **142**: 3135-3141.
205. Panda DK , Miao D, Tremblay ML, Sirois J, Farookhi R, Hendy GN, Goltzman D., *Targeted Ablation of the 25-Hydroxyvitamin D<sub>3</sub> 1alpha -Hydroxylase Enzyme: Evidence for Skeletal, Reproductive, and Immune Dysfunction*. *Proc Natl Acad Sci USA*, 2001. **98**: 7498-7503.
206. Kobayashi A , Kawai S, Obe Y, Nagashima Y., *Effects of Dietary Lactose and Lactase Preparation on the Intestinal Absorption of Calcium and Magnesium in Normal Infants*. *Am J Clin Nutr*, 1975. **28**: 681-683.
207. Kocian J , Skala I, Bakos K., *Calcium Absorption from Milk and Lactose-Free Milk in Healthy Subjects and Patients with Lactose Intolerance*. *Digestion*, 1973. **9**: 317-324.
208. Barltrop D , Oppe TE., *Absorption of Fat and Calcium by Low Birthweight Infants from Milks Containing Butterfat and Olive Oil*. *Arch Dis Child.*, 1973. **48**: 496-501.

209. Giles MM , Fenton MH, Shaw B, Elton RA, Clarke M, Lang M, Hume R, *Sequential Calcium and Phosphorus Balance Studies in Preterm Infants*. J Pediatr, 1987. **110**: 591-598.
210. Senterre J , Putet G, Salle B, Rigo J, *Effects of Vitamin D and Phosphorus Supplementation on Calcium Retention in Preterm Infants Fed Banked Human Milk*. J Pediatr, 1983. **103**: 305-307.
211. Venkataraman PS , Tsang RC, Steichen JJ, Grey I, Neylan M, Fleischman AR., *Early Neonatal Hypocalcemia in Extremely Preterm Infants. High Incidence, Early Onset, and Refractoriness to Supraphysiologic Doses of Calcitriol*. Am J Dis Child, 1986. **140**: 1004-1008.
212. Senterre J , Salle B., *Calcium and Phosphorus Economy of the Preterm Infant and Its Interaction with Vitamin D and Its Metabolites*. Acta Paediatr Scand Suppl, 1982. **296**: 85-92.
213. Abrams SA. , *Calcium and Vitamin D Requirements of Enterally Fed Preterm Infants*. Pediatrics, 2013. **131**: e1676-1683.
214. Campbell DE , Fleischman AR, *Rickets of Prematurity: Controversies in Causation and Prevention*. Clin Perinatol, 1988. **15**: 879-890.
215. McIntosh N , De Curtis M, Williams J, *Failure of Mineral Supplementation to Reduce Incidence of Rickets in Very-Low-Birthweight Infants (Letter)*. Lancet, 1986. **2**: 981-982.
216. Weisman Y , Sapir R, Harell A, Edelstein S, *Maternal-Perinatal Interrelationships of Vitamin D Metabolism in Rats*. Biochim Biophys Acta, 1976. **428**: 388-395.
217. Kooh SW , Vieth R, *25-Hydroxyvitamin D Metabolism in the Sheep Fetus and Lamb*. Pediatr Res, 1980. **14**: 360-363.
218. Gardella T , Jüppner H, Bringham FR, Potts JT Jr., ed. *Receptors for Parathyroid Hormone (Pth) and Pth-Related Protein*. New York, 2008.
219. Horwitz MJ , Tedesco MB, Sereika SM, Hollis BW, Garcia-Ocana A, Stewart AF, *Direct Comparison of Sustained Infusion of Human Parathyroid Hormone-Related Protein-(1–36)*. J Clin Endocrinol Metab, 2003. **88**: 1603-1609.
220. Horwitz MJ , Tedesco MB, Sereika SM, Syed MA, Garcia-Ocana A, Bisello A, Hollis BW, Rosen CJ, Wysolmerski JJ, Dann P, Gundberg C, Stewart AF., *Continuous Pth and Pthrp Infusion Causes Suppression of Bone Formation and Discordant Effects on 1,25(OH)<sub>2</sub> Vitamin D*. J Bone Miner Res, 2005. **20**: 1792-1803.
221. Kovacs CS "Interactions of Pthrp with Receptors and Signaling." In *The Parathyroids (3rd Ed.)*, edited by Marcus R Bilezikian JP, Levine MA, Marcocci C, Potts JT Jr, Silverberg SJ. San Diego, CA: Elsevier, 2014.
222. Somjen D , Weisman Y, Berger E, Earon Y, Kaye AM, Binderman I., *Developmental Changes in the Responsiveness of Rat Kidney to Vitamin D Metabolites*. Endocrinology, 1986. **118**: 354-359.
223. Song Y , Peng X, Porta A, Takanaga H, Peng JB, Hediger MA, Fleet JC, Christakos S, *Calcium Transporter 1 and Epithelial Calcium Channel Messenger Ribonucleic Acid Are Differentially Regulated by 1,25 Dihydroxyvitamin D<sub>3</sub> in the Intestine and Kidney of Mice*. Endocrinology, 2003. **144**: 3885-3894.
224. Senterre J , Salle B, *Renal Aspects of Calcium and Phosphorus Metabolism in Preterm Infants*. Biol Neonate, 1988. **53**: 220-229.
225. Thomas ML , Anast CS, Forte LR, *Regulation of Calcium Homeostasis in the Fetal and Neonatal Rat*. Am J Physiol Endocrinol Metab, 1981. **240**: E367-E372.
226. Mallet E , Basuyau JP, Brunelle P, Devaux AM, Fessard C, *Neonatal Parathyroid Secretion and Renal Receptor Maturation in Premature Infants*. Biol Neonate, 1978. **33**: 304-308.
227. Mantovani G. , *Clinical Review: Pseudohypoparathyroidism: Diagnosis and Treatment*. J Clin Endocrinol Metab, 2011. **96**: 3020-3030.
228. Ngai YF , Chijiwa C, Mercimek-Mahmutoglu S, Stewart L, Yong SL, Robinson WP, Gibson WT, *Pseudohypoparathyroidism Type 1a and the Gnas P. R231h Mutation: Somatic Mosaicism in a Mother with Two Affected Sons*. Am J Med Genet Part A, 2010. **152**: 2784-2790.
229. Tsang RC , Venkataraman P, Ho M, Steichen JJ, Whitsett J, Greer F., *The Development of Pseudohypoparathyroidism. Involvement of Progressively Increasing Serum Parathyroid*

- Hormone Concentrations, Increased 1,25-Dihydroxyvitamin D concentrations, and "Migratory" Subcutaneous Calcifications.* Am J Dis Child, 1984. **138**: 654-658.
230. Polykandriotis EP , Beutel FK, Horch RE, Gruert J., *A Case of Familial Tumoral Calcinosis in a Neonate and Review of the Literature.* Arch Orthop Trauma Surg., 2004. **124**(8): 563-567.
231. Slavin RE , Wen J, Barmada A., *Tumoral Calcinosis—a Pathogenetic Overview: A Histological and Ultrastructural Study with a Report of Two New Cases, One in Infancy.* Int J Surg Pathol., 2012. **20**(5): 462-473.
232. Palmer PE. , *Tumoural Calcinosis.* Br J Radiol, 1966. **39**: 518-525.
233. Moncrieff MW *Early Biochemical Findings in Familial Hypophosphataemic, Hyperphosphaturic Rickets and Response to Treatment.* Arch Dis Child., 1982. **57**(1): 70-72.
234. Carpenter TO. , *The Expanding Family of Hypophosphatemic Syndromes.* J Bone Miner Metab, 2012. **30**(1): 1-9.
235. Ekpebegh CO , Blanco-Blanco E., *Familial Hypophosphataemic Rickets Affecting a Father and His Two Daughters: A Case Report.* West Afr J Med., 2010. **29**(4): 271-274.
236. Santos F , Fuente R, Mejia N, Mantecon L, Gil-Peña H, Ordoñez FA., *Hypophosphatemia and Growth.* Pediatr Nephrol., 2013. **28**(4): 595-603.
237. Liu S , Zhou J, Tang W, Jiang X, Rowe DW, Quarles LD., *Pathogenic Role of Fgf23 in Hyp Mice.* Am J Physiol Endocrinol Metab., 2006. **291**(1): E38-49.
238. Lorenz-Depiereux B , Guido VE, Johnson KR, Zheng QY, Gagnon LH, Bauschatz JD, Davisson MT, Washburn LL, Donahue LR, Strom TM, Eicher EM., *New Intragenic Deletions in the PheX Gene Clarify X-Linked Hypophosphatemia-Related Abnormalities in Mice.* Mamm Genome., 2004. **15**(3): 151-161.
239. Ohata Y , Yamazaki M, Kawai M, Tsugawa N, Tachikawa K, Koinuma T, Miyagawa K, Kimoto A, Nakayama M, Namba N, Yamamoto H, Okano T, Ozono K, Michigami T., *Elevated Fibroblast Growth Factor 23 Exerts Its Effects on Placenta and Regulates Vitamin D Metabolism in Pregnancy of Hyp Mice.* J Bone Miner Res., 2014. **29**(7): 1627-1638.
240. Xu X , Weinstein M, Li C, Naski M, Cohen RI, Ornitz DM, Leder P, Deng C., *Fibroblast Growth Factor Receptor 2 (Fgfr2)-Mediated Reciprocal Regulation Loop between Fgf8 and Fgf10 Is Essential for Limb Induction.* Development., 1998. **125**(4): 753-765.
241. MacIsaac RJ , Heath JA, Rodda CP, Moseley JM, Care AD, Martin TJ, Caple IW., *Role of the Fetal Parathyroid Glands and Parathyroid Hormone-Related Protein in the Regulation of Placental Transport of Calcium, Magnesium and Inorganic Phosphate.* Reprod Fertil Dev., 1991. **3**(4): 447-457.
242. Kovacs CS *The Role of Vitamin D in Pregnancy and Lactation: Insights from Animal Models and Clinical Studies.* Annu Rev Nutr., 2012. **32**: 97-123.
243. Turner M , Barré PE, Benjamin A, Goltzman D, Gascon-Barré M., *Does the Maternal Kidney Contribute to the Increased Circulating 1,25-Dihydroxyvitamin D Concentrations During Pregnancy?* Miner Electrolyte Metab., 1988. **14**(4): 246-252.
244. Bai X , Dinghong Q, Miao D, Goltzman D, Karaplis AC., *Klotho Ablation Converts the Biochemical and Skeletal Alterations in Fgf23 (R176q) Transgenic Mice to a Klotho-Deficient Phenotype.* Am J Physiol Endocrinol Metab., 2009. **296**(1): E79-88.
245. Yuan Q , Sato T, Densmore M, Saito H, Schüler C, Erben RG, Lanske B, *Deletion of Pth Rescues Skeletal Abnormalities and High Osteopontin Levels in Klotho-/- Mice.* PLoS Genet., 2012. **8**(5): e1002726.
246. Shibasaki Y , Etoh N, Hayasaka M, Takahashi MO, Kakitani M, Yamashita T, Tomizuka K, Hanaoka K, *Targeted Deletion of the Tybe Iib Na(+)-Dependent Pi-Co-Transporter, Napi-Iib, Results in Early Embryonic Lethality.* Biochem Biophys Res Commun, 2009. **381**(4): 482-486.
247. Takaiwa M , Aya K, Miyai T, Hasegawa K, Yokoyama M, Kondo Y, Kodani N, Seino Y, Tanaka H, Morishima T., *Fibroblast Growth Factor 23 Concentrations in Healthy Term Infants During the Early Postpartum Period.* Bone, 2010. **47**(2): 256-262.
248. Ramsey EM *The Placenta: Human and Animal.* New York: Praeger, 1982.

249. Cross JC , Rossant J. *Fetal Growth and Development* Development of the Embryo. Cambridge, UK: Cambridge University Press, 2001.
250. Sellars KB , Ryan BA, Kirby BJ, Kovacs CS. . "Fetal Fgf23 Is Required Only to Defend against Hyperphosphatemia Induced by Maternal Phosphate Loading." In *ASBMR*. Orlando, FL, USA, 2019.
251. Sellars KB , Ryan BA, Kirby BJ, Kovacs CS. . "Fetal Fgf23 Is Required Only to Defend against Hyperphosphatemia Induced by Maternal Phosphate Loading." In *2019 CSEM/Diabetes Canada Professional Conference & Annual Meetings*. Winnipeg, MB, Canada, 2019.

## 6 Appendix

### 6.1 Mouse Tail DNA Extraction Protocol

1. Cut 5 mm (5–10 mg) fresh or frozen mouse tail tissue into small pieces.
2. Dispense 300  $\mu$ l Cell Lysis Solution into a 1.5 ml microcentrifuge tube and add the tissue from the previous step.
3. Add 1.5  $\mu$ l Puregene Proteinase K to the lysate, and mix by inverting 25 times.
4. Incubate at 55°C overnight or until the tissue has completely lysed. Invert tube periodically during the incubation.
5. Optional: If RNA-free DNA is required, add 1.5  $\mu$ l RNase A Solution (cat. no. 158922), and mix by inverting 25 times. Incubate for 15–60 min at 37°C. Incubate for 1 min on ice to quickly cool the sample.
6. Add 100  $\mu$ l Protein Precipitation Solution, and vortex vigorously for 20 s at high speed.
7. Centrifuge for 3 min at 13,000–16,000 x g. The precipitated proteins should form a tight pellet. If the protein pellet is not tight, incubate on ice for 5 min and repeat the centrifugation.
8. Pipet 300  $\mu$ l isopropanol into a clean 1.5 ml microcentrifuge tube and add the supernatant from the previous step by pouring carefully. Be sure the protein pellet is not dislodged during pouring.
9. Mix by inverting gently 50 times.
10. Centrifuge for 1 min at 13,000–16,000 x g. The DNA may be visible as a small white pellet.
11. Carefully discard the supernatant, and drain the tube by inverting on a clean piece of absorbent paper, taking care that the pellet remains in the tube.
12. Add 300  $\mu$ l of 70% ethanol and invert several times to wash the DNA pellet.
13. Centrifuge for 1 min at 13,000–16,000 x g.

14. Carefully discard the supernatant. Drain the tube on a clean piece of absorbent paper, taking care that the pellet remains in the tube. Allow to air dry for up to 10 min. The pellet might be loose and easily dislodged.
15. Add 50  $\mu$ l DNA Hydration Solution and vortex 5 s at medium speed to mix.
16. Incubate at 65°C for 1 h to dissolve the DNA.
17. Incubate at room temperature overnight with gentle shaking. Ensure tube cap is tightly closed to avoid leakage. Samples can then be centrifuged briefly and transferred to a storage tube.

## 6.2 Phosphorus Assay

### Test Summary

Increased serum inorganic phosphorus concentrations (hyperphosphatemia) are usually the result of Vitamin D overdose, hypoparathyroidism, or renal failure. Decreased serum concentrations (hypophosphotemia) usually result from rickets, hyperparathyroidism, or Fanconi Syndrome (a defect in absorption of phosphorus and other metabolites from the glomerular filtrate).

The majority of methods for determining inorganic phosphorus are based on the reduction of a phosphorus-molybdate complex with a reducing agent resulting in the subsequent formation of molybdenum blue. In 1972, Daly and Ertingshausen introduced a method for inorganic phosphorus which measured the unreduced phosphorus-molybdate complex. This procedure is a modification of the Daly and Ertingshausen technique.

### Reagents

Phosphorus Blank Reagent (R1): An acidic solution (pH < 1 at 25°C) containing a surfactant.

Phosphorus Molybdate Reagent (R2): An acidic solution (pH < 1 at 25°C) containing 2.8 mmol/L ammonium molybdate.

Phosphorus Calibrator: 1 x 15 mL of a solution containing 6.2 mg/dL (2 mmol/L) phosphorus.

### Specimen

Fresh, clear, unhemolysed serum. Serum should be separated promptly from the red blood cells because erythrocytes contain phosphate concentrations several times greater than those found in sera.

### Reference Intervals

2.7-4.5 mg/dL (0.87-1.45 mmol/L)

These values are suggested guidelines. It is recommended that each laboratory establish the normal range for the area in which it is located.

### Calcium Assay

#### Test Summary

The majority of calcium in the body is present in bones. The remainder of the calcium is present in serum and has various functions. For example, calcium ions decrease neuromuscular excitability, participate in blood coagulation, and activate some enzymes.

Hypercalcemia can result from hyperparathyroidism, hypervitaminosis D, multiple myeloma, and some neoplastic diseases of bone. Hypocalcemia can result from hypoparathyroidism, steatorrhea, nephrosis, nephritis, and pancreatitis.

Calcium has traditionally been difficult to measure accurately and precisely, and a large variety of methods have been developed. Among these are flame photometry, oxalate precipitation with titration, atomic absorption spectrophotometry, EDTA chelation, and more recently calcium dye complexes which are measured spectrophotometrically. Examples of calcium dyes are o-cresolphthalein complexone and Arsenazo III, the latter being the dye used for calcium measurement in this method.

#### Reagents

Calcium Reagent: A solution containing ~ 0.15 mmol/L arsenazo III, a buffer, and a surfactant.

Calcium Calibrator for Manual Assays: 1 x 15 mL of a solution containing 10.0 mg/dL (2.50 mmol/L) calcium and a preservative (not included with Cat. No. 140-24).

#### Specimen

Fresh clear serum.

#### Reference Intervals

Serum:

Premature Infants 6.0-10.0 mg/dL 1.5-2.5 mmol/L

Full-term Infants 7.3-12.0 mg/dL 1.8-3.0 mmol/L

1 to 2 years 10.0-12.0 mg/dL 2.5-3.0 mmol/L

Adults 8.0-10.5 mg/dL 2.0-2.6 mmol/L

These values are suggested guidelines. It is recommended that each laboratory establish the normal range for the area in which it is located.

### 6.3 Mouse PTH 1-84 ELISA Kit

#### Introduction

Mouse intact parathyroid hormone (PTH 1-84) is an amino acid polypeptide produced by the parathyroid gland with its biological activity residing in the N-terminal region of the peptide. PTH plays an important role in maintaining the concentration of ionized calcium within the limits needed to achieve normal metabolic functions. When serum calcium levels are decreased the parathyroid gland increases secretion of the hormone which results in increased mobilization of calcium from skeletal reserves into the circulation. When levels of serum calcium are increased the secretion of PTH is reduced. The similarities between mouse and human physiology relative to calcium metabolism make the mouse an excellent live-animal model for studying human skeletal disease and in the pre-clinical evaluation of pharmacologic agents that may alter bone remodeling. Quantitation of biologically active mouse PTH 1-84 with this kit can provide a precise and sensitive assessment of changes in bone and mineral metabolism..

#### Test Principle

The Mouse PTH 1-84 ELISA Kit is a two-site enzyme-linked immunosorbent assay (ELISA) for the measurement of PTH in mouse plasma or cell culture media. Two different goat polyclonal antibodies have been affinity purified against mouse PTH to detect the biologically active intact

form of mouse PTH. The antibody which recognizes epitopes within the midregion/C-terminal portion (39-84) of the peptide is biotinylated for capture. The other antibody, which recognizes epitopes within the N-terminal region (1-34), is conjugated with the enzyme horseradish peroxidase (HRP) for detection. A sample containing mouse intact PTH is incubated simultaneously with the biotinylated capture antibody and the HRP conjugated antibody in a streptavidin coated microtiter well. Intact PTH (1-84) contained in the sample is immunologically bound by the capture antibody and the detection antibody to form a “sandwich” complex:

Well/Avidin-Biotin Anti-Rat PTH — Rat Intact PTH — HRP Anti-Rat PTH

At the end of this incubation period, the well is washed to remove any unbound antibody and other components. The enzyme bound to the well is then incubated with a substrate solution in a timed reaction and then measured in a spectrophotometric microtiter plate reader. The enzymatic activity of the antibody complex bound to the well is directly proportional to the amount of PTH 1-84 in the sample. A standard curve is generated by plotting the absorbance versus the respective PTH 1-84 concentration for each standard on linear or logarithmic scales. The concentration of mouse intact PTH in the samples is determined directly from this curve.

#### Reagents: Preparation and Storage

Store the kit at 2-8°C upon receipt. Store the standards and controls at -20°C or below after reconstitution. For the expiration date of the kit refer to the label on the kit box. All components are stable until this expiration date.

Prior to use allow all reagents to come to room temperature and mix by gentle swirling and inversion. Reagents from different kit lot numbers should not be combined or interchanged.

1. STREPTAVIDIN COATED MICROTITER PLATE (40-0010)

One plate with 12 eight well strips and frame (96 wells total). This reagent should be stored in the foil pouch with desiccant at 2 - 8°C and is stable until the expiration date on the kit.

2. MOUSE PTH 1-84 BIOTINYLATED ANTIBODY (40-2315)

One vial containing 2.7 mL of biotin labeled anti-mouse PTH in TRIS buffered saline with protein stabilizers and a non-azide, nonmercury preservative. This reagent should be stored at 2 - 8°C and is stable until the expiration date on the kit.

3. MOUSE PTH 1-84 HRP CONJUGATED ANTIBODY (40-2325)

One vial containing 2.7 mL of horseradish peroxidase conjugated to anti-mouse PTH in a stabilized protein solution with a non-azide, non-mercury preservative. This reagent should be stored at 2-8°C protected from light and is stable until the expiration date on the kit.

4. MOUSE PTH 1-84 STANDARDS (40-2331 to 40-2336)

Six vials each containing mouse PTH 1-84 lyophilized in a protein matrix with a non-azide, non-mercury preservative. Refer to vial label for exact concentration. Before use reconstitute the vial with the mouse intact PTH 1-84 concentration of 0 pg/mL with 2.0 mL of deionized water.

Before use reconstitute each of the other five vials of standards with 1.0 mL of deionized water.

Allow the vials to sit for approximately 20 minutes with occasional gentle swirling and inversion.

Assure complete reconstitution before use. Use the standards immediately after reconstitution; freeze the unused portion for later use. After reconstitution the standards are stable until the expiration date on the kit when stored at -20°C or below with up to 3 freeze/thaw cycles.

#### 5. MOUSE PTH 1-84 CONTROLS I & II (40-2341 & 40-2342)

Two vials each containing mouse PTH 1-84 lyophilized in a protein matrix with a non-azide, non-mercury preservative. Refer to vial label for control ranges. Before use reconstitute each control with 1.0 mL of deionized water. Allow the vials to sit for approximately 20 minutes with occasional gentle swirling and inversion. Assure complete reconstitution before use. Use the controls immediately after reconstitution; freeze the unused portion for later use. After reconstitution the controls are stable until the expiration date on the kit when stored at -20°C or below with up to 3 freeze/thaw cycles.

#### 6. ELISA WASH CONCENTRATE (40-0041)

One vial containing 20 mL of a 20 fold concentrate. Before use dilute the content to 400 mL with deionized water and mix well. Upon dilution this yields a working wash solution containing a surfactant in phosphate buffered saline with a non-azide, nonmercury preservative. The diluted wash solution should be stored at room temperature and is stable until the expiration date on the kit.

#### 7. ELISA HRP SUBSTRATE (40-0026)

One bottle containing 11 mL of tetramethylbenzidine (TMB) with hydrogen peroxide. This reagent should be stored at 2 - 8°C protected from light and is stable until the expiration date on the kit..

#### 8. ELISA STOP SOLUTION (40-0030)

One bottle containing 11 mL of 1 M sulfuric acid. This reagent may be stored at room temperature or at 2 - 8°C and is stable until the expiration date on the kit.

#### 9. PLATE SEALER (10-2016)

Two included in kit; use to prevent evaporation and cross contamination of wells.

#### Materials Required But Not Provided

1. 1.0 mL and 2.0 mL volumetric pipettes for reconstituting standards and controls.
2. Precision pipets capable of delivering 25  $\mu$ L, 100  $\mu$ L and 150  $\mu$ L.
3. Aluminum foil.
4. Automated microtiter plate washer OR
5. Repeating dispenser for delivering 350  $\mu$ L and suitable aspiration device.
6. Container for storage of wash solution.
7. Spectrophotometric microtiter plate reader capable of reading absorbance at 450 nm and at 595 - 650 nm.
8. Deionized water.
9. Horizontal rotator capable of maintaining 180 - 220 RPM.
10. Timer.

## Specimen Collection

The intact PTH molecule is unstable, resulting in decreased immunoreactivity over time. Sample collection and storage procedures should be carried out in an expeditious manner. Due to the variable lability of the molecule, measurement of the mouse PTH 1-84 concentration should be made using EDTA plasma or cell culture media. Forty microliters of plasma or culture media are required to assay the sample in duplicate. Centrifuge the sample and separate the plasma or media from the cells. Samples should be assayed immediately or stored frozen at -20°C or below. Avoid repeated freezing and thawing of specimens. The use of various anesthetics can cause significant elevations in blood PTH concentrations. It is therefore imperative to use consistent sample collection procedures within studies.

## Assay Procedure

1. Place a sufficient number of Streptavidin Coated Strips in a holder to run PTH standards, controls and unknown samples.
2. Pipet 20  $\mu$ L of standard, control, or sample into the designated or mapped well. Freeze the remaining standards and controls as soon as possible after use.
3. Pipet 50  $\mu$ L of the Working Antibody Solution consisting of equal volumes of Mouse PTH 1-84 Biotinylated Antibody and Mouse PTH 1-84 HRP Conjugated Antibody into each well.
4. Cover the plate with one plate sealer, then cover with aluminum foil to avoid exposure to light.
5. Incubate plate at room temperature for three hours on a horizontal rotator set at 180 - 220 RPM.

6. Remove the aluminum foil and plate sealer. Using an automated microtiter plate washer aspirate the contents of each well. Wash each well five times by dispensing 350  $\mu\text{L}$  of working wash solution into each well and then completely aspirating the contents.
7. Pipet 100  $\mu\text{L}$  of ELISA HRP Substrate into each of the wells.
8. Re-cover the plate with the Plate Sealer and aluminum foil. Incubate at room temperature for 30 minutes on a horizontal rotator set at 180 - 220 RPM.
9. Remove the aluminum foil and plate sealer. Read the absorbance at 620 nm (see Note) within 5 minutes in a microtiter plate reader against the 0 pg/mL Standard wells as a blank.
10. Immediately pipet 100  $\mu\text{L}$  of ELISA Stop Solution into each of the wells. Mix on a horizontal rotator for 1 minute.
11. Read the absorbance at 450 nm within 10 minutes in the microtiter plate reader against a reagent blank of 100  $\mu\text{L}$  of Substrate and 100  $\mu\text{L}$  of Stop Solution.

If dual wavelength correction is available set the Measurement wavelength to 450 nm and Reference wavelength to absorbance used in step #9.

### Calculation of Results

The two absorbance readings taken before and after the addition of the ELISA Stop Solution allow for the construction of two standard curves using the mouse PTH 1-84 standards contained in the kit. Refer to the individual vial label for exact concentration. The primary curve used for calculation of results is the second reading taken after the addition of the ELISA Stop Solution and read at 450 nm. This data utilizes the absorbance values obtained with the first five standards. The first reading taken before the addition of the ELISA Stop Solution and read at 595

nm – 650 nm is intended to extend the analytical range to the value of the sixth (highest) standard provided in the kit. It should be used only for sample results that fall between the value of the fifth and sixth standard. Results obtained with the first reading should not replace the on-scale reading at 450 nm. Each curve should be generated as follows:

Primary Procedure — Read at 450 nm

1. Calculate the average absorbance for each pair of duplicate assay wells.
2. Subtract the average absorbance of the 0 pg/mL Standard from the average absorbance of all other readings to obtain corrected absorbance.
3. The standard curve is generated by plotting the corrected absorbance of the first five standard levels on the ordinate against the standard concentration on the abscissa using linear-linear or log-log paper. Appropriate computer assisted data reduction programs may also be used for the calculation of the mouse PTH 1-84 results. The PTH 1-84 concentration of the controls and samples are read directly from the standard curve using their respective corrected absorbance. If log-log graph paper or computer assisted data reduction programs utilizing logarithmic transformation are used, samples having corrected absorbance between the 0 pg/mL Standard and the next highest standard should be calculated by the formula:

Value of unknown = [Corrected Absorbance (unknown)/Corrected Absorbance(2<sup>nd</sup> Std.)] x

Value of the 2<sup>nd</sup> Std.

Secondary Procedure — Read at 595 nm – 650 nm

1. Calculate the average absorbance for each pair of duplicate assay wells.

2. The standard curve is generated by plotting the absorbance of the three highest standards on the ordinate against the standard concentration on the abscissa using linear-linear or log-log graph paper.
3. The PTH 1-84 concentration of samples reading only between the fifth and sixth standard are read directly from this standard curve.

#### 6.4 1,25-Dihydroxy Vitamin D EIA kit

##### Summary and Explanation

Vitamin D is a commonly used collective term for a family of closely related molecules derived from naturally occurring 7-dehydrocholesterol (pro-vitamin D<sub>3</sub>). Pro-vitamin D<sub>3</sub> undergoes photolytic conversion in the skin to 'parent' vitamin D<sub>3</sub> (cholecalciferol) upon exposure to sunlight. This compound is biologically inactive, but enters the circulation and is hydroxylated in the liver to active 25-hydroxyvitamin D (25D). A small proportion of this becomes further hydroxylated in the kidney to the highly potent calcitropic hormone 1,25D. 1,25D is largely bound to Vitamin D Binding Protein and albumin in the circulation.

1,25D is one of the major regulators of calcium (and phosphate) metabolism, stimulating intestinal calcium absorption and increasing bone resorption. It also inhibits parathyroid hormone (PTH) production both by direct action on the parathyroid glands and indirectly by raising serum calcium levels. 1,25D production is itself stimulated by parathyroid hormone (PTH), thus providing an effective control loop.

Hypovitaminosis D is commonly associated with dietary insufficiency, most frequently with vegetarianism, and is also associated with low exposure to sunlight (e.g. the elderly and institutionalised) and skin pigmentation. 1,25D production appears to be impaired in early renal failure though this may not be a renal effect. In late-stage renal failure, 1 $\alpha$ -hydroxylation may be impaired, with low 1,25D levels as a result.

#### Method Description

The IDS 1,25-Dihydroxy Vitamin D EIA kit is a complete assay system for the purification of 1,25D in patient samples by immunoextraction followed by quantitation by EIA. Patient samples are delipidated and 1,25D extracted from potential cross-reactants by incubation for 90 minutes with a highly specific solid phase monoclonal anti-1,25D. The immunoextraction gel is then washed and purified 1,25D eluted directly into glass assay tubes. Reconstituted eluates and calibrators are incubated overnight with a highly specific sheep anti-1,25D. Then a portion of this is incubated for 90 minutes with shaking in microplate wells which are coated with a specific anti-sheep antibody. 1,25D linked to biotin is then added and the plate shaken for a further 60 minutes before aspiration and washing. Enzyme (horseradish peroxidase) labelled avidin is added and binds selectively to complexed biotin and, following a further wash step, colour is developed using a chromogenic substrate (TMB). The absorbance of the stopped reaction mixtures are read in a microtitre plate reader, colour intensity developed being inversely proportional to the concentration of 1,25D.

#### Preparation of Reagents

Calibrators CAL: Calibrators CAL are supplied in lyophilised form. Reconstitute immediately before use. Add 1 mL distilled or deionised water to each bottle. Replace stopper and leave to reconstitute for 5-10 minutes, inverting several times to ensure complete reconstitution. DO NOT RECONSTITUTE ON A ROLLING MIXER - this will result in potency loss.

Controls CTRL: Controls CTRL are supplied in lyophilised form. Reconstitute immediately before use. Add 1.2 mL distilled or deionised water to each bottle. Replace stopper and leave 15 - 20 minutes to reconstitute, inverting several times to ensure complete reconstitution.

If Calibrators CAL or Controls CTRL are to be used more than once, they must be frozen (-20°C) within 15 minutes of reconstitution. When re-using frozen Calibrators CAL or Controls CTRL, thaw at room temperature, mix well and use within 15 minutes.

Primary Antibody Solution Ab SOLN: Primary Antibody Concentrate Ab 6x is supplied as a concentrate. Add the entire contents of the bottle of Primary Antibody Buffer Ab BUF, replace the stopper and invert several times to ensure complete mixing.

1,25D Biotin solution 1,25D BIOTIN SOLN: 1,25D Biotin Concentrate 1,25D BIOTIN 6x is supplied lyophilised. Add the entire contents of the bottle of the 1,25D Biotin Buffer 1,25D BIOTIN BUF. Replace the stopper and stand for 10-15 minutes at room temperature. Invert several times to ensure complete reconstitution. If 1,25D Biotin solution 1,25D BIOTIN SOLN is to be used more than once, it must be frozen (-20°C) within 2 hours of reconstitution. When using frozen 1,25D Biotin solution 1,25D BIOTIN SOLN thaw at room temperature, mix well and use within 2 hours.

Wash Solution: Prepare by adding the contents of each bottle of Wash Concentrate WASHBUF 20x to 950 mL of distilled or de-ionised water. Store at room temperature.

All other reagents are supplied ready for use.

Allow all reagents to come to room temperature before use.

Reagents should be mixed by repeated inversion prior to use in the assay

### Specimen Collection and Storage

The assay should be performed using serum or plasma (EDTA or heparin) specimens. Specimens should be separated as soon as possible after collection. For long term storage, store at -20°C.

Avoid repeated freeze/thaw of samples.

Note:

The specimens' storage and stability information stated above are general recommendations for use in a variety of settings of laboratories. Each laboratory should follow the guidelines or requirements of local, state, and/or federal regulations or accrediting organizations to establish its own specimens handling and storage stability. For guidance on appropriate practices, please refer to the CLSI GP44-A4, Procedures for the Handling and Processing of Blood Specimens for Common Laboratory Tests; Approved Guideline - Fourth Edition

### Procedure

#### Materials Provided

1. CAL 0 – 6 – Calibrators (REF AC-6201A - AC-6201G): Lyophilised BSA buffer containing 1,25-dihydroxy-vitamin D and <0.4% sodium azide (0.01% reconstituted). The exact value of each calibrator is printed on the QC Report. 1 mL per bottle, 7 bottles per kit.
2. Ab 6x - Primary Antibody Concentrate (REF AC-6202): Sheep anti-1,25-dihydroxyvitamin D in BSA-phosphate buffer with 0.09% sodium azide, 2 mL per bottle.

3. Ab BUF - Primary Antibody Buffer (REF AC-6202B): Proprietary reagent containing phosphate buffer with 0.09% sodium azide. 10 mL per bottle.
4. Sac-Wel™ SHEEP - Anti-Sheep coated plate (REF AC-SH02W): Microplate with anti-sheep IgG linked to the inner surface of the polystyrene wells, 12 x 8 well strips in a foil pouch with desiccant.
5. 1,25D BIOTIN 6x - 1,25D Biotin Concentrate (REF AC-6203): Lyophilised buffer containing 1,25-dihydroxy-vitamin D labelled with biotin, and proprietary stabilisers, 2mL per bottle.
6. 1,25D BIOTIN BUF - 1,25D Biotin Buffer (REF AC-6203B): Phosphate buffered saline with 0.09% sodium azide, 12 mL per bottle.
7. ENZYMCNJ - Enzyme Conjugate (REF AC-6204): Phosphate buffered saline containing avidin linked to horseradish peroxidase, protein, enzyme stabilisers and preservative, 24mL per bottle.
8. CTRL 1 - CTRL 2 - Controls (REF AC-6205A - AC-6205B): Lyophilised human serum containing 1,25-dihydroxyvitamin D and <1% sodium azide (0.09% reconstituted), 1.2 mL per bottle, 2 bottles per kit.
9. SORB - Immunocapsules (REF AC-6206): Capsules containing monoclonal antibody to 1,25-dihydroxyvitamin D linked to solid phase particles in suspension with vitamin D binding protein inhibitor, 80 immunocapsules per kit.
10. REAG 1 - Delipidation Reagent (REF AC-6207): A solution of dextran sulphate and magnesium chloride, 2.5 mL per bottle.
11. REAG 2 - Elution Reagent (REF AC-6208): Ethanol, 44 mL per bottle.
12. BUF - Assay Buffer (REF AC-6209): BSA buffer with 0.09% sodium azide, 12 mL per bottle.

13. TMB - TMB Substrate (REF AC-TMB): A proprietary aqueous formulation of tetramethylbenzidine (TMB) and hydrogen peroxide, 24 mL per bottle.
14. HCL - Stop Solution (REF AC-STOP): 0.5M Hydrochloric acid, 14 mL per bottle.
15. WASHBUF 20x - Wash Concentrate (REF AC-WASHL): Phosphate buffered saline containing Tween, 50 mL per bottle.
16. Adhesive Plate Sealer 8 per kit.
17. Documentation: Package Insert and QC report.

#### Materials Required but not Provided

1. Disposable 12 x 75 mm borosilicate glass tubes.
2. Disposable 12 x 75 mm polystyrene tubes (optional).
3. Precision pipetting devices to deliver 50  $\mu$ L, 100  $\mu$ L, 150  $\mu$ L, 200  $\mu$ L, 500  $\mu$ L and 1 mL.
4. Repeating pipetting devices to deliver 150 $\mu$ L and 500  $\mu$ L, e.g. Eppendorf Multipipette 4780 or similar.
5. Precision multi-channel pipettes to deliver 100  $\mu$ L and 200  $\mu$ L.
6. Vortex mixer.
7. End-over-end or roller mixer.
8. Heating block or water bath at 40°C.
9. Nitrogen supply and manifold.
10. Centrifuge capable of achieving 2000g.
11. Orbital shaker.
12. Automatic microplate washer (optional).
13. Photometric microplate reader and data analysis equipment.

14. Distilled or deionised water.

#### Sample Preparation

1. Prepare labelled glass or plastic tubes, one for each Control CTRL and unknown sample. DO NOT DELIPIDATE CALIBRATORS CAL.

2. Add 500 µL of each Control CTRL or sample to appropriately labelled tubes.

3. Add 50 µL of Delipidation Reagent REAG 1 to each tube. Vortex all tubes.

4. Centrifuge all tubes at 2000 g for 15 minutes.

Note: Take care not to disturb the pellet when handling delipidated samples. If the pellet becomes suspended or if the sample is not clear, then repeat the centrifugation.

#### Alternative Sample Preparation:

Suitable for samples where the volume available is less than 500 µL.

1. Prepare labelled conical-bottom plastic tubes or microcentrifuge tubes, one for each sample .

2. Add sample (e.g. 250 µL) to appropriately labelled tubes.

3. Add 0.1 x sample volume of Delipidation Reagent REAG 1 (e.g. 25 µL) to each tube. Vortex all tubes.

4. Centrifuge all tubes at 2000 g for 15 minutes, or at 10000 g for 10 minutes (microcentrifuge).

#### Immunoextraction Procedure

1. Prepare labelled Immunocapsules SORB, two for each Control CTRL and sample DO NOT IMMUNOEXTRACT CALIBRATORS CAL . Note: If a Immunocapsule SORB shows signs of leakage or incorrect volume - do not use.

2. Vortex Immunocapsules SORB and allow solid phase to settle. Stand Immunocapsules SORB upright in foam rack for 3-5 minutes.
3. Remove top screw caps from Immunocapsules SORB. Add 100  $\mu$ L of delipidated sample or control to Immunocapsules SORB in duplicate. Replace caps securely.
4. Place Immunocapsules SORB in foam rack and rotate end over-end at 5-20 revolutions per minute for 90 minutes at room temperature (18-25°C). Foam racks can be easily attached to a blood tube rotator by means of cut out slots. Alternatively, foam rack may be wedged inside a suitable plastic beaker and rotated on a bottle roller.
5. Stand Immunocapsules SORB upright in foam rack for 3-5 minutes to allow gel to settle. Tap to dislodge any gel adhering to the screw caps. Allow gel to settle for a further 1-2 minutes. Remove screw cap and break off (do not twist off) bottom stopper from Immunocapsules SORB and place each Immunocapsule SORB in a plastic (or glass) tube. Centrifuge at low speed (500-1000g) for approximately 1 minute to remove sample.
6. Add 500  $\mu$ L of deionised water to each Immunocapsule SORB. Add carefully to avoid solid phase splashing out of the Immunocapsule SORB Centrifuge at low speed (500-1000g) for approximately 1 minute to wash immunoextraction gel.
7. Repeat the above wash step a further two times.
8. Prepare labelled borosilicate glass tubes, one for each Immunocapsule SORB , and transfer Immunocapsules SORB to the glass tubes.
9. Add 150  $\mu$ L of Elution Reagent REAG 2 to all Immunocapsules SORB . Allow reagent to soak into solid phase for 1 to 2 minutes. Centrifuge at low speed (500-1000g) for approximately 1 minute to collect eluate.

10. Repeat above step a further two times. The total elution volume collected is therefore 450  $\mu$ L for each sample.

11. Discard Immunocapsules SORB and place tubes in a heating block or water bath set to 40°C. Evaporate the eluates under a gentle flow of nitrogen. Evaporation should take 20 - 30 minutes. Ensure there is no remaining liquid in the tubes.

12. Add 100  $\mu$ L of Assay Buffer BUF to each tube and vortex to dissolve residues.

The immunopurified samples are now ready for assay.

#### Assay Procedure

Reconstitute Calibrators CAL immediately before assay as described in Preparation of Reagents, or thaw previously reconstituted materials. Allow all reagents to come to room temperature before use. Mix all reagents gently before use in the assay. Prepare labelled borosilicate glass tubes, two for each Calibrator CAL.

1. Add 100  $\mu$ L of each Calibrator CAL to the appropriately labelled tubes. Pipette directly to the bottom of the tube.

2. Assemble sample extract tubes from step 12 above.

3. Add 100  $\mu$ L of Primary Antibody Solution Ab SOLN to all tubes.

4. Vortex all tubes gently without foaming. Incubate at 2-8°C overnight (16-20 hrs).

5. Add 150  $\mu$ L of solution from step 4 to the Coated plate MICROPLAT. Leave the first two wells empty for substrate blanks. Cover the plate with an adhesive plate sealer and incubate the plate on an orbital shaker (500-750rpm) at 18-25°C for 90 minutes.

6. Add 100  $\mu$ L of 1,25D Biotin solution 1,25D BIOTIN SOLN to all wells except for the substrate blanks. Cover the plate with an adhesive plate sealer and incubate the plate on an orbital shaker (500-750rpm) at 18-25°C for 60 minutes.

7. Wash all wells three times with Wash Solution:

a. Automatic plate wash: Set plate washer to dispense at least 300  $\mu$ L of Wash Solution per well. Fill and aspirate for 3 cycles.

b. Manual Wash: decant the contents of the wells by inverting sharply. Dispense 250  $\mu$ L of Wash Solution to all wells. Decant and repeat twice.

Tap the inverted plate firmly on absorbent tissue to remove excess Wash Solution before proceeding to the next step.

8. Add 200  $\mu$ L of Enzyme Conjugate ENZYMCNJ to all wells except for the substrate blanks using a multichannel pipette. Cover the plate with an adhesive plate sealer and incubate the plate at 18-25°C for 30 minutes.

9. Repeat Wash Step 7

10. Add 200  $\mu$ L of TMB Substrate TMB to all wells including the substrate blanks using a multichannel pipette. Cover the plate with an adhesive plate sealer and incubate the plate at 18-25°C for 30 minutes.

*Note: TMB Substrate is easily contaminated. Only remove the required amount for the assay from the bottle. Dispose of unused TMB Substrate. Do not return to bottle.*

11. Add 100  $\mu$ L of Stop Solution HCL to all wells using a multichannel pipette.

12. Measure the absorbance of each well at 450nm (reference 650nm) using a microplate reader within 30 minutes of adding the Stop Solution.

## Calculation of Results

Calculate the percent binding (B/Bo%) of each Calibrator, Control and unknown sample as follows:

$$B/B_0\% = [(\text{mean abs.} - \text{mean abs. substrate blank})] \times 100 / (\text{mean abs. for '0' cal.} - \text{mean abs. substrate blank})$$

Prepare a calibration curve on semi-log graph paper by plotting B/Bo% on the ordinate against concentration of 1,25-dihydroxyvitamin D on the abscissa. Calculate B/Bo% for each unknown sample and read values off the curve in pmol/L. Alternative data reduction techniques may be employed, such as automated data reduction programs, but users should confirm that the selected curve fit is appropriate and gives acceptable results. Smoothed spline or 4PL curve fits are recommended. IDS calculates results using MultiCalc (PerkinElmer) data reduction software with a 4PL curve fit plotting net absorbance versus log concentration.

The reportable range of the assay is 6 – 500 pmol/L. Any value that reads below the lowest calibrator, 6 pmol/L, is an extrapolated value and may be reported as “less than 6 pmol/L”.

## 6.5 FGF23 ELISA Kit

### [REFERENCES AND CUSTOMER SERVICE]

#### 1. REFERENCES

1) Yuji Yamazaki : J Clin Endocrinol Metab, Vol. 87, No. 11 : 4957-4960 (2002)

#### 2. CUSTOMER SERVICE

Kainos Laboratories, Inc.  
38-18, Hongo 2-Chome Bunkyo-ku, Tokyo, Japan 113-0033  
E-mail : fgf-23@kainos.co.jp

Research use only, not for use  
in diagnostic procedures

## FGF-23 ELISA Kit

This product is warranted to perform as described in its labeling  
and literature when used in accordance with all instructions.

### [INTRODUCTION]

Recently FGF-23 was discovered as 22th protein of fibroblast growth factor family. FGF-23 is produced as a 226 amino acid polypeptide which has a cleavage site and the fragmented peptides are recognized in serum with full length peptide.

It is suggested that serum full length FGF-23 level may be useful as an indicator for severity of osteomalacia such as tumor-induced osteomalacia, X-linked hypophosphatemic rickets and autosomal dominant hypophosphatemic rickets.

FGF-23 is a new regulatory element for mineral metabolism.

### [PRINCIPLE OF THE ASSAY]

The FGF-23 ELISA Kit is a two-site enzyme-linked immunosorbent assay for the measurement of FGF-23 in serum. Two specific murine monoclonal antibodies bind to full-length FGF-23. One antibody is immobilized onto the microtiter plate well for capture. The other antibody is conjugated to HRP ( horseradish peroxidase ) for detection.

In first reaction, a sample containing FGF-23 is incubated with the immobilized antibody in a microtiter well. FGF-23 in sample is captured by the antibody. At the end of this reaction, the well is washed to remove unbound FGF-23 and other components.

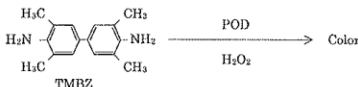
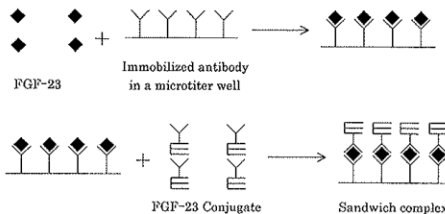
In second reaction, this immobilized FGF-23 is incubated with HRP labeled anti FGF-23 antibody to form a "sandwich" complex :

Anti FGF-23 antibody - FGF-23 - HRP labeled anti FGF-23 antibody  
( N-terminal ) ( C-terminal )

At the end of this reaction, the well is washed to remove unbound components.

In enzyme reaction, sandwich complex immobilized on the well is incubated with a substrate solution and then measured by a spectrophotometric microtiter plate reader. The enzymatic activity of the complex bound to the well is directly proportional to the amount of FGF-23 in the sample.

A standard curve is generated by plotting the absorbance versus the each concentration of FGF-23 standard. The concentration of FGF-23 in the sample is determined from this curve.



### [FEATURE]

- 1) High specificity  
Measurable without the influence of serum components
- 2) High sensitivity  
The minimal detectable concentration is 3 pg/mL
- 3) Wide range  
The maximal detectable concentration is 800 pg/mL

### MANUFACTURE

**KAINOS LABORATORIES, INC.**

38-18, Hongo 2-Chome Bunkyo-ku, Tokyo, Japan 113-0033  
E-mail : fgf-23@kainos.co.jp

※Revised : October 2010

TCY4000E

※ [REAGENTS ( Catalog No. CY-4000 )]

- 1) FGF-23 Antibody coated Microplate ( FGF-23 Microplate )  
96 well microplate ( 12 strips of 8 well ) coated with a murine monoclonal antibody against FGF-23.
- 2) HRP labeled FGF-23 Antibody ( FGF-23 Conjugate )  
12 mL of murine monoclonal antibody against FGF-23 conjugated to horseradish peroxidase, with preservatives.  
This reagent should be stored at 2-10°C protected from light.
- 3) FGF-23 Standards ( Std1~Std7 )  
12 mL ( Std1 ) and 0.5 mL ( Std2~Std7 ) of buffered FGF-23 with preservative.  
7 vials of FGF-23 in buffered base with preservative.
- 4) Assay Diluent ( Assay Diluent )  
12 mL of buffer.
- 5) Color Reagent ( Substrate )  
12 mL of tetramethylbenzidine ( TMBZ ) with urea hydrogen peroxide.
- 6) Wash Buffer Concentrate ( Wash Buffer ( × 5 ) )  
60 mL of a 5-fold concentrated solution of buffered surfactant with preservative.  
Before using, dilute the contents to 5-fold with deionized water and mix well.
- 7) Stop Solution ( Stop Solution )  
12 mL of 0.5 mol/L Sulfuric acid.
- 8) Plate Sealer  
Three included in kit.

These reagents should be stored at 2-10°C at in dark.  
Bring all reagent to room temperature before use.

[ASSAY PROCEDURE]

1. METHODS

- 1) Prepare a sufficient number of Antibody Coated Strip in a holder.
- 2) Add 50  $\mu$ L of Assay Diluent into the well.
- 3) Add 50  $\mu$ L of FGF-23 Standards or sample into the each well, and cover the plate with a plate sealer.
- 4) Incubate plate at room temperature for 2 hr on a plate mixer.
- 5) Remove plate sealer. Aspirate the contents of each well. Wash each well 4 times with 300  $\mu$ L of working Wash Buffer and completely aspirate the contents.
- 6) Add 100  $\mu$ L of FGF-23 Conjugate into each well and cover the plate with a plate sealer.
- 7) Incubate plate at room temperature for 1 hr on a plate mixer.
- 8) Remove plate sealer. Aspirate the contents of each well. Wash each well 4 times with 300  $\mu$ L of working Wash Buffer into each well and completely aspirate the contents.
- 9) Add 100  $\mu$ L of Substrate into each well and cover the plate with a plate sealer and a aluminum foil.
- 10) Incubate plate at room temperature for 30 minutes.
- 11) Remove plate sealer and aluminum foil. Immediately add 100  $\mu$ L of Stop Solution into each well. Shake the plate on the plate mixer for 1 minutes.
- 12) Read the absorbance at 450 nm within 10 min by microtiter plate reader.

2. ASSAY PROCEDURE SUMMARY

Prepare all reagents and standards  
↓  
Add 50  $\mu$ L of Assay Diluent to each well  
↓  
Add 50  $\mu$ L of FGF-23 Standards or sample to each well  
↓  
Incubate at room temperature for 2 hr on a plate mixer  
↓  
Aspirate and wash 4 times  
↓  
Add 100  $\mu$ L of FGF-23 Conjugate into each well  
↓  
Incubate at room temperature for 1 hr on a plate mixer  
↓  
Aspirate and wash 4 times  
↓  
Add 100  $\mu$ L of Substrate into each well  
↓  
Incubate at room temperature for 30 minutes  
Protect from light  
↓  
Add 100  $\mu$ L of Stop Solution into each well  
Read at 450 nm within 10 minutes

3. CALCULATION RESULTS

The standard curve is generated by plotting the corrected absorbance of the Std1 ~ Std7 levels on the ordinate against the standard concentration on the abscissa using linear-linear or log-log graph paper. Appropriate computer assisted data reduction programs may also be used for the calculation of results.

Samples with values greater than the highest standard should be dilute with Std1 and reassayed.

[SAFETY PRECAUTION]

- 1) Handle samples, standards and the materials that contact them as potential biohazards.
- 2) Avoid contact with reagents containing TMBZ, hydrogen peroxide, or sulfuric acid ( i.e. ELISA HRP Substrate and ELISA Stop Solution ). TMBZ is dissolved in a solution which contains urea hydrogen peroxide, an irritant to skin and mucous membrane. In case of contact with any of these reagents, wash thoroughly with water. TMBZ is a suspected carcinogen. Use Good Laboratory Practices. Wash hands before eating. Do not eat, drink or smoke in the work area.

[SPECIMEN COLLECTION]

The intact FGF-23 molecule appears to be highly unstable resulting in decreased immunoreactivity over time. Specimen collection and assay or storage procedures should be carried out in an expeditious manner.

[PROCEDURAL NOTES]

- 1) Store any unused Antibody Coated strips in the resealable aluminum pouch with desiccant to protect from moisture.
- 2) The sample and all reagents should be pipetted carefully to minimize air bubbles in the well.
- 3) The sequence and timing of each reagent addition is important as both the immunological and enzymatic reactions are in kinetic modes. The washing step is also an important part of the total assay procedure. The use of an automated microtiter plate washer is strongly recommended. All pipetting and washing steps should be performed such that the timing is as consistent as possible.
- 4) Samples with values greater than the highest standard should be dilute with Std 1 and reassayed.

[LIMITATION OF THE PROCEDURE]

- 1) The lowest concentration of human intact FGF-23 measurable is 3 pg/mL ( assay sensitivity ) and the highest concentration of human intact FGF-23 measurable without dilution is the value of the highest standard.
- 2) The reagents in this Human Intact FGF-23 ELISA kit have been optimization so that the high dose "hook effect" is not a problem for samples with elevated FGF-23 values. Sample with values greater than the highest standard should be dilute with Std 1 and reassayed.

[WARRANTY]

This product is warranted to perform as described in its labeling and literature when used in accordance with all instructions. KAINOS LABORATORIES, Inc. DISCLAIMS ANY IMPLIED WARRANTY OF MERCHANTABILITY OR FITNESS FOR A PARTICULAR PURPOSE, and in no event shall KAINOS LABORATORIES, Inc. be liable for consequential. Replacement of the product or refund of the purchase price is the exclusive remedy for the purchaser. This warranty gives you specific legal right and you may have other rights which vary from state to state.

TCY4000E